AUTONOMIC ASSESSMENT FOR GI DYSMOTILITY AND NEUROMODULATION

DEVELOPMENT OF METHODOLOGIES TO ASSESS AUTONOMIC NERVOUS SYSTEM FUNCTIONING AND NEUROMODULATION FOR THE DIAGNOSIS AND TREATMENT OF COLONIC MOTILITY DISORDERS

M. KHAWAR ALI, B.Sc. ENG., M.ENG.

A Thesis Submitted to

The School of Graduate Studies

In Partial Fulfillment of the Requirements for the Degree

Doctor of Philosophy

McMaster University

McMaster University

Doctor of Philosophy (2022)

Hamilton, Ontario (School of Biomedical Engineering)

TITLE: DEVELOPMENT OF METHODOLOGIES TO ASSESS AUTONOMIC NERVOUS SYSTEM FUNCTIONING AND NEUROMODULATION FOR THE DIAGNOSIS AND TREATMENT OF COLONIC MOTILITY DISORDERS

AUTHOR: M. Khawar Ali, B.Sc. Engineering (Bahauddin Zakariya University), M.Eng. (McMaster University)

SUPERVISOR: Professor Jan D. Huizinga, Ph.D.

PAGES: xxv, 250

Abstract

Although parasympathetic activity (PNS) is the primary driver and sympathetic activity (SNS) is a significant inhibitor of colonic propulsive activity, they are rarely measured, and hence, they almost play no role in diagnosing dysfunction or standard treatments for chronic conditions such as refractory constipation. We aimed to develop methodologies for the assessment of autonomic nervous system (ANS) activity, establish criteria for autonomic dysfunction, and study if stimulation of lumbar and sacral autonomic nerves using low-level laser therapy (LLLT) could affect the ANS and explore it as a potential treatment of autonomic dysfunction to restore colonic motility. By studying the active standing test and the table tilt test as a method to evoke activity in the ANS, we rejected LF power, SD1 and SD2 of Poincare plot, Pre-ejection-period (PEP), complex-correlation-measure (CCM) and detrended fluctuation analysis (DFA). Respiratory-Sinus-Arrhythmia (RSA), Root-Mean-Square-of-Successive-Differences (RMSSD) were selected for PNS activity, the Baevsky's-Stress-Index (SI) was chosen for SNS activity, and SI/RSA and SI/RMSSD were introduced as a measure of autonomic balance. We explored high-resolution-colonic-manometry with concurrent electrocardiography to observe whether these parameters could be associated with ANS changes during colonic motor patterns. High-amplitude-propagating-pressure-waves were associated with a strong parasympathetic activity and decreased sympathetic activity. Comparing ANS reactivity of patients with severe motility disorders to controls in response to postural changes, we observed that most patients have low PNS and elevated SNS baseline activity and reactivity. This established a way to evaluate autonomic dysfunction in patients with colon motor disorders. A single session of LLLT using LED and laser light on the lumbar and sacral spine in 41 patients with chronic gastrointestinal motor

dysfunction indicated that treatments with LED light followed by laser light significantly increased parasympathetic activity and decreased sympathetic nervous system activities. These results initiated a study into the effects of LLLT on restoring autonomic dysfunction in chronic refractory colonic motility disorders.

Acknowledgments

Foremost, I would like to express my gratitude to my supervisor Professor Jan D. Huizinga, for the continuous support during the entire period of my Ph.D. study and research, for his leadership, patience, guidance, motivation, enthusiasm, and immense knowledge. Thank you, Dr. Huizinga, for providing the endless supply of opportunities for me to grow, the independence to figure out how to pursue them and your immense support when I struggled throughout these years.

This work could not have been possible without input from Dr. Jihong Chen. Thank you, Dr. Chen, for your continuous advice, passion, inspiration, and support. You and Dr. Huizinga complemented each other very well and created a great learning environment in the Lab.

I would also like to thank my supervisory committee members, Professor Michael Noseworthy and Prof. Qiyin Fang, for their encouragement, insightful comments, and critical analysis to improve my work. My sincere thanks to Dr. Juan Guzman and Dr. Chen for their collaboration and for allowing me to use their clinical data for this work. I thank my fellow lab members Dr. Sean Parsons, Natalija Milkova, Lijun Liu, Christie Yuan, Amer Hussain and Ashley Barbier for your stimulating discussions, sharing ideas and constant willingness to help. I would also like to thank Kartik Sharma, Shrayasee Saha, and Sharjana Nirmalathasan for their help.

It is a pleasure to acknowledge the facilities and research funds generously provided by the School of Biomedical Engineering, the Farncombe Family Digestive Health Research Institute at McMaster University and the National Sciences and Engineering Research Council of Canada (NSERC).

Above all, I want to thank my family for inspiring me and their unconditional support and love.

Table of Contents

List of Figures

List of Tables

List of Abbreviations

ANS	Autonomic Nervous System
AST	Active Standing Test
ATL	Autonomic Testing Laboratory
CAN	Central Autonomic Network
CNS	Central Nervous System
DRG	Dorsal Root Ganglia
ENS	Enteric nervous system
GI	Gastroenterology
HAPW	High-Amplitude Propagating Pressure Wave
HAPW-SPW	High-Amplitude Propagating Pressure Wave followed by a Simultaneous Pressure Wave
HF	High Frequency
HRCM	High Resolution Colonic Manometry
HRV	Heart rate Variability
LF	Low Frequency
LLLS	Low Level Laser Stimulation
LLLT	Low Level Laser Therapy
MC	Motor Complex
NTS	Nucleus Tractus Solitarius
PEP	Pre-Ejection Period

PNS	Parasympathetic Nervous System
RMSSD	Root Mean Square of Successive Differences
RSA	Respiratory Sinus Arrythmia
SD1	Standard Deviation of Minor Axis of Poincare´ Plot
SD2	Standard Deviation of Major Axis of Poincare´ Plot
SI	Sympathetic Index
SNS	Sympathetic Nervous System
SPW	Simultaneous Pressure Waves
TTT	Tilt Table Test

Declaration of Authorship and Preface

Declaration of Authorship

I, M Khawar Ali, declare that the work included in this thesis titled "Development of methodologies to assess autonomic nervous system functioning and neuromodulation for the diagnosis and treatment of colonic motility disorders," is my own. I confirm that:

I participated in all experimental designs and analyses in cooperation with the co-authors. I was subsequently responsible for the data collection, analysis, and manuscript preparation, including primary and supplemental texts, figures, and tables.

- For Chapter 4, a paper published in *Frontiers in Neurosciences*: All studies were conducted at the McMaster University Medical Center. MKA and YY are the shared first authors. J-HC performed the HRCM studies. J-HC and JH developed HRCM at McMaster University. YY and MKA executed the HRV analyses assisted by MF, KS, NM, and LL. MKA made substantial contributions to the Baevsky index implementation. WT, KZ, NM, and LL took part in the execution and data analysis of HRV. SP was instrumental in designing HRCM and the early stages of HRV analysis. KM and LS were critical for HRV analysis and statistical analysis. ER and DA were instrumental in the execution of HRCM. JH supervised all analyses. All authors were involved in discussing and revising the manuscript.
- For Chapter 5, a paper published *in Frontiers in Physiology:* MKA analyzed all the data, generated all the figures, incorporated Baevsky's Stress Index, and wrote the first draft of the manuscript. LL assisted with data analysis and manuscript writing. J-HC directed and performed all-volunteer HRCM studies and discussed manuscript writing. JDH

oversaw the autonomic nervous system analysis and manuscript writing. All authors approved the manuscript.

- For Chapter 6, all the work presented is my own which includes data collection, analyses and writing the chapter. Part of this work has been incorporated in a manuscript titled "Diagnosis of colonic dysmotility associated with autonomic dysfunction in patients with chronic refractory constipation" published in *Nature's Scientific Reports* on July 14, 2022, authored by: Lijun Liu, Natalija Milkova, Sharjana Nirmalathasan, M. Khawar Ali, Kartik Sharma, Jan D. Huizinga and Ji-Hong Chen.
- For Chapter 8, a paper submitted to *Frontiers in Neuroscience | Autonomic Neuroscience*: MKA collected and analyzed all the data, contributed to interpretation, and wrote the manuscript draft, generated all the figures. SS assisted in data analysis and data interpretation at the beginning of the project. NM and LL contributed to patient assessment and data analysis. KS made a substantial contribution to data analysis. JDH and J-HC designed the study and contributed to the manuscript's data collection, analysis, interpretation, and revisions.
- In chapters 2 and 3 and 7, I performed all the literature research, programming, data analysis and collection and presentation under the supervision of JDH.

Preface

Heart rate variability provides a window into cardiac autonomic function; it also is a window to more general autonomic function in an individual. Part of our objective was to evaluate its use to assess ANS activity related to the GI tract. The first step of this project was to identify the best heart rate variability parameters for parasympathetic and sympathetic nervous system

activity. In Chapter 2, Heart rate variability parameters are evaluated that have been proposed related to a procedure that produces known changes in the autonomic nervous system activity during the supine-sitting-standing protocol (the active standing test). The criteria for normal autonomic nervous system modulation are established from the HRV parameters values generated during each posture for healthy controls, which is used as a standard to test the patients' autonomic nervous system activity and reactivity.

The selected HRV parameters for ANS assessment and the active standing test results are then evaluated against the established tilt table test. This comparison enabled us to optimize the protocol for the active standing test, which has been discussed in chapter 3. The patients selected for this study had cardiac and GI symptoms. The HRV parameters were also applied during the deep breathing test, beta-adrenergic hypersensitivity test, intrinsic heart rate test and catecholamine level test.

After identifying the heart rate variability parameters for the sympathetic and parasympathetic nervous system activity, the next step (Chapter 4) was to determine the associations of the autonomic nervous system with colonic motility. The general autonomic activity and reactivity to postural change were first tested for each individual and compared to the established normal ranges for each posture. High-resolution colonic manometry was used to record the activity of the human colon. Meal, prucalopride, proximal and distal balloons distention and rectal bisacodyl were used as stimuli to evoke the motor patterns during the recording. The ECG and impedance cardiography were simultaneously recorded during the whole session and time-matched with high-resolution colonic manometry. The HRV parameters were used to

study the autonomic nervous system activity before, during and after each recorded motor pattern. The baseline autonomic activity was also correlated to the autonomic nervous system modulation during motor patterns.

In Chapter 5, The association of the autonomic nervous system activity with the colonic motor function was further optimized by identifying the most suitable heart rate variability parameters for sympathetic and parasympathetic activity. In addition, two new parameters of autonomic balance were introduced. The sympathetic and parasympathetic nervous system activity was visually associated with the colonic activity. The visual representation and quantification enabled us to study the baseline autonomic activity without colonic motor patterns and during the different motor patterns.

To test the hypothesis of the involvement of autonomic nervous system dysfunction in motility disorders, the baseline autonomic nervous system activity and the reactivity to the postural change from supine to sitting and standing were compared between the motility disorder patients and the healthy controls in chapter 6. In addition, different groups of patients based on their age and medical history, including constipation, back pain, bladder symptoms, anxiety, and stress, were also compared with the control groups.

It is hypothesized that stimulating the lumbar and sacral autonomic nerves using low-level laser therapy can improve the autonomic function related to colonic motility. We used an LED array with 240 LEDs generating red and Infrared light and an infrared laser probe developed by

Bioflex Inc. to stimulate the lumbar and sacral autonomic nerves, and the reactivity of the autonomic nervous system was assessed by heart rate variability. In chapter 7, the properties of light and its propagation from one medium to another medium, like biological tissue, are discussed, and the penetration of light and delivered energy is calculated for LED array (Red and Infra-red) and laser probe.

In chapter 8, the effect of one session of LLLT is evaluated on ANS in patients with motility disorders. The patients received light stimulation on their lumbar and sacral spine using red and infrared LED arrays and infrared laser probes. Their autonomic nervous system activity was recorded before, during, and after the LED and laser stimulations. The effect of sham LLLT is also studied in healthy volunteers to rule out the ANS modulations due to the sham effect. Finally, chapter 9 is the overall discussion, which refers to this research's overall results and limitations and future recommendations.

Chapter 1

Introduction

1.1 Introduction

The autonomic nervous system (ANS) is critical for maintaining the normal motility functions, yet we have very little insight into its role in actual human colon motor activities[1]. Despite our understanding of the extrinsic innervation of the colon, it is largely ignored in the diagnosis of functional colonic disorders. Hence, there is a requirement to establish a methodology to study the associations between autonomic sympathetic and parasympathetic nervous system activity and the colonic motor functions, the autonomic dysfunction's association with motility disorders and to identify the potential treatment for autonomic dysfunction. Heart rate variability (HRV) has been used as a non-invasive technique to quantitatively measure the autonomic nervous system activity; however, the criteria for normal autonomic testing in association with motility functions must be established.

The gastrointestinal tract (GI tract) is innervated by the intrinsic enteric nervous system (ENS) and extrinsic autonomic nervous system (ANS), with their respective neurotransmitter receptors widely distributed in various intestinal cells. Although the GI functions exhibit a significant amount of autonomy via the enteric nervous system, which is located within the submucosal and myenteric plexuses in the wall of the GI tract, the central nervous system (CNS) provides extrinsic neural inputs by communicating with the ENS via autonomic innervations to regulates, modulate, and control the GI functions like digestion, nutrient absorption, and

elimination of waste [2] [1], [3]. Below we will identify the extrinsic neural pathways involved in colonic motor functions and the association between cardiac and colonic autonomic activities.

1.1.1 Autonomic innervation and control of the GI tract

The parasympathetic innervation of the GI tract is supplied by the vagus nerve and the sacral or pelvic nerves. The upper part of the GI tract, including the esophagus, stomach, small intestine, and ascending colon, gets its parasympathetic innervation from the vagus nerve. In contrast, the lower GI tract, which includes the transverse, descending and sigmoid colon and the striated muscles of the external anal canal, receive their parasympathetic innervations from the preganglionic neurons within the lumbosacral spinal cord, prominently from S1–S4 regions. The parasympathetic nerve fibres are long and synapse inside the walls of the GI tract in myenteric and submucosal plexuses, where the parasympathetic inputs are synchronized and transmitted to the smooth muscles, endocrine and secretory cells. The parasympathetic neurons are either cholinergic releasing acetylcholine (Ach) or peptidergic releasing neuropeptides as neurotransmitters[4].

The sympathetic preganglionic neurons innervating the GI tract ascend from the thoracic and lumbar spinal cord. Four sympathetic ganglia, celiac, superior mesenteric, inferior mesenteric and hypogastric located at spinal L2–L5 lumbar levels provide the sympathetic innervations to the GI tract out of which the inferior mesenteric ganglion or pelvic ganglion innervate the colon. The postganglionic nerve fibres synapse either on ganglia in the myenteric and submucosal plexuses or directly innervate the smooth muscle cells. The sympathetic nerve fibres are adrenergic, which release norepinephrine as a neurotransmitter. Sympathetic fibres can

function both pre-synaptically and post-synaptically to modulate the enteric nervous system activity via direct action on the enteric nervous system [5][6] [].

1.1.2 Nucleus Tractus Solitarius (NTS)

The central nervous system provides the homeostatic control of the colon by modulating the activity of the sympathetic and parasympathetic innervation to the colon. The vagal efferent activity is controlled by synaptic inputs from the brainstem and higher central nervous system nuclei. Although the dorsal motor neurons of the vagus receive the innervation from several brainstem and higher CNS nuclei, most of these modulatory inputs arise from the nucleus tractus solitarius (NTS). The NTS also receives the sensory information from the vagal afferent fibres, which innervate the thoracic and adnominal viscera. The cell bodies of the vagal afferent fibres lie within the nodose ganglia, and their central terminals enter the brainstem through the NTS, also affecting the NTS neurons, which are organized in subnuclei according to their afferent inputs like gastric afferent input, esophageal afferent input, cardiovascular and respiratory afferent inputs. The dendric projections of NTS spread throughout the nucleus and interact within the subnuclei because of which the autonomic reflexes may be synchronized across all the organs with autonomic innervations[2]. Therefore, the inputs from CNS to the efferent fibres to modulate the GI function in response to the sensory inputs from the GI tract also affect the cardiovascular function because of the crosstalk between the subnuclei in the NTS affecting the heart rhythm. Therefore, any autonomic input to modulate the GI function may be measured via heart rate variability[7][6].

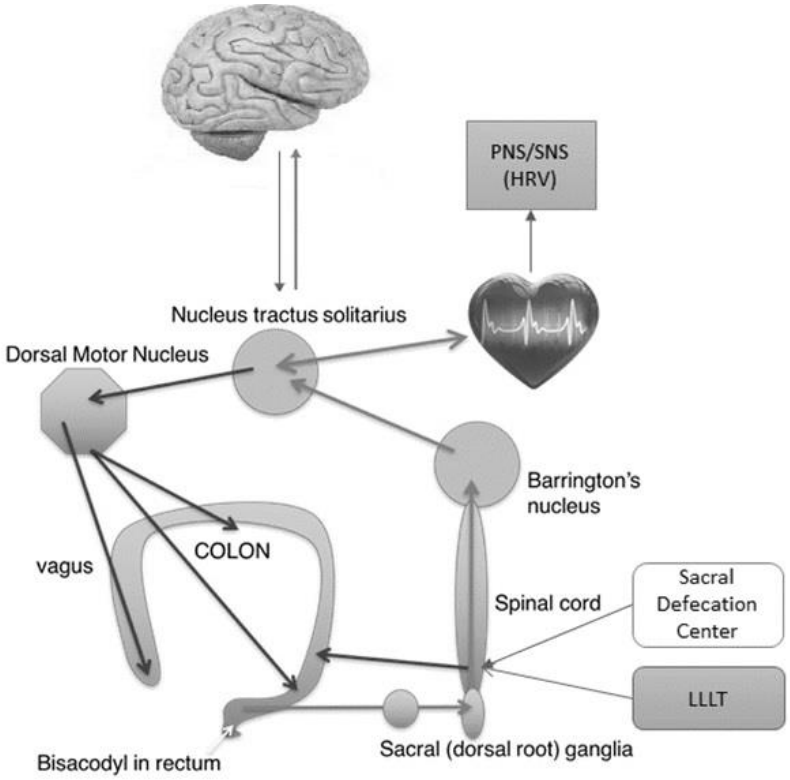

Figure 0-1: Neural Pathways involved in colonic motility

A study presented in the later section of this thesis indicated that injecting bisacodyl in the rectum causes the generation of contractions starting from the most proximal end of the ascending colon. The bisacodyl in the rectum causes the activation of chemical receptors in the rectum, which communicate through the sacral afferent fibres to the higher brain centers via spinal pathways through Barrington's nucleus and the Nucleus Tractus Solitarius (NTS). This information is treated as an urge to defecate, and in response to this information, the CNS modulates the vagal input to initiate the contractions in the proximal colon. Figure 1.1 shows the communication channels of the sensory information from the sacral defecation center to the CNS and the autonomic input from the CNS to the proximal colon via the NTS which is also reflected in the cardiovascular system and can then be measured by the heart rate variability.

This indicates the importance of the autonomic nervous system in normal colonic functions. Therefore, unlike in current clinical practices, patients with colonic motility disorders should be assessed for autonomic dysfunction. One of the objectives of this project is to establish the methodology to assess the autonomic nervous system and autonomic nervous system dysfunction.

1.1.3 Autonomic Innervations of Heart

The central autonomic network (CAN) controls the autonomic outflow to the heart via the vagal and sympathetic nerve fibres innervations. The sinoatrial node (SA Node) is innervated by the right vagus nerve, while the AV (atrioventricular) node gets its innervations from the left vagus nerve, but there can be a significant amount of overlap in the anatomical distribution. Atrial muscle and ventricular myocardium are also innervated by vagal efferent. In comparison, the sympathetic efferent nerves are present throughout the atria and ventricles and the conduction system of the heart. The nucleus tractus solitarius receives sensory information from the baroreceptors and chemoreceptors. The neuronal connections originating from the nucleus tractus solitarius modulate the parasympathetic and sympathetic activity. The medulla containing the NTS also receives input from other brain regions like the hypothalamus, which is vital for stimulating cardiovascular responses in various situations like stress and danger. The autonomic nervous system affects many aspects of cardiac electrophysiology by the complex interaction between neurotransmitters and their effect on the receptors located in the SA node, AV node and left ventricle[8], [9].

1.1.4 Heart Rate Variability

Heart rate variability (HRV) measures the time variations between the consecutive inter-beat intervals (RR intervals) caused by the central nervous system's autonomic input to the heart. In addition to the central autonomic network, respiration and baroreceptor reflex also induce changes in the heart rate. The heart rate variability has been used as a tool for the non-invasive study of the autonomic activity in the body using the RR interval obtained from the electrocardiogram. Studies have shown that the blocking of vagal input via a high dose of atropine causes the disappearance of variability in the RR intervals. This indicates the dominance of vagal control over sympathetic control of the heart rate variability and the role of autonomic input in generating the heart rate variability. The average of RR intervals indicates the balance between the vagal and sympathetic neural activity, and the difference of an RR interval from the mean RR values indicates the spontaneous modulation of sympathetic and parasympathetic input [10] [11]. Several heart rate variability parameters have been developed to measure parasympathetic and sympathetic activity. Although heart rate variability provides a window into cardiac autonomic function, it also is a window to more general autonomic function in an individual. Part of our objective was to evaluate its use to assess ANS activity related to the GI tract.

1.2 Development of Treatment Technique

After identifying the role of the autonomic nervous system in motility function, our objective was to establish a technique to treat autonomic dysfunction. Low-level laser therapy (LLLT) is a therapeutic method founded on the photobiomodulation principle, which generates biological

modifications in organisms in response to the interactions of photons in the visible or infrared spectral regions with biological cells in the target region. It has been successfully used to promote cellular functions and speed up cellular healing and has been proved helpful in treating inflammation, pain, nerve regeneration, hair growth and bone repair[12].

1.2.1 Low-Level Laser Therapy (LLLT)

Low-level laser therapy (LLLT) uses continuous or pulsed, low-powered (1-5 mW) red and infra-red light with a wavelength ranging from 600–1100 nm with low energy density to modulate the biological functions in the cells of the target biological tissue. Unlike high-powered lasers, which have ablative or thermal effects, low-level laser therapy has a photochemical effect like photosynthesis. Therefore, it is also known as cold or non-thermal, soft, biostimulation, and photobiomodulation laser and has been used for physical therapy. LLLT is performed either by LED arrays or laser diode, or both; LED arrays stimulate a larger area, but they have less penetration depth, while a laser diode produces monochromatic, unidirectional light that can deliver substantial levels of concentrated energy at more penetration depth inside the biological tissue compared to LEDs. Despite low-level laser therapy's clinical and pre-clinical benefits, its underlying action mechanism for biological tissues is not fully understood[13]. According to many studies, the mitochondria in the cells are the major red and IR light-absorbing chromophores. During the event of an inelastic collision between photons and mitochondrial chromophores, the energy is transferred from the incoming photon to the chromophores, which is then converted into chemical energy, increasing the production of Adenosine Triphosphate (ATP) in the cell. The photons are absorbed by the cytochrome c oxidase of the electron transport chain (ETC) of the mitochondria, which leads to the elevated

movement of protons across the mitochondrial membrane, which causes an increase in the proton gradient across the membrane of mitochondria generating a membrane potential. This causes an increase in ATP, reactive oxygen species (ROS) and intracellular calcium (Ca^{2+}) and nitric oxide (NO) from cytochrome C oxidase. These molecules cause activations of signal transduction leading to gene transcription and cause visible effects like wound healing, pain management and treatment of inflammation[13].

Patients with motility disorders due to autonomic dysfunction may have problems in their neural autonomic pathways, and low-level laser therapy of the lumbar and sacral autonomic nerves may restore the normal autonomic function by stimulating the neural circuitry the motility function (**Error! Reference source not found.**). Therefore, another objective of this t hesis was to study the effect of one-time low-level laser therapy on the autonomic nervous system activity of the patients with motility dysfunctions to identify if LLLT is a candidate for restoring the autonomic dysfunction.

1.3 Hypotheses

It is hypothesized that the autonomic nervous system plays a crucial role in normal colonic motility, and abnormal autonomic activity or reactivity might contribute to motility disorders. Therefore, patients with motility disorders should be assessed and treated for autonomic dysfunction.

The neuromodulation of lumbar and sacral autonomic nerves by low-level laser therapy may restore the regular autonomic activity and hence colonic motility.

1.4 Objectives

The objectives of this thesis work were:

1. To develop methodologies to assess autonomic nervous system activity and develop criteria for autonomic dysfunction.
2. To identify the association of sympathetic and parasympathetic nervous system activity with colonic motor functions and to identify the role of autonomic dysfunction in colonic motility disorders
3. To study the effect of neuromodulation of the autonomic nerves originating from the lumbosacral spine and innervating the colon, using one session of low-level laser therapy to find out if any evidence could be obtained that LLLT actually affects the autonomic nervous system.

Chapter 2

Developing Autonomic Nervous System Assessment As It Relates To The Active Standing Protocol, To Provide Baseline General Autonomic Functioning.

2.1 Introduction

Heart Rate Variability (HRV) signal analysis is an important tool for studying the autonomic nervous system. Several time and frequency domain and nonlinear analysis techniques have been applied to HRV signals to generate information about parasympathetic nervous system (PNS) and sympathetic nervous system (SNS) activity and reactivity. Most of these analysis techniques like RSA, RMSSD, high frequencies band power (0.15-0.4 Hz.) of HRV signal, SD1 of Poincare plot provide information about the PNS, while the ratio of low frequencies band power (0.04-0.15 Hz.) to high frequencies (LF/HF) are considered as measures of sympathovagal balance. Pre-Ejection-Period (PEP) is considered a measure of SNS activity; however, it requires impedance measurement. This chapter provides the basic information about RSA, RMSSD, Poincare plot (SD1, SD2 and their ratios), frequency analysis (HF power band, LF power band and their ratios), complex correlation measure (CCM), detrended fluctuation analysis (DFA), PEP and Baevsky's stress index (S.I.) in response to active standing test (Supine, Sitting, Standing, Walking, sitting after the walking or sitting 2) Suitable parameters were then selected for SNS and PNS activity. Their normal ranges were calculated for each posture of the active standing test and used as a criterion for normal autonomic activity and reactivity.

2.1.1 Root Mean Square of Successive Differences (RMSSD)

Root Mean Square of Successive Differences (RMSSD) is one of the frequently used time-domain heart rate variability parameters to measure parasympathetic activity. It is obtained by

first calculating the successive differences between the R.R. intervals in milliseconds and then calculating the root mean square of these differences as follows:

$$RMSSD = \sqrt{\frac{1}{N-1}\sum_{i=1}^{N-1}(RR_{i+1} - RR_i)^2}$$

Where N is the total number of R.R. intervals, RR_i is the current R.R. interval, and RR_{i+1} is the next R.R. interval[10]. An increased parasympathetic reactivity causes more variations in successive R.R. intervals (short-term variability), which leads to higher values of successive differences (RR_i-RR_{i+1}) and, ultimately, a higher value of RMSSD. RMSSD correlates to the high-frequency power of the HRV signal and is used as a measure of parasympathetic reactivity[10].

2.1.2 Frequency Spectrum analysis of HRV signal

The frequency analysis enables quantifying the various frequencies in the HRV signal. The R.R. interval signal is generated from the ECG recording after removing the artifacts and converted into the frequency domain using Fast Fourier Transform (FFT) or continuous wavelet transform (CWT). Four frequency bands are of interest in HRV signal analysis (i) Ultra-low Frequency Band (ULF) ranging from 0-0.003 Hz., Very low-frequency band (VLF) ranging from 0.003-0.04 Hz., Low-frequency band (LF) ranging from 0.04-0.15 Hz. and high-frequency band (HF) ranging from 0.15-0.5 Hz. Out of these four bands, the LF band and HF band, their ratio (LF/HF) are usually used for ANS assessment. The LF band is associated with both the SNS and PNS activity; the ratio LF/HF is considered to represent the autonomic balance [14].

The HF band, also known as the respiratory band, is associated with the variation in the heart rate due to respiration. The heart rate increases during inhalation due to the inhibition of vagal

outflow by the cardiovascular center and decreases during exhalation due to the restoration of vagal outflow by the release of acetylcholine [15]. Therefore, the respiration frequency highly influences the HF band power. The HF band ranges from 0.15-0.5 Hz, which corresponds to 9-24 breaths/min respiration frequency. Colombo and Aurora et al. explained that since the respiration frequency highly influences the HF band power, therefore, it is the marker of the PNS activity only within the frequency ranges of 9-24 breaths/min and the frequency range of the HF band should be adjusted continuously based on breathing frequency [16]. If the breathing rate is outside these ranges, then the calculated HF power will only be due to noise or harmonics of lower frequency bands, and the respiration frequency power will not be included in the HF power. Also, the HF band of 0.15-0.5 Hz. is too broad, including power due to noise. If the respiration frequency is lower than 9 breathes/min, as in the case of deep breathing, the most prominent component of HF band power (respiration frequency power) will lie in the LF band, and without adjusting the HF band, it will indicate low HF power and high LF power and lead to erroneous results. Similarly, during exercise, the breathing frequency of over 24 breaths/min, the prominent component of HF power, will be out of the range and will wrongly represent low HF power.

Instead of HF power, the term Respiratory Frequency Area (RFa) is used as a marker of PNS activity [16]. LF power, which is influenced by both SNS and PNS activity, will also be adjusted by adjusting the HF band to RFa. For example, in the case of deep breathing (< 9 breaths/min), the respiration frequency will lie in the LF region, and using RFa instead of HF will also decrease the LF band, and the new adjusted LF band power is termed as Low-Frequency area (LFa) which is smaller than LF power. It is claimed by Aurora et al. that LFa is purely the measure of SNS

activity as the PNS component is included in RFa [16][17] . Nguyen et al. have also used LFa and RFa instead of LF and HF power in their recent study of autonomic function in gastroparesis using a machine developed by ANSAR medical technologies Inc. to record the SNS and PNS activities [16][17] . This adjustment is valuable only if the respiration frequency changes during the recording due to deep breathing or exercise requirements. [16][17]. Since LF band power is influenced by both the SNS and PNS, we will not use it in our ANS assessment. For PNS assessment, the HF power will be used; however, it will be converted into respiratory sinus arrhythmia (RSA).

2.1.3 Respiratory Sinus Arrhythmia (RSA)

A cyclical variation in heart rate characterized by faster heart rate during inspiration and slower heart rate during expiration, but otherwise normal ECG, is termed respiratory sinus arrhythmia (RSA). RSA is primarily vagally mediated, with negative intrathoracic pressure of inspiration causing less pressure on the paired vagus nerves and, therefore, lower vagal tone (heart rate increases), and the reverse sequence causing a decrease in heart rate during exhalation [18]. The average respiration frequency for adults in supine position ranges from 12 to 20 per minute (0.2 Hz. to 0.33 Hz.). Therefore, the strongest frequency components in the HF range of the HRV spectrum are due to respiration. The more the variation in the heart rate due to breathing, the higher the value of the HF power band, which indicates a higher value of RSA. RSA is defined and calculated as:

$$RSA = \ln (HF\ Power)$$

A higher value of RSA represents a higher variation in heart rate during inhalation and exhalation, which is mediated by vagal tone variations during breathing[19]. In addition, it

represents increased short-term variability in R.R. intervals and improved heart rate variability. Hence, RSA is used to measure parasympathetic (re)activity [20].

2.1.4 Poincaré Plot (SD1 and SD2)

Poincare´ plot is the geometrical representation of heart rate variability time series in a cartesian plane. Each R.R. interval is plotted against another R.R. interval (next R.R. interval in case lag 1 Poincare´ plot). RR_i represents the current R.R. interval and RR_{i+1} represents the next R.R. interval in milliseconds. The first point on the cartesian plane is obtained by taking RR_i on the x-axis and RR_{i+1} on the y-axis. The next point is plotted by taking RR_{i+1} on the x-axis and RR_{i+2} on the y-axis. Similarly, each R.R. interval is plotted against its next R.R. interval in the time series to obtain the Poincare´ plot as shown below.

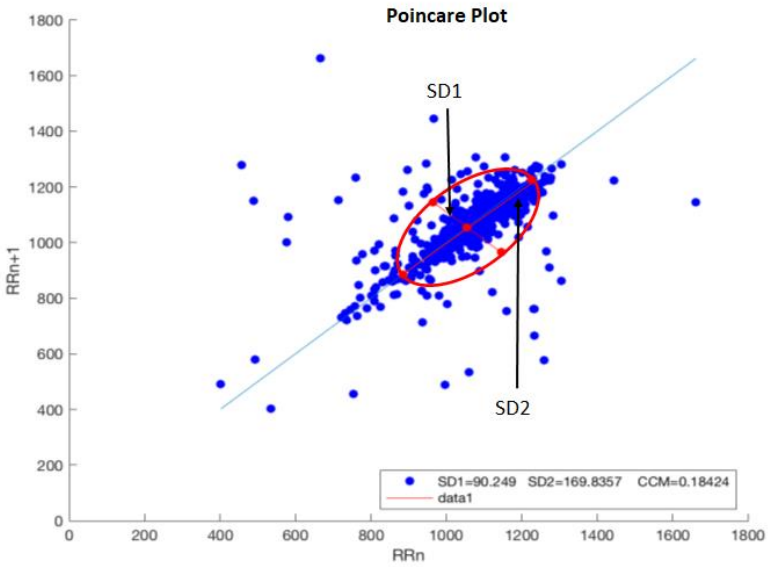

Figure 2-1: Poincare´ Plot

The quantitative analysis of the Poincare´ plot involves the fitted eclipse technique. The first step is to plot the line of identity across the plot. It is done by plotting each R.R. interval against itself, as represented by the blue line in the figure. The next step is to draw a fitted eclipse on

the Poincare´ plot. The eclipse centre is the point obtained by plotting the mean value of R.R. intervals used on both the x-axis and y-axis. The minor and major axes of the eclipse are represented as SD1 and SD2, respectively and are calculated as follows:

$$SD1 = \sqrt{\frac{1}{N-1}\sum_{i=1}^{N-1}\left\{\frac{RR_i - RR_{i+1}}{\sqrt{2}}\right\}^2}$$

And

$$SD2 = \sqrt{\frac{1}{N-1}\sum_{i=1}^{N-1}\left\{\frac{RR_i + RR_{i+1} - 2\overline{RR}}{\sqrt{2}}\right\}^2}$$

RR_i and RR_{i+1} represent the current and next R.R. interval, and $\overline{RR}$ is the mean value of R.R. intervals used [21]. Like RMSSD, SD1 also represents the beat-to-beat variations (short-term variability) mediated by parasympathetic reactivity. It is also correlated to HF band power, which indicates parasympathetic reactivity. SD2, on the other hand, is correlated to the LF band, which represents the long-term variability and is mediated by both sympathetic and parasympathetic reactivities. The ratio SD2/SD1 correlates with LF:HF ratio and measures the autonomic balance. [22][23]

2.1.5 Complex Correlation Measure (CCM)

The fitted eclipse technique provides information about the overall shape of the Poincare plot without any information about its temporal structure. Complex Correlation Measure (CCM) is a method that, in addition to its dependence upon the values of SD1 and SD2, takes into account the temporal structure of the R.R. interval time series, and it is calculated using a moving

window consisting of three consecutive points say *an* (x_1,y_1), $b(x_2,y_2)$ and $c(x_3,y_3)$ of Poincare plot. Each set of three points forms a triangle whose area is calculated. The area of the triangle (*A(i)*) in the window depends upon the temporal variation of the data points, e.g., if all the three points lie in the same line, then the area of the triangle will be equal to zero, which represents a linear alignment of three points. Similarly, positive, and negative values of A(i) represent counterclockwise and clockwise orientation of points *a, b* and *c*. The window is moved continuously with a lag of one point[24]. The area of the triangle formed by these points is calculated as:

$$A(i) = \frac{1}{2}\begin{vmatrix} x_1 & y_1 & 1 \\ x_2 & y_2 & 1 \\ x_3 & y_3 & 1 \end{vmatrix}$$

The complex correlation measure of the Poincare plot consisting of N points consisting of all the overlapping three points windows is calculated as:

$$CCM = \frac{1}{C_n(N-2)} \sum_{i=1}^{N-2} ||A(i)||$$

Where

$$C_n = \pi * SD1 * SD2$$

(Area of the fitted curve of Poincare plot)

After applying the CCM method to the volunteer HRV data during different postures of the active standing test, it was identified that the trend of the CCM is the same as SD1/SD2; it did not give additional information. Therefore, the Poincare plot will only be used in our studies instead of CCM. The figure below shows the CCM and SD1/SD2 ratios calculated for a volunteer during the active standing test.

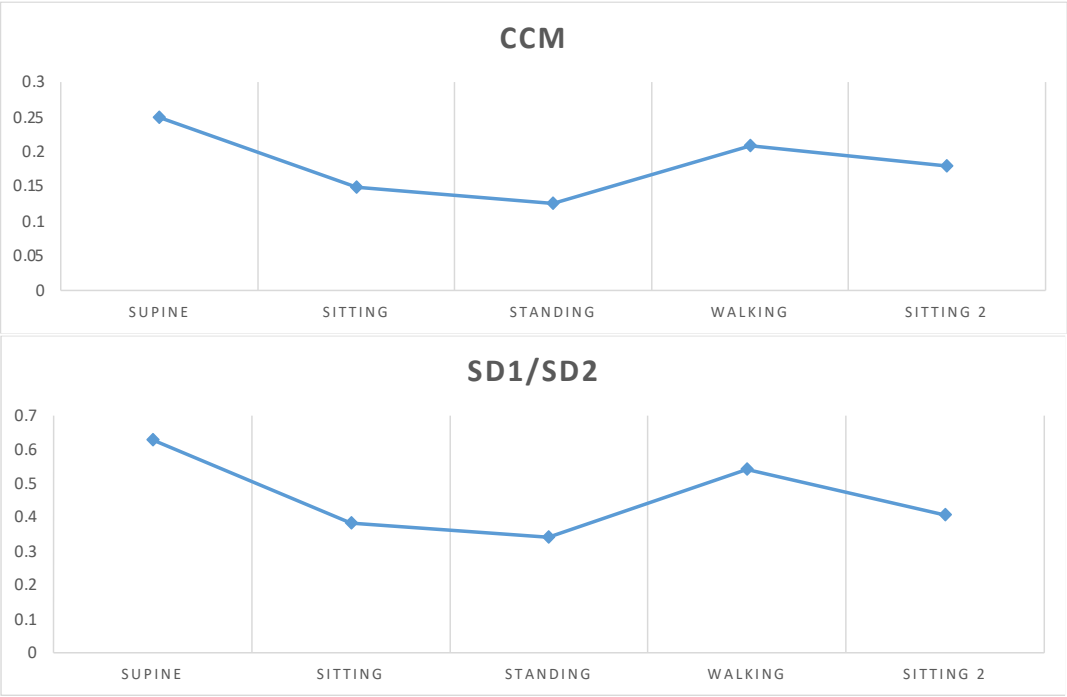

Figure 2-2: CCM and SD1/SD2 trends during active standing test for LW

2.1.6 Detrended Fluctuation Analysis (DFA)

The detrended fluctuation analysis (DFA) is used to measure the fractal correlation properties of non-stationary signals quantitively, and it has been used to assess long-term and short-term correlations in time series. The root mean square (RMS) of the integrated and detrended fluctuations in the HRV signal is calculated in observation windows of different sizes and then plotted against the window size on a log-log plot. The slope (α) of the trend line, which represents the log of fluctuation to the log of window size scaling exponent, is calculated. Two different window sizes, one ranging from 4 to 16 and the other window with a size more than 17, are used to calculate the two scaling exponents α_1 and α_2 respectively. α_1 represents short-term variability while α_2 represents medium to long-term variability[25], [26].

The R.R. interval signal is first integrated as follows:

$$y(k) = \sum_{i=1}^{k} [RR(i) - RRavg]$$

Where RRi is the current R.R. interval and R.R. avg is the mean of the R.R. intervals. Then the integrated time y(k) series is divided into equal-length boxes with length n, and the least square fitted line is drawn. In the next step, the integrated time series y(k) is detrended by subtracting the local trend $y_n(k)$ in each box. The rms of the detrended integrated time series is calculated as:

$$F(n) = \sqrt{\frac{1}{N} \sum_{k=1}^{N} [y(k) - y_n(k)]^2}$$

The above calculation is repeated for varied window lengths to find the relationship between F(n) and the box size n. The scaling exponent $\alpha 1$ is calculated as the slope of the line relating log F(n) to log(n) from the smaller window (4-16), while $\alpha 2$ is calculated as the slope of the trend line with larger window sizes (>16). [26]. I developed the MATLAB code to calculated the values of $\alpha 1$ and $\alpha 2$. The figure below shows the result of DFA calculations for a volunteer in the supine position.

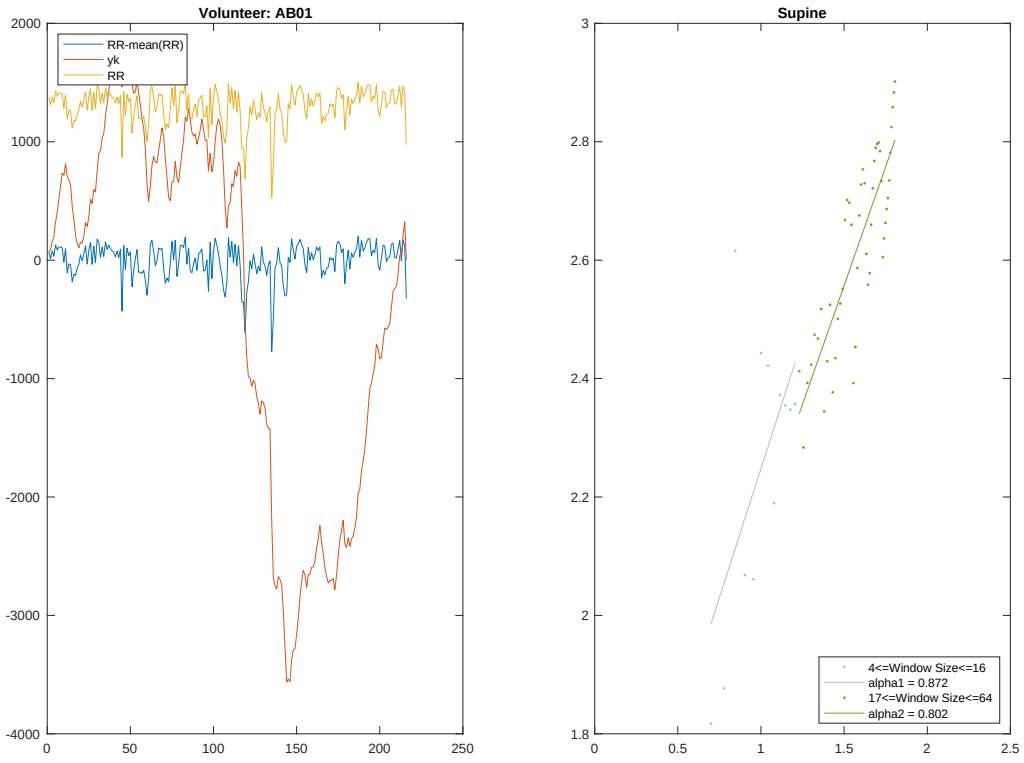

Figure 2-3 Detrended fluctuation analysis results for a volunteer in the Supine position

After applying the DFA to the recorded HRV signal during active standing tests for several patients and volunteers, it was identified that for active standing test, the changes in the values of alpha1 and alpha2 were random and not correlated to the ANS modulation due to postural change, as shown for one of our volunteers (Figure 2.4). Therefore, DFA was not selected in our ANS assessment protocol.

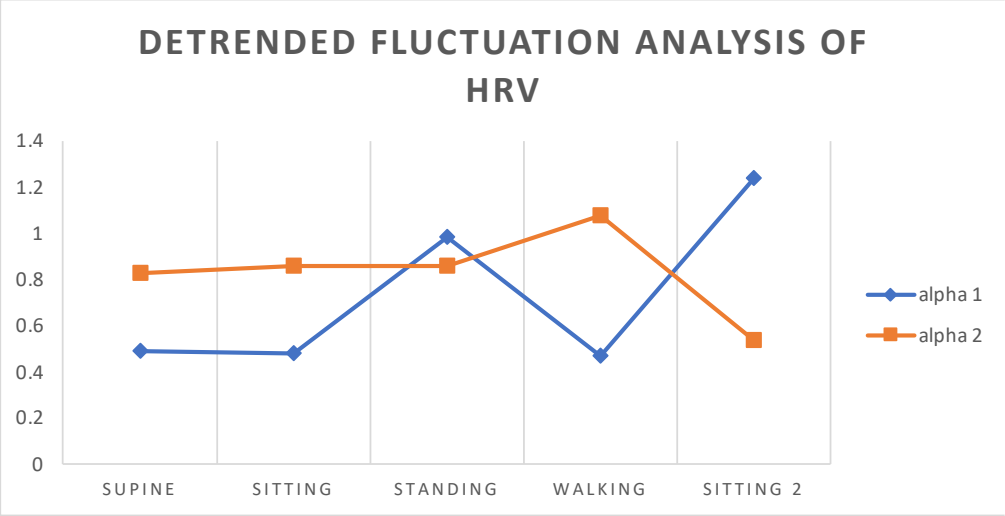

Figure 2-4: alpha 1 and alpha2 values during the active standing test for patient GP

2.1.7 Pre-Ejection Period (PEP)

The pre-ejection period (PEP) is known to represent cardiac sympathetic activity, and it is the duration from the start of electrical stimulation of the heart until the mechanical opening of the aortic valve[27]. PEP can be calculated from ECG and thoracic impedance cardiogram (ICG) signals as the time interval or time delay between the Q point on the ECG signal to the beginning of the rise in pressure in the left ventricle shown in the figure below.

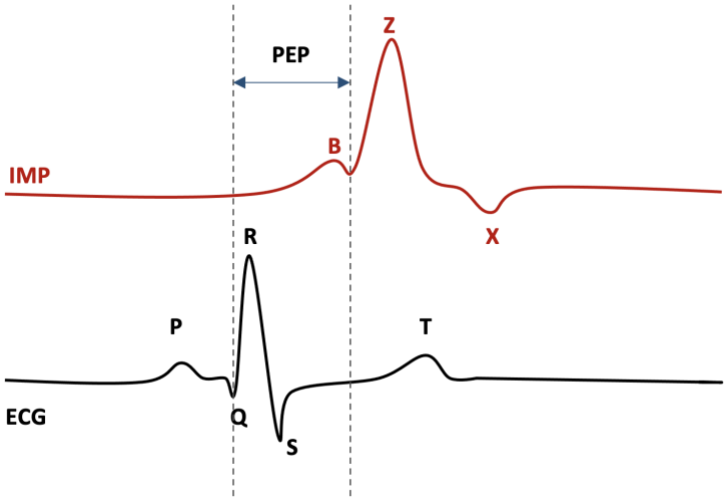

Figure 2-5: Pre-Ejection Period is the time duration from the Q point on ECG signal to the B point on Impedance Cardiography Signal (time on x-axis)

The resistance to the flow of alternating current is called impedance; similarly, the cardiac impedance is measured by injecting an alternating current into the chest, and the signal takes the path of least resistance through the blood. As the heart beats, the volume of blood in the aorta varies, which causes the change in the impedance to the constant current signal. An increase in blood volume causes a decrease in impedance and vice-versa. Four electrodes are used for ICG, 2 electrodes act as a constant current source, and the other two are used to sense the changes in impedance. The recorded impedance is represented by Z_0 with units of ohm (Ω).

The next step is to convert the Z_0 signal into dz/dt. It is simply done by taking the derivative of Z_0 signal. dZ/dt waveform is shown as the signal in white colour in the above figure, and it represents the mechanical function of the heart. The rate of impedance change increases sharply from point B, which indicates the change in impedance due to blood flow into the aorta due to the mechanical opening of the aortic valve [27], [28]. We tested PEP as a measure of SNS (re)activity as discussed later in this chapter.

2.1.8 Baevsky's Stress Index (SI)

Also known as the Stress Index, we refer to it as the Sympathetic index, SI is based on the RR intervals. With an increase in sympathetic activity, the heart rate variability decreases; hence the variation in RR intervals also decreases and vice versa. SI is based on this idea; the first step is to generate the histogram of RR intervals and we constructed it with a bin size of 50 milliseconds; the SI can be represented as the ratio of the height of the histogram to its width because the height represents the monotony of the RR intervals while the width represents the variations in RR intervals as shown in the figure below adapted from [23]

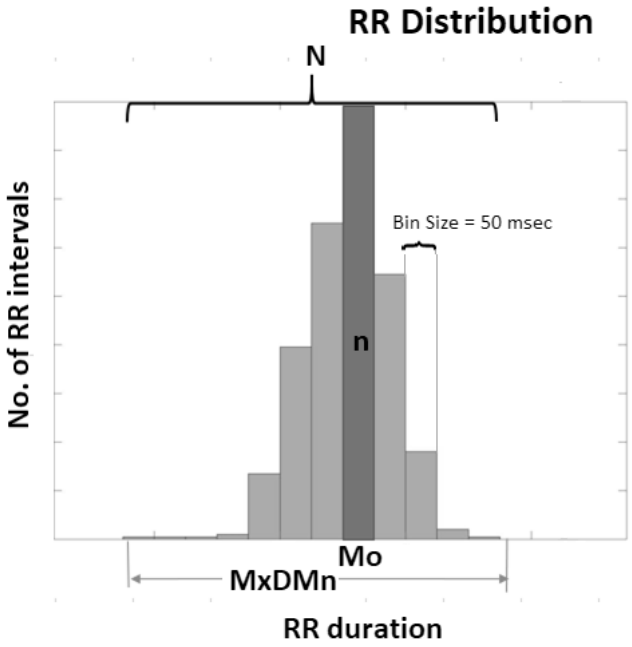

Figure 2-6: RR Histogram (adapted from www.kubious.com)

The SI is calculated as:

$$SI = \frac{AM_o * 100\%}{2M_o * MxDMn}$$

Where, M_o=mode of RR intervals

MxDMn= longest R.R. interval – shortest R.R. interval

$$AM_o = \frac{n}{N}$$

n is the number of RR intervals in the central bin containing Mo, and N is the total number of R.R. intervals. The SI is highly sensitive to the variations in sympathetic nervous system activity. [29][23], [30]. We generated MATLAB code to calculate the SI from RR interval data and used it as an SNS parameter as discussed below.

2.2 Objective

The objective of this exercise is to test RSA, RMSSD and SD1 as a measure of PNS activity and PEP and SI as a measure of SNS activity and their sensitivity to the change in ANS due to posture change, as well as to generate the control values for each of these parameters for each posture of the active standing test, which will be used as a standard for the ANS assessment of patients with motility disorders.

2.2.1 Methods

In healthy volunteers, we used posture changes from supine to sitting, sitting to standing, and then sitting back after walking to modulate the autonomic nervous system. Moreover, the parameters mentioned earlier were tested as a measure of PNS and SNS as well as to calculate the control values of each parameter during each posture to use as a criterion for normal ANS modulation. Thirty-three healthy volunteers were selected for this study, and anyone with heart disease, motility disorders and diabetes were excluded. Volunteers were advised not to have tea or coffee two hours prior to the recording. ECG and Impedance Cardiography (ICG) were recorded during different postures as per the following protocol:

Table 2-1: Active Standing test Protocol

Posture	Duration
Supine	6 min
Sitting	6 min
Standing	6 min
Walking	6 min
Sitting after walking	6 min

Recording during walking was not considered due to many movement artifacts and noise in the signal. The Mindware Technologies ECG and ICG recorder was used to record data, and Mindware HRV analysis Software 3.1.3 was used to remove artifacts and generate RR interval signal. The value of RSA and RMSSD was also calculated during each posture using the same software. Similarly, Mindware technology's IMP analysis software 3.1.3 was used to calculate PEP values. I developed the MATLAB code to calculate the Poincare plot parameters (SD1, SD2) and Sympathetic Index using the RR interval data generated from Mindware HRV analysis software.

The mean and standard deviation (SD) for each parameter was calculated for all the volunteers during each posture. We considered the maximum value of the normal range as the mean + 1 SD, and the minimum value was calculated as mean – 1 SD for each posture. Then, the mean, maximum and minimum values were plotted against their respective posture. This graph was termed as the normal range of each parameter during posture change and is presented for each measure of ANS in the results.

2.2.2 Results

RSA

The PNS was at its highest during supine position, as indicated by RSA, with a mean value of 6.60 ln(ms^2) which decreased to 6 ln(ms^2) during sitting and to 5.42 ln(ms^2) during standing and recovered back to 5.84 ln(ms^2). Figure 2.7 shows the values of the 40 healthy subjects with 1 S.D. above and below the mean value.

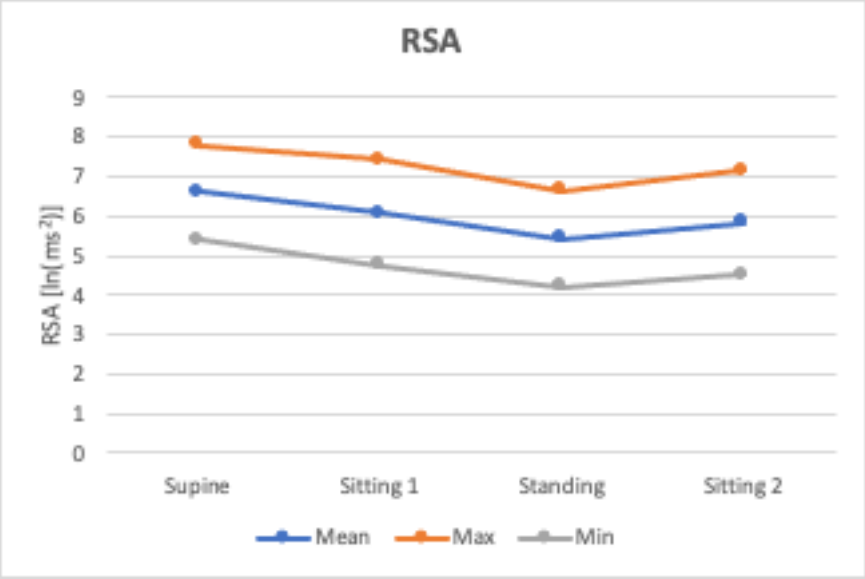

Figure 2-7: Range of RSA values from healthy controls' data

RMSSD

RMSSD was also highest during supine position with a mean value of 59.60*ms* which decreased to 44.69*ms* during sitting and to 25.71*ms* during standing and recovered back to 43.78*ms*. The normal range of RMSSD for healthy volunteers is shown in Figure 2.8.

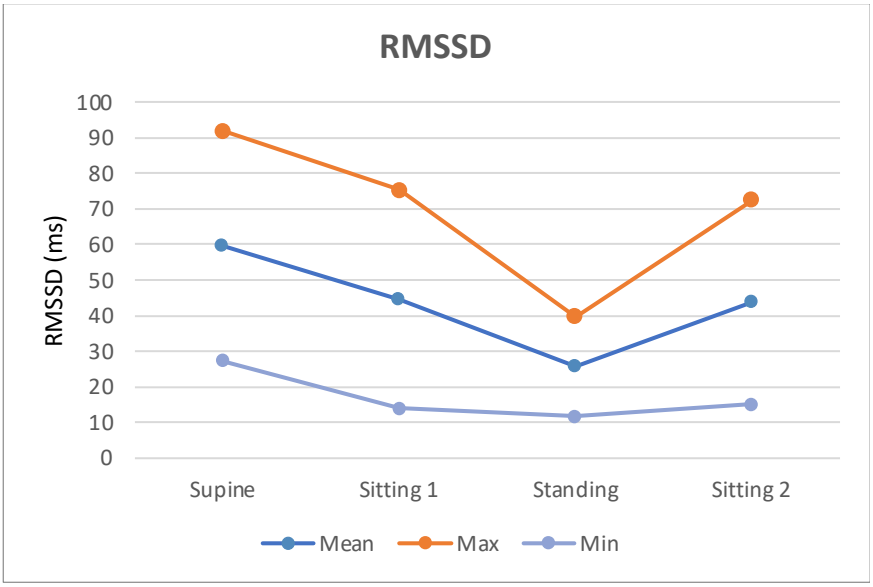

Figure 2-8: Range of RMSSD values from healthy controls' data

SD1

SD1 was also highest during supine position with a mean value of 56.00ms which decreased to 44.93ms during sitting and 28.11ms during standing and recovered back to 44.86ms. The normal range of SD1 for healthy volunteers is shown in the figure below.

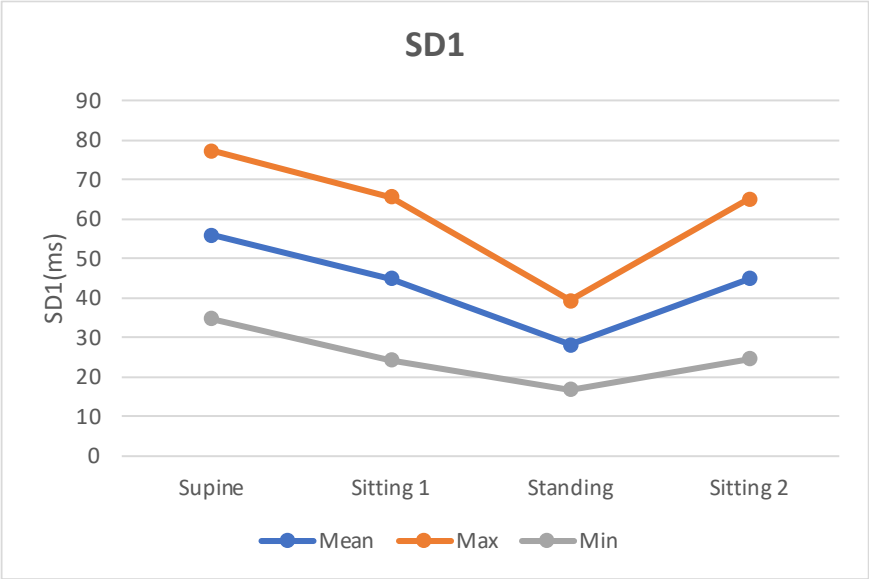

Figure 2-9: Range of SD1 values from healthy controls' data

PEP

The mean value of PEP during supine was 112.47*ms* which increased to 116.22*ms* during sitting and 117.07*ms* during standing. The mean value decreases to 109.05*ms* during sitting after the walk. The normal range of PEP for healthy volunteers is shown in the figure below.

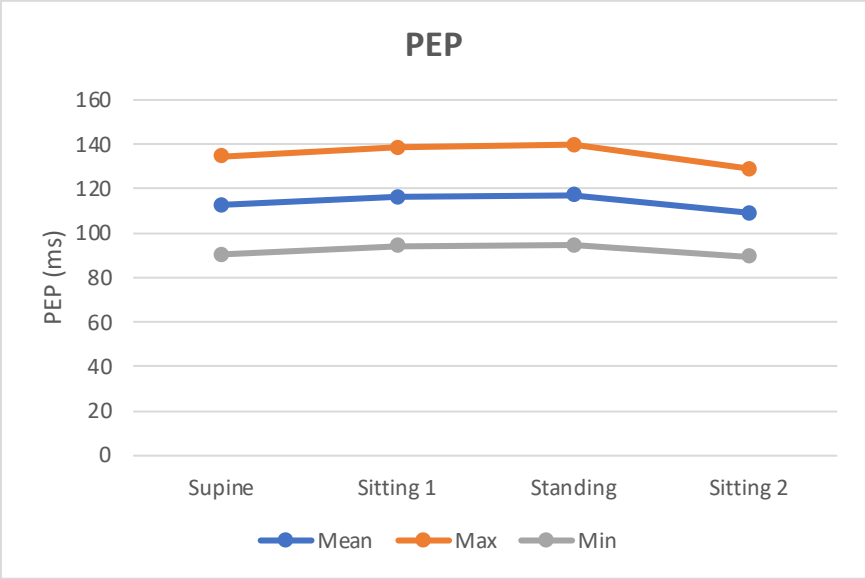

Figure 2-10: Range of PEP values from healthy controls' data

Sympathetic Index (SI)

The mean value SI was 28.84 s^{-2} during supine, which increased to 33.43 s^{-2} and increased to 56.22 s^{-2}. The mean value decreases back to 41.07 s^{-2} during sitting after the walk. The normal range of S.I. for healthy volunteers is shown in the figure below.

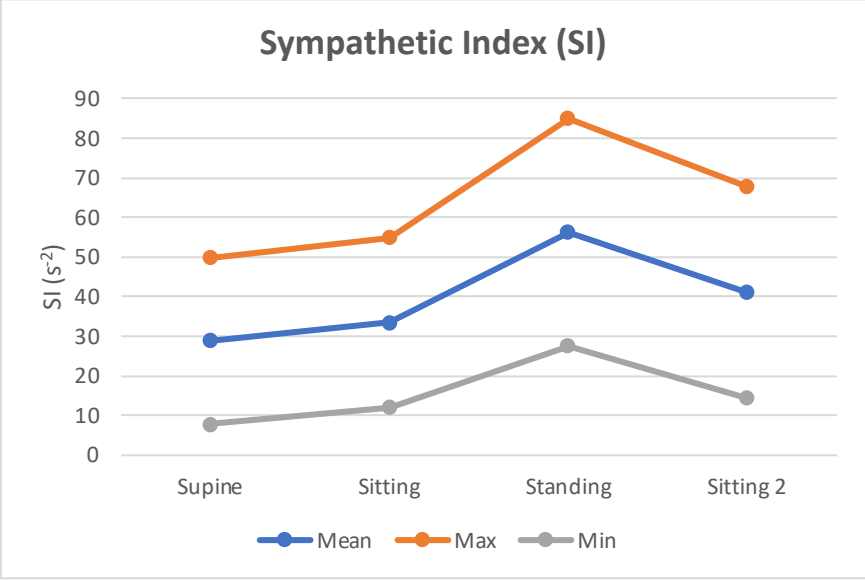

Figure 2-11: Range of S.I. values from healthy controls' data

2.3 Case Study

In this case study, the autonomic assessment for one of the patients with colonic motility disorders is presented. The patent underwent the active standing test, and their HRV parameters were calculated and compared to the control values as discussed above. Data presented as patient's value (healthy controls' lower limit - healthy controls' upper limit)

Heart Rate

Supine 63.22(55.14-76.18), Sitting 73.44 (61.10-82.27), Standing 89.41 (69.90-93.34), Sitting after walking 74.81 (61.08-83.32)

Parasympathetic activity

RSA:

Supine **4.91** (5.40-7.80), Sitting **4.22** (4.75-7.40), Standing **3.14** (4.21-6.63), Sitting after walking 4.74 (4.52-7.16)

RMSSD:

Supine **24.85** (27.22-91.86), Sitting **13.45** (14.06-75.32) Standing **4.08** (11.73-39.70), Sitting after walking 22.92 (15.00-72.55)

SD1:

Supine 39.81 (34.72-77.29), Sitting **16.62** (24.30-65.56) Standing **10.83** (16.87-39.37), Sitting after walking 38.69 (24.59-65.14)

Sympathetic activity

SI:

Supine 28.45(7.87-49.81), Sitting **119.06** (12.0-54.86), Standing **344.82** (27.52-84.92), Sitting after walking 45.30 (14.34-67.80)

PEP:

Supine 98.85 (90.37-134.59), Sitting 95.14(94.05-138.41), Standing 104.67 (94.63-139.52), Sitting after walking 105.60 (89.26-128.83)

Figure 2-12 below shows the autonomic assessment for the patient in comparison with the standard autonomic criteria.

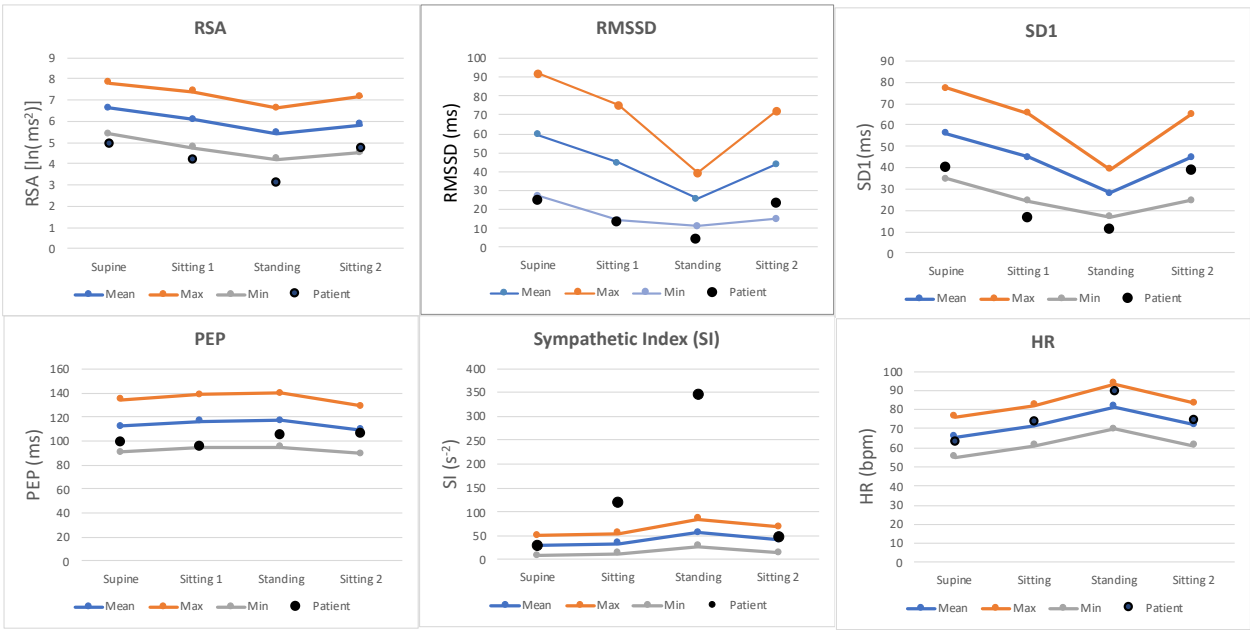

Figure 2-12: ANS assessment of a patient with motility disorder

These results show that the patient has low parasympathetic tone and reactivity as represented by the low values of RSA, RMSSD and SD1 and very high sympathetic reactivity to sitting and standing as represented by the very high values of SI during sitting and standing. The heart rate was normal throughout the test. PEP did not predict the high sympathetic reactivity to sitting and standing. After using this procedure of autonomic testing in over 40 patients, we found that PEP is less sensitive to the known changes in SNS activity compared to SI (discussed below).

2.4 Discussion

All the three measures of the parasympathetic nervous system used (RSA, RMSSD and SD1) indicated a decrease in PNS activity from supine to sitting and a further decrease during standing. However, the decrease from sitting to standing was more than that from supine to sitting. The PNS increases from standing to sitting. RSA is considered the measure of vagal tone; it is primarily affected by voluntary and natural changes in respiration. Therefore, the value of RSA decreases during rapid shallow breathing while increases during slow deep breathing under steady-state conditions. Grossman et al. reported that an increase of only 3-4 breaths/min might reduce the RSA magnitude significantly [31]. The Poincare plot is the best visual representation of HRV, and there was an evident change in shape and size of the Poincare plot during each posture upon visual inspection. The Poincare plot's SD1 showed a similar trend and degree of fluctuations to that of RMSSD, and both are also related mathematically, therefore, it can be used as another measure of PNS. However, the Poincare plot did not provide any quantitative information about SNS as SD2, like LF band power is known to be influenced by both the SNS and PNS.

With an increase in sympathetic activity, the heart rate variability decreases; hence the variation in RR intervals tends to decrease and vice versa[29]. Although the PEP and the Baevsky index are parameters of cardiac activity, general changes in autonomic activity due to a variety of stimuli (stress, pain) are reflected in HRV; hence these stimuli do reach the specific ANS branches that innervate the heart, but not all HRV parameters reflect non-cardiac ANS activity equally. PEP is the measure of the time difference between the electrical and

mechanical activity of the heart. The mechanical activity is not directly measured, but it is measured as the change in impedance caused by the change in blood flow due to the opening and closing of the ventricular opening of the heart. The opening of the valve may not cause the abrupt change in impedance because the blood flows linearly and changes the impedance as it flows out of the valve [28], [28]. It may cause a delay after valve opening. This delay may not be captured by using impedance measurement. Therefore, the change in time difference between the mechanical opening of the ventricular valve and the heart's electrical activity measured by this method can be less than the actual time difference. That may be why our results showed much less PEP change during posture changes. On the other hand, Sympathetic Index (SI) is measured only from the RR interval data and is very sensitive to SNS due to posture change. PEP was initially used for ANS assessment in this thesis along with SI, however, we stopped using it later on.

The autonomic assessment criteria developed in this chapter have been successively applied to the patients with motility disorder for their autonomic assessment. To further improve this ANS assessment protocol it is compared to the tilt table test protocol, which is discussed in the next chapter.

Chapter 3

Evaluation Of Our Autonomic Assessment Methodology In Comparison With The Established Tilt Table Test Procedure

3.1 Abstract

The objective of this study is to understand autonomic dysfunction in patients with cardiac and GI symptoms and to compare the autonomic testing methodology (developed in chapter 2) with the autonomic assessment test conducted for cardiac patients at the autonomic testing laboratory in Hamilton General Hospital by Dr. Guzman. The tests at the autonomic testing lab (ATL) include the tilt table test, deep breathing test, beta-adrenergic hypersensitivity test, catecholamine level determination during orthostatic stress and Intrinsic heart rate test. We used the RR interval data recorded during these tests by ATL to calculate the HRV parameters for each of these tests and their results were compared to that of our active standing test.

7 patients who had both cardiac and GI dysfunctions were selected for this study. 5 out of 7 patients underwent both the autonomic testing at the ATL as well as the active standing test while two patients did not do the active standing test. 3 out of 7 patients had lumbar and sacral neuromodulation by one session of LLLT (discussed in chapters 7 and 8) as well as transcutaneous electric nerve stimulations (TENS) while one patient had neuromodulation by TENS only. The autonomic modulations were analysed via HRV, calculated from RR intervals of patients, recorded during the TTT, Deep breathing test, beta-adrenergic hypersensitivity test, catecholamine level determination during orthostatic stress and Intrinsic heart rate test and

compared with the autonomic activity during the active standing test. RMSSD and RSA were used for parasympathetic tone and reactivity and SI for sympathetic tone and reactivity.

The results indicated that, Postural Orthostatic Tachycardia Syndrome, POTS (n=5) is associated with very high sympathetic reactivity during tilt and during the active standing test. One patient had high sympathetic tone, no POTS on test but had POTS in the past. Hence HRV is likely sensitive to the sympathetic condition of the patient. Syncope is associated with the inability to maintain sympathetic tone during standing. We saw this once during all our active standing tests, in this patient. It is possible that plasma noradrenaline levels are in sync with baseline SI levels (n=1). Five out of 7 patients had higher sympathetic reactivity compared to our controls in both TTT and active standing test, associated with constipation. Although these patients did not have overt cardiac autonomic dysfunction, they did have severe gastrointestinal symptoms which, we believe and show, are due to abnormal autonomic reflexes, in particular over-excitation of the sympathetic nervous system. This is consistent with the prevalence of POTS which is due to an exaggerated sympathetic response to standing.

One patient with POTS had high sympathetic reactivity during TTT but not during active standing test. (If patient has had POTS episodes, high sympathetic tone can be but does not have to be persistent). One patient with syncope had lower sympathetic activity during standing, did not have constipation, only upper GI issues.

The parameters SI/RSA and SI/RMSSD give a quantitative assessment of a shift in the balance between sympathetic and parasympathetic. There is good agreement between the TTT, and the active standing test related to HRV parameter changes. However, based on the results of this study, the active standing test procedure was further optimized by including the deep breathing

and removing the sitting phase between supine and standing, the new protocol for active standing test is currently being used at Dr. Chen's clinic. Sacral low level laser stimulation reduced sympathetic activity when high and increased sympathetic activity when low; HRV can be used to evaluate success of treatment.

3.2 Introduction:

The magnitude of gravity of the earth and its direction related to the body axis highly affect the systolic blood pressure and blood flow towards the head. Due to the shifting of body fluids towards the lower limbs during the postural change from supine or sitting and to standing, the neuronal regulatory mechanism triggers to maintain the blood flow to the upper limbs. This neuronal regulator mechanism includes the baroreceptor reflex and other aspects of the autonomic nervous system. The baroreceptor reflex acts as a feedback regulatory mechanism of the autonomic nervous system with aortic and sinus nerves as its afferent nerves. When the body posture changes, the baroreceptor reflex adjusts the heart rate and vascular resistance via sympathetic and vagal nerve activities to maintain the blood pressure. During the postural change the vestibulo-sympathetic reflex is elicited before change in blood pressure, hence it works in a predictive manner as a feedforward regulation. The postural change stimulates the otolith organs in humans which activate the sympathetic nervous system[32]. This otolith activation related sudden increase in sympathetic neural activity leads to vasoconstriction and an increase in total peripheral resistance. This vestibular-mediated increase in sympathetic activity is called vestibulo-sympathetic reflex and it helps maintain blood pressure[33]. Orthostatic hypotension occurs due to the shifting of body fluids to the lower body, if the

autonomic nervous system does not work efficiently after postural transition. To minimise the blood pooling in the lower limbs upon active standing, a series of responses activate in the body including the "skeletal muscle pump", increase in abdominal pressure, decrease in vagal tone and increase in cardiac and vascular activity [34].

3.3 General methodologies

3.3.1 Tilt Table Test

The tilt table test was performed at Dr. Guzman's Autonomic Laboratory at the Hamilton General Hospital in the fasting and conscious state. The patients were placed in supine position on the tilt table. The task force monitor was connected to the patients for non-invasive continuous hemodynamic monitoring. The mean values of Heart rate, Blood pressure (systolic/diastolic), Stroke Index, Cardiac Index and Total Peripheral Resistance Index were recorded. The beat-to-beat intervals (RR intervals) were extracted from the ECG signal. After recording for 10 minutes in supine position, the patient was tilted up to upright position at 70 degrees of inclination and the above-mentioned parameters were recorded for 10-30 minutes (based on the appearance of symptoms like dizziness, palpitation, nausea, visual disturbance, and blood pressure drop), the patients were then moved back to supine position and the parameters were recorded again.

3.3.2 Deep breathing Test

The deep breathing test was performed using controlled respiration with the respiration frequency of 6 bpm (5 sec of inhalation and 5 seconds of exhalation repeated 6 times without pause). The ratio of the means of the longest RR interval (the slowest heartbeat) during each of

the six expirations and the mean of the shortest RR intervals (the fastest heartbeat) during each of the six inspirations is calculated (E/I ratio).

I calculated the HRV parameters (SI, RSA, RMSSD, SI/RSA) from the RR intervals stored on the TTT apparatus during the deep breathing test. The entire period of deep breathing was assessed without separating the inhalation and exhalation. The deep breathing test evaluates respiratory sinus arrhythmia (increased HR during inhalation and decreased HR during exhalation) that involves several autonomic reflexes dominated by vagal afferent and efferent nerve activities between the NTS and the heart. Hence it primarily assesses parasympathetic (vagal) integrity. The calculated HRV results are compared to the E/I ratio reported by ATL.

3.3.3 Beta Adrenergic Hypersensitivity Test:

For the beta-adrenergic hypersensitivity test performed by ATL, the beta-adrenergic agonist isoproterenol was used to test the functional state of the beta-adrenergic receptor. The stepwise incremental (0.25 mcg) doses of isoproterenol were administered until HR increased by 30-35 bpm. The increased sensitivity to the isoproterenol was associated with the Postural Orthostatic Tachycardia Syndrome (POTS). The mean heart rate was calculated after each dose. From the RR interval data during the test, I calculated the SI, RSA, RMSSD and SI/RSA for each step to study the effect of isoproterenol doses on autonomic nervous system activity.

3.3.4 Catecholamine Level Determination during Orthostatic Stress:

Performed by ATL, the blood samples are taken during supine, 5 minutes after standing as well as 10 minutes after standing to test the change in Norepinephrine levels in the blood. The change in the norepinephrine levels in the blood are compared to the change SI values from supine to standing during active standing test.

Since both plasma norepinephrine and the sympathetic index (SI) represent neural release of norepinephrine, the plasma levels should correlate with SI, and it does so in the one patient where this could be analyzed.

3.3.5 Intrinsic Heart Rate Test:

To test the normal Sinus Node function, the intrinsic heart rate test was performed by complete autonomic blockade with atropine 2.6 mg IV push and propranolol (beta blocker) 13.2 mg IV. And the HR of the patient was compared to that of the predicted IHR by ATL. Failure to increase the HR suggests reduced parasympathetic function. A decreased IHR can contribute to the decreased cardiac output and may cause syncope. We calculated the HRV parameters (SI, RSA, RMSSD and SI/RSA) from the RR interval data provided by ATL to assess the changes in HRV during autonomic blockage.

3.3.6 Active standing test

The baseline autonomic nervous system activity as well as the ANS modulation due to postural change were also studied in the same patients separately in our laboratory. The ECG was recorded in the supine position for six minutes followed by sitting, standing, walking and back to sitting for six minutes each. The ECG signal is used to generate the heart rate variability signal (RR interval signal) during each posture which was then used to calculate the SI, RSA, RMSSD and SI/RSA as mentioned above.

3.3.7 Data Analysis

HRV analysis based on ECG obtained from the Guzman lab (ATL). The RR intervals signal recorded during each step of the Table Tilt Test at ATL was analysed for HRV using MATLAB. The Sympathetic Index (SI) was calculated as the parameter of the sympathetic nervous system

(SNS) activity, Respiratory Sinus arrythmia (RSA), and Root Mean Square of Successive Differences (RMSSD) were calculated to represent the Parasympathetic nervous system activity (PNS), while the ratio SI/RSA was used to represent the "Autonomic Balance"[30].

3.4 Results

3.4.1 Summary of results

All the results for every patient including the GI dysfunction diagnosis are summarized in table 3.1 below while the detailed analyses for each patient and cumulative analysis for each of the tests are given in following sections of this chapter.

Table 3-1: Summary of results for all patients

	Patient 1	**Patient 2**	**Patient 3**	**Patient 4**	**Patient 5**	**Patient 6**	**Patient 7**
CARDIOLOGY – GUZMAN LAB							
POTS (TTT)	✓	No-yes*	✓	✓	no	no	✓
Presyncope (TTT)	no	No-yes*	No-yes*	✓	no	no	no
Syncope (TTT)	no	No-yes*	No-yes*	no	No-yes*	✓	✓
Neurogenic orthostatic hypotension	no	no	no	no	no	no	no
Cardiovagal Reflex (Deep Breathing)	Normal	--	--	Normal	--	Normal	--
Orthostatic Plasma Catecholamine Level	--	--	--	--	Normal	Results not available	--
Beta Adrenergic Hypersensitivity Test	✓	--	--	Normal	Normal	--	--
Intrinsic Heart Rate Test	--	--	--	-(slightly)	--	--	--
Autonomic dysfunction (TTT) ATL	no	no	no	yes	no	no	yes
Autonomic dysfunction (GI clinic)	no	yes	yes	--	--	yes	yes
GASTROENTEROLOGY - CHEN CLINIC							

Active standing test PNS baseline (RSA)	Normal	--	Normal	--	--	Normal	-- (very low)
Active standing test PNS reactivity (RSA)	Normal	-^	- ^	--	--	↑	↑(but low)
Active standing test SNS baseline (SI)	Normal	↑↑	Normal	--	--	--	↑↑
Active standing test SNS reactivity (SI)	Normal	↑^	↑^	--	--	-	↑^
Autonomic dysfunction (Active standing) *PNS = parasympathetic tone and reactivity to standing* *SNS = sympathetic tone and reactivity to standing*	no	✓ (p**#) (sπ) PNS low SNS very high**	✓(s**π) PNS SNS very high react**	--	--	✓ **(₹) PNS abnormal increase to standing SNS low tone and abnormal opposite reactivity to standing**	✓(p**π)(sπ) PNS SNS**
LLLT PNS response (RSA)	--	--	↑	--	--	↑	- (slight)
LLLT SNS response (SI)	--	--	-	--	--	↑	↑
TENS PNS response (RSA)	↑	--	↑	--	--	-	-(slight)
TENS SNS response (SI)	↑	--	-	--	--	-	↑
GI dysfunction Diagnoses/History							
Acute Diarrhea		✓	✓	✓	✓	✓	
Fecal incontinence							
Acute constipation	✓	✓	✓	✓*			
Chronic constipation							
IBS		✓					
Upper GI dysmotility	✓		✓			✓	
Lower GI dysmotility			✓			✓	
Ehler's Danlos syndrome	✓		✓				
Abdominal bloating and/or Pain		✓	✓			✓	
Impaired gastric accommodation			✓				
Irregular Bowel movements			✓				
Nausea and Vomiting		✓	✓		✓		

Difficulty of Oral food intake					✓	✓	
Acute/Chronic intestinal pseudo-obstruction			✓?			✓	
Gastroparesis			✓		✓		

✓ : Positive diagnosis
-- : not tested
No : test is negative
No-yes*: Not during test but had it in the past
↑↑ : High outside 1 SD of normal range
-- : Low. Outside 1 SD of normal range
↑ : Increased
- : Decreased
↑^ : Increased abnormally high
-^ : Decreased abnormally low
✓? : Future risk
Autonomic Dysfunction via Active Standing Test:
The HRV parameters (SI, RSA, RMSSD, HR) for patient are compared with those of healthy volunteers.
Value within Mean±SD = Normal
: Value within Mean±SD and Mean±2SD = High tone or reactivity
π : Value greater than or less than Mean±2SD= Autonomic Dysfunction
₹ : Value within normal range but the reactivity to standing is opposite to that of normal reactivity = ANS dysfunction
p : PNS tone or reactivity
s : SNS tone or reactivity

3.4.2 Individual Analysis of Each Patient:

3.4.2.1 Patient 1:

Tilt Table Test

The patient was tilted to 70 degrees during the tilt table test and after 30 minutes of orthostatic stress, the patient was tilted down to supine position. The heart rate increased from 81 bpm in supine to 130 bpm during tilt which is an indication of Postural Orthostatic tachycardia Syndrome (POTS).

Table 3-2: Cardiac and HRV parameters during TTT for Patient 1

	Supine	**Tilt**	
Heart Rate (bpm)	81	130	POTS
Blood Pressure (mmHg)	102/73	115/79	No OH
Stroke index (mL/m2)	41.1	25.2	
Cardiac Index L/min/m2)	3.3	3.3	
Total peripheral index	2009	2247	

HRV parameters	**Supine**	**Tilt**	
Sympathetic Index	34.76	407.79	
RSA	6.86	4.04	
RMSSD	57.03	12.3	
HR	81.53	130.46	POTS
SI/RSA	5.07	100.94 (20x)	Dramatic increase in sympathetic activity
SI/RMSSD	0.61	33.15 (54x)	

There was no reduction of blood pressure during the tilt which indicated negative Orthostatic Hypotension. Over 10 times increase in SI and decreased RSA and RMSSD values indicate increased sympathetic activity and withdrawal of parasympathetic activity during the tilt (Table

3.2).

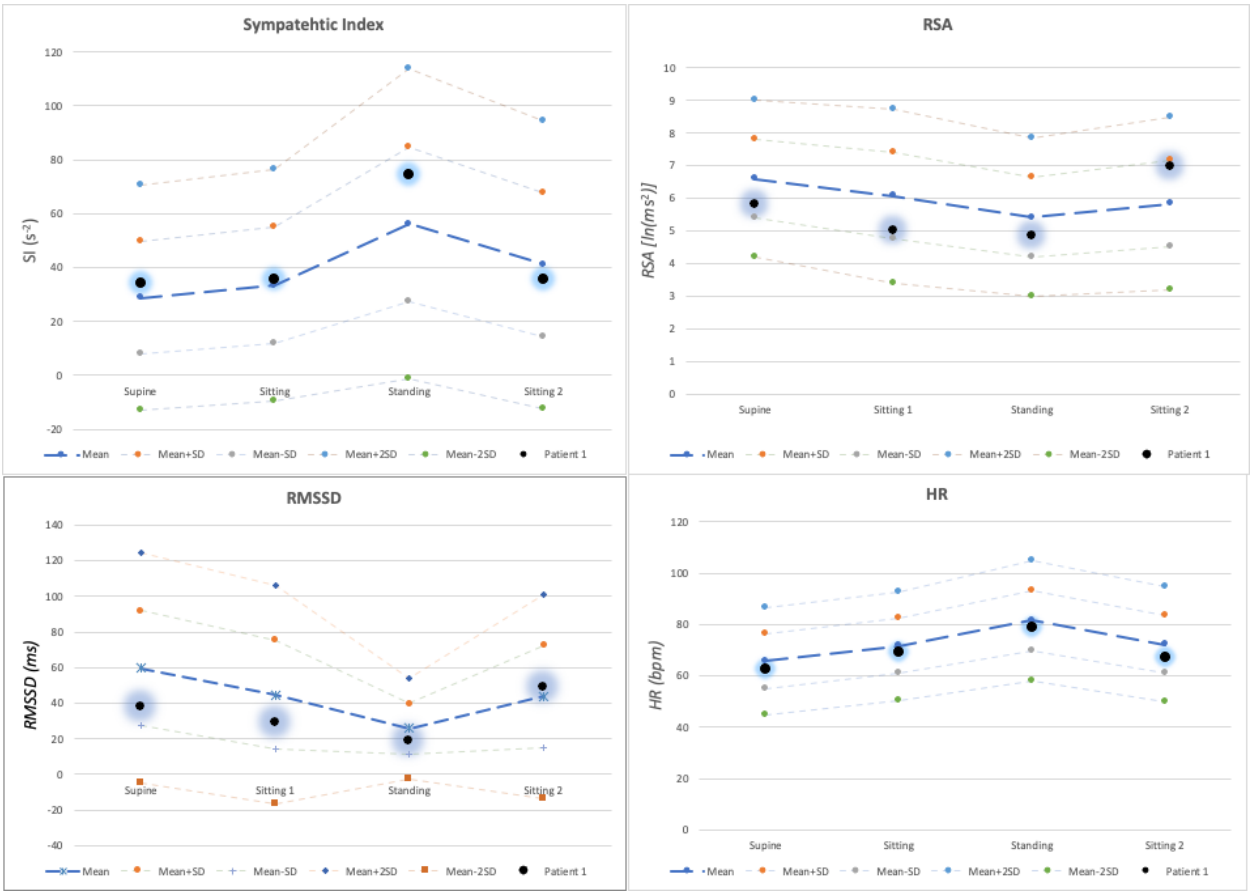

Figure 3-1: ANS assessment for Patient 1 via Active Standing test

The Active standing test values of HRV indicate normal baseline autonomic activity. The modulation of ANS activity was also normal with SI value within the normal range (Figure 3.1).

Deep Breathing Test

According to ATL report, the expiration/inspiration ratio of the heart rate was 1.4 which was considered normal.

Catecholamine Level Determination During Orthostatic Stress

The norepinephrine levels during lying down, 5 minutes after standing and 10 minutes after standing were 2.3, 4.4 and 7.8 respectively which were considered elevated catecholamine

levels by Dr. Guzman's ATL. The corresponding values of SI during active standing test were calculated to be 34.06 s^{-2} during supine, 76.47 s^{-2} during standing (1-3 min) and 112.59 s^{-2} for standing (4-6 min). Upon breaking down the 6 minutes of standing into first 3 minutes and last 3 minutes, and calculating SI in each case, it was observed that during the first 3 minutes of standing, the SI was 76.47 while during the last three minutes was 112.59. The normal range of SI during standing is 27.52-84.92 s^{-2}. The breakdown of SI indicated that the SI was within the normal range during first 3 minutes while it increased above the normal range during the last three minutes of standing. This indicates that the increase in SI was continuous during standing which is consistent with the Catecholamine levels shown in the table above. Both indicate an increase in sympathetic activity during prolonged standing.

Beta Adrenergic Hypersensitivity Test

The patient reached target heart rate with a dose of 0.5 mcg of isoproterenol. This is considered increased beta-adrenergic hypersensitivity (as reported by ATL).

ANS Diagnoses by ATL:

1. Positive tilt test for postural orthostatic tachycardia syndrome
2. Negative tilt test for autonomic dysfunction/Orthostatic hypotension
3. Elevated orthostatic catecholamine levels
4. Beta adrenergic hypersensitivity

ANS modulation due to Lumbar and Sacral Neuromodulation

The patient received lumbar and sacral neuromodulation by TENS. LLLT was not applied. The effect of one time TENS on HRV parameters are shown in the table below:

Table 3-3: ANS modulation by Lumbar and Sacral Neuromodulation for Patient 1

	SI	RSA	RMSSD	HR	SI/RSA
Baseline	19.82	6.21	54.77	61.9	3.19
TENS	25.76	7.19	55.49	66.28	3.58
Recovery	25.46	7.05	58.67	65.3	3.61

The active standing test indicated low parasympathetic tone (but still within the normal range) which might be contributing to POTS. The TENS increased the parasympathetic tone by 15.78% (RSA) as well as sympathetic tone by 29.97% (SI). Increase in SI was more dominant as indicated by increase in HR and SI/RSA ratio.

Summary of results for Patient 1

1. POTS and pos beta adrenergic sensitivity test
2. TTT_HRV; baseline normal, high SI reactivity; SI/RSA = 5 ->100; DB is normal
3. Ineffective oesophageal peristalsis / difficulty swallowing / bowel urgency, occasional incontinence.
4. According to Active standing test the HRV is normal
5. Norepinephrine levels in blood correlate with high SI reactivity to standing during active standing test

3.4.2.2 Patient 2

Table 3.4 summarizes the HRV parameters calculated from the RR interval data recorded during the tilt table test.

Table 3-4: Cardiac and HRV parameters during TTT for Patient 2

	Supine	**Tilt**	**Isuprel 1 mcg/min and NS 150 ml/HR**
Heart Rate (bpm)	84	103	126
Blood Pressure (mmHg)	112/75	125/85	133/87
Stroke index (mL/m2)	27.19	19.78	18.95
Cardiac Index L/min/m2)	2.28	2.02	2.38
Total peripheral index	3053	3900	3430
	Supine	**Tilt**	**Isuprel 1 mcg/min and NS 150 ml/HR**
Sympathetic Index	142.65	198.39	55.55
RSA	6.21	5.74	6.76
RMSSD	24.48	10.81	33.66
HR	84.03	102.69	125.57
SI/RSA	22.97	34.56 (1.5x)	8.22
SI/RMSSD	5.83	18.35 (3x)	

The HR increased from 84 bpm to 103 bpm from supine to tilt which is considered normal with no diagnosis of POTS. The blood pressure also increased during tilt. The patient tolerated 15 minutes of tilt with no complaints or symptoms, after which Isuprel was started 1 mcg per minute.

Isuprel or isoproterenol is a beta-adrenergic agonist, that mimics sympathetic neural activation although SI did not increase, HR increased. Isoproterenol is given to increase the chance of syncope.

Heart rate increased to approximately 140 beats per minute for which the dose of the Isuprel infusion was adjusted to 0.5 mcg per minute. The patient tolerated another 15 minutes with no further symptoms and no syncope or presyncope. The patient was returned to

supine position. After the Isuprel infusion there was an increase in HR to 126 bpm however, the SI decreased and RSA & RMSSD increased.

The patient has history of POTS as well as syncope, which was not diagnosed during the tilt table test, however, the active standing test indicated that the patient had very high sympathetic tone which increased almost ten times during standing. The RSA and RMSSD indicated low PNS tone.

The tilt table test came out negative for POTS and presyncope or syncope, however, the patient complains about continuous attacks of presyncope and/or syncope as well as orthostatic intolerance as well as palpation on daily basis. The 10 times increase in SI is an indicator of POTS.

Active standing test:

The active standing test results indicate that the patient has autonomic dysfunction because the SNS tone and reactivity are both very high (more that 2 Standard deviations). Similarly, the PNS tone is low as shown in the figure 3.2 below.

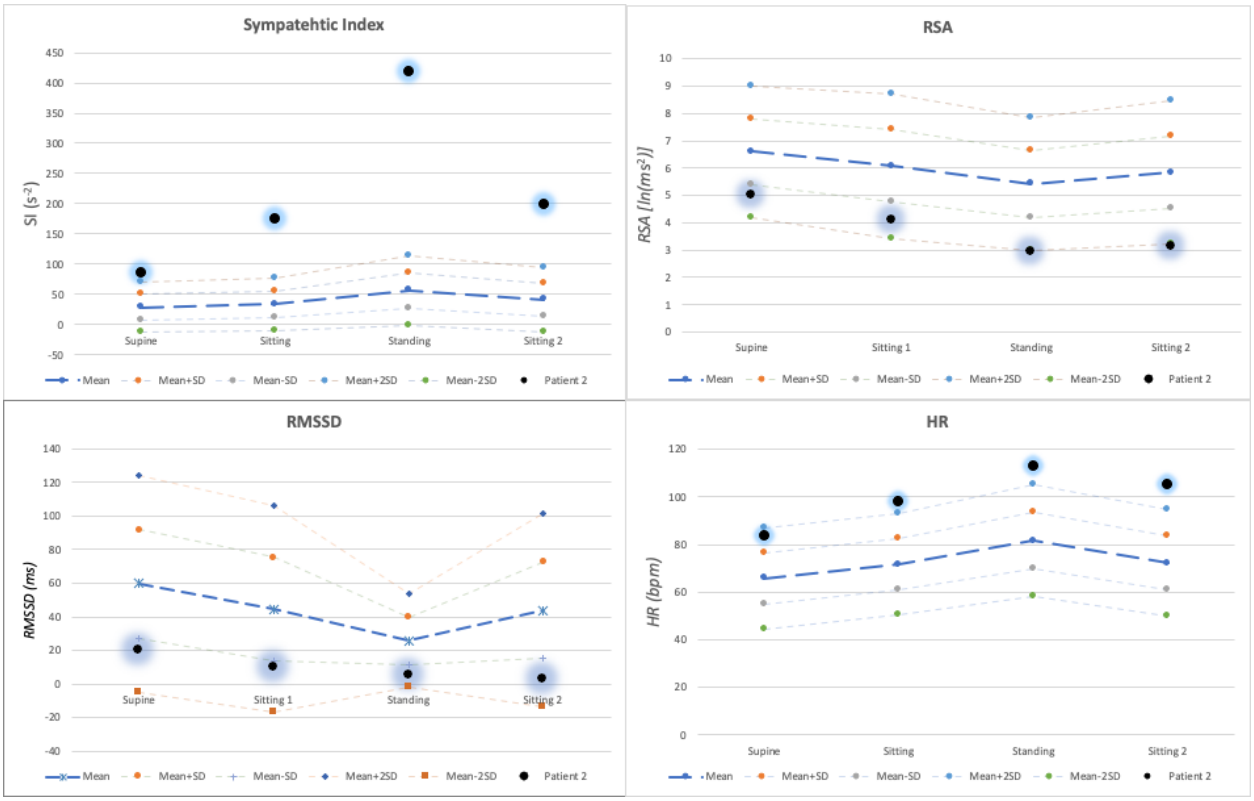

Figure 3-2:ANS assessment for Patient 2 via Active Standing test

Summary of results for Patient 2

1. Did not have OH, no POTS no syncope during TTT, all was normal. Did have POTS and syncope in the past.
2. HRV from ATL data: High supine SI; normal reaction to TTT. SI/RSA 23 -> 35.
3. HRV from active standing test showed very high sympathetic tone and reactivity, and low RSA; high reactive HR
4. IBS, nausea, vomiting, pain, bloating

3.4.2.3 Patient 3

Table 3.5 summarizes the HRV parameters calculated from the RR interval data recorded during the tilt table test for patient 3.

Table 3-5: Cardiac and HRV parameters during TTT for Patient 3

	Supine	**Tilt**	**End Head Tilt up**	
Heart Rate (bpm)	98	141	88	POTS
Blood Pressure (mmHg)	80/53	116/81	117/67	
Stroke index (mL/m2)	45.71	33.20	54.72	
Cardiac Index L/min/m2)	4.45	4.66	4.65	
Total peripheral index	1110	1633	1490	

	Supine	**Tilt**	**End Head Tilt up**	
Sympathetic Index	178.39	295.24	35.26	High symp tone
RSA	4.2	3.99	6.11	Low para tone
RMSSD	11.17	12.92	41.21	Low para tone
HR	98.14	141	87.76	POTS
SI/RSA	42.47	73.99	5.77	
SI/RMSSD	15.9	22.7		

Patient's HR increased from 98 bpm to 141 bpm from Supine to tilt which is more than 30 bpm, which is an indication of POTS. HRV variables indicate a very high sympathetic tone with a supine SI value of 178.39 which increased to 295.24 during tilt. RSA and RMSSD indicated low PNS baseline tone. However, after the tilt test there was a remarkable recovery in SNS and PNS parameters. The active standing test below indicates very high SI value while standing which might be correlated to the diagnosis of POTS.

The blood pressure changes are normal and there was no evidence of Syncope.

Active standing test

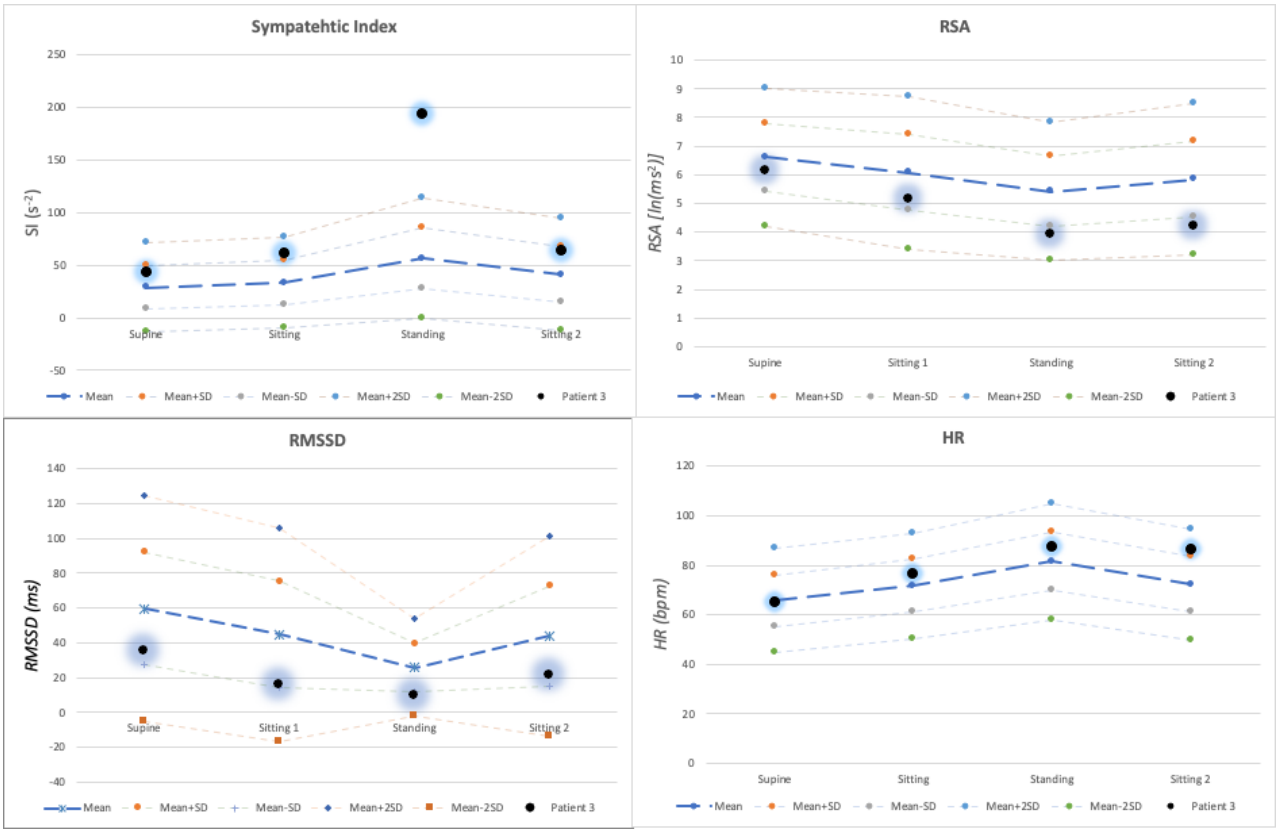

Figure 3-3:ANS assessment for Patient 3 via Active Standing test

The active standing test's results indicate that the patient has Autonomic dysfunction because the SNS reactivity to standing is very high (more that 2 Standard deviations).

ANS modulation due to Lumbar and Sacral Neuromodulation

Patient 3 had one-time sacral neuromodulation using Low level laser therapy (LLLT) followed by Transcutaneous Electric Nerve Stimulation (TENS).

The LLLT shows a decrease in sympathetic activity as shown by the decreased values of SI from 32.71 during baseline to 17.79 during Infrared laser probe; and an increase in parasympathetic activity as reflected by the increase in the value of RSA from baseline value of 6.55 to 6.88 during IR probe. However, a larger increase in RSA was recorded during TENS, when RSA was 8.87. From this data shown in the table below, it can be concluded that LLLT decreases the

sympathetic activity by 45.6% (SI value) while the parasympathetic activity increased by only 5% (RSA). On the other hand, the TENS increased the parasympathetic activity by 43.06% (RSA change from recovery to TENS) while the SI decreased by 32.20%. The HR remained almost the same with very slight changes during each step.

Table 3-6:ANS modulation by Lumbar and Sacral Neuromodulation for Patient 3

	SI	**RSA**	**RMSSD**	**HR**	**SI/RSA**
Baseline	32.71	6.55	38.44	70.01	4.99
Array AC	39.8	6.24	33.35	66.65	6.38
Array BD	25.7	6.51	36.88	65.80	3.95
Probe	17.79	6.88	47.73	66.73	2.59
Recovery	46.18	6.20	26.72	68.17	7.45
TENS	31.31	8.87	34.08	67.68	3.53

The tilt table test was negative for syncope and presyncope however, the patient was diagnosed with POTS with HR reaching 141 bpm during tilt. The value of SI was 178 during supine and 295 during tilt which are very high, similarly, the active standing test indicated very high SI value during standing.

Therefore, there should be more focus on decreasing the Sympathetic activity which can be achieved by using LLLT because it affected the SI more as compared to RSA.

Summary of results for Patient 3

1. POTS, no syncope, no OH. Previous syncope
2. TTT: high baseline and SI reactivity, and low RSA, [HRV gives additional info on POTS]
   SI/RSA: 42 -> 74
3. Both RSA and more so SI react very strongly to standing, normal tone. HR normal
4. Constipation and upper GI symptoms, nausea, bloating, pain
5. LLLT pretest shows promise; Ehlers Danlos syndrome also associated with high sympathetic tone

3.4.2.4 Patient 4

Table 3.7 summarizes the HRV parameters calculated from the RR interval data recorded during the tilt table test. According to ATL, the patient has a history of chronic orthostatic intolerance, POTS and recurrent syncope.

Tilt Table Test

After 10 minutes of baseline recording, the patient was tilted up to the upright position at 70 degrees of inclination. Following symptoms were reported by the patient:

- Dizziness
- Nausea
- Feeling warm after 10 min of orthostatic stress

There was evidence of initial orthostatic tachycardia at 160 bpm. However, at the end of the test, the patient developed symptoms of presyncope and there was a drop in blood pressure and heart rate.

Table 3-7: Cardiac and HRV parameters during TTT for Patient 4

	Supine	**Tilt**	**Pre-Syncopal Attack**	
Heart Rate (bpm)	122	160	89	POTS
Blood Pressure (mmHg)	108/71	116/76	89/49	
Stroke index (mL/m2)	28.4	24.95	20.2	
Cardiac Index L/min/m2)	3.5	3.99	3.1	
Total peripheral index	1974	1814	1139	

	Supine	**Tilt**	**End Tilt test**	
Sympathetic Index	158.26	574.45	79.67	High symp tone and reactivity
RSA	4.74	1.39	5.09	Strong para reactivity
RMSSD	17.46	2.09	8.34	Strong para reactivity
HR	122.24	160.82	120.42	POTS
SI/RSA	33.39	413.27 (12.5x)	15.65	
SI/RMSSD	9.1	287 (31.5x)		

After 7.32 minutes of orthostatic stress, the patient was tilted down to the supine position. Hemodynamic variables returned to baseline. Symptoms went away. The patient was then hydrated with IV fluids.

Patient has very high baseline SI value indicating very high sympathetic tone which increased during tilt in order to cope with maintaining the blood flow requirement to the upper limbs. There was a greater decrease in RSA (from 4.74 during supine to 1.39 during tilt) compared to other patients.

Deep Breathing Test

According to ATL, report, the expiration/inspiration ratio of the heart rate was 1.7 which was considered normal.

Catecholamine Level Determination During Orthostatic Stress

The norepinephrine levels during supine were 5.7 and results for standing were not available. Active standing test not performed, hence cannot compare catecholamine levels cannot be correlated with SI.

Beta Adrenergic Hypersensitivity Test

As reported by ATL, the target heart rate was 114 and 135 bpm that was achieved with 2mcg of isoproterenol. It was reported as negative beta-adrenergic hypersensitivity.

Intrinsic Heart Rate Test:

According to ATL report, the predicted intrinsic heart rate was 102 and actual was 100, which was reported to be a borderline increased sinus node automatism.

Conclusions:

1. Positive tilt table test for vasovagal presyncope/postural orthostatic tachycardia
2. Increased catecholamine response in supine position pending orthostatic stress
3. Normal cardiovagal reflexes
4. Normal beta-adrenergic hypersensitivity test
5. Borderline increased intrinsic heart rate

Active standing test was not done for this patient, hence no data available.

Summary of results for Patient 4

1. POTS and presyncope
2. TTT-HRV: high SI tone and reactivity. But also, very high supine HR of 122. Very low RSA reactivity; DB test normal, RSA up to 12. SI/RSA 33 -> 413
3. Chen-HRV: not done

3.4.2.5 Patient 5

Table 3.8 summarizes the HRV parameters calculated from the RR interval data recorded during the tilt table test for patient 5.

Table 3-8:Cardiac and HRV parameters during TTT for Patient 5

	Supine	**Tilt**	**ISOPREL 1.0 MCG/MIN & NS 150 ML/HR**	**Recovery**
Heart Rate (bpm)	95	117	129	105
Blood Pressure (mmHg)	108/73	112/84	120/84	N/A
Stroke index (mL/m2)	24.7	20.6	22.61	19.90
Cardiac Index L/min/m2)	2.0	2.42	2.93	2.09
Total peripheral index	N/A	N/A	N/A	N/A

	Supine	**Tilt**	**ISOPREL 1.0 MCG/MIN & NS 150 ML/HR**	**Recovery**
Sympathetic Index	54.83	241.48	645.29	369.19
RSA	5.52	2.3	3.38	3.39
RMSSD	46.54	9.72	2.71	8.09
HR	91.82	117.81	129.33	105.33
SI/RSA	9.93	104.99 (10.5x)	190.91	108.91
SI/RMSSD	1.2	24.9 (20.7x)		

The increase in HR from supine to tilt was less then 30 bpm which indicated negative POTS diagnosis. The SI and RSA values during supine are within normal ranges, however the RSA decrease in RSA and RMSSD during tilt was more compared to other patients.

Isoprel or isoproterenol is a beta-adrenergic agonist, that mimics sympathetic neural activation and when administered indeed increased SI significantly from 241.48 to 645.29 and increase in HR was also observed. Isoproterenol is given to increase the chance of syncope.

Catecholamine Level test during orthostatic stress:

The norepinephrine levels during lying down, 5 minutes after standing and 10 minutes after standing were 0.6, 1.7 and 2.1 respectively which were considered normal catecholamine levels by Dr. Guzman ATL. The Active standing test was not performed for this patient.

Beta Adrenergic Hypersensitivity Test

According to the ATL report, the incremental doses of isoproterenol were given to the patient. The target heart rate was 126 bpm that was reached with isoproterenol 2 mcg. This was reported to be considered normal and hence negative test for beta adrenergic hypersensitivity.

Conclusions:

1. Negative tilt table test for vasovagal syncope, autonomic dysfunction/postural orthostatic tachycardia.
2. Normal catecholamine level determination during orthostatic stress.
3. Negative beta-adrenergic hypersensitivity test.

Summary of results for Patient 5

1. All normal; previous syncope
2. TTT-HRV normal base but high SI reactivity; normal blood NE. SI/RSA 10 -> 105
3. Chen-HRV not done
4. Difficulty of oral food intake, Nausea, vomiting and diarrhea

3.4.2.6 Patient 6

Table 3.9 summarizes the HRV parameters calculated from the RR interval data recorded during the tilt table test. According to ATL, the patient has a history of chronic orthostatic intolerance, GI dysmotility and Mast cell activation disorder

Tilt Table Test

After 10 minutes of baseline recording, the patient was tilted up to the upright position at 70 degrees of inclination. Following symptoms were felt initially but subsided 1-minute orthostatic stress:

- Dizziness
- Tingling in limbs
- Ringing in ears

Table 3-9:Cardiac and HRV parameters during TTT for Patient 6

	Supine	**Tilt**	**Syncopal Attack**
Heart Rate (bpm)	69	80	47
Blood Pressure (mmHg)	103/50	121/78	61/30
Stroke index (mL/m2)	48	37.5	32.4
Cardiac Index L/min/m2)	3.3	3.0	2.0
Total peripheral index	1869	2501	739

	Supine	**Tilt**	**NTG 0.3 mg**	**End Head Tilt up with Syncope**
Sympathetic Index	12.82	95.02	47.59	19.51
RSA	6.68	5.24	4.51	7.66
RMSSD	56.51	21.72	30.3	67.52
HR	66.69	80.84	111.08	69.13
SI/RSA	1.92	18.13 (9.4x)	10.55	2.55
SI/RMSSD	0.23	4.3 (18.8x)		

After 15 minutes of orthostatic stress, 0.3 mg of nitroglycerin was administered. Five minutes later, the patient started experiencing:

- Dizziness

- Palpation
- Nausea
- Visual disturbances
- Sudden drop in blood pressure

The patient had a syncopal attack.

The patient was tilted down to the supine position and hemodynamic variables returned to the baseline and they regained consciousness almost immediately.

The change in HR from supine to tilt was less than 30 bpm which is normal hence, negative POTS diagnosis. The patient could not maintain the increased SNS activity during the tilt after the administration of NTG and had a syncopal attack during which the HR and blood pressure both decreased significantly. The baseline SI value of 12.82 indicates that the patient has abnormally low SNS tone. It was increased to 95 but patient could not maintain it. The low baseline SNS tone is also indicated by the low SI value during the active standing test. The interesting fact is, the SI increased from supine to sitting however, it was decreased during standing. Hence, patient could not maintain the increased SNS tone after sitting and hence it decreased while standing instead of increasing. The RSA and RMSSD increased during standing instead of decreasing. Which is in accordance with the inability to maintain the SNS tone during tilt and the patient had syncopal attack, during which the both the HR and BP decreased, Sympathetic Index (SI) decreased back to its baseline value (approx.). RSA and RMSSD increased.

Deep Breathing Test

As reported in ATL report, the calculated expiration/inspiration ratio of the heart rate was equal to 1.4 which was considered normal. Hence vagal, parasympathetic, reactivity was reported as normal.

Catecholamine Level Determination During Orthostatic Stress

As reported in reports from ATL, the catecholamine levels were taken at supine and upright position, but the values were not reported. However, From the active standing test data, the Sympathetic Index (SI) during supine (15.38 s^{-2}) and standing during first 3 minutes (25.60 s^{-2}) and for next three minutes (34.75 s^{-2}) was on the lower side of the normal range, indicating low sympathetic tone. The norepinephrine levels are not available to compare with SI.

Beta Adrenergic Hypersensitivity Test

Not performed by ATL.

Conclusions:

1. Positive tilt table test for vasovagal syncope, mixed response
2. Negative tilt table test for neurogenic orthostatic hypotension/autonomic failure
3. Negative tilt table test for postural orthostatic tachycardia syndrome
4. Pending catecholamine levels during orthostatic stress
5. Normal Cardiovagal reflexes

Active standing test

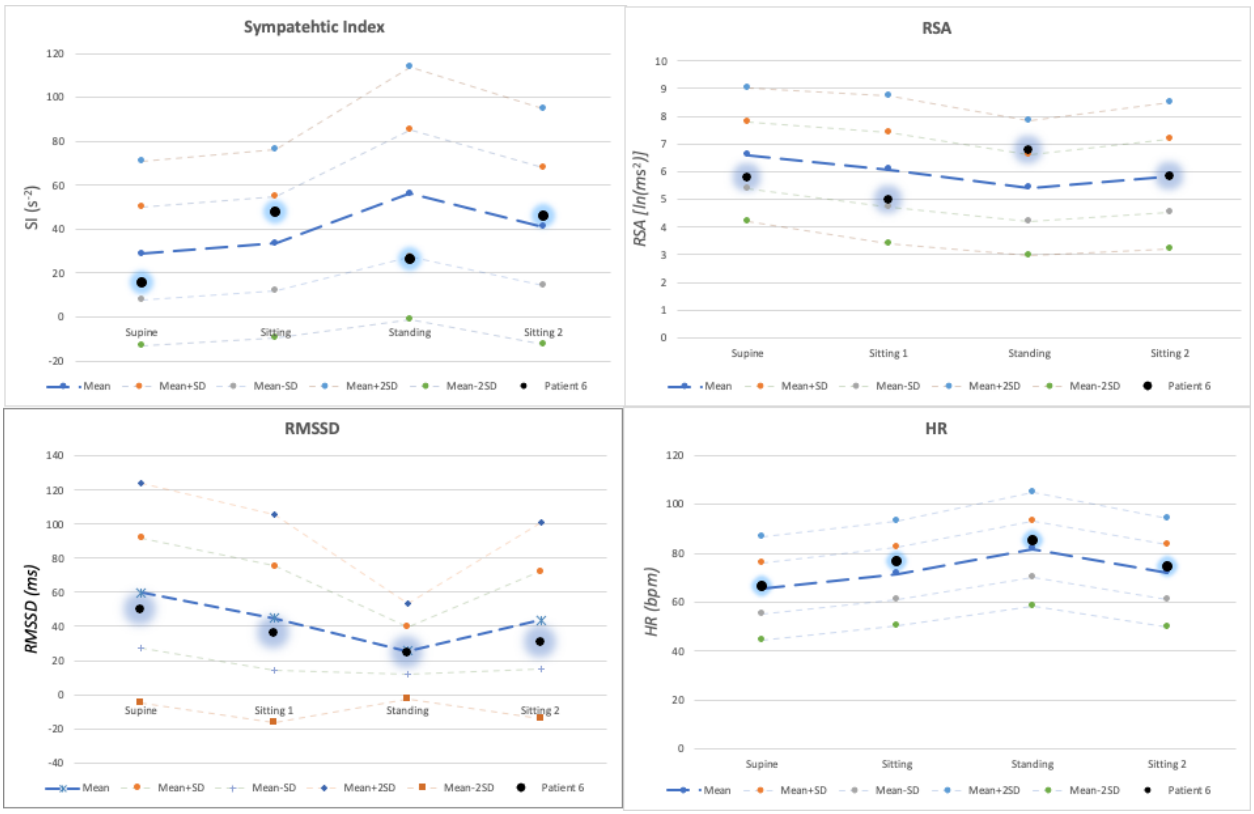

Figure 3-4:ANS assessment for Patient 6 via Active Standing test

The active standing result indicate that the patient's ANS response to standing is not normal (opposite), which indicates ANS dysfunction.

ANS modulation due to Lumbar and Sacral Neuromodulation

The patient had one-time sacral neuromodulation at Dr. Chen's clinic using LLLT as well as TENS. The results are shown in the table below:

Table 3-10:ANS modulation by Lumbar and Sacral Neuromodulation for Patient 6

	SI	RSA	RMSSD	HR	SI/RSA
Baseline					
Array AC RED	33.19	5.953	32.887	66.002	5.58
Array AC IR	21.59	6.319	39.654	65.353	3.42
Array BD RED	35.23	5.918	37.216	65.311	5.95
Array BD IR	28.33	5.99	43.627	63.311	4.73
Probe	34.02	6.175	41.842	66.437	5.51
Recovery	25.55	5.798	46.837	68.988	4.41
TENS	24.8	5.711	35.02	70.219	4.34
Recovery	36.03	5.388	38.038	74.969	6.69

In this case the effect of LLLT array stimulation was assessed separately for Red and Infrared light. Data indicated that the Infrared array stimulation influenced the AND more compared to Red light at both AC and BD positions. In both cases the SI decreased, and RSA increased. Probe did not decrease the SI but slightly increase the RSA. TENS also have very little effect.

A point of concern is, since the patient has syncopal attack during tilt table test, they had low sympathetic tone (active standing test) therefore, if the neuromodulation is desired to further decrease the SI to treat GI dysfunction, it may contribute further to syncope. Laser probe here indicated to only increase the PNS (as indicated by slight increase in RSA) without doing much to SNS activity (hence not contributing to syncope). The slight increase in RSA during laser probe will be helpful for GI dysfunction and it will not promote syncope at the same time.

Summary of results for Patient 6

1. No OH no POTS, syncope
2. TTT-HRV: Normal RSA but very low SI that cannot be maintained (SI explains syncope), normal HRV response to deep breathing, RSA up to 12 SI/RSA 2 -> 18
3. Chen-HRV: Low RSA and PNS abnormal increase during standing; SNS low tone and abnormal opposite reactivity to standing, both RSA and SI indicate inability to maintain sympathetic response to standing. Normal HR

3.4.2.7 Patient 7

Table 3.11 summarizes the HRV parameters calculated from the RR interval data recorded during the tilt table test for Patient 7.

Table 3-11: Cardiac and HRV parameters during TTT for Patient 7

	Supine	**Tilt**	**5-min Head Tilt up**	**Recovery**	
Heart Rate (bpm)	88	134	143	80	POTS
Blood Pressure (mmHg)	127/84	125/95	120/86	109/65	
Stroke index (mL/m2)	31.41	25.03	24.25	38.87	
Cardiac Index L/min/m2)	2.75	3.33	3.45	3.08	
Total peripheral index	2814	2424	2271	2093	

	Supine	**Tilt**	**5-min Head Tilt up**	**Recovery**	
Sympathetic Index	101.29	241.69	109.84	54.06	High symp base
RSA	7.55	3.2	3.16	7.13	
RMSSD	27.27	12.71	21.81	30.66	
HR	87.71	134.13	142.76	76.77	POTS
SI/RSA	13.42	75.53 (5.8x)	34.76	7.58	
SI/RMSSD	3.74	19.01 (5.1x)			

The HR increased from 88 bpm in supine to 134 bpm during tilt. This increase of more than 30 bpm is an indication of Postural Orthostatic Tachycardia Syndrome (POTS).

During head up tilt tested, her heart rate went up from 83 to maximum of 160 beats per minute. Blood pressure remained unchanged. Mean blood pressure was 124/90. Cardiac index increased from 2.6 to 3.3. She had some dizziness, nausea and shortness of breath and sweating but heart rate remained quite high above 130 beats per minute. Blood pressure was also remaining stable. Blood was drawn for estimated catecholamine levels in supine

position. After 15 minutes of head up tilt testing, she had a sudden drop in her blood pressure and heart rate. Heart rate went from 160 to 60 and blood pressure dropped to minimum of 40 mm systolic, and she had a syncopal episode.

The sympathetic Index value during the baseline is on the higher side. The Active standing test value of SI during supine was also high compared to the healthy controls which increased to over 250 during standing.

The systolic and diastolic blood pressures increased and maintained during the tilt. All the variables recovered back to normal after the tilt. During the recovery the values of SI decreased to 54.06 compared to its baseline value of 101.29.

Calculated predicted intrinsic heart rate was 103. The heart rate achieved was 102 beats per minute.

LLLT and TENS response

Table 3-12: ANS modulation by Lumbar and Sacral neuromodulation for Patient 7

	SI	**RSA**	**RMSSD**	**HR**	**SI/RSA**
Baseline	69.4	4.23	17.37	80.18	16.41
Array AC	88.19	3.88	12.94	79.08	22.73
Array BD	82.14	3.9	13.1	79.19	21.06
Probe	104.46	3.84	12.1	78	27.20
Recovery	65.06	3.79	13.14	80.36	17.17
TENS	78.78	3.44	9.61	82.1	22.90
Recovery	89.42	3.95	15.4	84.27	22.64

There was very little effect on sympathetic and parasympathetic nervous system due to one-time sacral neuromodulation as indicated by the values given in table above. Both LLLT and TENS indicated to further increase the sympathetic activity and decrease the parasympathetic activity.

The patient has low PNS activity during supine as indicated by RSA value during active standing test (Figure 3.5) however, the RSA seems to move towards the normal range during sitting and standing.

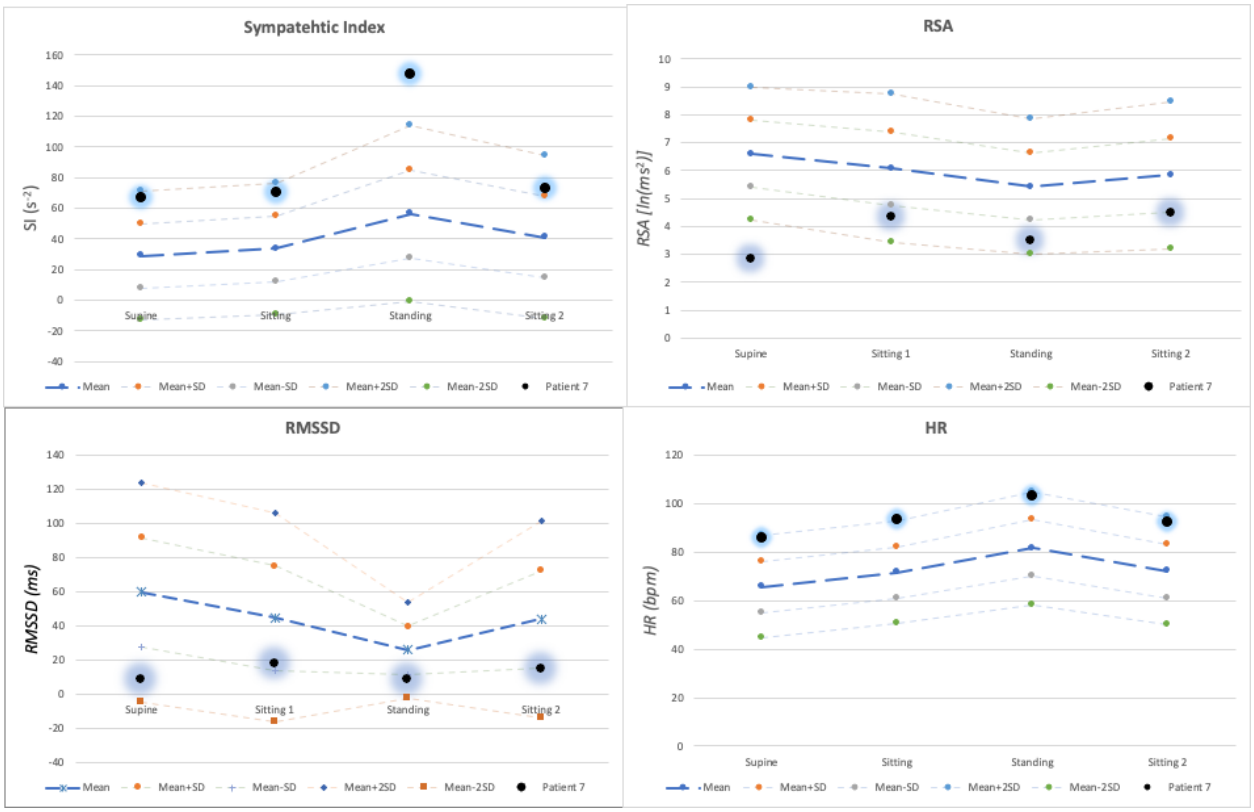

Figure 3-5: ANS assessment for Patient 7 during Active Standing test

Baseline SNS tone is high and baseline PNS tone is very low, the SNS rectivity to standing is very high (more than 2 SD), which indicates ANS dysfunction.

Summary of results for Patient 7

1. POTS and syncope.
2. TTT-HRV: high SI reactivity, normal RSA tone but very low RSA reactivity SI/RSA 13 -> 75
3. Chen-HRV very low RSA, very high SI and very high SI reactivity; HR high
4. High SI without major cardiac or GI disorders

3.5 Summative Evaluations

3.5.1 POTS and HRV

Five (Patients# 1,2,3,4,7) out of seven patients had a positive test of Postural Orthostatic Tachycardia Syndrome (POTS). The normal maximum value of SI in supine position for healthy control is 49.81 (generated in chapter 2). Patient 4 was not tested using Active Standing test, for remaining four, the values of SI are shown in the Table 3-13 below and their comparison with healthy controls is also shown in the figure below. It can be noted that out of the four patients, Patient 2 and Patient 7 had their supine SI value well above the maximum normal value during supine, while Patient 3 has their SI supine value near the upper limit. Only Patient 1 had the supine SI value near the mean of the normal range. Looking at the HRV parameters during Active standing test, it was observed that in addition to high SI values during supine, there was a remarkable increase in SI during standing in all these cases except patient 1. Table below shows the SI values of these patients. Active standing test was not conducted for Patient 4.

Table 3-13: Sympathetic Index (SI) during Active Standing Test for all the patients with POTS

Sympathetic Index (s^{-2})			
	Supine	Standing	Sitting
Patient 1	34.06	74.51	35.62
Patient 2	86.09	419.41	199.09
Patient 3	42.67	193.47	63.22
Patient 7	66.38	147.34	72.58

Figure 3.6 below shows the comparison of SI values Patients 1,2,3 and 7. The pattern of SI modulation in all these patients is the same. The SNS activity is very high (>Mean±2SD) compared to baseline during standing. In case of Patient 1 only, the value of SI during standing

was within the normal range however, it is near the upper limit of the normal range. Therefore, it can be stated that the Active standing test can correctly predict the diagnosis of POTS.

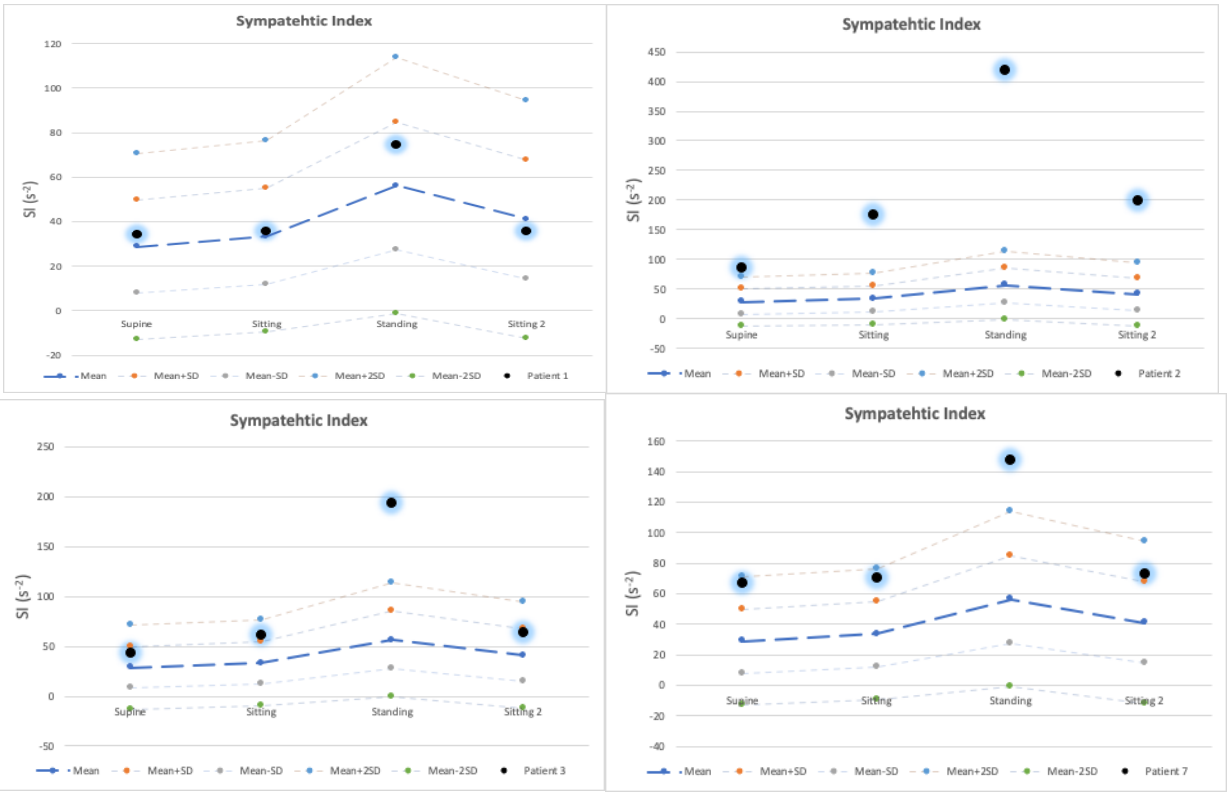

Figure 3-6: Sympathetic Index for all the patients with POTS

Tentative Conclusion:

POTS appears to be associated with a very high sympathetic reactivity (SI) upon standing in our Active Standing Test

3.5.2 Syncope and HRV

Patients 4 and 6 are the only two patients who had a syncopal attack. The active standing test was conducted only for patient 6. The patient increased the SNS and decrease the PNS tone during standing. In contrast, during TILT, there was a decrease in SI and an increase in RSA and RMSSD while standing which is similar to the situation of not being able to maintain the required increased SNS tone, and hence the patient had a syncopal attack. Although the data is

from one patient only, it appears that from the active standing test HRV pattern, the syncopal attack can be predicted. Figure 3.7 below indicate the decreased SI value during standing instead of increase.

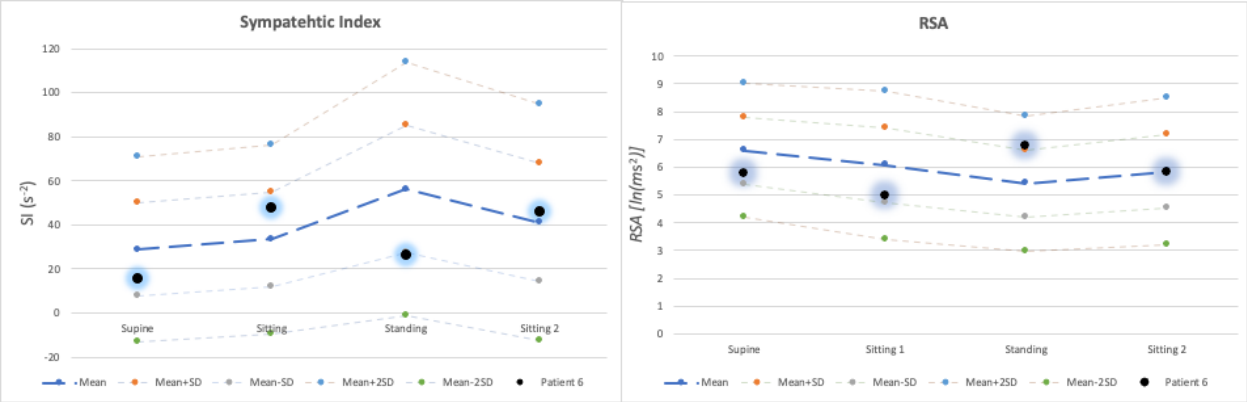

Figure 3-7: ANS modulation during active standing test for patient6, diagnosed with Syncope during TTT

Tentative Conclusion:

It may be that a syncope attack is associated with the inability to maintain appropriate sympathetic reactivity (SI) upon standing, hence, it can be evaluated using HRV analysis.

3.5.3 Catecholamine Level Determination During Orthostatic Stress

The ATL reported that Patient 1 had elevated norepinephrine levels during standing and Patient 4 had elevated norepinephrine level during supine. The SI calculated from active standing test indicated abnormally increased sympathetic activity during active standing during last three minutes which is consistent with the increased norepinephrine levels for Patient 1. For Patient 6, the values of SI were normal during supine while during standing the SI was near the lower range and it deceased after sitting instead of increasing, Patient 6's norepinephrine levels are not available. In the third patient, only the supine norepinephrine levels were reported by ATL,

and they are elevated while those during standing were not available (Table 3.14). The active standing test was not performed for Patient 4

Table 3-14:: Norepinephrine Levels in comparison with SI during the active standing test

Norepinephrine Levels

	Supine	**Standing (5 min)**	**Standing (10 min)**
Patient 1	2.3	4.4 (191%)	7.8 (339%)
Patient 6	Results not reported	Results not reported	Results not reported
Patient 4	5.7	Results not reported	Results not reported

Sympathetic Index (SI)

	Supine	**Standing (1-3 min)**	**Standing (4-6 min)**
Patient 1	34.06	76.47 224%	112.59 330%
Patient 6	15.38	25.60	34.75
Patient 4	N/A	N/A	N/A

Tentative Conclusion:

From the data of it can be concluded that there is a good correlation between the SI and plasma NE levels

3.5.4 Deep breathing test

Three patients underwent the deep breathing test. An increase in parasympathetic activity and a decrease in sympathetic activity was observed during the deep breathing. The average value of sympathetic index (SI) decreased to 62.05 s^{-2} during the first deep breathing session and increased back to 260.29 s^{-2} after the first session of deep breathing. In the second session the SI decreased to 77.31 s^{-2} and recovered back to 299.06 s^{-2} after the deep breathing test. Similarly, the RSA increased from the mean value of 5.81 $ln(ms^2)$ to 8.93 $ln(ms^2)$ on average during first deep breathing session after which it decreased back to 5.57 $ln(ms^2)$. During the second session of deep breathing the RSA increased to 8.64 $ln(ms^2)$ and recovered back to 5.34 $ln(ms^2)$ after deep breathing session. The heart rate decreased slightly during each deep

breathing session. Figures below show the changes in each HRV parameter of each individual during deep breathing.

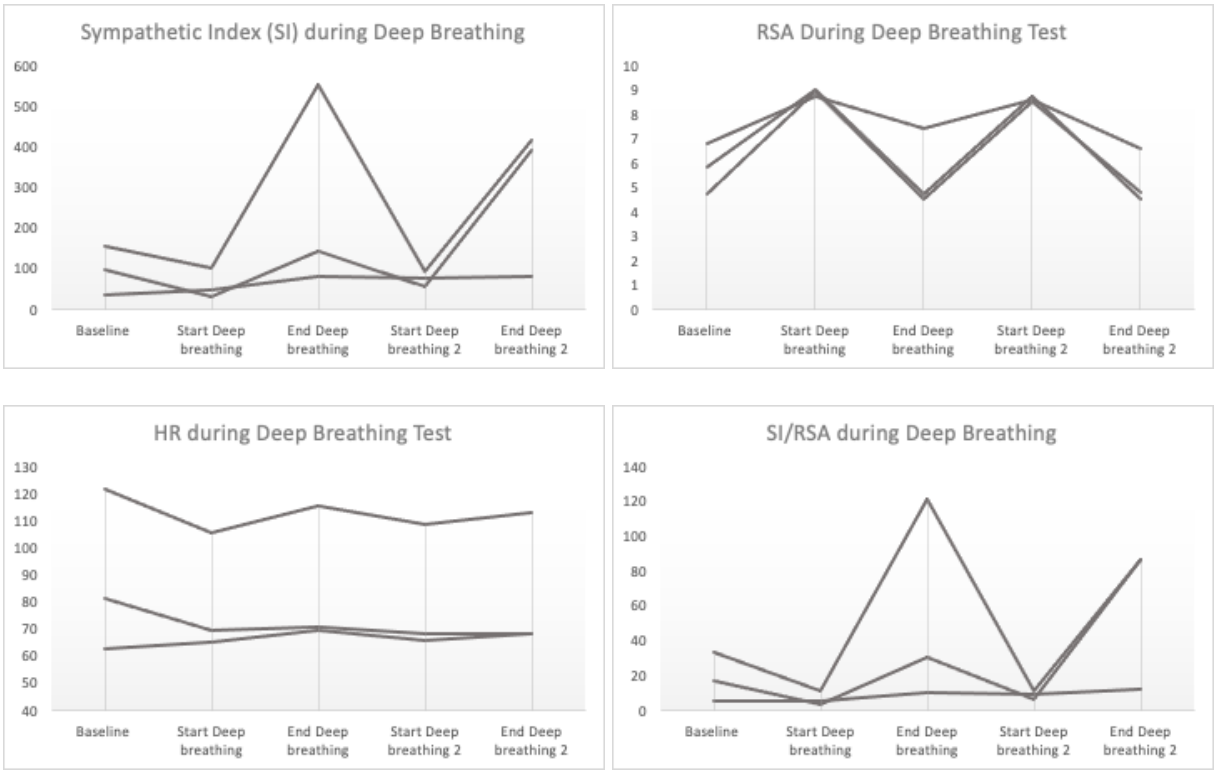

Figure 3-8: ANS modulation during deep breathing

In ATL reports, only the HR is taken into account such that the ratio of heart rate during expiratory/inspiratory is calculated and reported. However, the calculated HRV results indicate that change in SI and RSA are more sensitive during deep breathing as compared to heart rate. The Table below indicate the changes in HRV parameters during deep breathing test for each individual.

Table 3-15: HRV during Deep Breathing

Sympathetic Index (SI)					
	Baseline	**Start Deep breathing**	**End Deep breathing**	**Start Deep breathing 2**	**End Deep breathing 2**
Patient 1	34.76	50.43	80.5	78.39	83.72
Patient 4	158.26	102.96	554.14	96	418.52
Patient 6	99.01	32.76	146.22	57.53	394.94
Average	**97.34**	**62.05**	**260.29**	**77.31**	**299.06**
RSA					
	Baseline	**Start Deep breathing**	**End Deep breathing**	**Start Deep breathing 2**	**End Deep breathing 2**
Patient 1	6.86	8.79	7.42	8.62	6.63
Patient 4	4.74	8.97	4.56	8.56	4.82
Patient 6	5.84	9.03	4.74	8.75	4.56
Average	**5.81**	**8.93**	**5.57**	**8.64**	**5.34**
RMSSD					
	Baseline	**Start Deep breathing**	**End Deep breathing**	**Start Deep breathing 2**	**End Deep breathing 2**
Patient 1	57.03	53.75	37.64	48.42	28.04
Patient 4	17.46	40.93	6.25	37.8	6.83
Patient 6	44.32	62.76	19.57	51.99	19.76
Average	**39.60**	**52.48**	**21.15**	**46.07**	**18.21**
SI/RSA					
	Baseline	**Start Deep breathing**	**End Deep breathing**	**Start Deep breathing 2**	**End Deep breathing 2**
Patient 1	5.65	5.74	10.85	9.09	12.63
Patient 4	33.39	11.48	121.52	11.21	86.83
Patient 6	16.95	3.63	30.85	6.57	86.61
Average	**18.66**	**6.95**	**54.41**	**8.96**	**62.02**
Heart Rate					
	Baseline	**Start Deep breathing**	**End Deep breathing**	**Start Deep breathing 2**	**End Deep breathing 2**
Patient 1	81.53	69.92	71.09	68.75	68.46
Patient 4	122.24	105.6	115.72	109.15	113.53
Patient 6	63.11	65.65	69.56	66.21	68.3
Average	**88.96**	**80.39**	**85.46**	**81.37**	**83.43**

As discussed in the method section, the deep breathing test was conducted to diagnose the cardiovagal reflex. As reported by ATL, the cardiovagal reflex was normal for all the three patients. Looking at the HRV parameters, the RSA and RMSSD values increased during deep breathing and SI decreased during the deep breathing for all the three patients indicating the dominant vagal influence. As discussed above, during inhalation, the HR increases and during exhalation, the HR decreases. But during inhalation only and similarly during exhalation only,

there are not many variations in HR. Since HRV parameters are based on the variability of the HR and if the HR is constant the value of RMSSD and RSA will be zero and value of SI will be infinite. Therefore, if the HRV is used to test the deep breathing instead of HR itself, the HRV parameter should be calculated for the whole session (inhalation and exhalation) instead of only inhalation or exhalation, so the variation of HR during deep breathing should be captured correctly in HRV. To use RSA for PNS measurement during deep breathing, the HF band needs to be adjusted to capture the breathing frequency band.

The breathing frequency used for deep breathing test is 6 bpm which is equivalent to 0.10 Hz. To include this frequency the HF band needs to be adjusted. For these patients the HF band of 0.09-0.5 Hz was used which include the deep breathing frequency of 0.10 Hz.. The resultant values of RSA calculated from the adjusted HF band power are shown in the table 3.15 above. Deep breathing is the only test used to assess the cardiovagal reflex therefore we decided to include it in our active standing test protocol which will be implemented for the future studies in our lab. The updated protocol of active standing test is given at the end of this chapter.

Tentative Conclusion:

Deep breathing assesses the functioning of the parasympathetic (vagal) integrity. Normally the deep breathing increased RMSSD and RSA and decreased sympathetic tone (SI).

3.5.5 Beta Adrenergic Hypersensitivity Test:

Four out of seven patients underwent Beta-adrenergic hypersensitivity test. Patient 1 reached the target heart rate with only two doses of Beta-Isoprel (beta-agonist) 0.25mg each, they were reported by ATL to be hypersensitive. The beta-adrenergic hypersensitivity is a contributor of POTS.

The other three patients received four doses with total dose of 2.0 mg. The HRV parameters were calculated after each dose of 0.25 mg beta-isuprel. The table 3.16 below presents the calculated values of HRV parameters in each case.

The most likely receptor influencing HR is the beta 1 adrenergic receptor on cardiac cells. This will be activated by isuprel. Isoproterenol also evokes release of norepinephrine from sympathetic nerves via B2 receptors on sympathetic nerves [35].

Table 3-16:HRV during Beta Adrenergic Hypersensitivity Test

Sympathetic Index (SI) during Beta Adrenergenic Hypersensitivity Test					
	BETA-ISUPREL 0.25 mcg	BETA-ISUPREL 0.5 mcg	BETA-ISUPREL 1.0 mcg	BETA-ISUPREL 2.0 mcg	End BETA testing
Patient 1	175.36	21.48			26.83
Patient 3	1213	501.79	595.97	394.94	190.96
Patient 5	780.2	256.28	513.72	532.17	159.03
Patient 4	1132	1116	296.95	206.84	
Average	**825.14**	**473.89**	**468.88**	**377.98**	**125.61**

RSA during Beta Adrenergenic Hypersensitivity Test					
	BETA-ISUPREL 0.25 mcg	BETA-ISUPREL 0.5 mcg	BETA-ISUPREL 1.0 mcg	BETA-ISUPREL 2.0 mcg	End BETA testing
Patient 1	5.73	7.3			9.82
Patient 3	2.75	2.97	3.14	3.82	6.17
Patient 5	1.99	3.2	1.74	2.95	4.14
Patient 4	4.43	3.91	5.72	5.39	
Average	**3.73**	**4.35**	**3.53**	**4.05**	**6.71**

RMSSD during Beta Adrenergenic Hypersensitivity Test					
	BETA-ISUPREL 0.25 mcg	BETA-ISUPREL 0.5 mcg	BETA-ISUPREL 1.0 mcg	BETA-ISUPREL 2.0 mcg	End BETA testing
Patient 1	21.92	78.81			264.49
Patient 3	6.17	6.61	4.84	4.95	11.35
Patient 5	4.52	7.66	3.78	7.05	9.27
Patient 4	5.37	4.39	5.9	7.96	
Average	**9.50**	**24.37**	**4.84**	**6.65**	**95.04**

SI/RSA during Beta Adrenergenic Hypersensitivity Test					
	BETA-ISUPREL 0.25 mcg	BETA-ISUPREL 0.5 mcg	BETA-ISUPREL 1.0 mcg	BETA-ISUPREL 2.0 mcg	End BETA testing
Patient 1	30.60	2.94			2.73
Patient 3	441.09	168.95	189.80	103.39	30.95
Patient 5	392.06	80.09	295.24	180.40	38.41
Patient 4	255.53	285.42	51.91	38.37	
Average	**279.82**	**134.35**	**178.99**	**107.39**	**24.03**

Heart Rate during Beta Adrenergenic Hypersensitivity Test					
	BETA-ISUPREL 0.25 mcg	BETA-ISUPREL 0.5 mcg	BETA-ISUPREL 1.0 mcg	BETA-ISUPREL 2.0 mcg	End BETA testing
Patient 1	76.56	89.31			103.14
Patient 3	103.1	104.3	108.02	112.71	103.02
Patient 5	101.11	98.68	105	108.79	100.41
Patient 4	112.93	116.38	120.52	118.03	
Average	**98.43**	**102.17**	**111.18**	**113.18**	**102.19**

3.5.6 Intrinsic Heart Rate Test:

Atropine blocks cholinergic muscarinic receptors and propranolol is an antagonist to the beta-adrenergic receptors. Three patients had the Intrinsic Heart Rate test during which Atropine and Propranolol were administered to block the autonomic input to the sinus node and to obtain the Intrinsic Heart rate (IHR). After the autonomic blockage, the value of HR was compared to predicted value of IHR. Since there is no autonomic modulation to the sinus node, the heart beats at a constant rate which is equal to IHR in ideal case. Hence, there is no variability in the HR which is represented by the lower values of RSA and RMSSD (near zero) and very high value of SI (tends to be infinity in case of constant HR). Therefore, the HRV can only confirm the autonomic parasympathetic withdrawal. HR should be used instead of HRV to test the intrinsic sinus node activity.

Sympathetic Index (SI) indicated a substantial increase in sympathetic activity with average SI value increased from 309.64 s^{-2} to 4451.18 s^{-2}, while the parasympathetic activity was completely withdrawn as indicated by the decrease in the average value of RSA to 0.97 $ln(ms^2)$. two out of three patients had normal sinus node functionality as their HR reached the predicted value of IHR while in case one patient (Patient 4) the slight increased intrinsic heart rate was observed. If the HR cannot reach the IHR after autonomic blockage and remain lower than the predicted IHR, it may not be able to fully increase the cardiac output during the tilt. The table 3.17 below indicates the absolute values of HRV parameters and Heart rate in each case. Atropine abolishes RSA as expected, hence HRV goes down which is reflected in high increase in SI, a subsequent beta antagonist decreases SI suggesting that part of the high SI was due to sympathetic activity.

Table 3-17: HRV during Intrinsic Heart Rate test

Sympathetic Index (SI) during Intrinsic Heart Rate Test				
	Start Atropine	End Atropine	Start PROPRANOLOL	End PROPRANOLOL
Patient 3	444.26	1921	458.02	1565
Patient 4	395.71	11170	391.14	181.74
Patient 7	88.94	262.53	490.46	936.13
Average	**309.64**	**4451.18**	**446.54**	**894.29**

RSA during Intrinsic Heart Rate Test				
	Start Atropine	End Atropine	Start PROPRANOLOL	End PROPRANOLOL
Patient 3	2.7	0.08	-0.0352	-0.93
Patient 4	3.03	0.1696	0.64	4.64
Patient 7	5.38	2.67	1.64	1.31
Average	**3.70**	**0.97**	**0.75**	**1.67**

RMSSD during Intrinsic Heart Rate Test				
	Start Atropine	End Atropine	Start PROPRANOLOL	End PROPRANOLOL
Patient 3	4.28	1.79	1.79	3.84
Patient 4	3.69	0.59	2.82	23.08
Patient 7	14.54	31.63	5.54	6.4
Average	**7.50**	**11.34**	**3.38**	**11.11**

SI/RSA during Intrinsic Heart Rate Test				
	Start Atropine	End Atropine	Start PROPRANOLOL	End PROPRANOLOL
Patient 3	164.54	24012.50	13011.93	1682.80
Patient 4	130.60	65860.85	611.16	39.17
Patient 7	16.53	98.33	299.06	714.60
Average	**103.89**	**29990.56**	**4640.72**	**812.19**

Heart Rate during Intrinsic Heart Rate Test				
	Start Atropine	End Atropine	Start PROPRANOLOL	End PROPRANOLOL
Patient 3	110.16	136.18	128.5	105.16
Patient 4	133.82	149.81	132.54	97.35
Patient 7	97.18	119.43	110.58	100.19
Average	**113.72**	**135.14**	**123.87**	**100.90**

3.6 Tilt table test vs Active standing test:

3.6.1 Sympathetic Response:

All the seven patients indicated increased Sympathetic Index (SI) during tilt and recovery afterwards with an average increase of 260% during tilt compared to supine and average decrease of 292% after tilt. The average value of SI during supine was 97.57 s^{-2} which increased to 351.12 s^{-2} during tilt and recovered back to 89.63 s^{-2} after tilt back to supine. The highest increase (1073%) in SI during tilt was observed in Patient 1, while the smallest increase in SI due to tilt was observed in Patient 2 (39%).

The active standing test was performed in 5 patients. The change in SI during postural change was similar to that in TTT, with an increase in SI from supine to standing (127% average increase) and recovery (72%) during sitting. The average value of SI during supine for five patients was 48.92 s^{-2} which increased to 110.90 s^{-2} during standing and recovered back to 64.42 s^{-2} during sitting. The smallest increase in SI during standing was observed in Patient 2 who also indicated smallest change in SI during tilt table test.

It was observed that the baseline values of SI during tilt table test were higher (average = 97.57 s^{-2}) compared to baseline values during active standing test (average= 48.92 s^{-2}). Patient 1 was the only patient with almost same baseline value of SI during both tilt table test and the active standing test. The elevated SI value during TTT might be because of higher stress levels in patients during the tilt table test. The Figure below indicates the individual changes in SI during table tilt test and postural change.

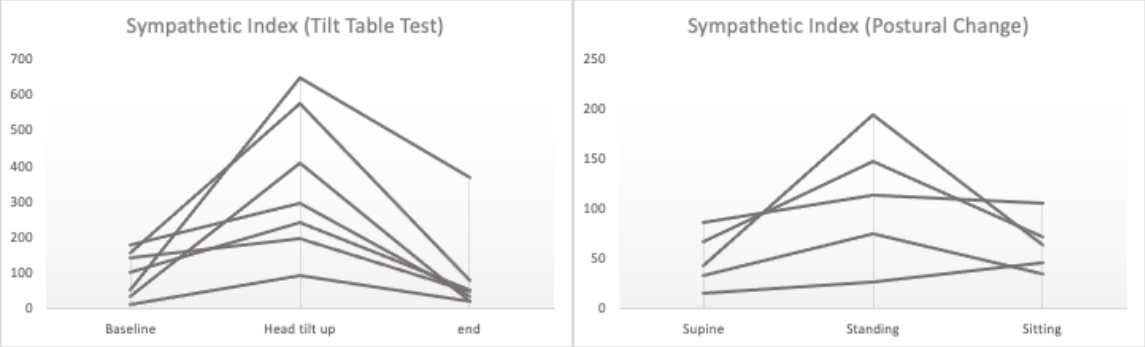

Figure 3-9:Comparison of Sympathetic activity during TTT and Active Standing Test

3.6.2 Parasympathetic Response:

All the seven patients indicated decreased RSA during tilt and recovery afterwards with an average decrease of 37% during tilt compared to supine and average increase of exactly 37% after tilt. The average value of RSA during supine was 6.14 which decreased to 3.85 during tilt and recovered back to 6.13 after tilt, back to supine. The highest decrease (58%) in RSA during tilt was observed in Patient 7 with the highest recovery of 55%. While the smallest decrease in RSA due to tilt was observed in Patient 2 (8%) with a recovery of 2%. The Patient 5 did not show any recovery in RSA after the tilt while their RSA value decreased 39% during the tilt.

The active standing test was performed in 5 patients. The change in RSA during active standing test was similar that in TTT, with decrease in RSA from supine to standing (14% average decrease) and recovery (11%) during sitting. The average value of RSA during supine for five patients was 5.11 ln(ms^2) which decreased to 4.38 ln(ms^2) during standing and recovered back to 4.91 ln(ms^2) during sitting. The highest decrease in RSA during standing was observed in Patient 2 (42%) who also indicated smallest change in RSA during tilt table test.

It was observed that the baseline values of RSA during tilt table test were higher (average = 6.14 ln(ms^2)) compared to baseline values during postural change test (average= 5.11 ln(ms^2)). Figure below indicates the individual changes in RSA during table tilt test and postural change.

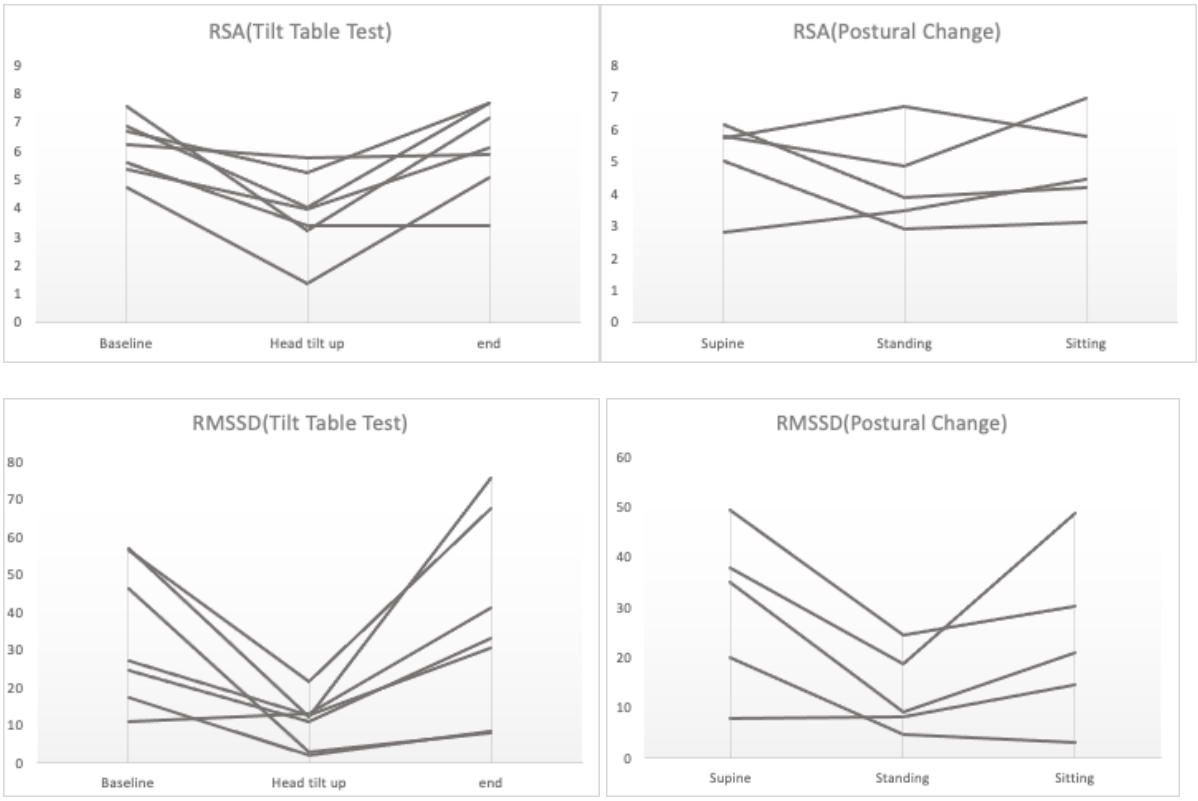

Figure 3-10:Comparison of Parasympathetic activity during TTT and Active Standing Test

3.6.3 Autonomic Balance and Heart Rate:

The autonomic balance, the SI/RSA ratio, indicated that the sympathetic nervous system activity dominated the vagal activity during tilt position in table test and in standing position in postural change test, with 657% increase in SI/RSA values on average during tilt position and a recovery of 499% after tilt, while 167% increase from supine to standing in postural change test and 92% recovery after standing.

The heart rate increased from the average value of 90.22 bpm during supine to 126.84 bpm during tilt and recovered back to 92.11 bpm. In the postural change test, the HR increased from average value of 75.21 bpm during supine to 97.10 bp during standing and recovered back to 89.58 bpm during sitting.

3.7 Discussion and Conclusions

The results indicate that there was an increase in sympathetic nervous system activity during head tilt up position (70 degrees) and a decrease in parasympathetic activity as represented by the sympathetic index (SI) and respiratory sinus arrhythmia (RSA) values respectively. The same autonomic response was also observed during the postural change test, where the sympathetic activity increased, and parasympathetic activity decreased from supine to standing and both recovered back during sitting after standing. However, the amount of increase in sympathetic and decrease in parasympathetic activity during postural change test was not as higher as during the tilt table test because, in postural change test there was a sitting phase between supine and standing while in tilt test, the position changed directly from supine to 70-degree tilt, hence there was an abrupt change in posture in tilt test which was not the case in postural change test. Due to the sitting phase between supine and standing the decrease in blood flow toward the upper limb and mind is not as much as it can be in case of direct supine to standing or during tilt, hence there is less amount of cardiac and hence autonomic modulation required to sustain the blood supply. Similarly, the SI and RSA were not fully recovered to their baseline values in postural change test because during the tilt table test the recovery was taken in supine position (similar to baseline) while in postural change test, the recovery was taken

during sitting position instead of supine (baseline) also there was a 6-minute walking phase between standing and sitting back. While in tilt table test both SI and RSA recovered almost fully. Therefore, if the postural change test is modified by removing the sitting and walking phases and taking the recovery in supine instead of sitting, it may give equivalent results to the tilt table test. (Supine-Standing-Supine). The active standing test has been modified accordingly for our new patients at Dr. Chen's clinic; however, the studies presented in next sections of this thesis, the active standing test developed in chapter 2 was used. Our team has decided on the following test for ANS assessment for future patients:

Modified ANS testing for patients and volunteers for future studies

Patient will be asked to go into supine position on massage table.

Deep Breathing: assessment of vagal parasympathetic integrity.

1. Adjustment period of 5 min
2. Baseline: 5 min in supine position
3. Breath at a rate of 6 breaths/min using metronome for about 2 min or until comfortable.
4. ECG recording for 5 minutes with a breathing frequency for 6 breaths/min
5. 5 min recovery with normal breathing frequency

Active Standing Test: Assessment of Autonomic Control to Maintain Blood Pressure.

1. After resting in supine position for 5 mins, blood pressure will be measured. Thereafter ECG recording for 5 min as a baseline.

2. After slowly standing up, wait for 1 minute and start recording ECG for 9 minutes, the standing period will be divided into 3 periods of 3 minutes each and blood pressure recording after each period of 3 minutes while standing.
3. Move back to supine for 1 minute before recording ECG for 5 minutes as recovery.

Table 3.18 below compares the changes in HRV parameters from baseline to tilt and supine to standing.

Table 3-18: HRV parameters in comparison with their normal ranges (TTT and AST)

			Tilt Table Test (Supine-Tilt)					Active Standing Test (Supine-standing)				
			SI/RSA	SI/RMSSD	RSA	SI	HR	SI/RSA	SI/RMSSD	RSA	SI	HR
Patient 1	POTS and pos beta	All GI	5-**100**	0.6-**33.2**	6.9-4.0	35-**408**	81-**130**	5.9-15.4	0.9-3.9	5.8-4.9	34-75	62-75
Patient 2	Normal (prev POTS syncope)	Upper /IBS	**23**-35	**5.8-18.4**	6.2-5.7	**143-198**	84-103	**17**-144	4.3-85.9	5.0-2.9	**86-419**	85-112
Patient 3	POTS (prev syncope)	Upper	**42-74**	**15.9-22.7**	**4.2**-4.0	**178-295**	98-**141**	6.9-49.6	1.2-21.1	6.2-3.9	43-**193**	65-85
Patient 4	POTS and presyncope	Upper	**33-413**	**9.1-287**	**4.7**-1.4	**158-574**	122-**160**	x				
Patient 5	Normal (prev syncope)	All GI	10-**105**	1.2-**24.9**	5.5-2.3	55-**242**	95-117	x				
Patient 6	syncope	All GI	2-18	0.2-4.3	6.7-5.2	13-95	69-80	2.7-**3.9**	0.3-1.1	5.8-**6.7**	15-**26**	65-85
Patient 7	POTS and syncope	Upper Pain	13 -**75**	**3.7-19.1**	7.6-3.2	**101-242**	88-**134**	**23**-42	8.3-17.9	**2.8-3.5**	**66-147**	85-100

Bold = Values outside 1 SD from the control values of active standing test.

Conclusions

1. All patients with POTS during test had high sympathetic reactivity to tilt based on Sympathetic Index (SI) and SI/RSA
2. Although POTS alone does not constitute cardiac autonomic dysfunction, TILT HRV clearly shows sympathetic over-reactivity.

3. 2 out of 4 patients with POTS and severe upper GI symptoms had low baseline parasympathetic activity and very high sympathetic tone and reactivity
4. Overall, sympathetic dysfunction (high) is much more common than low parasympathetic activity.
5. There was excellent consistency between SI/RSA and SI/RMSSD, both indices of balance between sympathetic and parasympathetic activity.
6. Most patients did not have severe cardiac issues to show autonomic dysfunction although TILT-HRV (Table 3.18) showed sympathetic overactivity in all but one.
7. One patient with syncope alone, showed no overt HRV-TILT abnormalities but during TILT but in our active standing test, the patient could not maintain sympathetic activity during standing, consistent with syncope.
8. Both patients with syncope during TILT showed an abnormal parasympathetic reaction to active standing such that their PNS activity increased instead of going down during standing, consistent with the pathophysiology of syncope. Both also had the lowest increase in sympathetic activity in response to standing.

Contribution of HRV in understanding pathophysiology

1. HRV can determine if POTS is associated with high sympathetic tone and/or abnormal sympathetic reactivity to standing
2. HRV (SI and RSA) is very sensitive to assess the vagal and sympathetic reaction to deep breathing
3. The autonomic dysfunction can be demonstrated by HRV even without OH, POTS or syncope; correlated with previous POTS and/or previous syncope.

4. Blood levels of norepinephrine (low for neurogenic OH and high for sympathetic overexcitation) correlate with how SI reacts to TILT
5. On average, the baseline HR was 15 bpm higher on TTT table compared to baseline HR during active standing test, possibly because TILT is more stressful compared to active standing test.

Chapter 4

Associations Between Colonic Motor Patterns and Autonomic Nervous System Activity Assessed by High-Resolution Manometry and Concurrent Heart Rate Variability

Published January 23, 2020, in Frontiers in Neuroscience | Autonomic Neuroscience.

https://doi.org/10.3389/fnins.2019.01447

Yuhong Yuan[1,2]†, M. Khawar Ali[2,3]†, Karen J. Mathewson[4], Kartik Sharma[2], Mahi Faiyaz[2], Wei Tan[2,5], Sean P. Parsons[2], Kailai K. Zhang[2], Natalija Milkova[2], Lijun Liu[2], Elyanne Ratcliffe[6],David Armstrong[2],Louis A. Schmidt[4],Ji-Hong Chen[2*‡] and Jan D. Huizinga[2,3‡]

† Shared First Authorship

‡ Shared senior Authorship

- [1]Department of Gastroenterology, Sun Yat-sen Memorial Hospital, Sun Yat-sen University, Guangzhou, China
- [2]Department of Medicine, Division of Gastroenterology, Farncombe Family Digestive Health Research Institute, McMaster University, Hamilton, ON, Canada
- [3]School of Biomedical Engineering, McMaster University, Hamilton, ON, Canada
- [4]Department of Psychology, Neuroscience, and Behaviour, McMaster University, Hamilton, ON, Canada
- [5]Department of Gastroenterology, Renmin Hospital of Wuhan University, Wuhan, China
- [6]Department of Pediatrics, Farncombe Family Digestive Health Research Institute, McMaster University, Hamilton, ON, Canada

4.1 Abstract

Abnormal colonic motility may be associated with dysfunction of the autonomic nervous system (ANS). Our aim was to evaluate if associations between colonic motor patterns and autonomic neural activity could be demonstrated by assessing changes in heart rate variability (HRV) in healthy volunteers. A total of 145 colonic motor patterns were assessed in 11 healthy volunteers by High-Resolution Colonic Manometry (HRCM) using an 84-channel water-perfused catheter. Motor patterns were evoked by balloon distention, a meal and luminal bisacodyl. The electrocardiogram (ECG) and cardiac impedance were assessed during colonic manometry. Respiratory sinus arrhythmia (RSA) and root mean square of successive differences of beat-to-beat intervals (RMSSD) served as measures of parasympathetic reactivity while the Baevsky's Stress Index (SI) and the pre-ejection period (PEP) were used as measures of sympathetic reactivity. Taking all motor patterns into account, our data show that colonic motor patterns are accompanied by increased parasympathetic activity and decreased sympathetic activity that may occur without eliciting a significant change in heart rate. Motor Complexes (more than one motor pattern occurring in close proximity), High-Amplitude Propagating Pressure Waves followed by Simultaneous Pressure Waves (HAPW-SPWs) and HAPWs without SPWs are all associated with an increase in RSA and a decrease in SI. Hence RSA and SI may best reflect autonomic activity in the colon during these motor patterns as compared to RMSSD and PEP. SI and PEP do not measure identical sympathetic reactivity. The SPW, which is a very low amplitude pressure wave, did not significantly change the autonomic measures employed here. In conclusion, colonic motor patterns are associated with activity in the ANS which is reflected

in autonomic measures of heart rate variability. These autonomic measures may serve as proxies for autonomic neural dysfunction in patients with colonic dysmotility.

4.2 Introduction

Colonic motility is regulated by a multitude of control systems. The colonic musculature receives rhythmic depolarization from the colonic pacemaker networks of interstitial cells of Cajal (ICC) and on-demand depolarization from the enteric nervous system (Furness, 2012; Huizinga, 2018). Motor patterns are generated in response to stimuli that are mediated by sensory and motor neurons, intrinsic and extrinsic to the musculature (Bharucha et al., 1993, 2008; Brierley et al., 2004; Costa and Brookes, 2008; Wang et al., 2009; Knowles et al., 2013; Callaghan et al., 2018). The extrinsic nervous system facilitates brain – colon communication, which plays a critical role in many aspects of colonic motility such as the defecation reflex (Szurszewski et al., 2002; Tache, 2003; Brookes et al., 2016).

The defecation reflex starts with a sensation of urgency mediated by rectal stimulation followed by sacral sensory nerve activation. This impulse initiates activity in the sacral defecation center, which sends signals to brain stem areas and the frontal cortex, which in turn activate motor nerves from the ANS and the enteric nervous system to produce a bowel movement (Furness, 2012; Spencer et al., 2016). The essential role of the ANS is demonstrated by the fact that the defecation reflex is lost when sacral parasympathetic activity is absent due to spinal injury (Devroede and Lamarche, 1974). Similarly, children with bowel dysfunction show significantly lower parasympathetic reactivity (Fazeli et al., 2016). Dramatic reduction in colonic motor activity may also occur when sympathetic activation is prolonged during stress (McIntyre and Thompson, 1992). Attempts have been made to gain insight into brain-gut communication

through analysis of heart rate variability (HRV); Irritable Bowel Syndrome (IBS) patients with constipation appear to have decreased levels of resting parasympathetic activity or increased resting sympathetic activity, suggesting that parasympathetic withdrawal with or without sympathetic activation could be an important contributing factor to constipation (Mazurak et al., 2012; Polster et al., 2018).

Heart rate is the net outcome of the intrinsic sinus node pacemaker activity that is influenced by sympathetic and parasympathetic innervation of the heart (Draghici and Taylor, 2016). HRV analysis is based on the peak R-R interval time series obtained from the ECG. HRV reflects physiological variation in heart rate caused by its autonomic innervation, but heart rate regulation may be influenced by events that are only indirectly related to physiological regulation of the heart rate; HRV may reflect ANS activity more generally, including associations with the gut (Mathewson et al., 2014; Bonaz et al., 2016; Draghici and Taylor, 2016; Ernst, 2017). The NTS in the brain stem plays a key role in this since it is involved in regulation of both heart rate and gut motility (Browning and Travagli, 2014; Babic et al., 2015).

Parasympathetic regulatory activity is typically represented by the intensity of a high frequency component (0.15–0.40 Hz) of HRV that fluctuates with the phase of respiration (Bonaz et al., 2016), known as RSA. Higher levels of resting RSA in healthy individuals are associated with the ability to adapt quickly to internal and external changes in the environment (Beauchaine and Thayer, 2015). An additional measure of parasympathetic activity is the root mean square of successive differences (RMSSD) between adjacent beat-to-beat intervals, which is calculated in the time domain.

The PEP, refers to the latency of the ejection of blood into the aorta, an index that correlates with ventricular contractility (Quigley and Stifter, 2006) and measured by impedance cardiography. Lower PEP values reflect greater contractility (increased sympathetic activation), whereas higher values reflect lower contractility (decreased sympathetic activation). In addition, we employed the Baevsky's Stress Index (SI), calculated from the main characteristics of the histogram of beat-to-beat intervals, the mode (the RR interval value repeating the most in the signal), the amplitude of the mode, and the range in variation. SI values increase with increases in sympathetic nervous system activity (Baevsky and Chernikova, 2017).

Autonomic measures are influenced by exercise, sleep, postprandial activity, smoking, alcohol, and coffee consumption in normal healthy individuals (Ernst, 2017). Other factors, such as gender, age, breathing frequency, body mass index, blood pressure, negative feelings (eg., depression, stress, pain), hormonal activity, medications, even family history and genetic background may influence HRV (Parati and Di Rienzo, 2003), indicating that HRV reflects more than cardiac health.

The objective of the present study was to test the hypothesis that activity in the ANS associated with colonic motor patterns can be observed as changes in HRV and impedance measurements. If so, these measures may provide a way to assess autonomic dysfunction in patients with colonic dysmotility. To this end, we conducted HRCM while simultaneously recording the ECG and cardiac impedance measures.

4.3 Materials and Methods

4.3.1 Participants

Eleven healthy participants were recruited by local advertisement (Table 1). Participants with any history suggestive of current or prior cardiovascular or gastrointestinal disease were excluded. Participants were not taking drugs that might affect cardiac or gastrointestinal function. Ethics approvals were obtained from McMaster University, the Hamilton Integrated Research Ethics Board, and written consent was obtained from all participants. The entire study was conducted at McMaster University.

Table 4-1: Normal values of Baseline ANS

Gender: male:7(64%); female 4(36%)	**Mean ±SD**	**Range**
Age (yr)	32.2±11.3	21-54
BMI (kg/m^2)	25.7±3.8	19.6-31.5
Baseline autonomic function (Supine)		
RSA(ln ms)	6.7±0.97	5.47-8.68
RMSSD (ms)	57.9±30.46	27.9-134.3
PEP (ms)	121.64±17.17	88-145.33
SI (s^{-2})	32.85±23.09	8.03-87.01
HR (bpm)	63.78±8.9	54.0±81.3

4.3.2 Methodologies and Nomenclature

High-Resolution Colonic Manometry was performed using an 84-sensor water perfused catheter that detected luminal pressures at 1 cm intervals from the proximal colon to the anal sphincter (Chen et al., 2017). The catheter was custom-made by Mui Scientific (Mississauga, ON, Canada) and the acquisition hardware was custom made by Medical Measurement Systems (Laborie, Toronto, ON, Canada). The manometric analysis was aided by customized Image-J and

MATLAB software. This study reports on the ECG and impedance data [30] obtained simultaneously with the HRCM data from the entire colon (Chen et al., 2018).

The following motor patterns were analyzed in conjunction with the autonomic measures:

• High-Amplitude Propagating Pressure Waves (HAPWs), occurring as single isolated events (Bharucha, 2012; Figure 1A).

• High-Amplitude Propagating Pressure Waves followed by SPWs referred to as HAPW-SPWs (Chen et al., 2017, 2018; Figure 1B).

• Motor Complexes (MCs): when two or more distinct motor patterns followed each other closely so that HRV changes could not be assessed for the individual patterns, e.g., two or more HAPWs (Figure 1C), or 1 HAPW and 1 HAPW-SPW etc.

• Simultaneous Pressure Waves (SPWs), most often pancolonic, occurring as single isolated events (Chen et al., 2017, 2018).

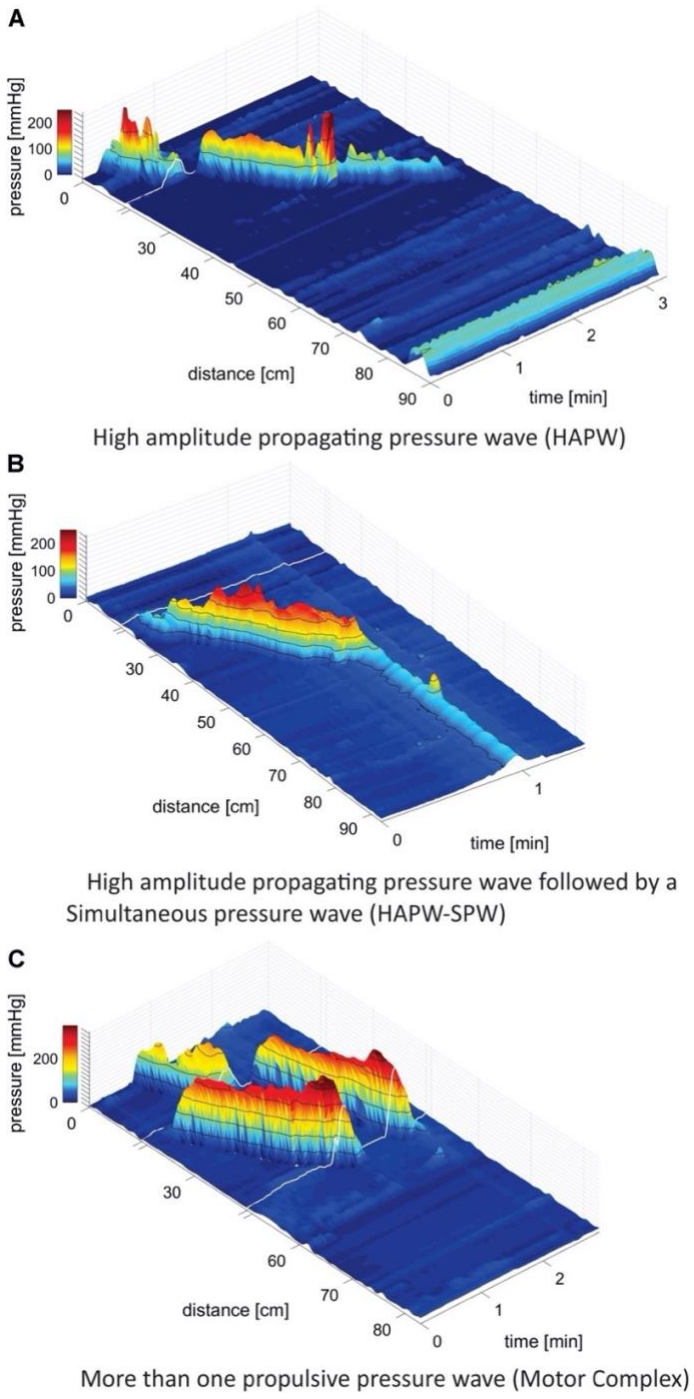

Figure 4-1:Motor patterns.

(A)High-Amplitude Propagating Pressure Waves (HAPWs) occurring as a single isolated event. White line indicates the presence of a 10 cm long balloon in the catheter where no data could be collected. The anal sphincter pressure is seen at 86 cm. 0 cm is in the proximal colon. (B) A HAPW followed by a simultaneous pressure wave (SPW) referred to as HAPW-SPW. White line indicates the presence of a 10 cm long balloon in the catheter where no data could be collected. The catheter was fully inside the colon such that the anal sphincter activity was not recorded.

The HAPW started distal to the balloon. (C) Motor Complexes, defined as two or more distinct propulsive motor patterns that followed each other closely so that HRV changes could not be assessed for the individual patterns. In this catheter, two balloons were present at the white lines so that two sections of 10 cm did not have pressure sensors. No anal activity was recorded.

ECG and impedance cardiography were recorded from seven electrodes on the subject's torso. Three electrodes formed a modified Lead II configuration for ECG recording. Four more electrodes were used in a standard tetrapolar electrode configuration for impedance recording, where two electrodes supplied a constant current source and two electrodes registered the changes in the transfer impedance (reflecting changes in activity of the sympathetic nervous system). Signals were recorded using a MindWare impedance cardio GSC monitor. HRV and impedances were analyzed by MindWare HRV 3.1 and IMP 3.1 software (MindWare Technologies Ltd., Gahanna, OH, United States). To assess general parasympathetic reactivity, we recorded changes in RSA and RMSSD in response to changes in body position during a resting baseline and posture change. Similarly, sympathetic reactivity was assessed by changes in PEP and in the Baevsky's stress index (SI).

4.3.3 General Autonomic Testing Prior to HRCM

Visit 1

Resting autonomic measures appear highly stable within an individual (Schmidt et al., 2012). Therefore, all volunteers underwent autonomic testing between 1 and 4 weeks prior to HRCM testing. Participants were accommodated in a quiet room with normal lighting and temperature. They had been asked to refrain from smoking, caffeine, alcohol and heavy eating in the 2 h before testing. After lying quietly in supine position for at least 10 min, ECG and impedance were measured for a 6 min rest period in the supine position. To test general

autonomic reactivity, the ECG was monitored while the subject was sitting on the edge of the bed, standing still, and while walking on the spot, each for 6 min (Jáuregui-Renaud et al., 2001).

4.3.4 HRCM, HRV and Impedance Recording

Visit 2

In addition to the general autonomic testing, all participants underwent simultaneous HRCM, ECG, and impedance recording. Bowel preparation with a high-volume polyethylene glycol electrolyte solution (Peglyte 280g, Pendopharm, Montreal, QC, Canada) was performed starting at 4 PM the day before HRCM (Chen et al., 2018). No other stimuli were used for bowel cleaning. The catheter was placed into the colon via colonoscopy and attached in the proximal colon mucosa with a clip. In six subjects, two balloons were part of the catheter, placed between sensors 10 and 11 and 40 and 41. In five subjects only a proximal balloon was part of the catheter placed between sensors 10 and 11. The balloons take up 10 cm space in which no pressure recordings can be made; these data omissions are indicated by a white line in the figures showing three-dimensional color manometry graphs. Manometric and autonomic recordings were performed during 90 min of baseline rest after colonoscopy, followed by 20 min of proximal balloon distention, 20 min of rectal balloon distention using a standard anorectal manometry balloon assembly, 90 min following intake of a meal, consisting of organic yogurt fortified by organic milk fat to make it 1000 kcal (Mapleton Organic, Ontario, Canada), and 45 min after administration of rectal bisacodyl. Participants were supine during all recordings except during the actual intake of the meal.

Autonomic reactivity was examined in the following conditions. (1) Baseline rest: supine autonomic activity obtained during general autonomic testing. This measure was taken to

evaluate whether changes in HRV due to motor patterns were related to the subject's "basal" autonomic activity. (2) Autonomic reactivity in response to body position changes from supine to sitting, then standing and walking. (3) Autonomic reactivity to colonic motor patterns by comparing three conditions: (a) pre-motor-pattern, the 2 min prior to the occurrence of the motor pattern. (b) the motor-pattern: autonomic activity during the entire period in which the motor pattern was present. (c) the recovery period, measured in the first 2 min immediately after the motor pattern.

4.3.5 Statistical Analyses

All data sets were assessed for normal distribution by applying the Shapiro–Wilk normality test (Ghasemi and Zahediasl, 2012) using GraphPad Prism version 8, RSA, RMSSD, PEP, SI, and HR values were assessed or compared during different postures and in response to motor patterns. Data were expressed as mean ± S.E.M. *N* = number of motor patterns. *n* = number of subjects.

4.3.6 General Autonomic Testing

At the first visit, general autonomic activity was assessed across postural conditions (supine, sitting, standing, walking) for each autonomic measure (Jáuregui-Renaud et al., 2001). All data sets were normally distributed except SI data. Normally distributed data sets were analyzed using one-way ANOVA with follow up multiple comparison Bonferroni test. The SI data were assessed using the non-parametric Friedman test followed by Dunn's multiple comparison test.

4.3.7 HRCM and HRV

At a second visit, 1–4 weeks later, A HRCM assessment was performed while simultaneously measuring heart rate and impedance. Then HRV parameters were calculated associated with the motor patterns. To be eligible for analysis, each motor pattern needed to be preceded by a

2 min baseline period and followed by a 2 min recovery period, both without movement artifact or other motor patterns. The Shapiro–Wilk normality test indicated that the data sets were not normally distributed.

First, all the motor patterns in all subjects were assessed as a single group to measure the changes in HRV parameters. Second, each category of motor patterns was assessed separately. First, the question was answered whether or not the occurrence of a motor pattern was associated with a change in any of the HRV parameters using the non-parametric Wilcoxon matched pairs signed rank test, comparing 2 min before to time during motor pattern. The data were averaged per individual hence n= 11, indicated as W-M (Wilcoxon-Mean) in the text when p values are noted.

Second, the question was answered whether or not there was recovery from a change in any of the HRV parameters within the 2 min following the motor patters. This was a comparison between three data sets (before – during – after) and the data sets were not normally distributed and were paired. Hence, the Friedman test was applied followed by the Dunn's multiple comparisons test. For each of the analyses, values of the motor patterns within one subject were averaged and considered an n = 1, indicated by F-D-M (Friedman-Dunn-Mean).

To provide a complete data set for all individual motor patterns in each category, graphs were presented with % change to emphasize the strength of the autonomic reactivity and its recovery. Within each category, the data were subjected to the Friedman test followed by Dunn's multiple comparisons test, based on the number of motor patterns (N), indicated by (F-D).

4.3.8 Correlation Between General Autonomic Testing and Autonomic Reactivity During Motor Patterns

Anticipating that patients with dysmotility might have reduced autonomic reactivity associated with motor patterns, and that this might be related to low general autonomic reactivity, we tested in the present study on healthy subjects whether or not any of the motor pattern associated changes in autonomic activity (comparing before and during motor patterns), was associated with two parameters of the general autonomic test, namely the supine value and the change from supine to standing. This was done using the Pearson Correlation Coefficient, two tailed test. Results with $R^2 > 0.5$ and $p < 0.05$ were considered significantly correlated. In the text, data related to correlations between general autonomic testing and autonomic reactivity during motor patterns supine HRV and changes in HRV parameters only show significant changes, while the results with no correlation ($R^2 < 0.05$ and/or $p > 0.05$) are provided in Supplementary Figures.

4.4 Results

4.4.1 General Autonomic Reactivity

The ability of the ANS to facilitate the generation of colonic motor patterns, may be related to a person's general autonomic reactivity (Shaffer and Ginsberg, 2017), which was therefore measured. General autonomic reactivity of the subjects was tested 1–4 weeks prior to HRCM in supine, sitting, standing, and walking positions. In pairwise tests, RSA decreased from supine to standing and walking, and from sitting to standing and walking (Figure 2A). RMSSD decreased from supine to sitting, standing and walking (Figure 2B). SI decreased significantly from supine to walking and from sitting to walking (Figure 2C). PEP did not show any significant change in

response to posture change (Figure 2D). The heart rate changed significantly during each posture change (Figure 2E). In general, the parasympathetic activity showed a decrease and the sympathetic activity showed an increase in responses to changes in posture.

4.4.2 Autonomic Reactivity Associated With Motor Patterns

A total of 145 eligible motor patterns from the 11 participants were included in the analysis. The motor patterns were comprised of 42 Motor Complexes; 28 HAPWs, 45 HAPW-SPWs, and 30 isolated SPWs. We first asked the question whether or not the occurrence of a motor pattern was associated with changes in HRV parameters, comparing activity in the 2 min before a motor pattern to the period in which the motor pattern took place using the Wilcoxon matched pair signed-rank test. Parasympathetic reactivity (both RSA and RMSSD) increased significantly (W-M); $p < 0.0001$) during the motor activity. Furthermore, both SI (W-M; $p < 0.0001$) and PEP (W-M; $p < 0.001$) showed a significant decrease in sympathetic reactivity during the motor activity. The heart rate did not change significantly during motor activity. Then we asked the question whether or not a recovery of autonomic activity to pre-motor pattern levels took place in the first 2 min after the motor pattern. Here we compared the 2 min before a motor pattern, the period during the motor pattern and the 2 min period after the motor pattern using the Freidman test followed by the Dunn's multiple comparison test. The data shown in Figure 3confirm that parasympathetic activity increased during a motor pattern compared to its baseline and then recovered during the 2 min following the motor pattern. According to the SI, sympathetic activity decreased during a motor pattern, and recovered in the next 2 min. For PEP, only the recovery phase showed a significant decline (increased sympathetic activity). Heart rate did not change significantly.

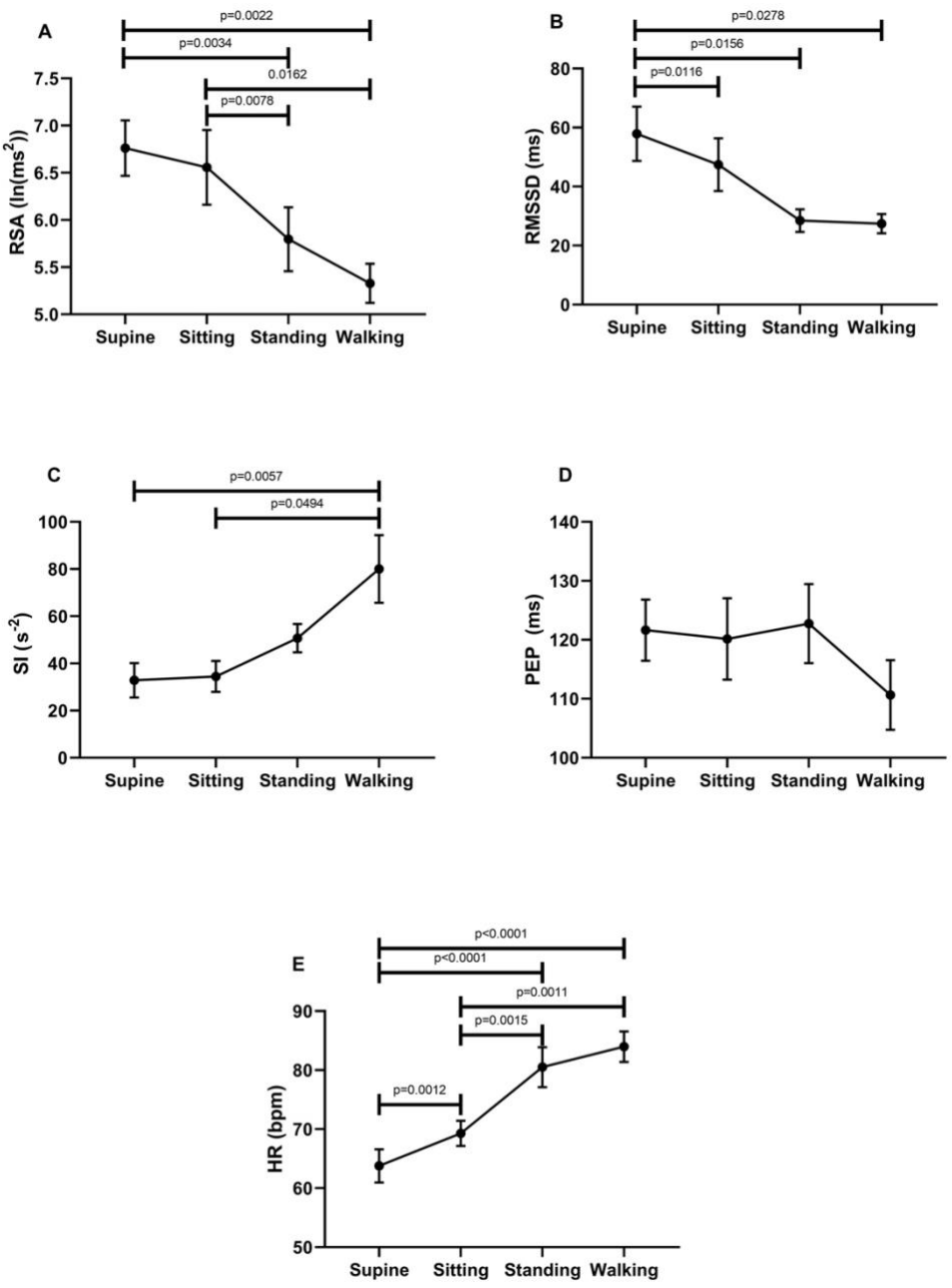

Figure 4-2: Changes in autonomic activity in response to posture changes

(n = 11), Significance was assessed by one-way ANOVA with repeated measures and Bonferroni correction for (A,B,D,E). Friedman test followed by Dunn's multiple comparison tests was used to assess significance for (C). (A) RSA declined upon standing and walking compared to the supine baseline position. (B)RMSSD declined upon standing and walking compared to the supine baseline position. (C) SI increased upon standing and walking compared to baseline position. (D) PEP decreased significantly only during walking. (E) Heart rate increases upon standing and walking compared to the supine baseline position.

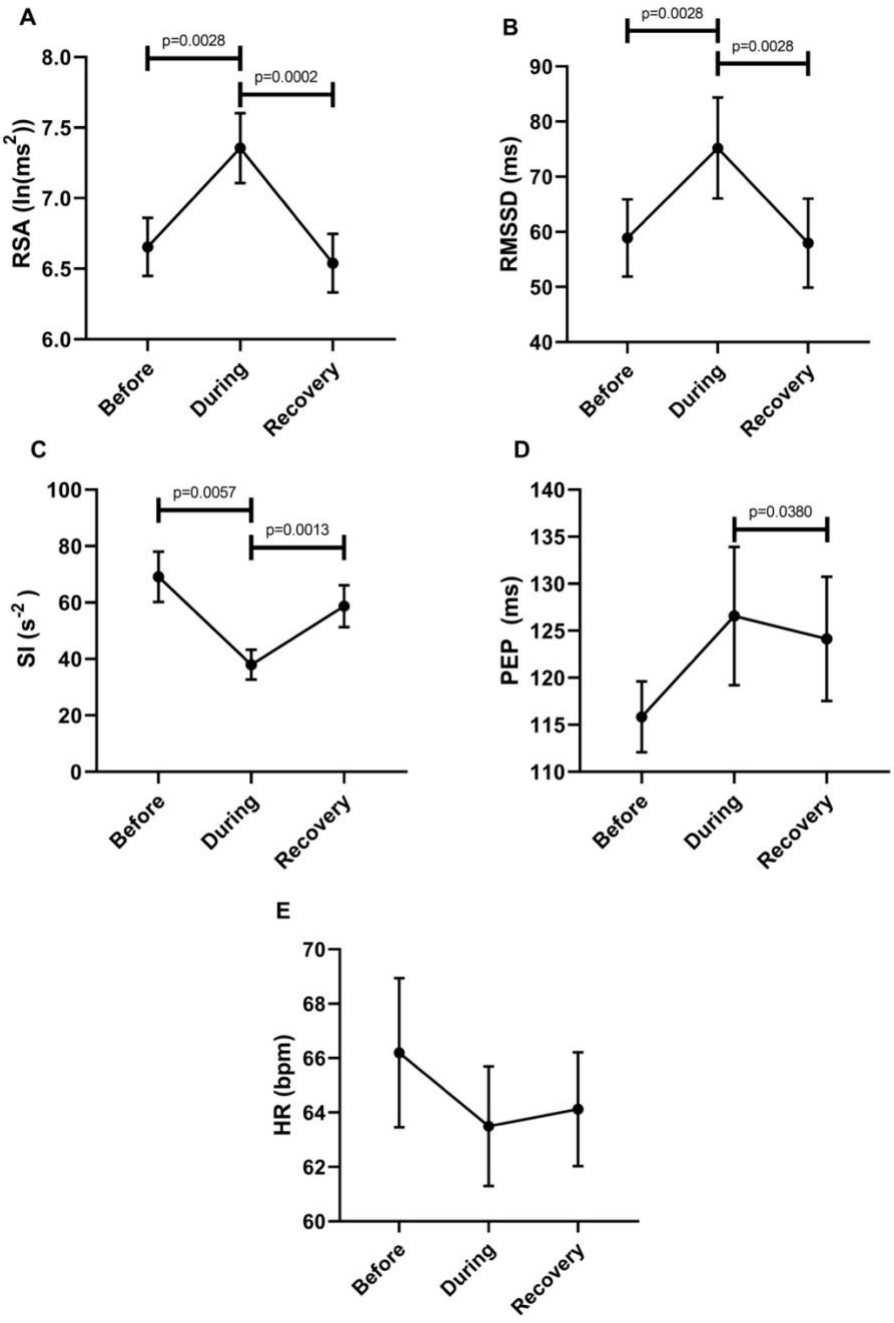

Figure 4-3: Changes in autonomic activity in response to all motor patterns.

Data sets are derived by averaging all 145 motor patterns within subjects, hence n = 11. The Friedman test was applied for assessment of significance, followed by the Dunn's multiple comparisons test. (A) RSA increased significantly during the motor activity and recovered within 2 min. (B) RMSSD increased significantly during the motor activity and recovered. (C) SI decreased significantly during the motor activity. (D)PEP decreased significantly after motor activity. (E) Heart rate remained unchanged.

4.4.3 Changes in Autonomic Reactivity Associated With the Different Motor Pattern Categories

4.4.3.1 Motor Complexes

Comparison of the 2 min quiet period preceding Motor Complexes with the period during the motor pattern revealed that this motor pattern was associated with an increase in parasympathetic activity reflected by an increase in RSA (W-M; $p = 0.0039$) and RMSSD (W-M; $p = 0.0078$) ($n = 11$). Motor Complexes were associated with a simultaneous decrease in sympathetic activity as reflected by an increase in the PEP value (W-M; $p = 0.0078$). During the Motor Complexes, the heart rate did not change.

In order to evaluate a potential recovery, we analyzed autonomic parameters before, during and after the Motor Complexes. This confirmed an increase in parasympathetic activity reflected by an increase in RSA, and a decrease in sympathetic activity reflected by both SI and PEP (Figure 4). Recovery was significant for RSA, RMSSD and PEP (Figure 4). The heart rate was significantly higher in the recovery period compared to during the motor pattern (Figure 4).

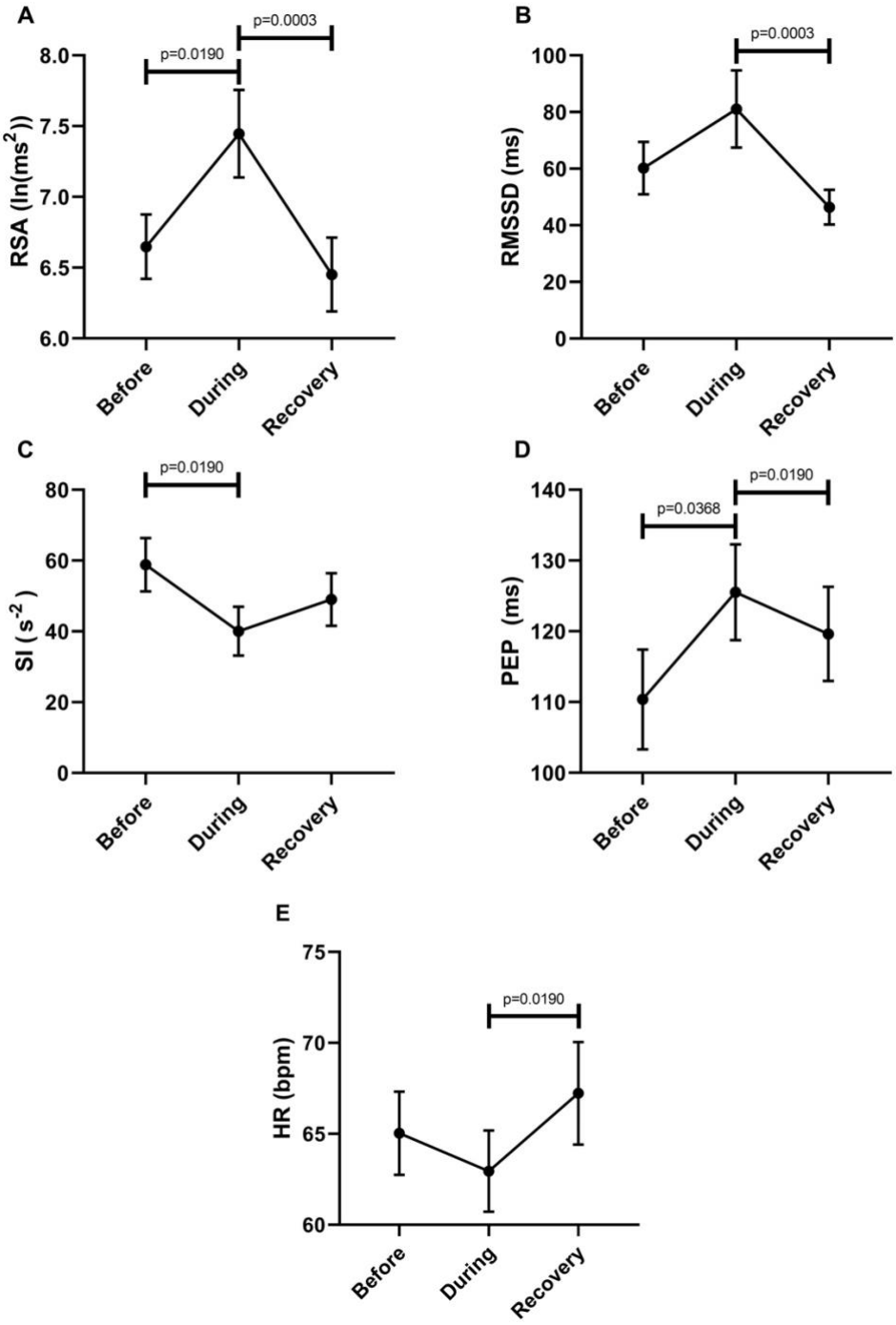

Figure 4-4: Overall changes in autonomic activity in response to Motor Complexes

(N = 42; n = 9). The following HRV parameters were assessed: RSA (A), RMSSD (B), the Baevsky's Stress Index (SI) (C), PEP (D), and heart rate (E). Data sets were derived by averaging all motor patterns within subjects, hence n = 9). The Friedman test was applied for assessment of significance followed by Dunn's multiple comparisons test (F-M).

Figure 5 shows RSA and SI reactivity of all 42 Motor Complexes as percent change. RMSSD and PEP are shown in Supplementary Figure S1.

The analysis of the other motor patterns were executed in the same manner as the Motor Complexes.

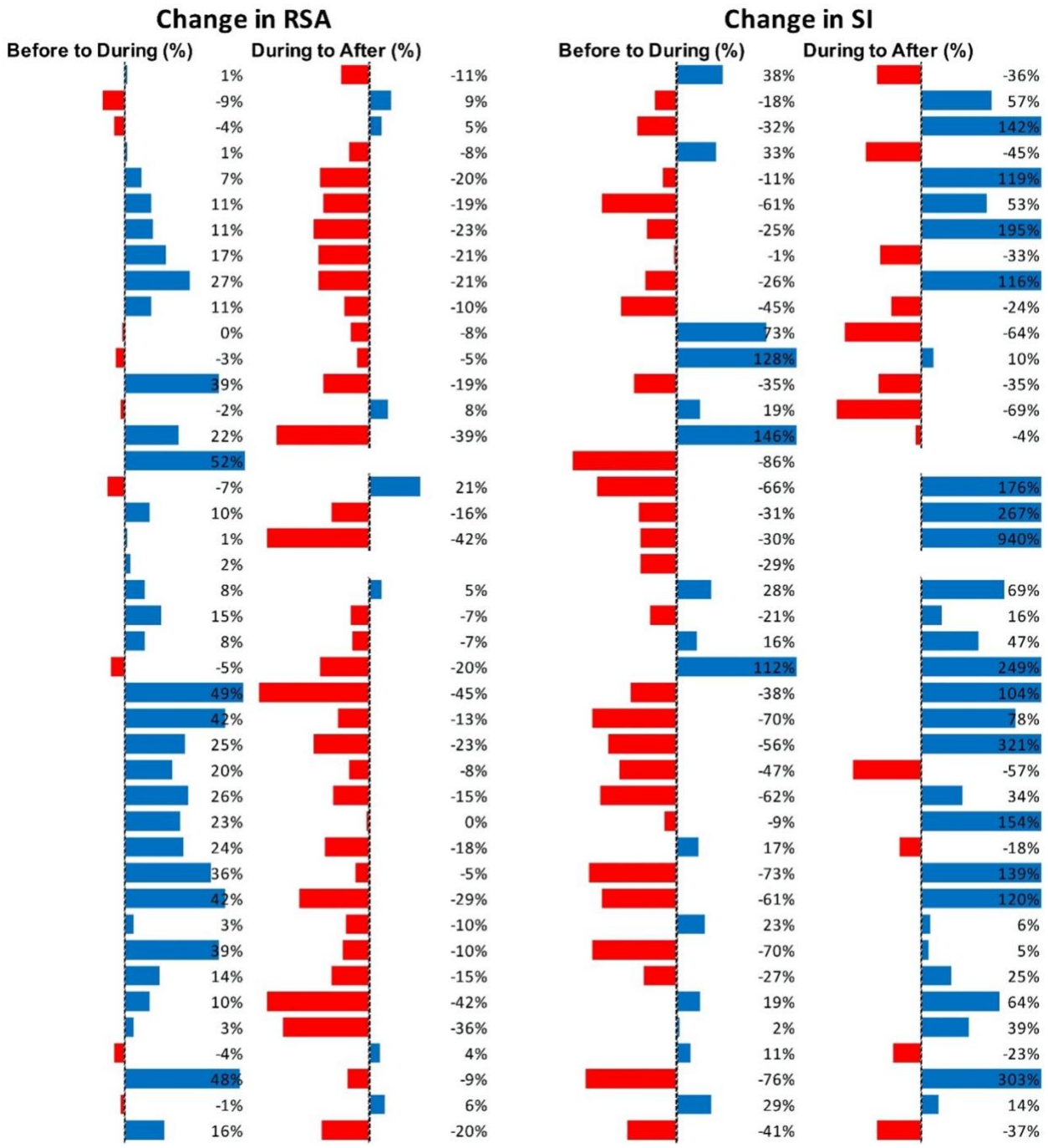

Figure 4-5: Changes in autonomic activity in response to all individual Motor Complexes

(N = 42). Data are shown as% change. The Friedman test was applied for assessment of significance followed by Dunn's multiple comparisons test. RSA: before to during p = 0.0007; during to recovery, p < 0.0001. SI: before to during p = 0.0104; during to recovery, p ≤ 0.0001 (F-D).

4.4.3.2 **HAPW-SPWs**

Compared to the 2 min quiet period preceding the HAPW-SPWs, this motor pattern was associated with an increase in RSA (W-M; $p = 0.0469$) and a decrease in SI ($p = 0.0313$). Other parameters did not change significantly.

To assess potential recovery, the data sets before, during and after motor activity were compared (Figure 6). First, this confirmed an increase in parasympathetic activity (RSA) and a decrease in sympathetic activity (SI). Only the recovery after SI reached significance (Figure 6C). The heart rate did not change significantly.

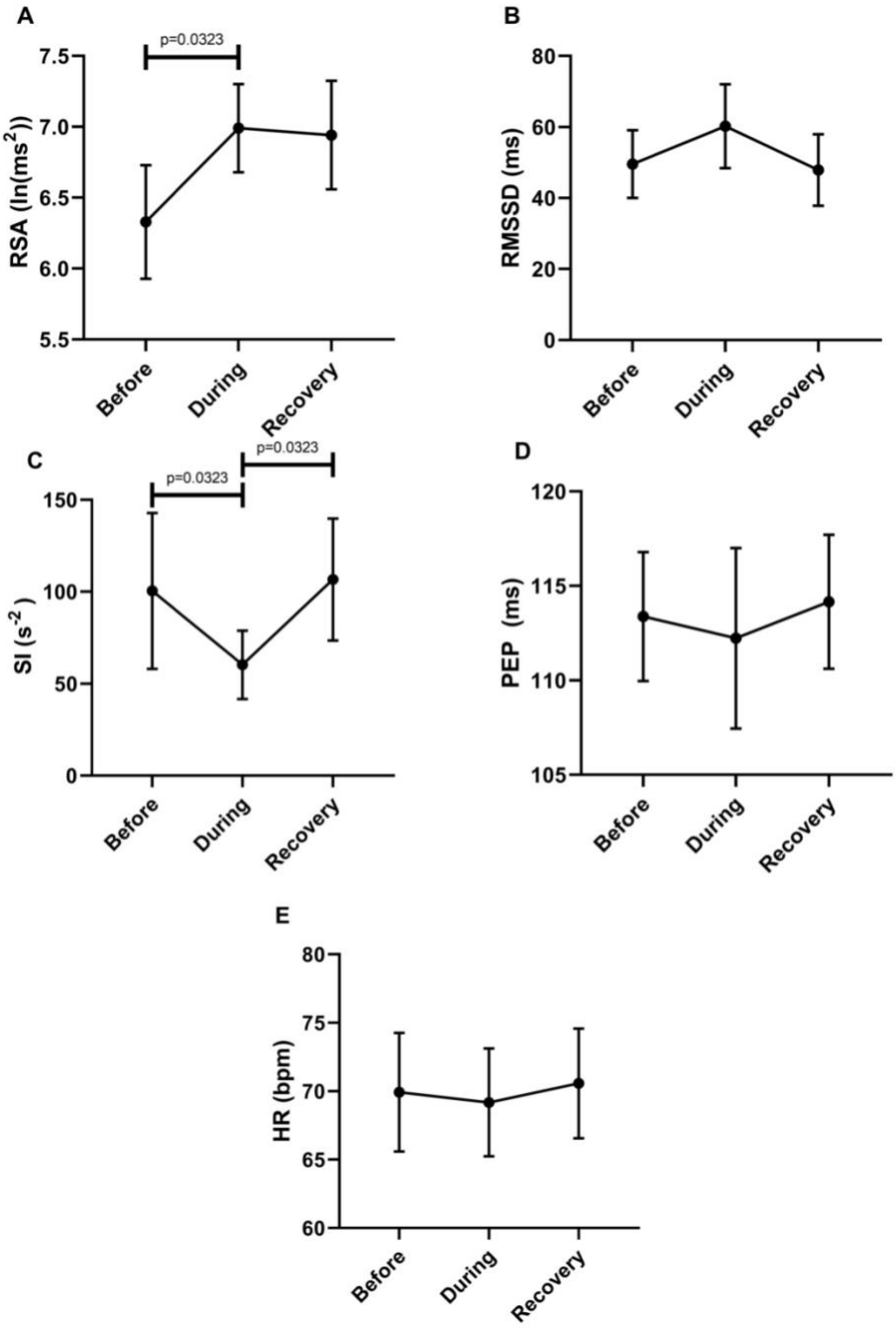

Figure 4-6: Overall changes in autonomic activity in response to HAPW-SPW's.

Data sets are derived by averaging all 45 motor patterns within 7 subjects, hence n = 7. The following HRV parameters were assessed: RSA (A), RMSSD (B), the Baevsky's Stress Index (SI) (C), PEP (D), and heart rate (E). The Friedman test was applied for assessment of significance followed by Dunn's multiple comparisons test (F-D-M).

Figure 7 shows RSA and SI reactivity of all 45 HAPW-SPWs as percent change. RMSSD and PEP are shown in Supplementary Figure S2.

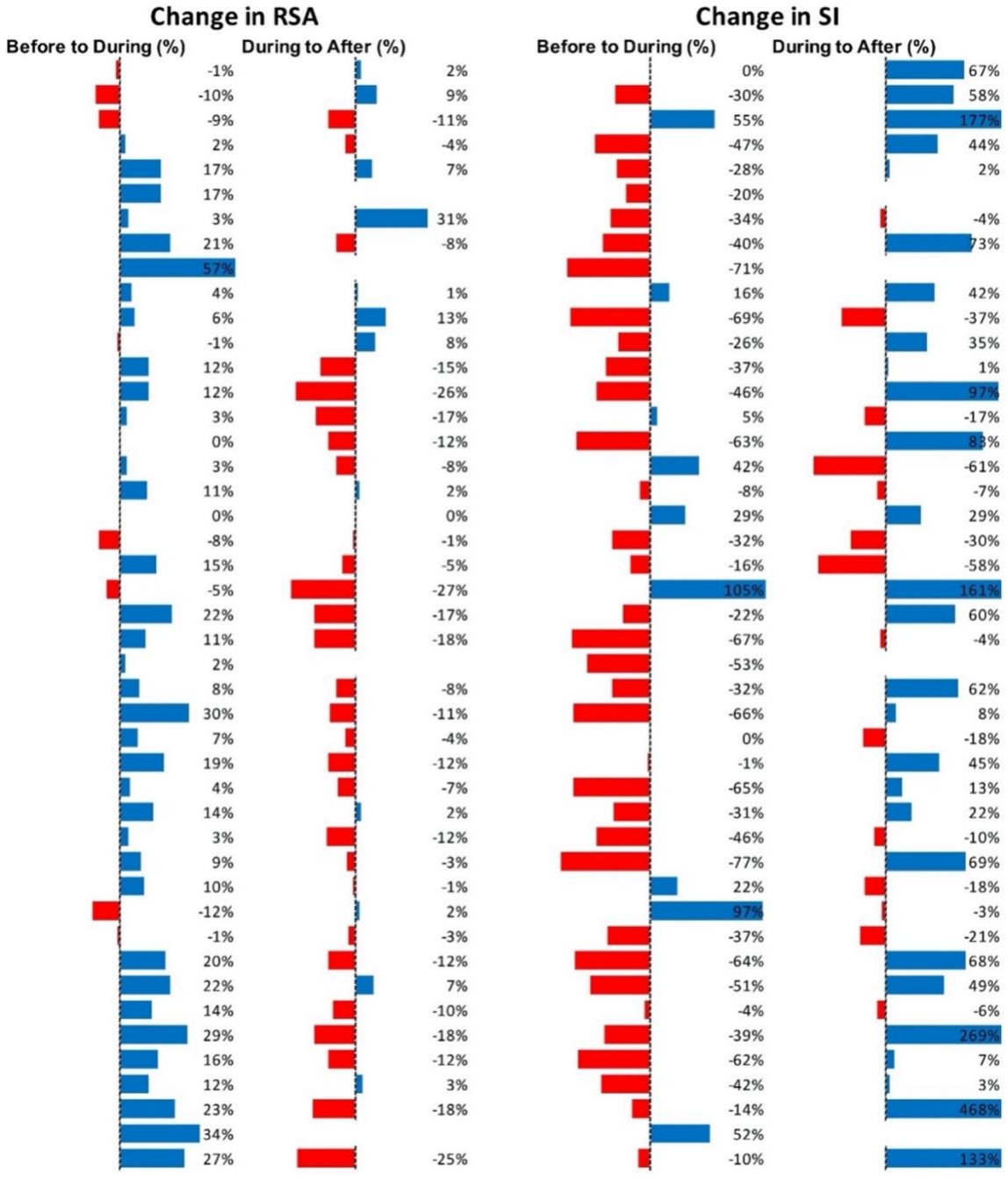

Figure 4-7: Changes in autonomic activity in response to all HAPW-SPW's

N = 45. Data are shown as % change. The Friedman test was applied for assessment of significance followed by Dunn's multiple comparisons test. RSA: before to during p = 0.0018;

during to recovery, p ≤ 0.0001. SI: before to during p = 0.0022; during to recovery, p < 0.0001 (F-D).

4.4.3.3 **HAPWs**

Comparing to the 2 min quiet period preceding the HAPWs, this motor pattern was associated with an increase in RSA (W-M; p = 0.0313) and a decrease in SI (W-M; p = 0.0313). Other parameters did not change significantly.

To assess potential recovery, the data sets before, during and after motor activity were compared, based on mean values from each individual (n = 6) (Figure 8). First, this confirmed that RSA increased significantly from before to during and that the SI decreased significantly comparing before to during. The SI recovered significantly within 2 min after the HAPW. Heart rate did not change.

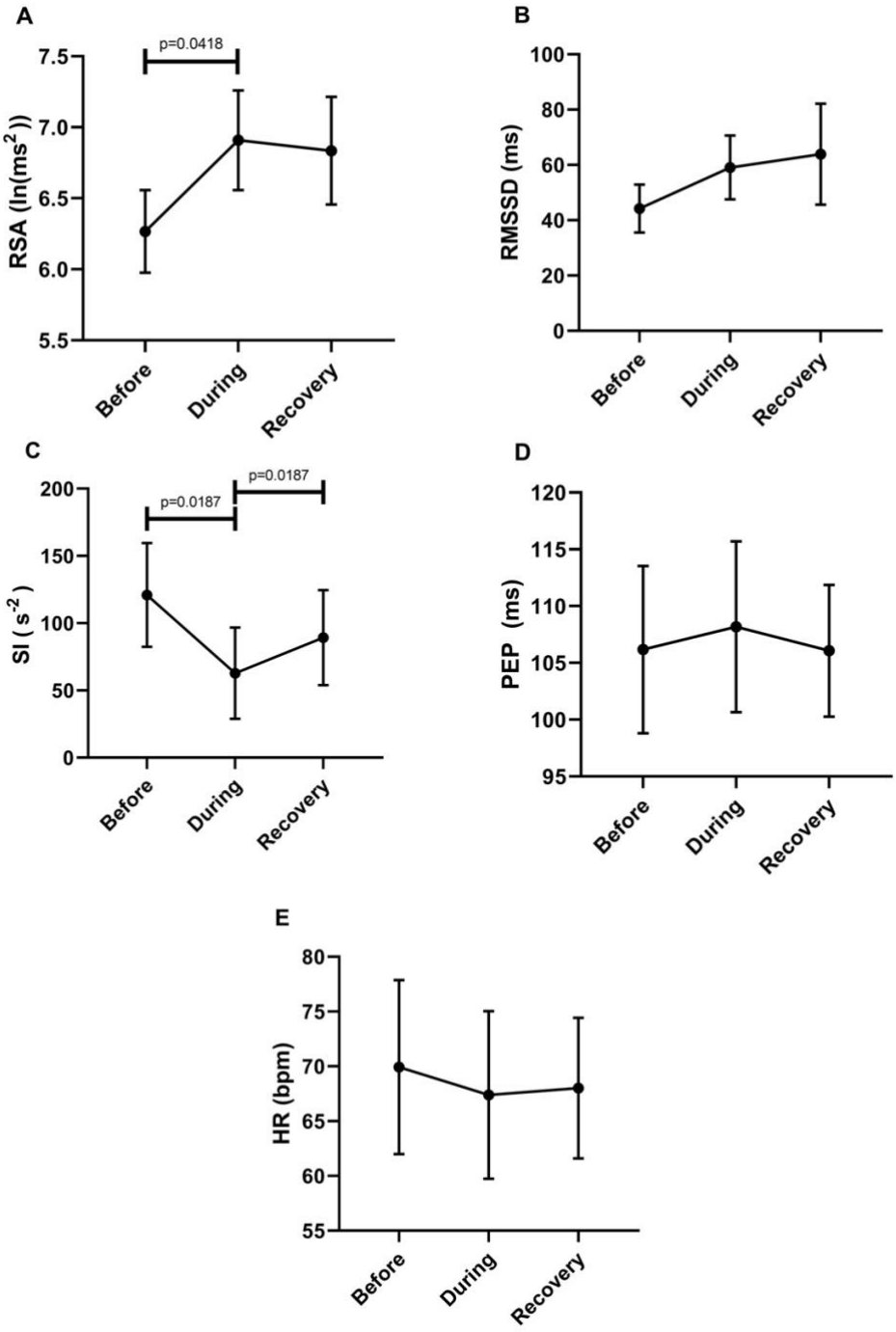

Figure 4-8: Overall changes in autonomic activity in response to HAPW's.

Data sets are derived by averaging all motor patterns within subjects, hence n = 6). The following HRV parameters were assessed: RSA (A), RMSSD (B), the Baevsky's Stress Index (SI) (C), PEP (D), and heart rate (E). The Friedman test was applied for assessment of significance followed by Dunn's multiple comparisons test (F-D-M).

Figure 9 shows RSA and SI reactivity of all 28 HAPWs as percent change. RMSSD and PEP are shown in Supplementary Figure S3.

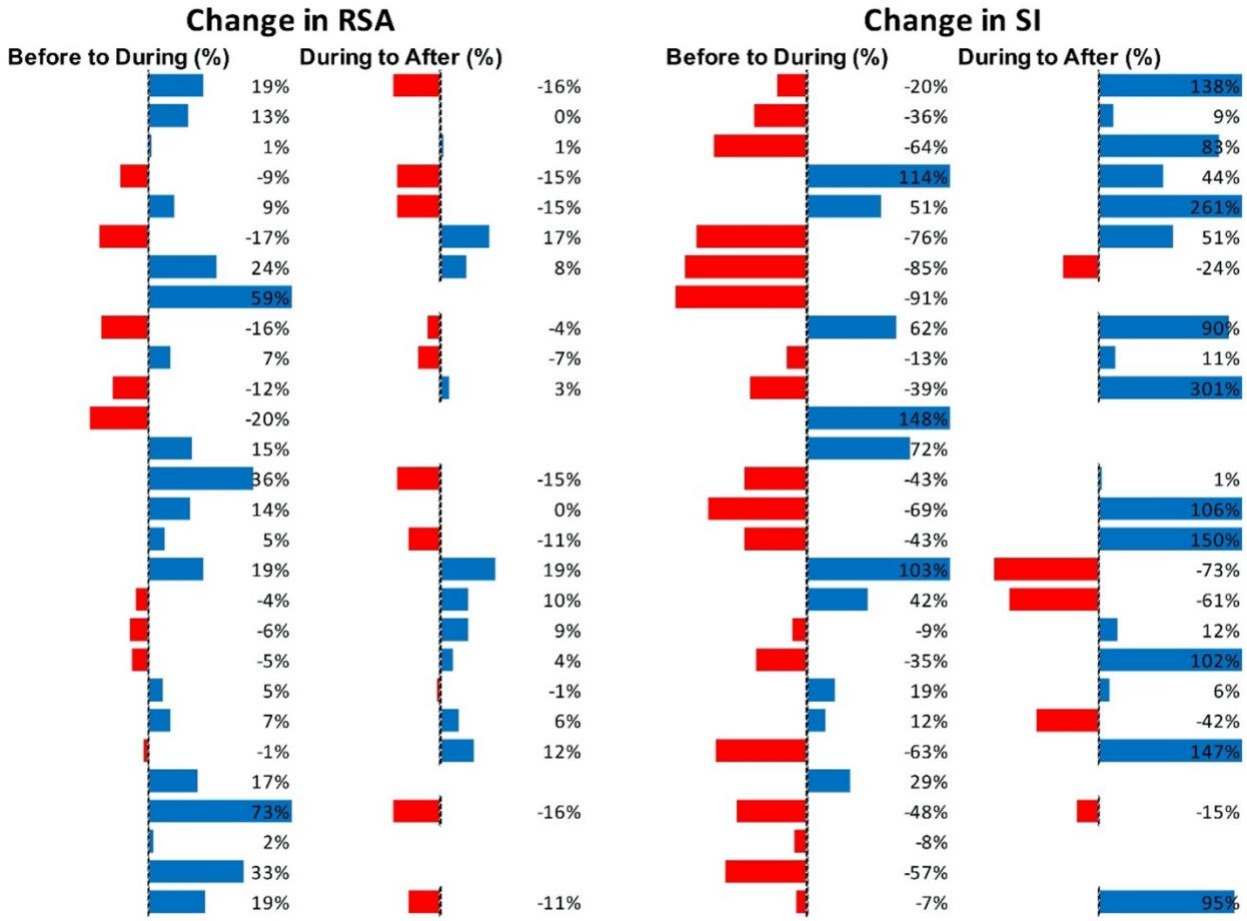

Figure 4-9: Changes in autonomic activity in response to all HAPW's

(N = 28). Data are shown as % change. The Friedman test was applied for assessment of significance followed by Dunn's multiple comparisons test. RSA: before to during, not significant; during to recovery, not significant. SI: before to during p = 0.0389; during to recovery, p = 0.004 (F-D).

4.4.3.4 **SPWs**

Compared to the 2 min quiet period preceding the SPWs, this motor pattern was not associated with any significant changes in HRV parameters.

To assess potential recovery, the data sets before, during and after motor activity were compared, based on mean values from each individual (n = 6) (Figure 10). Recovery of RSA was significant, but the differences between during and after did not reach significance in the first 2 min after the motor pattern for any of the other HRV parameters (F-D-M). The heart rate did not change significantly.

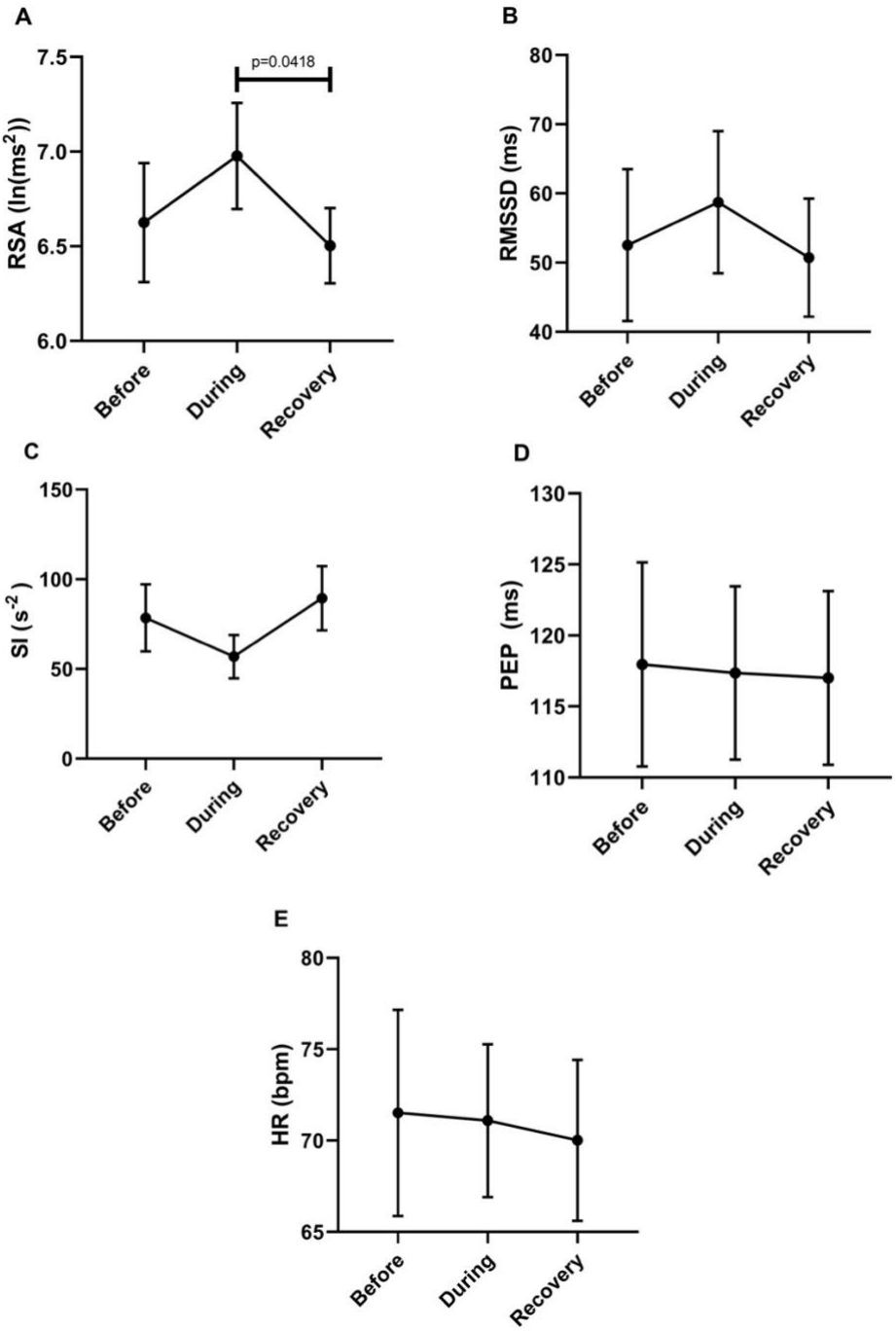

Figure 4-10: Overall Changes in autonomic activity in response to 30 SPW's.

Data sets were derived by averaging all motor patterns within subjects, hence n = 6. The following HRV parameters were assessed: RSA (A), RMSSD (B), the Baevsky's Stress Index (SI) (C), PEP (D), and heart rate (E). The Friedman test was applied for assessment of significance followed by Dunn's multiple comparisons test (F-D-M).

Figure 11 shows RSA and SI reactivity of all SPWs as percent change. RMSSD and PEP are shown in Supplementary Figure S4.

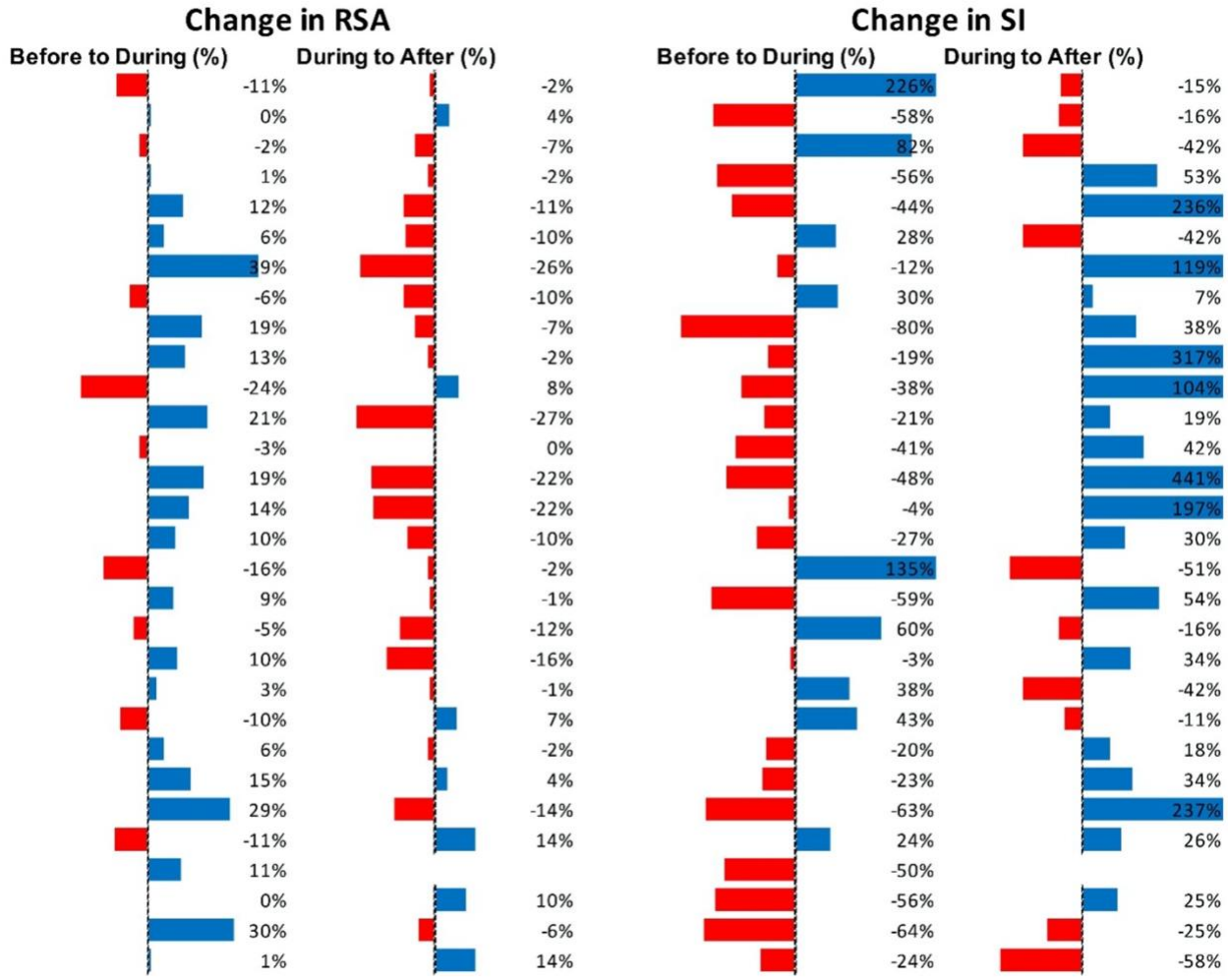

Figure 4-11: Changes in autonomic activity in response to all SPW's (N = 30).

Data are shown as % change. The Friedman test was applied for assessment of significance followed by Dunn's multiple comparisons test. RSA: before to during, ns; during to recovery, p = 0.0142. SI: before to during: ns.; during to recovery, p = 0.0021 (F-D).

4.4.4 Correlations Between General Autonomic Reactivity and Reactivity Associated With Motor Patterns

The HAPW associated change in RSA from before to during the motor pattern was correlated with the supine value of RSA (R^2 = 0.6057, p < 0.05) (Figure 12A). The HAPW associated change was also correlated with the supine value of RMSSD (R^2 = 0.7952, p < 0.05) as well as the change in RMSSD from supine to standing (R^2 = 0.8330, p < 0.05) (Figures 12B,C). The supine value of PEP showed a correlation to the change in PEP value during HAPW-SPW (R^2 = 0.6645, p < 0.05) (Figure 12D).

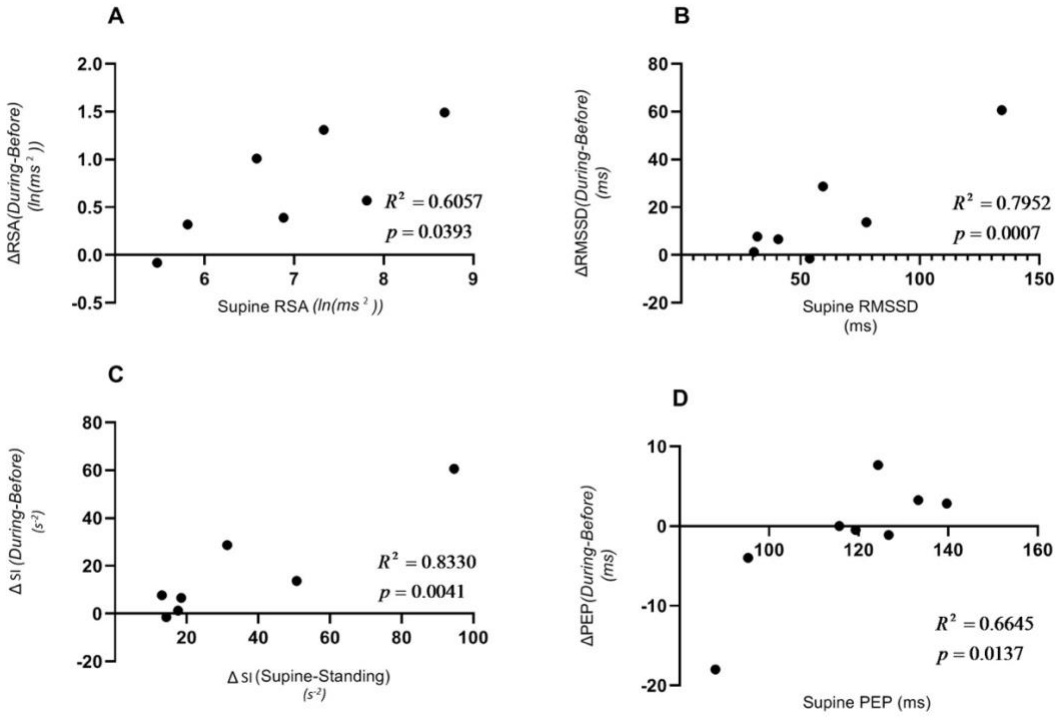

Figure 4-12: Correlations between supine HRV parameters and changes in HRV parameters due to posture changes compared to the changes in those measures due to motor activity. (A)Correlation between RSA during supine rest and change in RSA during HAPW. (B) Correlation between RMSSD during supine rest and change in RSA during HAPW. (C) Correlation between change in RMSSD from supine to standing and change in RSA during HAPW. (D)Correlation between PEP during supine rest and change in PEP during HAPW-SPW.

The remaining measures of autonomic reactivity during supine as well as change from supine to standing were not significantly correlated to changes in autonomic activity during motor patterns ($p > 0.05$) (Supplementary Figures S5–S8).

4.5 Discussion

Abnormal colonic motility, incontinence, and constipation including the inability to have spontaneous bowel movements may be associated with organic pathophysiology such as dysfunction of the enteric nervous system (Obermayr et al., 2013) or a marked reduction in ICC (Knowles and Farrugia, 2011). Alternatively, colonic motility may be abnormal due to dysfunctional brain-gut communication, such as an inability to sense a stimulus that would generate an urge to defecate, or an inability to properly respond to an urge to defecate. The ANS is involved in both sensation (a trigger for initiation of colonic motor patterns) and execution of motility and this is controlled or affected by the CAN (Roy and Green, 2019). Brain-gut communication dysfunction may also result in more subtle changes leading to hard stool or hyper-responsiveness to environmental stress (Chen et al., 2011; Mayer and Tillisch, 2011; Mazurak et al., 2012). The present study suggests some tools to investigate this further. A better understanding of the role of (abnormal) autonomic activity in conjunction with colonic motor dysfunction will lead to better understanding of underlying pathophysiology and may pave the way for evidence based treatment involving the autonomic control systems (Knowles et al., 2001; Knowles and Farrugia, 2011; Knowles et al., 2013; Bonaz et al., 2016).

The goal of this study was to assess whether autonomic activity associated with colonic motor patterns would be reflected in changes in HRV. Taking all motor patterns into account, it is clear that colonic motor patterns are accompanied by increased parasympathetic activity and

decreased sympathetic activity, reflected in HRV changes, that may occur without eliciting a significant change in heart rate (Figure 3).

Motor Complexes, HAPW-SPWs and HAPWs are all associated with an increase in RSA and a decrease in SI. Hence RSA and SI may best reflect autonomic activity in the colon during these motor patterns as compared to RMSSD and PEP. It is important to state that SI and PEP do not measure identical sympathetic reactivity, SI is based on HRV whereas PEP is based on vascular tone changes.

The SPW, which is a very low amplitude pressure wave, did not significantly change the autonomic measures employed here.

Measurements of supine RSA and RSA changes due to changes in body position are deemed to be stable measures of general autonomic health (Ernst, 2017) and deemed relevant for assessment of ANS function in IBS (Jarrett et al., 2016; Polster et al., 2018). In the present study, the magnitudes of RSA and RMSSD change evoked by change in body position from supine to standing showed a marked decrease in parasympathetic reactivity, as expected (Mestanik et al., 2019). There was no significant change in PEP between supine and standing, which is consistent with the fact that moderate exercise may not show significant changes in sympathetic reactivity *as measured by PEP*(Alex et al., 2013). Nevertheless, SI showed a significant increase in sympathetic reactivity from supine or sitting to walking.

We show here that the magnitude of RSA and RMSSD changes evoked by change in body position from supine to standing was positively correlated with the magnitude of RSA and RMSSD changes associated with the HAPW. Hence, RSA or RMSSD reactivity to posture change may be a useful predictor of the ability to generate motor patterns that are dependent on

parasympathetic activity. This may not be of clinical significance for healthy subjects, but if such correlations would be confirmed and/or other correlations were to be discovered in patients with colon motor dysfunction, general autonomic reactivity may have predictive value and/or develop into parameters that might be evaluated for improvement in pathophysiology in response to treatment.

The NTS is critical for regulation of both heart rate and gut motility (Browning and Travagli, 2014; Babic et al., 2015) involving distinct regions within the NTS; nevertheless, there is significant cross talk between neurons affecting heart rate and gut function (Castle et al., 2005). Indeed, functionally identified NTS neurons appear to lack viscerotopic organization despite the fact that many distinct reflex pathways for the gastrointestinal tract, the lung and the heart are routed through the NTS (Janig, 2006). The NTS may therefore be a nexus for interactions between autonomic regulation of the three systems. In addition to significant integration of inputs from all these areas within the NTS (Janig, 2006), there are direct projections to the NTS from the cortex, amygdala and the hypothalamus (van der Kooy et al., 1984). Hence specific activities from higher brain centers likely influence both cardiac and gut regulation through the NTS (Castle et al., 2005; Roy and Green, 2019). We hypothesize a model in which the autonomic changes observed in the present study are associated with the following actions: motor patterns associated with rectal balloon distention or rectal bisacodyl start with rectal stimulation leading to sensory neural activity entering the defecation center in the sacral cord followed by sensory neural activity going up the spinal cord to Barrington's nucleus and the NTS (Taché et al., 2004, 2005; Grundy et al., 2006). The Barrington nucleus has control over the sacral parasympathetic nucleus and thus has control over the motility of the bladder and the

distal colon (Valentino et al., 1999; Sasaki and Sato, 2013). Multi-directional communication between the NTS, the vagal motor nucleus and higher brain center follows (van der Kooy et al., 1984). Parasympathetic vagal and sacral motor activity then initiate colonic motor patterns that start in the proximal colon and proceed all the way to the rectum ending with relaxation of the anal sphincter (Chen et al., 2018). Although the vagal motor nucleus is predominantly associated with proximal colon activity, and hence is likely involved in triggering motor patterns that start in the proximal colon, it may well be that vagal fibers are controlling motor patterns all the way to the rectum (Powley, 2000). Spontaneous propulsive motor patterns may use similar pathways. We propose that it is this neural activity within the extrinsic ANS which accompanies initiation and execution of motor patterns, that is reflected in changes in HRV. The preejection period or PEP is the time elapsed between the electrical depolarization of the left ventricle (Q in the QRS complex in the ECG) and the beginning of ventricular ejection and represents the period of left ventricular contraction with the cardiac valves closed (Lanfranchi et al., 2017); it is an index of cardiac sympathetic (β-adrenergic) activity (Krohová et al., 2017). The SI is purely based on the RR intervals. With an increase in sympathetic activity, the HRV decreases, hence the variation in RR intervals tends to decrease (Baevsky and Chernikova, 2017). Although PEP and the SI are based on different metrics, both showed responsivity to motor patterns elicited during manometry, in the expected directions; but it is likely that not all HRV parameters reflect non-cardiac autonomic activity equally (Massaro and Pecchia, 2019). Only the Motor Complexes were associated with a change in PEP. in contrast, the Baevsky index was markedly affected during all motor patterns except the SPW, suggesting that the Baevsky index better reflects changes in sympathetic activity related to colon motor patterns.

Although the number of participants was relatively small, a large number of motor patterns (145) was available for analysis. Strong arguments have been put forward for the relevance of studies where a large number of observations are made on a relatively small number of experimental participants (Smith and Little, 2018). The temporal relationship between motor patterns and changes in autonomic measures of HRV demonstrates that colonic motor patterns are accompanied by significant parasympathetic autonomic neural activity and by withdrawal of sympathetic activity. Sacral nerves to the colon contain sensory and motor neurons, hence the autonomic activity may reflect motor neuron activity that initiates the motor patterns and/or sensory neural activity that precedes the motor patterns or is induced by the motor patterns. The distinction between the influences of sensory factors versus motor activities needs more stringent investigation. In the present study, motor patterns were initiated by different stimuli such as meal and bisacodyl; in the future, when more data become available, it will be important and interesting to subdivide the motor patterns according to their particular initiators. It is possible that motor patterns such as the SPW are associated with parasympathetic autonomic changes but that these changes do not exceed the magnitude of the inevitable physiologic “noise” in the recordings.

In conclusion, colonic motor patterns are associated with activity in the ANS that is reflected in HRV parameters. These autonomic measures may serve as proxies for autonomic neural dysfunction in patients with colonic dysmotility.

Data Availability Statement

All datasets generated for this study are included in the article/Supplementary Material.

Ethics Statement

The studies involving human participants were reviewed and approved by the Hamilton Integrated Research Ethics Board. The participants provided their written informed consent to participate in this study.

Funding

This study was supported by the Canadian Institutes of Health Research (CIHR) grants 12874 and 152942, as well as a Natural Sciences and Engineering Research Council (NSERC) grant 386877 to JH. MA and LL received full salary support from the Farncombe Family Digestive Health Research Institute, awarded to JH and J-HC, respectively. SP and J-HC were supported in part by research scholarships from the Farncombe Family Digestive Health Research Institute. Further support was received from the Hamilton Academic Health Sciences Organization (HAHSO) to ER and the Canadian Foundation for Innovation Leadership fund to JH. YY was supported by the Department of Gastroenterology at the Sun Yat-sen Memorial Hospital in Guangzhou, Guangdong, China. WT was supported by the National Natural Science Foundation of China (NSFC 81600423) and the Chinese Scholarship Council.

Conflict of Interest

The authors declare that the research was conducted in the absence of any commercial or financial relationships that could be construed as a potential conflict of interest.

Acknowledgments

Prof. Paul Moayyedi, assistant dean of clinical studies at McMaster University was consulted for the statistical analysis.

Supplementary Material

The Supplementary Material for this article can be found online at: https://www.frontiersin.org/articles/10.3389/fnins.2019.01447/full#supplementary-material

4.6 References

Alex, C., Lindgren, M., Shapiro, P. A., McKinley, P. S., Brondolo, E. N., Myers, M. M., et al. (2013). Aerobic exercise and strength training effects on cardiovascular sympathetic function in healthy adults: a randomized controlled trial. *Psychosom. Med.* 75, 375–381. doi: 10.1097/psy.0b013e3182906810

PubMed Abstract | CrossRef Full Text | Google Scholar

Babic, T., Ambler, J., Browning, K. N., and Travagli, R. A. (2015). Characterization of synapses in the rat subnucleus centralis of the nucleus tractus solitarius. *J. Neurophysiol.* 113, 466–474. doi: 10.1152/jn.00598.2014

PubMed Abstract | CrossRef Full Text | Google Scholar

Baevsky, R. M., and Chernikova, A. G. (2017). Heart rate variability analysis: physiological foundations and main methods. *Cardiometry* 66–67. doi: 10.12710/cardiometry.2017.10.6676

CrossRef Full Text | Google Scholar

Beauchaine, T. P., and Thayer, J. F. (2015). Heart rate variability as a transdiagnostic biomarker of psychopathology. *Int. J. Psychophysiol.* 98, 338–350. doi: 10.1016/j.ijpsycho.2015.08.004

PubMed Abstract | CrossRef Full Text | Google Scholar

Bharucha, A. E. (2012). High amplitude propagated contractions. *Neurogastroenterol. Motil.* 24, 977–982. doi: 10.1111/nmo.12019

PubMed Abstract | CrossRef Full Text | Google Scholar

Bharucha, A. E., Camilleri, M., Low, P. A., and Zinsmeister, A. R. (1993). Autonomic dysfunction in gastrointestinal motility disorders. *Gut* 34, 397–401. doi: 10.1136/gut.34.3.397

PubMed Abstract | CrossRef Full Text | Google Scholar

Bharucha, A. E., Low, P. A., Camilleri, M., Burton, D., Gehrking, T. L., and Zinsmeister, A. R. (2008). Pilot study of pyridostigmine in constipated patients with autonomic neuropathy. *Clin. Auton. Res.* 18, 194–202. doi: 10.1007/s10286-008-0476-x

PubMed Abstract | CrossRef Full Text | Google Scholar

Bonaz, B., Sinniger, V., and Pellissier, S. (2016). Vagal tone: effects on sensitivity, motility, and inflammation. *Neurogastroenterol. Motil.* 28, 455–462. doi: 10.1111/nmo.12817

PubMed Abstract | CrossRef Full Text | Google Scholar

Brierley, S. M., Jones, R. C., Gebhart, G. F., and Blackshaw, L. A. (2004). Splanchnic and pelvic mechanosensory afferents signal different qualities of colonic stimuli in mice. *Gastroenterology* 127, 166–178. doi: 10.1053/j.gastro.2004.04.008

PubMed Abstract | CrossRef Full Text | Google Scholar

Brookes, S., Chen, N., Humenick, A., Spencer, N. J., and Costa, M. (2016). Extrinsic sensory innervation of the gut: structure and function. *Adv. Exp. Med. Biol.* 891, 63–69. doi: 10.1007/978-3-319-27592-5_7

PubMed Abstract | CrossRef Full Text | Google Scholar

Browning, K. N., and Travagli, R. A. (2014). Central nervous system control of gastrointestinal motility and secretion and modulation of gastrointestinal functions. *Compr. Physiol.* 4, 1339–1368. doi: 10.1002/cphy.c130055

PubMed Abstract | CrossRef Full Text | Google Scholar

Callaghan, B., Furness, J. B., and Pustovit, R. V. (2018). Neural pathways for colorectal control, relevance to spinal cord injury and treatment: a narrative review. *Spinal Cord* 56, 199–205. doi: 10.1038/s41393-017-0026-2

PubMed Abstract | CrossRef Full Text | Google Scholar

Castle, M., Comoli, E., and Loewy, A. D. (2005). Autonomic brainstem nuclei are linked to the hippocampus. *Neuroscience* 134, 657–669. doi: 10.1016/j.neuroscience.2005.04.031

PubMed Abstract | CrossRef Full Text | Google Scholar

Chen, J. H., Parsons, S. P., Shokrollahi, M., Wan, A., Vincent, A. D., Yuan, Y., et al. (2018). Characterization of simultaneous pressure waves as biomarkers for colonic motility assessed by high-resolution colonic manometry. *Front. Physiol. Gastrointest. Sci.* 9:1248. doi: 10.3389/fphys.2018.01248

PubMed Abstract | CrossRef Full Text | Google Scholar

Chen, J. H., Yu, Y., Yang, Z., Yu, W. Z., Chen, W. L., Kim, M. J. M., et al. (2017). Intraluminal pressure patterns in the human colon assessed by high-resolution manometry. *Sci. Rep.* 7:41436. doi: 10.1038/srep41436

PubMed Abstract | CrossRef Full Text | Google Scholar

Chen, J. Y., Blankstein, U., Diamant, N. E., and Davis, K. D. (2011). White matter abnormalities in irritable bowel syndrome and relation to individual factors. *Brain Res.* 1392, 121–131. doi: 10.1016/j.brainres.2011.03.069

PubMed Abstract | CrossRef Full Text | Google Scholar

Costa, M., and Brookes, S. H. (2008). Architecture of enteric neural circuits involved in intestinal motility. *Eur. Rev. Med. Pharmacol. Sci.* 12(Suppl. 1), 3–19.

PubMed Abstract | Google Scholar

Devroede, G., and Lamarche, J. (1974). Functional importance of extrinsic parasympathetic innervation to the distal colon and rectum in man. *Gastroenterology* 66, 273–280. doi: 10.1016/s0016-5085(74)80114-9

CrossRef Full Text | Google Scholar

Draghici, A. E., and Taylor, J. A. (2016). The physiological basis and measurement of heart rate variability in humans. *J. physiol. anthropol.* 35:22.

PubMed Abstract | Google Scholar

Ernst, G. (2017). Heart-rate variability-more than heart beats. *Front. Public Health* 5:240. doi: 10.3389/fpubh.2017.00240

PubMed Abstract | CrossRef Full Text | Google Scholar

Fazeli, M. S., Collet, J. P., MacNeily, A. E., and Afshar, K. (2016). Cardiac autonomic nervous system activity in children with bladder and bowel dysfunction. *J. Urol.* 195, 1245–1249. doi: 10.1016/j.juro.2015.11.020

PubMed Abstract | CrossRef Full Text | Google Scholar

Furness, J. B. (2012). The enteric nervous system and neurogastroenterology. *Nat. Rev. Gastroenterol. Hepatol.* 9, 286–294. doi: 10.1038/nrgastro.2012.32

PubMed Abstract | CrossRef Full Text | Google Scholar

Ghasemi, A., and Zahediasl, S. (2012). Normality tests for statistical analysis: a guide for non-statisticians. *Int. J. Endocrinol. Metab.* 10, 486–489. doi: 10.5812/ijem.3505

PubMed Abstract | CrossRef Full Text | Google Scholar

Grundy, D., Al-Chaer, E. D., Aziz, Q., Collins, S. M., Ke, M., Tache, Y., et al. (2006). Fundamentals of neurogastroenterology: basic science. *Gastroenterology* 130, 1391–1411. doi: 10.1053/j.gastro.2005.11.060

PubMed Abstract | CrossRef Full Text | Google Scholar

Huizinga, J. D. (2018). "The physiology and pathophysiology of interstitial cells of cajal: pacemaking, innervation, and stretch sensation," in *Physiology of the Gastrointestinal Tract*, eds H. Said, J. K. Kaunitz, F. Ghishan, J. Merchant, and J. Wood, (Amsterdam: Elsevier), 305–336.

Google Scholar

Janig, W. (2006). *The Integrative Action of the Autonomic Nervous System: Neurobiology of Homeostasis*. Cambridge, MA: Cambridge University Press.

Google Scholar

Jarrett, M. E., Cain, K. C., Barney, P. G., Burr, R. L., Naliboff, B. D., Shulman, R., et al. (2016). Balance of autonomic nervous system predicts who benefits from a self-management intervention program for irritable bowel syndrome. *J. Neurogastroenterol. Motil.* 22, 102–111. doi: 10.5056/jnm15067

PubMed Abstract | CrossRef Full Text | Google Scholar

Jáuregui-Renaud, K., Hermosillo, A. G., Márquez, M. F., Ramos-Aguilar, F., Hernández-Goribar, M., and Cárdenas, M. (2001). Repeatability of heart rate variability during simple cardiovascular reflex tests on healthy subjects. *Arch. Med. Res.* 32, 21–26. doi: 10.1016/s0188-4409(00)00255-1

PubMed Abstract | CrossRef Full Text | Google Scholar

Knowles, C. H., and Farrugia, G. (2011). Gastrointestinal neuromuscular pathology in chronic constipation. *Best Pract. Res. Clin. Gastroenterol.* 25, 43–57. doi: 10.1016/j.bpg.2010.12.001

PubMed Abstract | CrossRef Full Text | Google Scholar

Knowles, C. H., Lindberg, G., Panza, E., and De Giorgio, R. (2013). New perspectives in the diagnosis and management of enteric neuropathies. *Nat. Rev. Gastroenterol. Hepatol.* 10, 206–218. doi: 10.1038/nrgastro.2013.18

PubMed Abstract | CrossRef Full Text | Google Scholar

Knowles, C. H., Scott, S. M., and Lunniss, P. J. (2001). Slow transit constipation: a disorder of pelvic autonomic nerves? *Dig. Dis. Sci.* 46, 389–401.

PubMed Abstract | Google Scholar

Krohová, J., Czippelová, B., Turianiková, Z., Lazarová, Z., Tonhajzerová, I., and Javorka, M. (2017). Preejection period as a sympathetic activity index: a role of confounding factors. *Physiol. Res.* 66, S265–S275.

PubMed Abstract | Google Scholar

Lanfranchi, P. A., Pepin, J. L., and Somers, V. K. (2017). "Cardiovascular physiology: autonomic control in health and in sleep disorders," in *Principles and Practice of Sleep Medicine*, eds M. Kryger, T. Roth, and W. C. Dement, (Philadelphia, PA: Elsevier), 142–154.

Google Scholar

Massaro, S., and Pecchia, L. (2019). Heart rate variability (HRV) analysis: a methodology for organizational neuroscience. *Organ. Res. Methods* 22, 354–393. doi: 10.1177/1094428116681072

CrossRef Full Text | Google Scholar

Mathewson, K. J., Van Lieshout, R. J., Saigal, S., Boyle, M. H., and Schmidt, L. A. (2014). Reduced respiratory sinus arrhythmia in adults born at extremely low birth weight: evidence of premature parasympathetic decline. *Int. J. Psychophysiol.* 93, 198–203. doi: 10.1016/j.ijpsycho.2014.04.005

PubMed Abstract | CrossRef Full Text | Google Scholar

Mayer, E. A., and Tillisch, K. (2011). The brain-gut axis in abdominal pain syndromes. *Annu. Rev. Med.* 62, 381–396. doi: 10.1146/annurev-med-012309-103958

PubMed Abstract | CrossRef Full Text | Google Scholar

Mazurak, N., Seredyuk, N., Sauer, H., Teufel, M., and Enck, P. (2012). Heart rate variability in the irritable bowel syndrome: a review of the literature. *Neurogastroenterol. Motil.* 24, 206–216. doi: 10.1111/j.1365-2982.2011.01866.x

PubMed Abstract | CrossRef Full Text | Google Scholar

McIntyre, A. S., and Thompson, D. G. (1992). Adrenergic control of motor and secretory function in the gastrointestinal tract. *Aliment. pharmacol. ther.* 6, 125–142. doi: 10.1111/j.1365-2036.1992.tb00257.x

PubMed Abstract | CrossRef Full Text | Google Scholar

Mestanik, M., Mestanikova, A., Langer, P., Grendar, M., Jurko, A., Sekaninova, N., et al. (2019). Respiratory sinus arrhythmia–testing the method of choice for evaluation of cardiovagal regulation. *Respir. physiol. neurobiol.* 259, 86–92. doi: 10.1016/j.resp.2018.08.002

PubMed Abstract | CrossRef Full Text | Google Scholar

Obermayr, F., Hotta, R., Enomoto, H., and Young, H. M. (2013). Development and developmental disorders of the enteric nervous system. *Nat. Rev. Gastroenterol. Hepatol.* 10, 43–57. doi: 10.1038/nrgastro.2012.234

PubMed Abstract | CrossRef Full Text | Google Scholar

Parati, G., and Di Rienzo, M. (2003). Determinants of heart rate and heart rate variability. *J. Hypertens.* 21, 477–480. doi: 10.1097/00004872-200303000-00007

PubMed Abstract | CrossRef Full Text | Google Scholar

Polster, A., Friberg, P., Gunterberg, V., Öhman, L., Le Nevé, B., Törnblom, H., et al. (2018). Heart rate variability characteristics of patients with irritable bowel syndrome and associations with symptoms. *Neurogastroenterol. Motil.* 30:e13320. doi: 10.1111/nmo.13320

PubMed Abstract | CrossRef Full Text | Google Scholar

Powley, T. L. (2000). Vagal input to the enteric nervous system. *Gut* 47(Suppl. 4), iv30–iv32. discussion iv36,Google Scholar

Quigley, K. S., and Stifter, C. A. (2006). A comparative validation of sympathetic reactivity in children and adults. *Psychophysiology* 43, 357–365. doi: 10.1111/j.1469-8986.2006.00405.x

PubMed Abstract | CrossRef Full Text | Google Scholar

Roy, H. A., and Green, A. L. (2019). The central autonomic network and regulation of bladder function. *Front. neurosci.* 13:535. doi: 10.3389/fnins.2019.00535

PubMed Abstract | CrossRef Full Text | Google Scholar

Sasaki, M., and Sato, H. (2013). Polysynaptic connections between Barrington's nucleus and sacral preganglionic neurons. *Neurosci. Res.* 75, 150–156. doi: 10.1016/j.neures.2012.11.008

PubMed Abstract | CrossRef Full Text | Google Scholar

Schmidt, L. A., Santesso, D. L., Miskovic, V., Mathewson, K. J., McCabe, R. E., Antony, M. M., et al. (2012). Test-retest reliability of regional electroencephalogram (EEG) and cardiovascular measures in social anxiety disorder (SAD). *Int. J. Psychophysiol.* 84, 65–73. doi: 10.1016/j.ijpsycho.2012.01.011

PubMed Abstract | CrossRef Full Text | Google Scholar

Shaffer, F., and Ginsberg, J. P. (2017). An overview of heart rate variability metrics and norms. *Front. Public Health* 5:258. doi: 10.3389/fpubh.2017.00258

PubMed Abstract | CrossRef Full Text | Google Scholar

Smith, P. L., and Little, D. R. (2018). Small is beautiful: in defense of the small-N design. *Psychon. bull. rev.* 25, 2083–2101. doi: 10.3758/s13423-018-1451-8

PubMed Abstract | CrossRef Full Text | Google Scholar

Spencer, N. J., Dinning, P. G., Brookes, S. J., and Costa, M. (2016). Insights into the mechanisms underlying colonic motor patterns. *J. Physiol.* 594, 4099–4116. doi: 10.1113/JP271919

PubMed Abstract | CrossRef Full Text | Google Scholar

Szurszewski, J. H., Ermilov, L. G., and Miller, S. M. (2002). Prevertebral ganglia and intestinofugal afferent neurones. *Gut*51(Suppl. 1), i6–i10. doi: 10.1136/gut.51.suppl_1.i6

PubMed Abstract | CrossRef Full Text | Google Scholar

Tache, Y. (2003). “The parasympathetic nervous system in the pathophysiology of the gastrointestinal tract,” in *Handbook of the Autonomic Nervous System*, eds C. L. Bolis, J. Licinio, and S. Govoni, (Basel: Marcel Dekker Inc.), 463–504.

Google Scholar

Taché, Y., Martinez, V., Wang, L., and Million, M. (2004). CRF1 receptor signaling pathways are involved in stress-related alterations of colonic function and viscerosensitivity: implications for irritable bowel syndrome. *Br. J. Pharmacol.* 141, 1321–1330. doi: 10.1038/sj.bjp.0705760

PubMed Abstract | CrossRef Full Text | Google Scholar

Taché, Y., Million, M., Nelson, A. G., Lamy, C., and Wang, L. (2005). Role of corticotropin-releasing factor pathways in stress-related alterations of colonic motor function and viscerosensibility in female rodents. *Gend. Med.* 2, 146–154. doi: 10.1016/s1550-8579(05)80043-9

PubMed Abstract | CrossRef Full Text | Google Scholar

Valentino, R. J., Miselis, R. R., and Pavcovich, L. A. (1999). Pontine regulation of pelvic viscera: pharmacological target for pelvic visceral dysfunctions. *Trends Pharmacol. Sci.* 20, 253–260. doi: 10.1016/s0165-6147(99)01332-2

PubMed Abstract | CrossRef Full Text | Google Scholar

van der Kooy, D., Koda, L. Y., McGinty, J. F., Gerfen, C. R., and Bloom, F. E. (1984). The organization of projections from the cortex, amygdala, and hypothalamus to the nucleus of the solitary tract in rat. *J. Comp. Neurol.* 224, 1–24. doi: 10.1002/cne.902240102

PubMed Abstract | CrossRef Full Text | Google Scholar

Wang, L., Martínez, V., Larauche, M., and Taché, Y. (2009). Proximal colon distension induces fos expression in oxytocin-, vasopressin-, CRF- and catecholamines-containing neurons in rat brain. *Brain Res.* 1247, 79–91. doi: 10.1016/j.brainres.2008.09.094

PubMed Abstract | CrossRef Full Text | Google Scholar

Chapter 5

Optimizing Autonomic Function Analysis Via Heart Rate Variability Associated with Motor Activity of The Human Colon

Published June 29, 2021, in Frontiers in Physiology | Autonomic Neuroscience |Research Topic: Horizon 2030: Innovative Applications of Heart Rate Variability

https://doi.org/10.3389/fphys.2021.619722

M. Khawar Ali[1,2], Lijun Liu[2], Ji-Hong Chen[2] and Jan D. Huizinga[1,2,*]

1. Faculty of Engineering, School of Biomedical Engineering, McMaster University, Hamilton, ON, Canada
2. Division of Gastroenterology, Department of Medicine, Faculty of Health Sciences, Farncombe Family Digestive Health Research Institute, McMaster University, Hamilton, ON, Canada

5.1 Abstract

The parameters of heart rate variability (HRV) can non-invasively assess some autonomic activities, and HRV is influenced by many bodily actions. Although parasympathetic activity is the primary driver of colonic propulsive activity, and sympathetic activity a major inhibitor of colonic motility, they are rarely measured and almost play no role in diagnosis of colon motor dysfunction or in standard treatments. Here we set out to optimize HRV analysis of autonomic nervous system changes related to human colon motility. The electrocardiogram and impedance were recorded in synchrony with colonic motor patterns by high-resolution manometry. Respiratory sinus arrhythmia (RSA), root mean square of successive differences of beat-to-beat intervals (RMSSD), the Baevsky Index or Sympathetic Index (SI), and the ratios of

SI/RSA and SI/RMSSD were shown to indicate a marked increase in parasympathetic and withdrawal of sympathetic activity during the high-amplitude pressure waves (HAPWs). Strong associations were seen with HAPWs evoked by a meal and rectal bisacodyl indicating a marked increase in parasympathetic and withdrawal of sympathetic activity during the gastrocolic reflex and the defecation reflex. When HAPWs occurred in quick succession, parasympathetic activation (RSA and RMSSD) occurred in a rhythmic fashion. Hence, during propulsive motor patterns, an overall shift in autonomic activity towards increased parasympathetic control was shown to be reflected in HRV. HRV assessment may therefore be valuable in the assessment of autonomic dysfunction related to colonic dysmotility.

KEY TERMS

High amplitude propagating pressure waves, RMSSD, RSA, Baevsky's Stress Index, autonomic nervous system, colonic motility

5.2 Introduction

Measurement of autonomic function does not yet play a significant role in colon dysmotility diagnosis, despite the fact that propulsive contractions in the human colon are orchestrated by the parasympathetic nervous system (Browning & Travagli, 2019) (de Groat & Krier, 1976). Some studies have linked gastrointestinal activity such as the postprandial state (Lu *et al.*, 1999) and gastric hypersensitivity (Ouyang *et al.*, 2020), to high frequency (HF) and low frequency (LF) parameters. Autonomic activity associated with Irritable Bowel Syndrome (IBS) (Bharucha *et al.*, 1993) and chronic intestinal pseudo obstruction (Camilleri *et al.*, 1993) were studied using heart rate interval parameters, heart rate response to deep breathing and

other tests. Autonomic function associated with functional dyspepsia was studied using HF power and root mean square of successive differences (RMSSD) (Lorena *et al.*, 2002).

Heart rate can react momentarily to changes in nervous input from the autonomic nervous system to the sinoatrial node, and this property establishes heart rate variability (HRV) (Thayer *et al.*, 2012; Shaffer & Ginsberg, 2017; Baevsky & Chernikova, 2017). Several time and frequency domain analyses and nonlinear methods have been developed to analyse HRV. Especially spectral analysis of beat-to-beat intervals, assessing the band power of low-frequency (LF; 0.04-0.15 Hz) and high-frequency (HF; 0.15-0.4 Hz), are used as matrices of the sympathetic and parasympathetic nervous systems (Hayano & Yuda, 2019). The HF band power is considered a measure of parasympathetic nervous system activity, the effect of activity of the final vagal fibers innervating the sinoatrial node, a culmination of vagal innervation that was influenced by a myriad of factors, primarily breathing but also activity from regulatory nuclei such as the nucleus tractus solitarius (NTS) that orchestrate coordination between respiratory, cardiac and gastrointestinal activities to optimize responses to metabolic demands and hence influence the autonomic outflow to the heart (Singh & Jaryal, 2020; Grossman & Taylor, 2007; Browning & Travagli, 2014). Dendritic projections from efferent vagal motor neurons to the colon extent throughout the NTS and intermingle within the various subnuclei so as to co-ordinate autonomic reflexes across autonomically controlled organs (Browning & Travagli, 2014). The NTS is a key structure for autonomic and neuroendocrine integration (Jean, 1991). The coordination of gastrointestinal, respiratory and cardiac function is dramatically seen in cases of emergency. The afferent information from the airways is first processed at the level of

NTS and results in various reflexes that are required for modification of ongoing breathing along with modulation of autonomic output to the cardiovascular and respiratory systems (Singh & Jaryal, 2020). It may be assumed that similar processes are involved in the central control of colon motility where the NTS plays a critical role (Browning & Travagli, 2014).

Effects of organ activities on HRV are difficult to predict and sometimes counterintuitive (La Rovere *et al.*, 2003). The major motor pattern of the human colon, the high-amplitude propagating pressure wave is associated with the autonomic nervous system in two ways. It is orchestrated by the parasympathetic and enteric nervous system and its occurrence, due to increased intraluminal pressure and distention of the colon, will activate stretch sensitive neurons. The role of the autonomic nervous in orchestrating colonic motility is exemplified by the sacral defection reflex (Bharucha & Brookes, 2018) that starts with rectal sensation, which activates the sacral sensory nerves. Then information is signaled into the sacral parasympathetic nucleus (also called the sacral defecation center) from where information travels into the brain stem and frontal cortex to either prevent or initiate a defecation. A bowel movement may be produced via activation of sacral parasympathetic nerves and via the enteric nervous system (Brookes *et al.*, 2016) (Furness *et al.*, 2014) (Browning & Travagli, 2014) (Bharucha & Brookes, 2018). The primary driver of the HAPWs is the parasympathetic nervous system (Devroede & Lamarche, 1974) (Callaghan *et al.*, 2018) (De Groat & Krier, 1978). Resection of the parasympathetic pelvic splanchnic nerves causes loss of the defecation reflex (Devroede & Lamarche, 1974). HAPWs are not observed in ex vivo preparations of the human colon (Dinning *et al.*, 2016) In the cat, HAPWs and HAPW-SPWs were identified in vivo and

shown to be associated with firing of parasympathetic efferents (De Groat & Krier, 1978). Stimulation of sacral extrinsic nerves has also been shown to be a treatment for constipation (Leblanc *et al.*, 2015). Interestingly, propulsive motor patterns can be evoked by injection of a ghrelin agonist in the sacral spinal cord (Shimizu *et al.*, 2006) or by stimulation of surgically placed electrodes in the S2 region of the spinal cord (Devroede *et al.*, 2012).

This study was designed to evaluate which of the myriad of HRV parameters best reflect autonomic nervous system activity using an established supine to standing protocol, and autonomic tone and reactivity associated with the high-amplitude pressure wave that is associated with human colon transit and defecation. We included HF and LF power, to directly compare RSA and HF power for statistical analysis, and to compare the disputed LF power as a measure of sympathetic activity with the Baevsky Index. We also separated the analysis by intervention, so that we could assess shifts in autonomic activity during HAPWs in response to a meal (the gastrocolonic reflex), and in response to rectal bisacodyl (the sacral autonomic (defecation) reflex, and in response to distention. We chose a combination of high amplitude propagating pressure waves (HAPWs) and high amplitude propagating pressure waves followed by simultaneous pressure waves (HAPW-SPWs) to incorporate all individual HAPWs in the statistical analysis, *excluding* in this analysis bisacodyl-induced multiple HAPWs since they sometimes are accompanied by pain and changes in breathing pattern. For bisacodyl-induced multiple HAPW activity we devised a new method for continuous assessment of HRV parameters. To study shifts in autonomic balance we propose new ratios of sympathetic over parasympathetic parameters.

5.3 Methods

5.3.1 Participants

Eleven healthy volunteers (7 males, 4 females, age 30 ± 10 yrs, without any current or prior history of cardiovascular or gastrointestinal disease and not on any medications affecting cardiac or gastrointestinal function were recruited by local advertisement (wall posters) for this study. Each participant was paid 600 CA$ to complete this study. The study was carried out at McMaster University with ethics approval from the Hamilton Integrated Research Ethics Board, and written consent from all participants.

5.3.2 Heart rate and impedance measurements

The electrocardiogram (ECG) was recorded using seven electrodes on the subject's torso. Three electrodes formed a modified Lead II configuration for ECG recording. Four electrodes were used in a standard tetrapolar electrode configuration for impedance recording, where two electrodes supplied a constant current source, and two electrodes registered the changes in the transfer impedance (reflecting changes in activity of the sympathetic nervous system). ECG and impedance were recorded using a MindWare impedance cardio GSC monitor with a sampling frequency of 500 Hz. (MindWare Technologies Ltd., Gahanna, OH, United States) and MindWare BioLab Recording Software. MindWare HRV 3.1 was used for artifact correction of the ECG signal, to generate beat-to-beat intervals (RR intervals) and for the calculation of RSA, RMSSD, HF and LF band powers. PEP was generated by Mindware Cardiac Impedance software (MindWare Technologies Ltd., Gahanna, OH, United States). MATLAB codes were generated to calculate SD1 and SD2 (Poincare plot) as well as the sympathetic Index (SI) using the RR interval signal. The breathing frequency was generated by the Mindware impedance analysis software.

5.3.3 HRV related to posture change

To test general autonomic reactivity using a standard method, heart rate and heart rate variability changes of all participants were measured related to posture change. The participants refrained from smoking, caffeine intake and heavy eating for 2 hours prior to the testing. During the test, they were accommodated in a quiet room with normal lighting and room temperature. After resting in supine position for a minimum 10 min, the ECG and impedance were recorded for 6 min in the supine position, 6 min in sitting position and immediately upon standing for 6 min. The HRV parameters tested are shown in Table 1. We calculated the Baevsky's stress index (SI) (Baevsky & Chernikova, 2017) according to the formula

$$SI = \frac{AM_o \times 100\%}{2M_o \times M_x DM_n}$$

where the mode (M_o) is the most frequent RR interval expressed in seconds. The amplitude of mode (AM_o) was calculated, using a 50ms bin width, as the number of the RR intervals in the bin containing to the M_o, expressed as a percentage of the total number of intervals measured. The variability is reflected in M_xDM_n as the difference between longest (M_x) and shortest (M_n) RR interval values, expressed in seconds. The SI is expressed as s^{-2}.

5.3.4 HRV related to colonic motor patterns

Raw data were obtained from a study that was reported on previously (Milkova *et al.*, 2020) (Yuan *et al.*, 2020). High-Resolution Colonic Manometry was performed using an 84-sensor water perfused catheter that detected luminal pressures at 1 cm intervals from the proximal colon to the anal sphincter. The catheter was custom-made by Mui Scientific (Mississauga, ON,

Canada) and the acquisition hardware was made by Medical Measurement Systems (Laborie, Toronto, ON, Canada). The sampling frequency of the system is 10 Hz. After the catheter was placed inside the colon with the assistance of colonoscopy, a 6-8 hours high-resolution colonic manometry (HRCM) procedure was executed. All participants underwent synchronized HRCM, ECG, and impedance recording during 90 min of baseline, followed by 20 min of proximal balloon distention, 20 min of rectal balloon distention using a standard anorectal manometry balloon assembly, 90 min following intake of a meal, consisting of organic yogurt fortified by organic milk fat to make it 1000 kcal (Mapleton Organic, Ontario, Canada), and 45 min after administration of rectal bisacodyl. Participants were supine during all recordings except during the actual intake of the meal.

The manometric analysis was carried out in ImageJ and MATLAB. All High-Amplitude Propagating Pressure Waves (HAPWs) with or without an associated SPW, occurring as single isolated events (Chen *et al.*, 2017) were included in the present study; the motor pattern needed to have a 2 min quiet period before and after the motor pattern. All analysis for the present study was based only on raw data from our studies. Autonomic reactivity to HAPWs was identified by comparing the 2 min period prior to the occurrence of an HAPW, during the occurrence of an HAPW, and the first 2 min immediately after the HAPW. The HRV signal was divided into segments of 1 minute and the HRV parameters were calculated for each individual segment. Even if the HAPW lasted 50 sec, the whole segment of 1 min was taken into account. In case of before and after, where the time period taken into account was 2 minutes, the data was analysed for each minute separately (using a one minute window) and the mean of the results of the two segments was taken to represent the HRV parameter. RSA, RMSSD, HF power

and SD1 were calculated as measures of parasympathetic activity and LF power, PEP and SI were calculated as measures of sympathetic activity. LF/HF, SD2/SD1 and SI/RSA and SI/RMSSD ratios were also calculated for each phase.

5.3.5 Analysis of HRV in association with Motor Complexes

Autonomic activity related to motor complexes, more than one HAPW as a cluster, was assessed graphically by generating time matched images of the motor complexes in HRCM with the frequency domain HF band (the RSA band) images of the HRV data. The process of generating the HF power (RSA band power) image started by importing the ECG and impedance signal into ImageJ using the Cardio Images plugins (Parsons). In the Cardio Images plugin, the peak detection and correction of the ECG signal was carried out by a Pan-Tomkins algorithm as well as by a Neural Networks model generated and trained in TensorFlow, followed by manually checking and editing the wrongly detected/edited R peaks. The tachogram of RR intervals was plotted as a raster image using a sampling frequency of 10 Hz., image width of 5 seconds with cubic interpolation in Intervals plugin. The Frequency Win Plugin was used to calculate FFT spectra of the tachogram raster image using window length of 60 s and intervals of 10 s. The power spectra are collated into an image with time on the y-axis and frequency on the x-axis with pixel intensity as amplitude (ms). Similarly, the HRCM data was converted into an image using the Event Series plugin in ImageJ. Both the images were then imported, and time matched in MATLAB as shown in Figure 1. A Win frequency plugin generated the HRV spectrogram from 0 to 5 Hz, to study the RSA/HF band only; the lower frequency band (0-0.14 Hz.) as well as the frequency band above 1Hz was removed in MATLAB, and the spectrogram with the frequency band of 0.14 to 1 Hz. was plotted as an aligned image with the HRCM image

as shown in figure 1(b). Similarly, the raster image of RR intervals was imported into Matlab and was used to calculate RMSSD and SI, which were also plotted as aligned images with the HRCM figures 1(c) and 1(d).

5.3.6 Statistical Analysis

Supine to standing

To evaluate HRV related to posture change, all the HRV parameters were analysed independently. Each HRV parameter was calculated for supine and standing position for all the participants (n=11) and tested for normal distribution using the Shapiro-Wilk Normality test. If the data for both supine and standing was normally distributed, the comparison was carried out using the paired t-test. The Wilcoxon Matched Pair Signed Rank test was used in case one or both of the supine and standing HRV parameter data was not distributed normally. The change in each HRV parameter was considered significant between supine and standing, if the calculated p-value was less than 0.05.

High-Resolution Colonic Manometry (HRCM)

All HAPWs (n=65) that had a 2 min period before and after without major motor patterns, in order to obtain a “baseline” and “recovery” period, from all the participants were investigated. For each HRV parameter, the results from all HAPWs were averaged for each subject and were presented as one reading with three data points (Before-During-After). These averaged results from all the participants were used for further analysis. Initially, the data was tested for normal distribution using the Shapiro-Wilk Normality test. If the data was normally distributed, the parametric test ANOVA followed by Bonferroni Multiple Comparison test was used for comparison. While the non-parametric Friedman test followed by Dunn's Multiple Comparison

test was used for data sets that were not normally distributed. The p-value was calculated for before-to-during (p-value (B-D)) and during-to-after (p-value (D-A)). A difference was considered significant when $p<0.05$. The t-values and degrees of freedoms are reported with parametric tests while the z-value is reported with non-parametric tests.

In addition, the HAPW's were grouped based on the HRCM condition with 12 HAPW's observed during baseline, 16 during meal, 14 during prucalopride, 5 during proximal balloon distension, 7 during distal balloon distension and 11 during bisacodyl. The same statistical procedures as mentioned above were applied to each group separately to identify the effect of the stimulus conditions on the association of autonomic nervous system with HAPW's.

5.4 Results

5.4.1 Autonomic reactivity associated with posture change

The parasympathetic parameters RSA, RMSSD, SD1 and HF power all decreased from supine to standing consistent with a decrease in parasympathetic reactivity. The sympathetic parameter SI showed a significant increase from supine to standing. PEP did not show any significant change. The shift from parasympathetic to sympathetic going from supine to standing was reflected in the change in LF/HF ratio, SD2/SD1 ratio, SI/RSA as well as the SI/RMSSD ratio. The posture change resulted in an increase in heart rate. SD2 and LF power did not change, likely a reflection of the fact that these parameters are associated with both sympathetic and parasympathetic changes (Table 5.1).

5.4.2 Autonomic Reactivity Associated with HAPWs

A significant increase in RSA indicated activation of the parasympathetic nervous system during the motor activity as compared to the period before the motor pattern and the change

recovered within 2 min (Table 5.2). An increase in RSA during the HAPWs was seen in all subjects, average 9.3 %, with recovery afterwards. Similarly, an increase in RMSSD was seen in all subjects except one. There was an average increase of 24.6 % in the RMSSD during the HAPW (Table 5.2). Due to one outlier, the change in RMSSD did not reach statistical significance. Similarly, SD1 also increased numerically in all volunteers but one, and did not reach statistical significance (Table 5.2).

Although RSA showed a significant increase, the HF power, derived from the same data set as the RSA, did not show a significant change (Table 5.2). RSA is the natural log (*ln*) of HF power and taking a natural log will remove the effect of large outliers. Indeed, when we removed 4 out of 65 values from the HF power data set that showed more than 3 SD units off the mean value, the HF power changed from 993.07 ± 300.47 before the motor pattern to 1769.64 ± 546.76 ($p = 0.0485$) and recovered to 1135.88 ± 403.85 ($p = 0.0485$); the increase in RMSSD during the HAPW and its decrease afterwards, also became significant.

The change in sympathetic index (SI) indicated a decrease in sympathetic activity during the motor patterns that recovered within 2 min (Table 5.2). The PEP did not show significant changes (Table 5.2).

The SI/RSA decreased 42% during an HAPW and recovered within 2 min, consistent with activity shifting towards parasympathetic activity during the motor activity. Similarly, SI/RMSSD showed a 64.4 % decrease. Both the LF/HF and SD2/SD1 ratios did not change significantly with motor activity. The heart rate did not show any significant change with motor activity (Table 5.2).

Since RSA is sensitive to respiratory rate changes and to respiratory tidal volume changes, the breathing frequency and volume were calculated before during and after all HAPWs. The breathing frequencies before and during all HAPWs, were 15.9 ± 0.4 and 15.4 ± 0.5 breaths/min (P=0.225), the values for volume were 0.0123 ± 0.0113 and 0.0131± 0.0008 V^2 (P > 0.999), respectively; hence, no significant change in breathing frequency was observed in response to an HAPW.

Autonomic activity associated with HAPWs may arise from the activity that initiates the HAPW and from potential mechanoreceptors activated by the actual HAPW. Although rectal bisacodyl almost always evoked HAPWs in the present cohort of healthy subjects, in one subject, two low amplitude simultaneous pressure waves were associated with an increase in RSA from 4.83 to 5.88 $ln(ms^2)$ with a concomitant decrease in SI from 159 to 84 s^{-2}; consistent with the notion that the initiating autonomic activity is seen by HRV and that the change may not solely dependent on the strong HAPW evoking distention.

5.4.3 Autonomic Nervous System Association with HAPW's in Different Conditions

Activity of autonomic nervous system activity during an HAPW may be different in different conditions, hence we assessed HRV parameter changes separately under each condition: baseline, meal, prucalopride, proximal balloon distension, distal balloon distension and bisacodyl, The dramatic shift in autonomic balance towards a dominant parasympathetic activity that was described above was observed during the HAPWs that were evoked by a meal (Table 5.3) and by rectal bisacodyl (Table 5.4) as reflected by RSA, RMSSD, SI and SI/RSA and SI/ RMSSD..

During baseline, HAPWs are quite rare, nevertheless, the mean values of all the HRV parameters during HAPW changed (5.03% increase in RSA, 6.53% increase is RMSSD, 24.79% increase in RMSSD, 38.68% increase in HF power, 30.44% decrease in SI), the changes did not reach statistical significance (Table 5.5).

The 90 min period after oral prucalopride, where we hypothesize that prucalopride stimulates the gastric mucosa to evoke HAPWs. both RSA and RMSSD increased significantly and SI decreased significantly during the HAPW's. and recovery afterwards in both RMSSD and SI was also significant. A significant shift in autonomic balance towards parasympathetic activity was indicated by a decrease in SI/RMSSD (Table 5.6).

The periods of balloon distention had low n numbers, nevertheless, distal balloon distension was accompanied by a significant increase in RSA and recovery after the HAPW (Table 5.7), but changes in response to proximal balloon distention did not reach significance (Table 5.8).

5.4.4 Autonomic Reactivity Associated with Motor Complexes.

Motor complexes are defined here as more than one HAPW and/or HAPW-SPW that occurred close together such that they could not be analyzed separately. In order to assess HRV during the motor complexes, a continuous assessment procedure was developed as outlined in the methods section. The major finding was that motor complexes were associated with an increase in HF power that was not continuous but rhythmic. The average duration of RSA reactivity, measured at 0.14-0.5 Hz, was 50 ± 10 sec and the frequency of occurrence was 0.8 ± 0.2 cycles/min which was similar to the HAPW frequency within motor complexes (Figure 2). However, with long HAPWs, more than one RSA band occurred, giving the RSA activity a distinct

rhythmic appearance (Figure 4). 37 out of a total 40 motor complexes studied, had RSA bands associated with them. Although there was complete synchronization of individual HAPWs and bursts of RSA activity, with motor complexes (n=34), rhythmic RSA activity sometimes (n=6) continued after the HAPW to slowly die out. Sometimes (n=3), the RSA activity started prior to the measured HAPW, but the HAPW likely originated earlier at a more proximal site, beyond the reach of the catheter. RMSSD also increased during the HAPWs and motor complexes. There was complete synchronization between RSA and RMSSD. SI changes were observed as more or less reciprocal to the RMSSD and RSA bands (Figures 1, 2). During all 90 min baseline periods, when HAPWs are rare, there was never rhythmic HF activity although very low amplitude HF activity was continuously observed (Figure 3).

5.5 Discussion

Assessment of sympathetic activity during posture change

In the assessment of sympathetic increase in the supine to standing protocol, the Baevsky Stress Index or Sympathetic Index increased 52%, whereas SD2, PEP and the LF power did not show significant changes. In order to maintain a near constant blood pressure, in response to the postural changes from supine to standing when blood is pooled in the legs and blood pressure decreases, the baroreceptor reflex increases sympathetic activity to increase heart rate. Baroreceptor action potentials are relayed to the nucleus tractus solitarius, which uses action potential frequency as a measure of blood pressure. The end-result of baroreceptor de-activation is excitation of the sympathetic nervous system and inactivation of the parasympathetic nervous system. Houtveen et al. recorded PEP at different breathing frequencies during supine, sitting and standing (Houtveen *et al.*, 2005); PEP increased from

supine to standing hence the sympathetic activity appeared to decrease. This was also observed by Cacioppo et al. (Cacioppo *et al.*, 1994). PEP is a measure of ventricular contractility, influenced by beta-adrenergic receptor mediated ventricular sympathetic innervation (van Lien *et al.*, 2015). Nitroprusside causes vasodilation, baroreceptor unloading and a reflex increase in sympathetic tone, which was associated with a significant decrease in PEP (Schächinger *et al.*, 2001). Our study indicates that the sympathetic activity that is increased upon standing is not reflected in the PEP value.

Sympathetic pathways within the body form a vast network; only those sympathetic activities that interact with, or directly or indirectly take part in sympathetic regulation of heart rate will be seen in HRV. For example, muscle sympathetic nerve activity measured at the peroneal nerve induces vasoconstriction and is modulated by the baroreflex but it represents regional sympathetic neural activity, it does not equal sympathetic discharge directed to the heart (Schächinger *et al.*, 2001).

Both LF power and SD2 did not significantly increase with posture change in the present study. Many studies continue to presume that LF power, especially if adjusted for HF power, total power, or respiration, provides an index of cardiac sympathetic “tone” and that the ratio of LF:HF power indicates “sympathovagal balance”, but strong evidence has been presented that LF power neither reflects cardiac sympathetic tone at supine nor in response to standing (Goldstein *et al.*, 2011). There is also no evidence that the LFa (low frequency area) (Nguyen *et al.*, 2020) is specific for sympathetic activity (Goldstein *et al.*, 2011) (Rahman *et al.*, 2011). Rahman et al. showed that SD2 as well as the ration of SD1 and SD2 are not related to cardiac sympathetic activity (Rahman *et al.*, 2018).

Baevsky et al. developed an index of regulation strain, or stress index, or, relevant to our study, a “Sympathetic Index” which illustrates the sympathetic or central regulation activity (Baevsky & Chernikova, 2017). The activation of sympathetic regulation results in the stabilization of the heart rhythm which causes a decrease in variation of RR intervals and an increase in the number of intervals with similar duration. The histogram of RR intervals becomes narrower and increases in height. Although the SI is not yet widely applied for sympathetic measurement, it is used by commercially available HRV data analysis software as one of the measures of sympathetic activity (Kubios); they use the square root of SI to minimize the effect of outliers. The marked change in SI due to posture change in the present study suggests it to be a sensitive marker for orthostatic sympathetic change.

Sympathetic activity and the colonic propulsive motor patterns

The HAPWs, the most significant propulsive motor pattern of the human colon, were accompanied by a significant decrease in SI, hence a decrease in sympathetic activity. During motor complexes, SI was always showing some value above zero, which indicates that there was continuous sympathetic activity which was inhibited during HAPWs. We infer that withdrawal of sympathetic activity is part of autonomic reflexes that initiate the HAPW, e.g. in response to a meal or rectal bisacodyl. Could stretch receptors be activated during the HAPW? Viscerofugal neurons, connecting to the sympathetic prevertebral ganglia allow the colon to fill, and when the circular muscle of the colon wall contracts to empty the segment, the mechanoreceptors are unloaded and synaptic input decreases (Szurszewski & Miller, 2006). Hence the marked reduction in SI observed in the present study is consistent with a withdrawal of sympathetic activity, allowing the HAPW to proceed.

Parasympathetic activity and the colonic propulsive motor patterns

All HRV parameters studied that are associated with parasympathetic activity, were decreased in response to posture change from supine to standing reflecting the well-known decrease in parasympathetic activity to prevent orthostatic hypotension.

Individual HAPWs, were associated with a significant increase in RSA. Many of these HAPWs occurred during baseline or in the aftermath of taking a meal where the HAPWs are not felt and do not cause a sensation and are not associated with evoked body movements, discomfort or changes in breathing patterns. We suggest that this may reflect the activity in the parasympathetic nervous system associated with the initiation of the HAPW. HAPWs occur most often after a meal as a result of the gastro-colonic reflex, or in response to rectal stimulation where they are the result of a sacral defecation reflex. The sacral defecation reflex involves the sacral defecation center (the parasympathetic nucleus), Barrington's nucleus and the NTS (Taché & Million, 2015). Barrington's nucleus and the NTS are also involved in cardiac autonomic regulation (Gasparini *et al.*, 2020), and in this way, the neuronal traffic in association with HAPWs can influence heart rate, similar to the influence of breathing on the heart rate: "breathing at different rates within the 9–24 bpm range, which changes HF power, does not change mean heart rate" (Shaffer & Ginsberg, 2017). The fact that a significant change occurred in RSA in association with the motor patterns without a change in heart rate is consistent with the hypothesis that the origin of the parasympathetic activity is the neural activity associated with gut activity and not cardiac activity. The fact that the heart rate does not change suggests

that the vagal tone, the mean vagal efferent effects to the sinus node, does not change (Grossman & Taylor, 2007).

Vagal afferent neurons are likely activated by colonic motor patterns and their dendritic projections extent throughout the NTS and intermingle within the subnuclei providing a potential means to coordinate respiratory and cardiac autonomic activities (Browning & Travagli, 2014). Sensory nerves in the pelvic plexus will also convey colonic information to the spinal cord (Smith-Edwards *et al.*, 2019). Hence neuronal traffic originating for an HAPW may also influence HRV. Research is ongoing to distinguish efferent and afferent neuronal traffic associated with HAPWs and to explore their role in HRV changes and diagnostic value. It is also possible that HAPWs induce colonic blood pressure changes that might influence HRV (Semba & Fujii, 1970).

When HAPWs occur in quick succession within motor complexes, overlapping in time, RSA was markedly increased. Strong motor patterns induced by bisacodyl sometimes results in discomfort and increased breathing frequency; increased breathing frequency results in decreased RSA but this was not found, likely superseded by processes that increased RSA. Importantly, there was never continuous RSA activity even when HAPWs were continuously present. RSA increases occurred in bursts that were not synchronous with individual HAPWs within the burst, and they continued for several minutes and then diminished gradually (Figure 4). The HF “rhythmicity” suggests that there is a refractory period in the parasympathetic neural activity. In some instances, the RSA bands started prior to the HAPW’s, however, in

those cases the HAPWs were seen in the most proximal sensor hence the true beginning of the HAPW was not captured by the catheter. Since contractions are ongoing, the rhythmicity of the parasympathetic activity suggests that it arises from activity orchestrating the HAPWs and not from distention, but this remains to be investigated.

HRV parameters associated with autonomic reflexes

When the HRV parameters associated with HAPWs were analyzed within each intervention separately, strong associations between HAPWs and sympathetic decrease and parasympathetic increase were observed in response to a meal, which reflect the gastrocolic reflex, in response to rectal bisacodyl that reflect the sacral autonomic (defecation) reflex and in a rapid response to oral prucalopride which we hypothesize is due to a gastrocolic reflex mediated by stimulation of gastric enterochromaffin cells and subsequent activation of vagal sensory nerves. In a subset of patients with chronic constipation, absence of the autonomic reflexes is associated with high sympathetic activity (Chen J-H and Liu, L, unpublished observations).

RSA vs RMSSD and HF power

The RMSSD increased one to one with the increase in RSA associated with HAPWs and within the motor complexes, confirming the marked association between parasympathetic activity and human colon propulsive motor patterns. The association between RMSSD and single HAPWs occurred despite the fact that the recording period of 1 min during the HAPW was too short for an ideal assessment as argued by Baek at al. (Baek *et al.*, 2015).

The RSA is the natural log of the HF power; the HF power did not show a significant change likely because with a few HAPWs (4/65), the HF power was more than 3 standard deviations

from the mean values. If we took these values out and assessed 61 out of 65 motor patters, the HF power showed a significant increase going from baseline to motor pattern and back to recovery.

The significance of changes in breathing frequency

The HF band, also known as the respiratory band, is associated with variation in heart rate due to respiration. The HF band has been set to range from 0.15 - 0.4 Hz. which corresponds to the respiration frequency of 9 - 24 breaths/min, the normal frequency range in adults. The heart rate increases during inhalation due to inhibition of vagal outflow and decreases during exhalation due to the restoration of vagal outflow by release of acetylcholine (Gasparini *et al.*, 2020). If the breathing rate is outside the range of 9-24 breaths/min, then the calculated HF power will be due to noise or harmonics of lower frequency bands and the respiration frequency power will not be included in the HF power. If the respiration frequency is lower than 9 breaths/min, as is the case with slow, deep breathing, the most prominent component of the respiration frequency power will lie in the LF band, and without adjusting the HF band, it will indicate low HF power and high LF power and lead to wrong interpretations of HF power. Similarly, during exercise, a breathing frequency of over 24 breaths/min, the prominent component of parasympathetic power will be out of the range and will wrongly represent low parasympathetic power. If during experimental conditions the breathing frequency goes outside the 9-24 breaths/min range, then the HF power band can be adjusted based on the respiration frequency. This was used in a recent study by Nguyen et al. where the HF or parasympathetic band was replaced by “RFa” (respiratory frequency area (Nguyen *et al.*, 2020; Colombo *et al.*, 2015)). In the present study the subjects were lying in a relaxed supine position

throughout the recording and were not asked to breathe deeply, they were only asked to change position from supine to sitting for a period of 15 minutes while eating. The respiration rate was within the range of 9-24 breaths/min almost all of the time. In our study, any incident for which the respiration frequency was out of the range of 9-24 breaths/min was rejected during analysis; hence, there appears to be no benefit in using RFa under our experimental conditions.

The new parameters SI/RSA and SI/RMSSD

The two branches of the autonomic nervous system can work reciprocally but they can also work independently. Hence a sympathetic over parasympathetic ratio may not reflect an autonomic "balance" and cannot be used as a singular parameter of autonomic balance. Furthermore, LF and SD2 are not considered good parameters for sympathetic activity, making the LF/HF and SD2/SD1 ratios less useful. These ratios in our study behaved significantly different from SI/RSA and SI/RMSSD. Hence, we calculated SI/RSA and SI/RMSSD *in conjunction with* the SI, RSA and RMSSD values as *additional* parameters to evaluate changes in autonomic activity. The SI/RSA and the SI/RMSSD decreased markedly with the HAPWs confirming a shift to parasympathetic activity.

In conclusion, we show that HAPWs are associated with measurable changes in HRV parameters reflecting parasympathetic and sympathetic activity. Most of the single HAPWs reported here were not noticed by the subjects, they occurred without discomfort or change in respiration pattern. Under normal conditions, they would just be part of everyday movement of content into anal direction without urge to defecate. These motor patterns were not associated with a change in heart rate, suggesting a physiological correlation between the HAPW, the

gastrocolic reflex, the sacral defecation reflex, and the autonomic parameters RSA, RMSSD and SI. Our inference is that these motor patterns and reflexes are directed by autonomic activity reflected in HRV, hence RSA, RMSSD, SI, SI/RSA and SI/RMSSD may develop as biomarkers of autonomic (dys)regulation of colonic motility.

Acknowledgements

This study was supported by the Natural Sciences and Engineering Research Council (NSERC) Grant 386877 to JDH. MKA was supported by a fellowship from the Farncombe Family Digestive Health Research Institute and NERC. We gratefully acknowledge that Dr. Sean Parsons provided all ImageJ plug-ins. An abstract of this work was presented at the 2021 Canadian Digestive Diseases Week.

Conflict Of Interest

The authors declare that they have no conflict of interest of any kind.

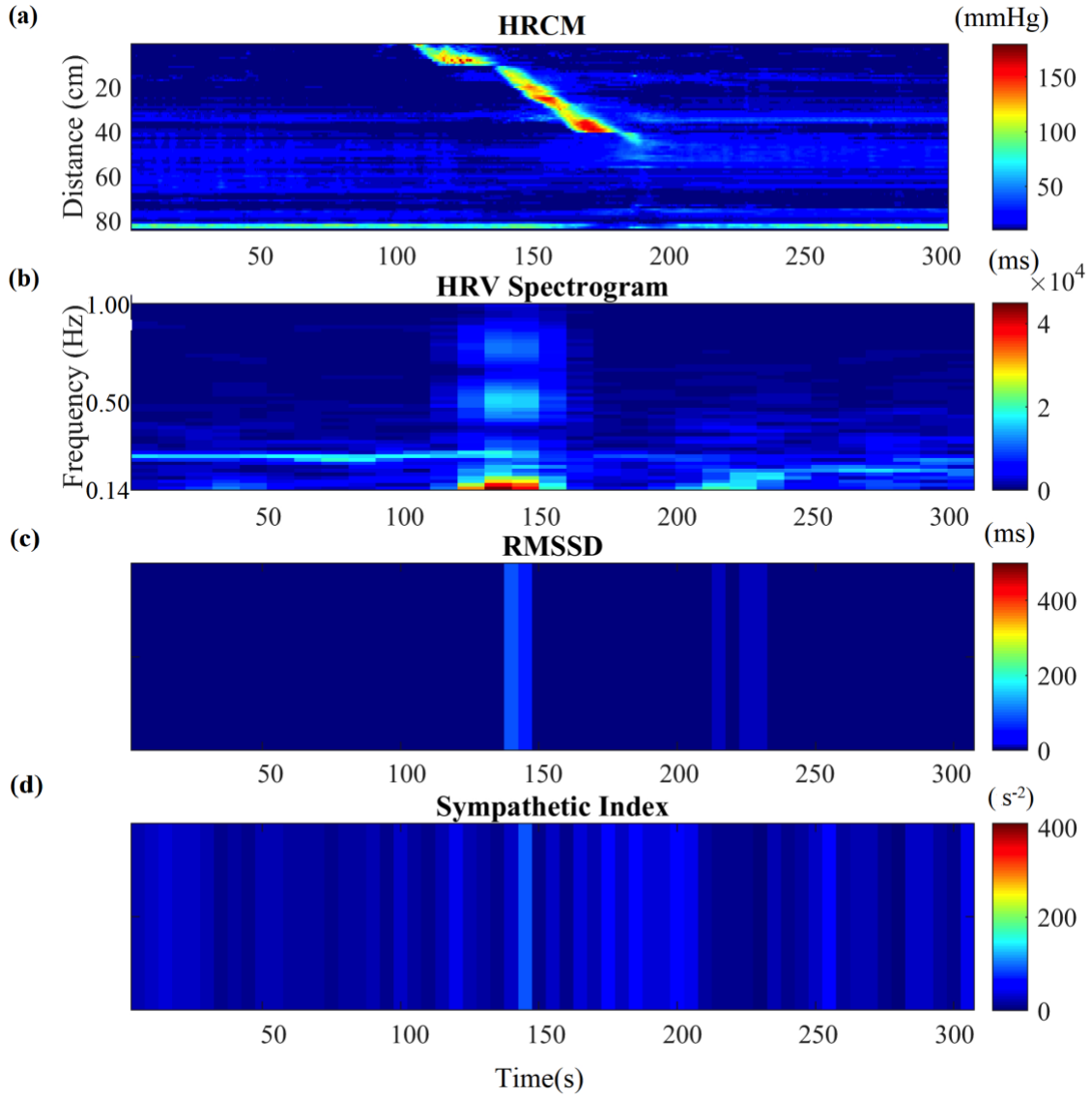

Figure 5-1: (a) 2-min before, during, and 2-min after HAPW recorded by HRCM (b) HF power/RSA band of HRV signal time matched with HRCM recording (c) RMSSD time matched with HRCM (d) SI time matched with HRCM. Distance at 0 cm is positioned at the proximal colon, distance at 80 cm is just proximal to the anal sphincter

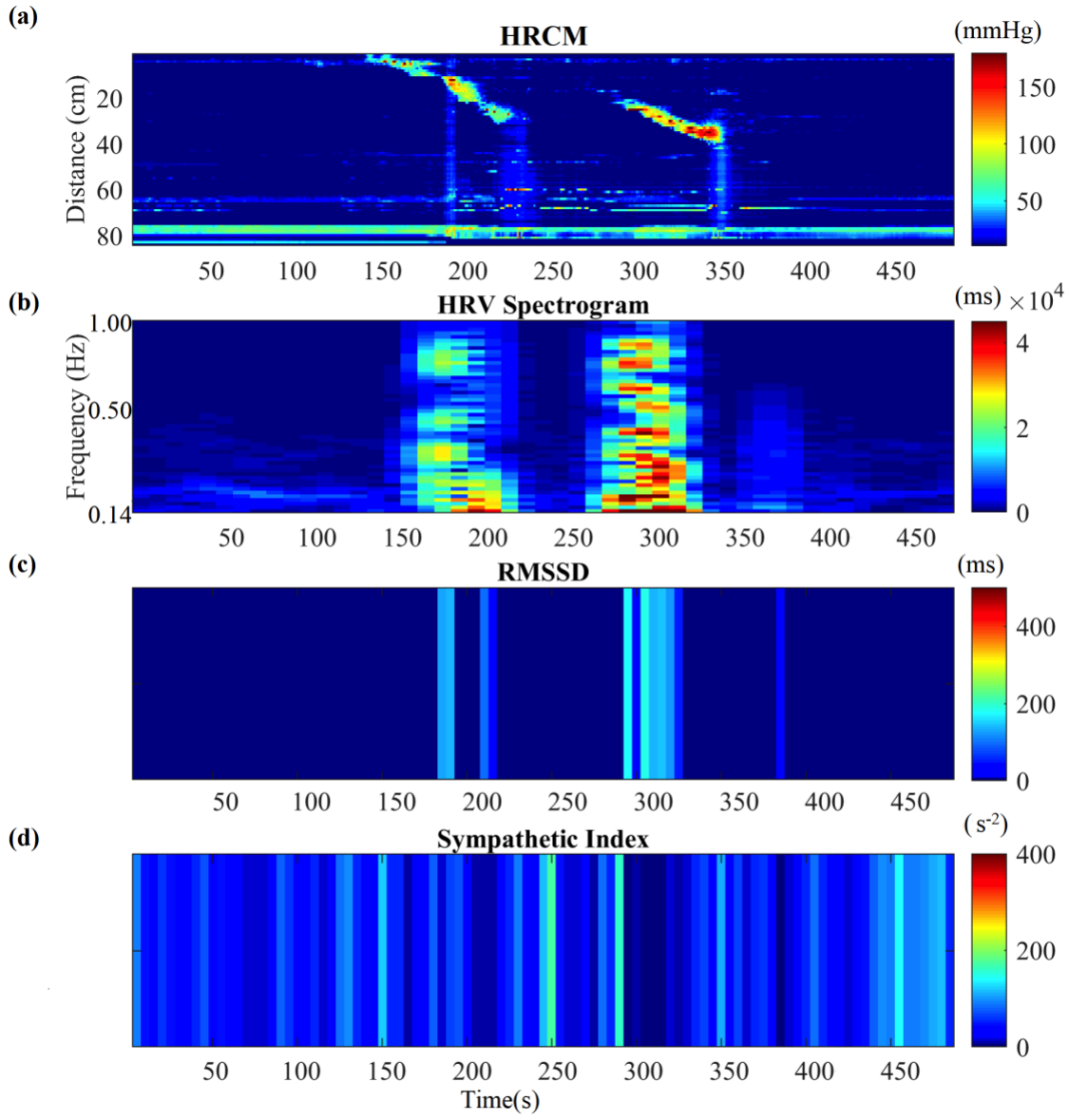

Figure 5-2: (a) Before-During and After a Motor Complex (b) Time matched HF Power/RSA band of the HRV signal before-during and after MC (c) RMSSD time matched with HRCM (d) SI time matched with HRCM

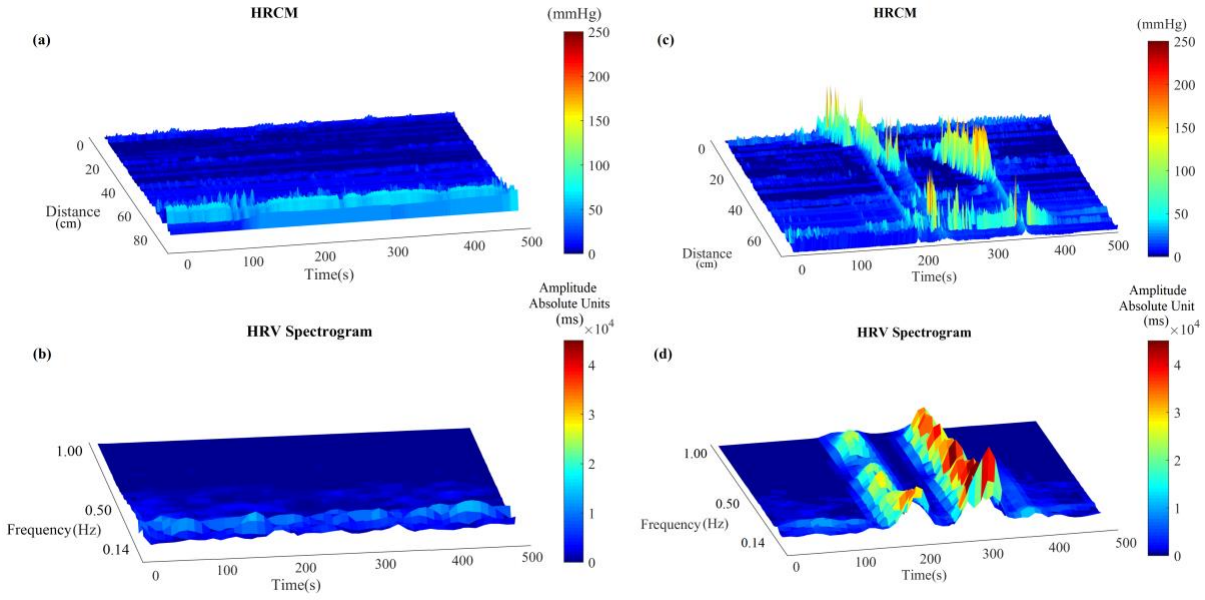

Figure 5-3: (a) Baseline HRCM recording without any colonic motor pattern (b) HF power/RSA band during the baseline (c) HRCM recording with Motor Complex (d) HF power/RSA band during the Motor Complex

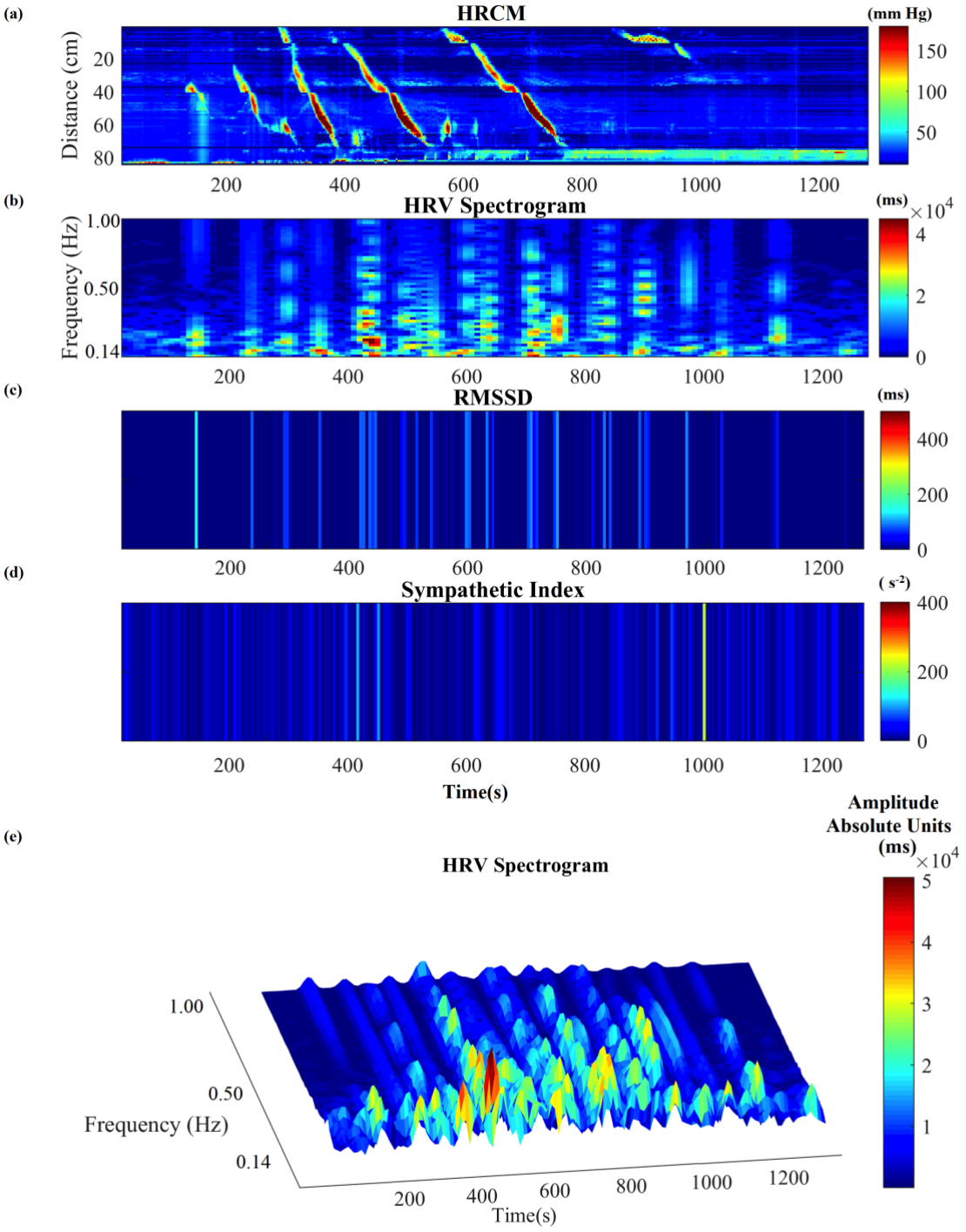

Figure 5-4: :(a) HRCM recording with Motor Complexes containing long overlapping HAPWs (b) HF power/RSA band of HRV signal (c) RMSSD (d) SI (e) HF/RSA power band in 3D.

Table 5-1: Autonomic reactivity associated with posture change

	Supine Mean ± SEM	Standing Mean ± SEM	P-Value	t, df (t-test)/ rs (Wilcoxon)
RSA (ln(ms^2))	6.76 ± 0.28	5.80 ± 0.32	***0.0006	t=4.958, df=10
RMSSD (ms)	57.90 ± 3.65	28.49 ± 3.65	***0.001	rs=0.7671
SD1 (ms)	58.77 ± 6.85	29.53 ± 2.64	**0.0012	t=4.459, df=10
SD2 (ms)	102.94 ± 12.52	82.99 ± 4.77	0.1434	t=1.588, df=10
HF Power (ms^2)	1552.88 ± 537.25	498.55 ± 120.61	**0.0020	rs=0.7455
LF Power (ms^2)	1064.53 ± 417.59	1122.36 ± 240.33	0.5771	rs=0.1182
PEP (ms)	121.64 ± 4.94	122.75 ± 6.40	0.8772	t=0.1585, df=10
SI (s^{-2})	32.85 ± 6.96	50.73 ± 5.72	*0.0322	rs=0.4455
LF/HF Ratio	0.69 ± 0.13	3.19 ± 0.64	**0.0049	rs=-0.02727
SD2/SD1	1.77 ± 0.07	2.97 ± 0.21	***0.0004	t=5.196, df=10
SI/RSA	5.20 ± 1.21	9.33 ± 1.30	*0.0244	rs=0.5727
SI/RMSSD	0.80± 0.22	2.38± 0.47	**0.0020	rs=0.5982
HR (bpm)	63.78 ± 2.68	80.50 ± 3.24	****<0.0001	t=9.854, df=10

Number of subjects N= 11, t-value and df are reported in case of t-test while rs(Spearman) value is reported where non-parametric Wilcoxon signed rank test was applied.

Table 5-2:Autonomic nervous system modulation in association with all individual HAPWs and HAPW-SPWs combined

	Before Mean ± SEM	During Mean ± SEM	After Mean ± SEM	p-value (B-D) (t, df) or (z-value)	p-value (D-A) (t,df) or (z-value)
RSA (ln(ms^2))	6.38 ± 0.27	6.90 ± 0.26	6.46 ± 0.24	*0.0182 (3.420, 8)	*0.0220 (3.290, 8)
RMSSD (ms)	53.24 ± 6.73	66.35 ± 10.35	52.03 ± 8.34	0.1609 (1.862, 8)	0.1608 (1.973,8)
SD1 (ms)	45.19 ± 4.66	56.44 ± 6.93	40.93 ± 4.42	0.1201 (2.189, 8)	0.0593 (2.641, 8)
SD2 (ms)	100.02 ± 7.64	126.93 ± 12.76	79.44 ± 0.18	*0.0069 (4.094,8)	*0.0166 (3.481,8)
HF Power (ms^2)	1675.88 ± 715.99	1594.33 ± 425.33	1074.31 ± 319.33	0.1979 (1.650)	0.1187 (1.886)
LF Power (ms^2)	1477.46 ± 241.43	1223.29 ± 200.60	588.49 ± 143.83	0.8796 (0.8128, 8)	*0.0128 (3.661,8)
PEP (ms)	115.04 ± 3.02	114.91 ± 4.14	118.06 ± 7.25	>0.9999 (0.053, 7)	0.4309 (1.362,7)
SI (s^{-2})	94.9 ± 29.1	51.92 ± 18.43	88.81 ± 25.62	*0.0190 (2.593)	**0.0044 (3.064)
LF/HF Ratio	2.75 ± 0.75	1.21 ± 0.24	0.88 ± 0.20	0.4772 (1.179)	0.1187 (1.886)
SD2/SD1	2.62 ± 0.19	2.53 ± 0.23	2.15 ± 0.18	>0.9999 (0.00)	0.1542 (1.768)
SI/RSA	18.76 ± 6.92	8.69 ± 3.69	16.13 ± 5.27	**0.0094 (2.828)	***0.0008 (3.536)
SI/RMSSD	5.53 ± 2.60	1.97 ± 1.24	3.52 ± 1.72	**0.0094 (2.828)	***0.0008 (3.536)
HR (bpm)	69.39 ± 3.98	66.73 ± 3.79	64.33 ± 3.64	0.1434 (2.075,8)	0.4711 (1.283,8)

The number of subjects, N=9 and the number of HAPW's, n=65, t-value and df are reported for parametric test (ANOVA) and z-value is reported in case of non-parametric Friedman test.

Table 5-3:HRV parameters associated with HAPWs in response to the meal (n=16)

	Before ± SEM	**During± SEM**	**After± SEM**	**p-Value (B-D)** (t,df) or (z-value)	**p-value (D-A)** (t,df) or (z-value)
RSA (ln(ms^2))	6.22±0.24	6.72±0.20	6.21±0.17	***0.0473 (2.54,14)**	****0.0013 (4.47,13)**
RMSSD (ms)	48.15±10.45	47.93±6.90	38.35±5.13	***0.0352 (2.37)**	****0.0038 (3.10)**
SD1 (ms)	40.24±6.68	46.34±4.85	35.53±4.69	0.0569 (2.19)	****0.002 (3.29)**
SD2 (ms)	94.45±15.96	112.38±10.387	79.72±9.3107	***0.0352 (2.37)**	***0.0212 (2.56)**
HF Power (ms^2)	1930.41±1100.6	1199.00±295.64	641.37±112.73	0.1358 (1.83)	****0.0038 (3.10)**
LF Power (ms^2)	1239.22±405	1296.89±355.38	667.15±135.33	0.4025 (1.28)	****0.0212 (2.56)**
PEP (ms)	120.91±2.29	123.27±2.36	124.00±1.72	0.2575 (1.58,13)	0.9107 (0.11,13)
SI (s^{-2})	77.34±10.17	55.30±7.01	89.57±12.22	***0.0467 (2.27)**	****0.0092 (2.84)**
LF/HF Ratio	2.06±0.84	1.26±0.27	1.43±0.37	>0.9999 (0.36)	0.9304 (0.73)
SD2/SD1	2.67±0.60	2.40±0.22	2.63±0.34	0.4025 (1.79)	>0.9999 (0.36)
SI/RSA	11.60±1.82	8.12±1.27	13.87±2.03	***0.0123 (2.78)**	****0.002 (3.29)**
SI/RMSSD	2.33±0.44	1.48±0.32	2.69±0.46	***0.0123 (2.74)**	****0.002 (3.29)**
HR (bpm)	71.50±1.96	70.33±1.80	70.35±1.80	>0.9999 (0.18)	>0.9999 (0.09)

t-value and df are reported for parametric test (ANOVA) and z-value is reported in case of non-parametric Friedman test.

Table 5-4: HRV parameters associated with HAPWs in response to the Bisacodyl (n=11)

	Before± SEM	**During± SEM**	**After± SEM**	**p-Value (B-D)** (t,df) or (z-value)	**p-value (D-A)** (t,df) or (z-value)
RSA (ln(ms^2))	5.67±0.57	6.13±0.48	5.68±0.47	***0.0407 (2.35,10)**	0.2529 (1.23,8)
RMSSD (ms)	32.95±7.45	46.00±9.52	33.79±7.90	****0.0007 (3.58)**	***0.0278 (2.46)**
SD1 (ms)	26.87±4.38	36.90±6.70	22.48±4.22	***0.0268 (2.99,10)**	**0.0582 (2.21,8)**
SD2 (ms)	75.42±9.70	78.24±7.89	62.71±8.77	0.2896 (1.12,10)	0.1159 (2.19,8)
HF Power (ms^2)	694.90±226.52	1037.75±296.52	544.23±142.21	0.3594 (1.34)	0.0883 (2.01)
LF Power (ms^2)	1181.99±409.5	1079.44±231.31	465.79±108.27	0.7422 (0.98)	***0.0278 (2.46)**
PEP (ms)	108.00±3.25	109.23±3.19	111.11±3.00	0.5032 (1.09,13)	0.5032 (1.09,9)
SI (s^{-2})	222.29±75.10	146.39±58.42	223.09±72.76	***0.0278 (2.46)**	****0.0073 (2.91)**
LF/HF Ratio	2.57±0.49	2.21±0.80	1.36±0.42	0.5271 (1.12)	0.5271 (1.12)
SD2/SD1	2.95±0.31	2.44±0.22	2.68±0.43	0.2544 (1.59,13)	0.6402 (0.48,9)
SI/RSA	54.98±21.95	29.75±13.02	45.09±15.53	***0.0146 (2.68)**	****0.0016 (3.35)**
SI/RMSSD	23.32±7.98	11.53±4.61	18.85±6.58	****0.0094 (2.83)**	****0.0094 (2.83)**
HR (bpm)	86.22±5.18	84.00±5.50	82.98±4.93	0.0883 (2.01)	>0.9999 (0.34)

t-value and df are reported for parametric test (ANOVA) and z-value is reported in case of non-parametric Friedman test.

Table 5-5:HRV parameters associated with HAPWs during baseline (n=12).

	Before± SEM	**During± SEM**	**After± SEM**	**p-Value (B-D)** (t,df) or (z-value)	**p-value (D-A)** (t,df) or (z-value)
RSA (ln(ms^2))	7.01±0.30	7.37±0.33	6.81±0.33	0.6419 (1.25,21)	0.0695 (1.91,21)
RMSSD (ms)	72.23±9.83	76.94±11.77	60.62±9.37	>0.9999 (0.43)	0.066 (2.12)
SD1 (ms)	64.65±7.83	80.68±8.91	66.18±7.31	0.0562 (2.31,11)	****0.0086 (3.67,10)**
SD2 (ms)	111.94±8.06	152.09±10.06	110.47±9.33	***0.0136 (2.93,11)**	****0.001 (5.06,10)**
HF Power (ms^2)	1964.75±519.63	2724.68±1146.1	1766.25±629.52	>0.9999 (0.21)	0.5728 (1.06)
LF Power (ms^2)	1649.09±397.7	1629.77±369.21	970.19±402.49	>0.9999 (0.61)	>0.9999 (0.61)
PEP (ms)	120.50±2.41	125.33±2.11	125.45±2.26	0.1181 (2.09,11)	0.9486 (0.07,10)
SI (s^{-2})	34.00±5.89	23.65±3.41	57.88±12.46	0.3316 (1.39)	****0.004 (3.09)**
LF/HF Ratio	2.04±0.77	1.08±0.30	1.04±0.23	0.7845 (0.85)	>0.9999 (0.21)
SD2/SD1	2.04±0.25	2.11±0.23	1.83±0.19	0.7648 (0.31,11)	0.2662 (1.59,10))
SI/RSA	4.99±0.94	3.35±0.52	9.27±2.25	0.4017 (1.28)	****0.0028 (3.20)**
SI/RMSSD	0.63±0.16	0.39±0.08	1.39±0.41	0.2712 (1.49)	*****0.0006 (3.62)**
HR (bpm)	56.92±2.18	54.42±1.93	54.36±1.50	0.0897 (2.25,11)	0.9206 (0.10,10))

t-value and df are reported for parametric test (ANOVA) and z-value is reported in case of non-parametric Friedman test.

Table 5-6:HRV parameters associated with HAPWs in response to the Prucalopride (n=14)

	Before± SEM	***During± SEM***	***After± SEM***	**p-Value (B-D)** *(t,df) or (z-value)*	**p-value (D-A)** *(t,df) or (z-value)*
RSA (ln(ms^2))	6.17±0.23	6.80±0.28	6.42±0.35	***0.0216 (2.55)**	0.2333 (1.57)
RMSSD (ms)	43.30±6.16	55.97±7.42	53.95±0.35	***0.0467 (2.27)**	***0.0467 (2.27)**
SD1 (ms)	35.68±5.253	45.74±6.24	41.2817±7.23	0.1025 (2.12,13)	0.2165 (1.30,13)
SD2 (ms)	76.897925±5.93	93.16±9.52	82.4542±10.48	0.0731 (2.32,13)	0.0731 (1.98,13)
HF Power (ms^2)	694.95±205.84	1327.93±351.56	1304.46±472.90	0.0997 (1.96)	0.6536 (0.98)
LF Power (ms^2)	595.53±119.8	911.97±274.02	607.13±242.66	>0.9999 (0.39)	0.5615 (1.08)
PEP (ms)	110.67±3.74	113.33±3.62	115.17±3.60	0.23 (1.65,13)	0.2692 (1.15,13)
SI (s^{-2})	91.06±12.60	65.34±11.87	87.27±19.55	***0.0465 (2.56,13)**	***0.0465 (2.34,13)**
LF/HF Ratio	1.20±0.23	0.75±0.10	0.64±0.16	0.2333 (1.57)	>0.9999 (0.39)
SD2/SD1	2.478±0.27	2.275±0.26	2.31167±0.32	0.8994 (0.76)	>0.9999 (0.38)
SI/RSA	15.17±2.15	10.43±2.17	15.00±3.62	0.2611 (1.51)	0.1176 (1.89)
SI/RMSSD	2.94±0.45	1.65±0.37	3.63±1.09	***0.0467 (2.27)**	***0.0092 (2.84)**
HR (bpm)	71.75±4.19	70.33±4.01	70.07±3.64	>0.9999 (0.38)	>0.9999 (0.19)

t-value and df are reported for parametric test (ANOVA) and z-value is reported in case of non-parametric Friedman test.

Table 5-7:HRV parameters associated with HAPWs in response to the Distal Balloon Distention (n=7)

	Before± SEM	**During± SEM**	**After± SEM**	**p-Value (B-D)** (t,df) or (z-value)	**p-value (D-A)** (t,df) or (z-value)
RSA (ln(ms^2))	6.56±0.41	7.31±0.20	6.25±0.21	***0.0138 (4.42,5)**	***0.0008 (10.88,4)**
RMSSD (ms)	51.73±8.29	61.19±8.43	43.51±3.59	0.7593 (1.85,5)	0.4863 (1.35,4)
SD1 (ms)	52.82±10.39	49.69±5.95	42.03±4.57	0.7649 (0.31,6)	0.7351 (0.77,4)
SD2 (ms)	105.08±11.97	120.76±13.77	90.732±11.20	0.2277 (1.58)	0.4118 (1.26)
HF Power (ms^2)	1449.08±561.1	1844.86±344.43	631.55±162.59	>0.9999 (0.53,5)	***0.0493 (4.20,3)**
LF Power (ms^2)	842.96±438.2	1574.24±370.03	520.67±212	0.3146 (1.41)	0.1542 (1.77)
PEP (ms)	123.43±2.09	126.00±2.68	127.60±1.91	0.6296 (0.92,6)	0.638 (0.51,4)
SI (s^{-2})	48.39±10.42	43.67±7.95	61.04±12.76	0.7077 (0.39,6)	0.6823 (0.86,4)
LF/HF Ratio	7.92±2.02	5.88±0.94	10.06±2.35	0.5777 (1.06)	0.5777 (1.06)
SD2/SD1	2.594±0.47	3.31±1.15	2.21±0.28	>0.9999 (0.32)	>0.9999 (0.63)
SI/RSA	7.92±2.02	5.88±0.94	10.06±2.35	0.4536 (0.88,6)	0.4536 (1.31,4)
SI/RMSSD	1.30±0.43	0.79±0.13	1.52±0.40	0.5194 (1.24,6)	0.5168 (1.32,4)
HR (bpm)	63.29±1.70	64.14±2.06	62.31±1.07	0.6954 (0.81,6)	0.6954 (0.76.4))

t-value and df are reported for parametric test (ANOVA) and z-value is reported in case of non-parametric Friedman test.

Table 5-8: HRV parameters associated with HAPWs in response to the Proximal Balloon Distention (n=5)

	Before± SEM	***During± SEM***	***After± SEM***	**p-Value (B-D)** *(t,df) or (z-value)*	**p-value (D-A)** *(t,df) or (z-value)*
RSA (ln(ms^2))	6.63±0.36	6.75±0.18	7.10±0.31	>0.9999 (0.33,4)	0.6283 (1.18,4)
RMSSD (ms)	46.44±0.36	43.99±5.85	48.88±3.65	>0.9999 (0.45,5)	>0.9999 (0.64,4)
SD1 (ms)	39.03±2.91	40.57±7.04	46.17±4.60	0.7593 (0.27,5)	0.4863 (0.66,4)
SD2 (ms)	87.99±14.16	85.74±9.28	100.57±11.71	>0.9999 (0.32)	>0.9999 (0.32)
HF Power (ms^2)	805.16±293	818.90±134.34	1119.5±444.78	>0.9999 (0.05,5)	>0.9999 (0.60,4)
LF Power (ms^2)	1347.52±529.7	601.13±212.58	879.83±444.92	0.6856 (0.95)	>0.9999 (0.00)
PEP (ms)	118.33±3.38	111.33±6.35	118.40±3.68	0.2225 (1.88,5)	0.2225 (1.87,4)
SI (s^{-2})	61.36±7.67	67.27±15.99	57.17±10.36	0.9121 (0.40,5)	0.9121 (0.35,4)
LF/HF Ratio	10.20±1.87	10.19±2.38	8.24±1.60	0.3095 (1.42)	>0.9999 (0.47)
SD2/SD1	2.28±0.32	2.34±0.31	2.39±0.49	0.993 (0.11,5)	0.993 (0.076,4)
SI/RSA	10.20±1.87	10.19±2.38	8.24±1.60	0.9942 (0.01,5)	0.8978 (0.44,4)
SI/RMSSD	1.16±0.21	1.61±0.57	1.23±0.25	0.7325 (1.02,4)	>0.9999 (0.45,4)
HR (bpm)	65.00±2.75	65.50±3.45	64.58±3.77	0.8425 (0.31,5)	0.8425 (0.56,4)

t-value and df are reported for parametric test (ANOVA) and z-value is reported in case of non-parametric Friedman test.

5.6 References

Baek, H. J., Cho, C. H., Cho, J., and Woo, J. M. (2015). Reliability of ultra-short-term analysis as a surrogate of standard 5-min analysis of heart rate variability. *Telemed. J. E Health* 21, 404–414. doi: 10.1089/tmj.2014.0104

PubMed Abstract | CrossRef Full Text | Google Scholar

Baevsky, R. M., and Chernikova, A. G. (2017). Heart rate variability analysis: physiological foundations and main methods. *Cardiometry* 66–67. doi: 10.12710/cardiometry.2017.10.6676

CrossRef Full Text | Google Scholar

Bharucha, A. E., and Brookes, S. J. H. (2018). "Neurophysiologic mechanisms of human large intestinal motility," in *Physiology of the Gastrointestinal Tract*, ed H. Said, (New York, NY: Elsevier), 517–564. doi: 10.1016/b978-0-12-809954-4.00023-2

CrossRef Full Text | Google Scholar

Bharucha, A. E., Camilleri, M., Low, P. A., and Zinsmeister, A. R. (1993). Autonomic dysfunction in gastrointestinal motility disorders. *Gut* 34, 397–401. doi: 10.1136/gut.34.3.397

PubMed Abstract | CrossRef Full Text | Google Scholar

Brookes, S., Chen, N., Humenick, A., Spencer, N. J., and Costa, M. (2016). Extrinsic sensory innervation of the gut: structure and function. *Adv. Exp. Med. Biol.* 891, 63–69. doi: 10.1007/978-3-319-27592-5_7

CrossRef Full Text | Google Scholar

Browning, K. N., and Travagli, R. A. (2014). Central nervous system control of gastrointestinal motility and secretion and modulation of gastrointestinal functions. *Compr. Physiol.* 4, 1339–1368. doi: 10.1002/cphy.c130055

PubMed Abstract | CrossRef Full Text | Google Scholar

Browning, K. N., and Travagli, R. A. (2019). Central control of gastrointestinal motility. *Curr. Opin. Endocrinol. Diabetes Obes.* 26, 11–16.

Google Scholar

Cacioppo, J. T., Berntson, G. G., Binkley, P. F., Quigley, K. S., Uchino, B. N., and Fieldstone, A. (1994). Autonomic cardiac control. II. Noninvasive indices and basal response as revealed by autonomic blockades. *Psychophysiology* 31, 586–598. doi: 10.1111/j.1469-8986.1994.tb02351.x

PubMed Abstract | CrossRef Full Text | Google Scholar

Callaghan, B., Furness, J. B., and Pustovit, R. V. (2018). Neural pathways for colorectal control, relevance to spinal cord injury and treatment: a narrative review. *Spinal Cord* 56, 199–205. doi: 10.1038/s41393-017-0026-2
PubMed Abstract | CrossRef Full Text | Google Scholar

Camilleri, M., Balm, R. K., and Low, P. A. (1993). Autonomic dysfunction in patients with chronic intestinal pseudo-obstruction. *Clin. Auton. Res.* 3, 95–100. doi: 10.1007/bf01818993
PubMed Abstract | CrossRef Full Text | Google Scholar

Chen, J.-H., Yu, Y., Yang, Z., Yu, W.-Z., Chen, W. L., Kim, M. J. M., et al. (2017). Intraluminal pressure patterns in the human colon assessed by high-resolution manometry. *Sci. Rep.* 7:41436. doi: 10.1038/srep41436
PubMed Abstract | CrossRef Full Text | Google Scholar

Colombo, J., Arora, R., DePace, N. L., and Vinik, A. I. (2015). *Clinical Autonomic Dysfunction. Measurement, Indications, Therapies, and Outcomes.* Heidelberg: Springer.
Google Scholar

De Groat, W. C., and Krier, J. (1976). An electrophysiological study of the sacral parasympathetic pathway to the colon of the cat. *J. Physiol.*260, 425–445. doi: 10.1113/jphysiol.1976.sp011523
PubMed Abstract | CrossRef Full Text | Google Scholar

De Groat, W. C., and Krier, J. (1978). The sacral parasympathetic reflex pathway regulating colonic motility and defaecation in the cat. *J. Physiol.* 276, 481–500. doi: 10.1113/jphysiol.1978.sp012248
PubMed Abstract | CrossRef Full Text | Google Scholar

Devroede, G., Giese, C., Wexner, S. D., Mellgren, A., Coller, J. A., Madoff, R. D., et al. (2012). Quality of life is markedly improved in patients with fecal incontinence after sacral nerve stimulation. *Female Pelvic Med. Reconstr. Surg.* 18, 103–112. doi: 10.1097/spv.0b013e3182486e60
PubMed Abstract | CrossRef Full Text | Google Scholar

Devroede, G., and Lamarche, J. (1974). Functional importance of extrinsic parasympathetic innervation to the distal colon and rectum in man. *Gastroenterology* 66, 273–280. doi: 10.1016/s0016-5085(74)80114-9

CrossRef Full Text | Google Scholar

Dinning, P. G., Sia, T. C., Kumar, R., Mohd Rosli, R., Kyloh, M., Wattchow, D. A., et al. (2016). High-resolution colonic motility recordings in vivo compared with ex vivo recordings after colectomy, in patients with slow transit constipation. *Neurogastroenterol. Motil.* 28, 1824–1835. doi: 10.1111/nmo.12884

PubMed Abstract | CrossRef Full Text | Google Scholar

Furness, J. B., Callaghan, B. P., and Rivera, L. R. (2014). The enteric nervous system and gastrointestinal innervation: integrated local and central control. *Adv. Exp. Med. Biol.* 817, 39–71. doi: 10.1007/978-1-4939-0897-4_3

CrossRef Full Text | Google Scholar

Gasparini, S., Howland, J. M., Thatcher, A. J., and Geerling, J. C. (2020). Central afferents to the nucleus of the solitary tract in rats and mice. *J. Comp. Neurol.* 528, 2708–2728.

Google Scholar

Goldstein, D. S., Bentho, O., Park, M., and Sharabi, Y. (2011). Low−frequency power of heart rate variability is not a measure of cardiac sympathetic tone but may be a measure of modulation of cardiac autonomic outflows by baroreflexes. *Exp. Physiol.* 96, 1255–1261. doi: 10.1113/expphysiol.2010.056259

PubMed Abstract | CrossRef Full Text | Google Scholar

Grossman, P., and Taylor, E. W. (2007). Toward understanding respiratory sinus arrhythmia: relations to cardiac vagal tone, evolution and biobehavioral functions. *Biol. Psychol.* 74, 263–285. doi: 10.1016/j.biopsycho.2005.11.014

PubMed Abstract | CrossRef Full Text | Google Scholar

Hayano, J., and Yuda, E. (2019). Pitfalls of assessment of autonomic function by heart rate variability. *J. Physiol. Anthropol.* 38:3.

Google Scholar

Houtveen, J. H., Groot, P. F., and Geus, E. J. (2005). Effects of variation in posture and respiration on RSA and pre-ejection period. *Psychophysiology* 42, 713–719. doi: 10.1111/j.1469-8986.2005.00363.x

PubMed Abstract | CrossRef Full Text | Google Scholar

Jean, A. (1991). [The nucleus tractus solitarius: neuroanatomic, neurochemical and functional aspects]. *Arch. Int. Physiol. Biochim. Biophys.*99, A3–A52.
Google Scholar

Kubios (2020). Available online at: https://www.kubios.com/about-hrv (accessed August 28, 2020).
Google Scholar

La Rovere, M. T., Pinna, G. D., Maestri, R., Mortara, A., Capomolla, S., Febo, O., et al. (2003). Short-term heart rate variability strongly predicts sudden cardiac death in chronic heart failure patients. *Circulation* 107, 565–570. doi: 10.1161/01.cir.0000047275.25795.17
CrossRef Full Text | Google Scholar

Leblanc, D., McFadden, N., Lebel, M., and Devroede, G. (2015). Fecal continence can be restored by sacral neurostimulation after traumatic unilateral pudendal neuropathy: a case report. *Int. J. Colorectal Dis.* 30, 569–570. doi: 10.1007/s00384-014-2019-3
PubMed Abstract | CrossRef Full Text | Google Scholar

Lorena, S. L., Figueiredo, M. J., Almeida, J. R., and Mesquita, M. A. (2002). Autonomic function in patients with functional dyspepsia assessed by 24-hour heart rate variability. *Dig. Dis. Sci.* 47, 27–31.
Google Scholar

Lu, C. L., Zou, X., Orr, W. C., and Chen, J. D. (1999). Postprandial changes of sympathovagal balance measured by heart rate variability. *Dig. Dis. Sci.* 44, 857–861.
Google Scholar

Milkova, N., Parsons, S. P., Ratcliffe, E., Huizinga, J. D., and Chen, J.-H. (2020). On the nature of high-amplitude propagating pressure waves in the human colon. *Am. J. Physiol. Gastrointest. Liver Physiol.* 318, G646–G660. doi: 10.1152/ajpgi.00386.2019
PubMed Abstract | CrossRef Full Text | Google Scholar

Nguyen, L., Wilson, L. A., Miriel, L., Pasricha, P. J., Kuo, B., Hasler, W. L., et al. (2020). Autonomic function in gastroparesis and chronic unexplained nausea and vomiting: relationship with etiology, gastric emptying, and symptom severity. *Neurogastroenterol. Motil.* 32:e13810.
Google Scholar

Ouyang, X., Li, S., Zhou, J., and Chen, J. D. (2020). Electroacupuncture ameliorates gastric hypersensitivity via adrenergic pathway in a rat model of functional dyspepsia. *Neuromodulation* 23, 1137–1143. doi: 10.1111/ner.13154
PubMed Abstract | CrossRef Full Text | Google Scholar

Parsons, S. (2019) Available online at: http://scepticalphysiologist.com.html (accessed August 28, 2020).
Google Scholar

Rahman, F., Pechnik, S., Gross, D., Sewell, L., and Goldstein, D. S. (2011). Low frequency power of heart rate variability reflects baroreflex function, not cardiac sympathetic innervation. *Clin. Auton. Res.* 21, 133–141. doi: 10.1007/s10286-010-0098-y
PubMed Abstract | CrossRef Full Text | Google Scholar

Rahman, S., Habel, M., and Contrada, R. J. (2018). Poincaré plot indices as measures of sympathetic cardiac regulation: responses to psychological stress and associations with pre-ejection period. *Int. J. Psychophysiol.* 133, 79–90. doi: 10.1016/j.ijpsycho.2018.08.005
PubMed Abstract | CrossRef Full Text | Google Scholar

Schächinger, H., Weinbacher, M., Kiss, A., Ritz, R., and Langewitz, W. (2001). Cardiovascular indices of peripheral and central sympathetic activation. *Psychosom. Med.* 63, 788–796. doi: 10.1097/00006842-200109000-00012
PubMed Abstract | CrossRef Full Text | Google Scholar

Semba, T., and Fujii, Y. (1970). Relationship between venous flow and colonic peristalsis. *Jpn. J. Physiol.* 20, 408–416. doi: 10.2170/jjphysiol.20.408
PubMed Abstract | CrossRef Full Text | Google Scholar

Shaffer, F., and Ginsberg, J. P. (2017). An overview of heart rate variability metrics and norms. *Front. Public Health* 5:258. doi: 10.3389/fpubh.2017.00258
PubMed Abstract | CrossRef Full Text | Google Scholar

Shimizu, Y., Chang, E. C., Shafton, A. D., Ferens, D. M., Sanger, G. J., Witherington, J., et al. (2006). Evidence that stimulation of ghrelin receptors in the spinal cord initiates propulsive activity in the colon of the rat. *J. Physiol.* 576, 329–338. doi: 10.1113/jphysiol.2006.116160
PubMed Abstract | CrossRef Full Text | Google Scholar

Singh, A., and Jaryal, A. K. (2020). "Neurophysiology of Respiratory System," in *Brain and Lung Crosstalk*, eds H. Prabhakar and C. Mahajan (Singapore: Springer), 1–38. doi: 10.1007/978-981-15-2345-8_1
CrossRef Full Text | Google Scholar

Smith-Edwards, K. M., Najjar, S. A., Edwards, B. S., Howard, M. J., Albers, K. M., and Davis, B. M. (2019). Extrinsic primary afferent neurons link visceral pain to colon motility through a spinal reflex in mice. *Gastroenterology* 157, 522–536.e2.
Google Scholar

Szurszewski, J., and Miller, S. M. (2006). "Physiology of prevertebral sympathetic ganglia," in *Physiology of the Gastrointestinal Tract*, ed. L. R. Johnson (San Diego, CA: Academic Press), 603–627. doi: 10.1016/b978-012088394-3/50025-8
CrossRef Full Text | Google Scholar

Taché, Y., and Million, M. (2015). Role of corticotropin-releasing factor signaling in stress-related alterations of colonic motility and hyperalgesia. *J. Neurogastroenterol. Motil.* 21, 8–24.
Google Scholar

Thayer, J. F., Ahs, F., Fredrikson, M., Sollers, J. J., and Wager, T. D. (2012). A meta-analysis of heart rate variability and neuroimaging studies: implications for heart rate variability as a marker of stress and health. *Neurosci. Biobehav. Rev.* 36, 747–756. doi: 10.1016/j.neubiorev.2011.11.009
PubMed Abstract | CrossRef Full Text | Google Scholar

Van Lien, R., Neijts, M., Willemsen, G., and de Geus, E. J. (2015). Ambulatory measurement of the ECG T-wave amplitude. *Psychophysiology*52, 225–237. doi: 10.1111/psyp.12300
PubMed Abstract | CrossRef Full Text | Google Scholar

Yuan, Y., Ali, M. K., Mathewson, K. J., Sharma, K., Faiyaz, M., Tan, W., et al. (2020). Associations between colonic motor patterns and autonomic nervous system activity assessed by high-resolution manometry and concurrent heart rate variability. *Front. Neurosci.* 13:1447. doi: 10.3389/fnins.2019.01447
PubMed Abstract | CrossRef Full Text | Google Scholar

Chapter 6

Autonomic Nervous System Assessment of patients with motility disorders in comparison with healthy controls

Part of this work has been incorporated in the manuscript titled “Diagnosis Of Colonic Dysmotility Associated With Autonomic Dysfunction In Patients With Chronic Refractory Constipation” published in *Nature’s Scientific Reports* on July 14, 2022. Authored by: Lijun Liu, Natalija Milkova, Sharjana Nirmalathasan, M. Khawar Ali, Kartik Sharma, Jan D. Huizinga and Ji-Hong Chen

DOI: https://doi.org/10.1038/s41598-022-15945-6

6.1 Abstract

Our recent study (presented in chapter 4) states that colonic motor patterns are associated with autonomic nervous system activity. The parasympathetic activity increases, and the sympathetic activity decreases during the motor patterns, and both recover afterwards. Based on these results, it was hypothesized that the patients with motility disorders might have abnormal autonomic nervous system activity during baseline and/or they might not be able to modulate their autonomic nervous system to generate the normal motor patterns. In this study, we have compared the autonomic nervous system activity of patients (n=40) with motility disorders, to that of healthy controls (n=20). The ECGs of the subjects were recorded during supine, sitting, standing, and sitting after walking. The heart rate variability parameters were calculated for each posture to represent the autonomic nervous system activity and reactivity to the postural change. RSA, RMSSD and HF power were used as measures of the parasympathetic nervous system, while SI was used to record the sympathetic nervous system

activity, and SI/RSA was used as a measure of autonomic balance. After overall comparison, the patients were divided into four age groups; 0-15y (n=3), 16y-35y (n=14), 36y-50y (n=13) and 50+y (n=10), and their autonomic tone and reactivity were compared with that of our own control group. In the next step, the patients were divided based on their different health conditions. We realized that our own control group does not match the patient group in age distribution, hence we are proposing ways to address this issue. What follows is first a comparison with our own control group. It was observed that the patients with a motility disorder have low parasympathetic tone and high sympathetic tone compared to the healthy controls during all the postures. The change in sympathetic and parasympathetic reactivity to sitting and standing was also higher in patients. The age group 0-15y has completely normal autonomic activity, the age group 16y-35y had normal parasympathetic activity and higher sympathetic tone and reactivity, while the last two groups (36-50y and 50+y) had low parasympathetic and high sympathetic tones and reactivities. The subgroup with anxiety/depression/suicide thoughts had normal parasympathetic but high sympathetic tone and reactivity. Patients in constipation and bladder disorder subgroups had lower parasympathetic tone and reactivity, while sympathetic tone and reactivity were both higher. While the patients with back pain and upper GI symptoms had very low PNS and very high SNS tones and reactivities.

An ideal comparison would be to divide the controls in the above-mentioned age groups as well and compare them with their respective patients' age group. However, in our control group we had no data for 0-15y (n=0) group, while 16 out of 20 controls belonged to 16y-35y group

(n=16), In 36y-50y group there was only 1 volunteer (n=1), and 3 volunteers were 50+ years old (n=3). Not all control values from the literature matched our experimental conditions, hence only the average values of supine RMSSD and HF power for the different age groups matched with this study and these values are provided for comparison. Our laboratory is currently working on generating the HRV control values for different age groups by hiring the volunteers for these age groups or by using online ECG databases if their protocol matches with ours which will be used in further comparison in future studies. Nevertheless, this study generates valuable hypotheses as to the contribution of elevated SNS and suppressed PNS activities in colonic motility disorders.

6.2 Introduction

Human colonic transit and defecation are neuronally regulated through multi-level neuronal reflexes, such as the gastrocolic reflex (a colon motor response to gastric distention) and the sacral defecation reflex (evoking propulsive activity in the left colon by rectal bisacodyl). A vagal autonomic reflex can be initiated by a meal, proximal colon distention or rectal bisacodyl stimulation to evoke propulsive activity starting from the proximal colon. The coloanal reflex involves the relaxation of the anal sphincters in response to a propulsive colon motor activity. Functional or structural deficits in the neural circuits may lead to colonic dysfunction due to abnormal or absent reflexes. Sensory information from the musculature and lumen of the colon, rectum and anal canal [1], [3] is sent to the spinal cord, including the sacral parasympathetic nucleus[36] and up into the brainstem[37], including the nucleus tractus solitarius (NTS) [38]. The sensory information is integrated into the brainstem, influenced by

the cortex, which can stimulate excitatory vagal and spinal parasympathetic motor neurons to initiate motor patterns in the proximal, transverse or descending colon[1], [39]. The importance of the extrinsic autonomic nervous system (ANS) in the regulation of defecation reflexes has been demonstrated in animal models [40] and in patients with a spinal injury who lost spontaneous bowel movements due to damage to sacral parasympathetic innervation [41], [42]. The autonomic dysfunction can be the root cause of motility disorders and restoring the normal autonomic tone and reactivity may restore the normal colonic motility. In this study, we will compare the autonomic tone and reactivity of patients with colonic motility patients with the healthy controls. The patients will also be divided into different age groups and based on various health conditions health conditions as mentioned in the next section.

6.3 Methods

Twenty healthy volunteers and forty patients with motility disorders participated in this study. The complete study was carried out at McMaster University with ethics approval from the Hamilton Integrated Research Ethics Board and written consent from all participants. All the participants underwent the active standing test, and their ECG and impedance were recorded during the whole procedure, which was then processed to generate the heart rate variability parameters to access the autonomic response to the postural change. The autonomic response of all the patients and their subgroups based on age and other health conditions, as explained below, were compared to that of healthy controls.

6.3.1 Literature values of HRV parameters for age groups

From the literature we obtained control values for heart rate variability parameters of interest stratified by age for various body postures (i.e., supine, standing, and sitting) [60]-[66]. These data were short-term (~5 mins) HRV recordings measured by ECG, where the average values (stratified for age) were pooled to capture estimated baseline values for the various HRV parameters. All the efforts were made to obtain all HRV parameters' values for each age group during supine, sitting and standing; however, there were several variations like, the population within the same age group varied in different studies, for example, one study included athletes who are considered to have higher heart rate variability, while other included normal population. The protocol followed during postural changes, the criteria for data preprocessing and calculations can be different in each study. The frequency bands used for the calculations of HF power may vary in each study. Only the HF power and RMSSD for age groups 16-35y, 36-50y and 50+y age groups were obtained for supine sitting and standing, the average values are shown in table 6.3 for comparison.

6.3.2 Active Standing Test and Autonomic Nervous System Assessment

The participants were asked to refrain from smoking, caffeine, alcohol, and heavy eating two hours before testing for the active standing test. After lying down quietly in the supine position for at least ten minutes in a quiet room with normal lighting and temperature, their ECG and impedance were recorded for 6 minutes in the supine position termed herein as baseline or supine. Immediately after baseline recording, the participants were asked to sit for six minutes, followed by six minutes of standing, six minutes of walking, and then back to sitting for six more minutes. Mindware technology's mobile recorder was used with seven electrodes

such that three of the seven electrodes were used to record the ECG. For impedance recording, the remaining four electrodes were used in a standard tetrapolar electrode configuration. ECG and impedance signals were recorded using MindWare BioLab Recording Software. MindWare HRV 3.1 software was used for artifact correction of the ECG signal and to calculate the beat-to-beat intervals (RR intervals), RSA, HF power and RMSSD. Baevsky's stress index (SI) was calculated in MATLAB using the RR interval time series. RSA, HF power and RMSSD were used as measures of parasympathetic reactivity; SI was used as a measure of sympathetic reactivity. In contrast, the ratio SI/RSA was used to measure shifts in combined parasympathetic and sympathetic activity (Autonomic Balance).

6.3.3 Patient subgroups

The patient group was subdivided into subgroups based on their age and different health conditions. The patients with age group *0-15* years had 3 patients (*n=3*), age group *16-35* had 14 patients(*n=14*) and age group *36-50* had 13 patients (*n=13*) and 50+ age group had 10 patients (*n=10*). Secondly, the patients were divided into subgroups based on their health conditions, smoking and marijuana use. There were 3 patients in the *smoking and marijuana* subgroup (*n=3; Age_{av}=39.33y*$\pm$10.34), 4 patients who had *tailbone injury* (*n=4; Age_{av}=37y*$\pm$14.21), and 6 patients in the subgroup suffering from scoliosis*/spinal bifida/thoracic outlet syndrome/meningitis/tarlov syst*, (*n=6; Age_{av}=29.50y*$\pm$12.15). *Anxiety/Depression/suicide thoughts* subgroup had 8 patients (*n=8; Age_{av}=42.13y*$\pm$11.69), *back pain* group had 16 patients (*n=16; Age_{av}=37.94y*$\pm$14.18), *constipation* subgroup had 14 patients (*n=14; Age_{av}=38.71y*$\pm$18.84), 3 patients had *Fecal incontinence* (n=3; *Age_{av}=36.67y*$\pm$0.47), 5 patients had both constipation and *fecal incontinence* (*n=5; Age_{av}=45.40y*$\pm$21.45), 12 patients had *upper*

GI symptoms (*n=12; Age_{av}=34.83y*±13.90), 2 patients had urinary difficulty (n=2; *Age_{av}=23.50y*±10.50), 3 had bladder symptoms (n=3; *Age_{av}=42.67y*±16.42) and 5 patients had urinary incontinence (n=5; *Age_{av}=38.20y*±21.10). Several patients had multiple disorders and were included in more than one subgroup.

6.3.4 Comparisons and Statistical Analyses

The HRV parameters (RSA, RMSSD, HF power, SI, SI/RSA) and HR were calculated from the recorded ECG signal for each stage of the active standing test protocol for each participant in both patients and control groups. All the HRV parameters for the control group (n=20) for supine, sitting, standing, and sitting after walking were used to compare with those of the patient group (n=40). To test the autonomic response to sitting and standing, the difference between the values of each parameter during supine and sitting and supine and standing was calculated for each participant, and the results were compared for patients and control groups. The data were first analyzed for Gaussian distribution using the Shapiro-Wilk Normality test. If both the data columns in comparison (patient vs control) were normally distributed, the Unpaired t-test was applied for comparison, and in the case of non-gaussian distribution, the Mann-Whitney test was applied. In the next step, each subgroup of the patients, as mentioned above, was compared to the controls' group individually for supine, sitting, standing, and sitting after walking for each HRV parameter generated. The data for walking was not included in the analysis because of more than 10% artifacts in the ECG recording during walking due to the noise from moving connecting cables while walking. The significance level was set at $p<0.05$. In all the tables $p<0.05$, $p<0.01$, $p<0.001$ and $p<0.0001$ are represented by *, **, *** and **** respectively. GraphPad Prism 9 was used for all the statistical analyses.

6.4 Results

6.4.1 Baseline Autonomic tone

The results indicated that the patients with motility disorders have considerably lower baseline (supine) parasympathetic and higher sympathetic tone compared to that of the control group. RSA for patients' group (n=40) was 5.74±0.21 ln(ms^2) which is significantly lower than the average baseline RSA of 6.57±0.30 ln(ms^2) for the controls (n=20). Similarly, the average RMSSD and HF power for the patients' group were 39.52±4.68 ms and 767.52±211ms^2 which are lower than the baseline average RMSSD and HF Power were 59.36±7.38 ms and 1392.28±346.55 ms^2 of the control group respectively. The SI, which represents the sympathetic tone, was more than double for patients (59.27±5.96 s^{-1}) compared to the SI for controls (28.71±4.72 s^{-1}). The patients had their autonomic balance dominated by the sympathetic nervous system compared to controls as indicated by the SI/RSA ratio, which is more than double for patients (12.30±1.76) as compared to controls (5.24±1.17). Table 6.1 represents the comparison with a statistical significance level (p-values) in each case.

6.4.2 Autonomic activity during different postures

The comparison of the autonomic activity of control and motility patient's groups indicated that the patients had slightly lower parasympathetic activity during sitting and higher sympathetic activity with sympathetically dominant autonomic balance. The average RSA, RMSSD and HF power values for the patient group were 14%, 39% and 65% lower than that of the control group. While the average SI for patients was 126% higher than the controls. The autonomic balance parameter SI/RSA was 151% higher for patients. Similarly, while standing, the parasympathetic parameters RSA, RMSSD, and HF power were 16%, 26% and 62.43% lower for

patients than in the control group. The SI was more than double (102%), and the autonomic balance (SI/RSA) was 166% higher for patients than in the controls group (Table 6.1).

The groups were compared again for sitting after walking to identify the recovery in the autonomic reactivity to the postural changes, termed "Sitting after walking". The RSA. RMSSD and HF Power for both patients' and controls' groups were not statistically different; however, the sympathetic activity for patients' groups was still 54% higher than in the controls' group. The autonomic balance (SI/RSA) was slightly higher for patients but not statistically significant (Table 6.1).

Table 6-1: Comparison of ANS activity and reactivity of the patients with motility disorders and healthy controls

		Controls (n=20) Age_{av}=28.65±11.70	**Patients (n=40)** Age_{av}=36.15±17.16	**p-value (C vs P)**
		Mean±SEM	**Mean±SEM**	
Supine	RSA *(ln(ms^2))*	6.57±0.30	5.74±0.21	***0.0302**
	SI *(s^{-2})*	28.71±4.72	59.27±5.96	****0.0001**
	RMSSD *(ms)*	59.36±7.38	39.52±4.68	***0.0121**
	HF Power *(ms^2)*	1392.28±346.55	767.52±211	0.0537
	SI/RSA	5.24±1.17	12.30±1.76	***0.0003**
Sitting	RSA *(ln(ms^2))*	6.20±0.35	5.31±0.19	***0.0181**
	SI *(s^{-2})*	33.62±4.77	75.85±8.93	***0.0003**
	RMSSD *(ms)*	49.97±8.31	30.44±3.18	***0.0196**
	HF Power *(ms^2)*	1295.90±438.38	454.83±121.13	***0.0161**
	SI/RSA	6.65±1.36	16.69±2.50	***0.0005**
Standing	RSA *(ln(ms^2))*	5.54±0.27	4.68±0.17	**0.0069**
	SI *(s^{-2})*	61.19±6.10	123.76±16.56	***0.0245**
	RMSSD *(ms)*	28.06±3.42	20.67±1.85	0.0699
	HF Power *(ms^2)*	524.10±179.79	196.84±45.76	**0.0083**
	SI/RSA	12.17±1.54	32.35±5.61	***0.0181**
Sitting after Walk	RSA *(ln(ms^2))*	5.66±0.35	5.55±0.20	0.7577
	SI *(s^{-2})*	43.73±6.56	67.18±6.61	***0.0246**
	RMSSD *(ms)*	45.18±8.21	34.74±4.28	0.1766
	HF Power *(ms^2)*	882.55±448.76	536.90±135.11	0.7644
	SI/RSA	9.18±1.78	13.75±1.99	0.1219

6.4.3 Comparison of ANS modulation in response to postural change for different age groups

To test the autonomic response in changing the posture from Supine to Sitting and standing. The difference of each HRV parameter during sitting and supine as well as during standing and supine for patients and control groups were compared, and the results indicated that the controls had a high parasympathetic response compared to patients while the patients had a

more sympathetic response compared to controls for both Sitting and Standing. The average change in RSA, RMSSD and HF power for patients going from supine to sitting were 26%, 44% and 45% less respectively, and the change in SI was 157% more than that in controls. The change in SI/RSA was 170% more in patients compared to controls; however not statistically significant as shown in Table 6.2.

Similarly, the average change in RSA for patients and controls was approximately similar from supine to standing, while ΔRMSSD and ΔHF power for patients in going from supine to standing were respectively 35% (p=0.0485) and 32%(p=<0.0001) less and change in SI was 116% more as compared to that in controls. The change in SI/RSA was more than double in patients compared to controls; however not statistically significant. Table 6.2 represents the comparison with a statistical significance level (p-values) in each case.

Table 6-2:Modulation of ANS in response to postural change (PvsC)

		Controls (n=20) Age_{av}=28.65±11.70	**Patients (n=40)** Age_{av}=36.15±17.16	**p-value (C vs P)**
		Mean±SEM	**Mean±SEM**	
△(Stand-Sup)	△RSA *(ln(ms²))*	1.11±0.20	1.23±0.15	0.5517
	△SI *(s^{-2})*	32.82±5.94	71.05±14.11	0.2145
	△RMSSD *(ms)*	33.19±5.86	21.47±3.95	***0.0485**
	△HF Power *(ms^2)*	891.56±216.48	608.66±197.89	****>0.0001**
	△SI/RSA	6.94±1.36	21.10±5.04	0.1128
△(Sitt-Sup)	△RSA *(ln(ms²))*	0.90±0.14	0.66±0.09	0.1582
	△SI *(s^{-2})*	11.48±3.02	29.53±2.46	****0.0086**
	△RMSSD *(ms)*	23.80±4.01	13.29±2.46	****0.0070**
	△HF Power *(ms^2)*	800.38±166.15	443.26±154.92	*****>0.0001**
	△SI/RSA	2.93±0.94	7.93±1.72	0.5621

6.4.4 Autonomic tone and reactivity for different age groups

The baseline autonomic activity of the patients in age groups 0-15 and 16-35 was similar to the baseline autonomic activity of the controls' group, with all the HRV parameters values within the normal range. The age group, 16-35, had significantly high sympathetic tone, on average the SI for patient was 70.64% higher compared to the control group. The parasympathetic tone of this age group was almost similar to that of controls. The age groups 36-50 and 50+ had both low parasympathetic tone and high sympathetic tone compared to controls. The baseline RSA, RMSSD and HF power for the 36-50 age group were respectively 15.83%, 46.39% and 65.17% lower compared the controls. Similarly for the 50+ age group, the RSA, RMSSD and HF power were 17.96%, 29.63% and 31.59% lower respectively from that of controls. The baseline sympathetic tone for 36-50 group was 115.12% and 50+ group was 121.63% higher compared to controls (Table 6.2).

The autonomic activity of the patients with age 15 years and under indicated no difference from that of control groups during both sitting and standing. While the patients in the age group 16-35 had significantly lower parasympathetic activity and higher sympathetic activity than the controls' group during sitting. The RSA and HF Power were not different during standing, while only RMSSD was significantly lower than controls; the SI indicated that this group had high sympathetic activity during standing compared to controls.

The age group, 36-50, did not show any change in parasympathetic activity during sitting, while they had a significantly higher sympathetic response as marked by the increased values of SI during sitting compared to controls. During standing, all the parasympathetic parameters (RSA,

HF Power, RMSSD) were lower, and the sympathetic parameter (S) was higher than that of the control. For the 50+ age group, the average values of RSA and HF power were significantly lower than controls, while RMSSD was slightly lower during sitting, while the parasympathetic nervous system activity was higher. The RSA and HF power remained higher during standing, but sympathetic reactivity (SI) to standing was similar to that of the control's group (Table 6.2).

6.4.5 Effects of various health conditions on autonomic tone

The baseline autonomic activity of the "*smoking and marijuana* subgroup, *tailbone injury"* subgroup, "scoliosis*/spinal bifida/thoracic outlet syndrome/meningitis/tarlov syst"*, "*Fecal incontinence", "*urinary difficulty" and "urinary incontinence" subgroups did not show any difference from that of control's group. All their parasympathetic and sympathetic parameters' values were within the normal range.

The "Anxiety/Depression/suicide thoughts" subgroup had a normal parasympathetic tone; however, their sympathetic tone was significantly higher than normal. Similarly, "*constipation and fecal incontinence"* and "*bladder symptoms"* subgroups had normal parasympathetic but higher than normal sympathetic tone.

The "*Back Pain"* and *"Upper GI Symptoms"* subgroups had lower parasympathetic and higher sympathetic activity than controls. The patients suffering from constipation only had higher than normal sympathetic tone, but their RSA and HF power were within the normal range, but RMSSD was lower than normal, indicating a decreased parasympathetic tone during baseline (Table 6.3).

6.4.6 Effects of various health conditions on Autonomic (re)activity during Sitting and Standing

"*Smoking and marijuana* and "*tailbone injury"*, "*Constipation and fecal incontinence"* and *"*urinary difficulty" subgroups' autonomic reactivities to both sitting and standing postures were within the normal ranges (or not significantly different in comparison with the control's group). "*Fecal incontinence"* subgroups' reactivity was also like that of the control in sitting and standing; the only difference was that this group had significantly lower RMSSD during standing than that of the control's group. Similarly, the "urinary incontinence" subgroup had the same sympathetic and parasympathetic response to sitting and the same parasympathetic response to standing as controls, with a markedly higher sympathetic response to standing than controls. *"Anxiety/Depression/suicide thoughts",* "scoliosis*/spinal bifida/thoracic outlet syndrome/meningitis/tarlov syst"* and "*Bladder Symptoms"* subgroups had a similar parasympathetic response to that of controls while higher sympathetic response compared to controls during the sitting.

The "*Back Pain", "Upper GI Symptoms" and* "*Constipation*" subgroups showed similar responses to the sitting posture. However, the patients in these groups had significantly lower parasympathetic activity and very high sympathetic activity during sitting compared to the healthy controls. During Standing posture, the "*Back Pain",* and *"Upper GI Symptoms" groups* were again hypersensitive, with a marked increase in SI (sympathetic response) compared to the control's SI and very low parasympathetic activity (RSA, HF Power and RMSSD) compared to that of controls. However, the "*Constipation*" subgroup's response was normal during standing in contrast to its response during sitting (Table 6.3).

The change in PNS parameters (△RSA, △RMSSD, △HF Power), SNS parameter (△SI) and autonomic balance (△SI/RSA) was not found to be statistically different for any health group from that of control group.

6.5 Discussions

While the vagus nerve innervates the proximal colon, parasympathetic innervation to the distal colon originates from the lumbosacral spinal cord regions of S1 to S4. Damage to parasympathetic nerves will cause dysregulated colonic motility[39]. A spinal injury can contribute to left colon dysmotility. Damage to the cauda equina or conus medullaris, where the sacral parasympathetic nucleus resides, decreases descending and sigmoid colon transit time[43]. Sympathetic innervation of the gastrointestinal tract originates from the thoracic and lumbar spinal cord, predominantly from L2 to L5. Stimulation of sympathetic nerves leads to inhibition of colonic motility via the release of norepinephrine on cholinergic nerves in the myenteric plexus and contraction of the anal sphincters via direct action on smooth muscle cells[44], [45], [46]. The high amplitude pressure waves (HAPWs), which are the primary drivers of colonic motility, are associated with increased parasympathetic activity and decreased sympathetic activity, while rhythmic parasympathetic activity is required to orchestrate motor complexes [30]. The low parasympathetic tone and reactivity in motility disorder patients indicate the patients' inability to effectively modulate parasympathetic activity to reach the threshold level required to generate strong HAPWs. The HAPWs might either be absent or very weak (low pressured) in patients with autonomic dysfunction. This opens the way for a future study to correlate the autonomic tone and reactivity of the patients with the amplitude of the HAPWs. The elevated SNS tone and activity to postural changes refer to the inhibition of the colonic activity. The autonomic tone or reactivity is highly influenced by age. As discussed earlier, a limitation of

this study was, the patients of all age groups and all the groups with different health conditions were compared to the same group of volunteers with an average age of 29.45 years. The objective was to gain a tentative assessment of relationships between certain health conditions and HRV parameters. This would help formulating study protocols for future studies. The tentative nature is due to the fact that we do not have optimal control values for the various health conditions, to the fact that the health conditions should also be subdivided by age, and that the various groups have a low n number. The data on the age group 16-35 where we have good control values shows that the literature data are far from our control values. As discussed earlier, there may be many reasons for that, the frequency range of the HF band is usually not given, a control group may be athletes who do not have "normal" control values, the difference in protocol compared to ours. This shows the importance of getting our own control values for all age groups. Our lab is in process of recruiting more volunteers to generate control values for all ages which will be used for comparison in future studies. The results for the age group of 16-35 for which we have good control values also indicated that the patients with motility disorder had increased sympathetic tone and reactivity to sitting with lowered PNS reactivity. The autonomic balance is shifted towards SNS activity during all of the supine, sitting and standing postures. This confirms our hypothesis of abnormal autonomic activity and reactivity associated with motility disorders.

The patients with upper GI symptoms, constipation, bladder function disorders and back pain had the most elevated SNS tone and reactivity and lowest PNS tone and reactivity. While other groups did not show abnormality in the autonomic function. Although it is very important to

obtain data for different pathophysiologies underlying GI motor disorders, the patients in the various groups will still be heterogeneous, and as we have emphasized in the submitted manuscript related to this chapter, our major goal is to provide individual diagnoses to the patients.

This study confirms the association of the autonomic abnormality with motility disorders; therefore, the patients with motility issues must be assessed for autonomic dysfunction. In current clinical practices, some patients with severe motility issues undergo surgeries which sometimes lead to the removal of the entire or some part of the colon, but the problem persists, where the problem might be in the autonomic dysfunction instead of the colon itself. Such patients may be able to fully restore their colonic activity by restoring their normal autonomic function and avoiding the removal of the colon.

Table 6-3: Comparison of ANS (re)activity of different age groups of the patients with motility disorders and healthy controls.

Average values from literature presented for comparison in brackets where available

		Control (n=20;Age_{av}=28.65±11.70)	**Age(0-15)** (n=3;Age_{av}=9±1.63)	**Age(16-35)** (n=14;Age_{av}=22.86±6.70)	**Age(36-50)** (n=13;Age_{av}=40.92±5.33)	**Age(50+)** (n=10;Age_{av}=56.7±12.5)
Supine	RSA *(ln(ms^2))*	6.57±0.30	6.28±0.75	6.08±0.32	***5.53±0.37**	***5.39±0.46**
	SI *(s^{-2})*	28.71±4.72	81.92±30.69	***48.99±8.61**	****61.76±11.35**	****63.63±8.57**
	RMSSD *(ms)*	59.36±7.38	48.73±16.42	43.08±5.77 (**Lit:**38.56±18.28)	****31.82±4.28** (**Lit:**30.74±16.53)	***41.77±14.45** (**Lit:**24.60±16.98)
	HF Power *(ms^2)*	1392.28±346.55	1161.65±738.02	813.30±243.45 (**Lit:**366.70)	***484.95±145.47** (**Lit:**204.96)	***952.5±691.1** (**Lit:**121.99)
	SI/RSA	5.24±1.17	15.32±6.79	***9.64±2.72**	****13.92±3.74**	****13±2.16**
Sitting	RSA *(ln(ms^2))*	6.20±0.35	6.76±0.84	5.27±0.28	5.27±0.31	***4.98±0.33**
	SI *(s^{-2})*	33.62±4.77	93.98±47.05	***69.54±11.75**	***88.70±19.34**	***62.53±9.28**
	RMSSD *(ms)*	49.97±8.31	51.94±15.16	***27.54±3.29** (**Lit:**34.37±16.35)	29.82±5.62 (**Lit:**29.59±17.84)	28.87±6.86 (**Lit:**23.37±18.45)
	HF Power *(ms^2)*	1295.90±438.38	1863.53±1001.13	***355.40±125.64** (**Lit:**405.58)	352.22±106.46 (**Lit:**242.34**)**	***304.8±155.1** (**Lit:**177.82)
	SI/RSA	6.65±1.36	17.70±10.37	***15.50±3.95**	***10.14±5.36**	***13.57±2.44**
Standing	RSA *(ln(ms^2))*	5.54±0.27	5.75±0.72	4.92±0.26	***4.44±0.28**	****4.31±0.27**
	SI *(s^{-2})*	61.19±6.10	88.96±20.41	104.79±20.83	***167.32±36.06**	104.13±28.6
	RMSSD *(ms)*	28.06±3.42	29±6.74	19.66±1.85 (**Lit:**25.15±12.31)	***18.41±3.31** (**Lit:**25.53±11.89)	22.51±4.57 (**Lit:**16.10±14.27)
	HF Power *(ms^2)*	524.10±179.79	655.05±408.67	218.46±59.11 (**Lit:**238.8)	****138.18±37.38**	**105.4±27.9 (**Lit:**53.69)
	SI/RSA	12.17±1.54	17.49±5.48	***24.66±6.02**	***46.49±12.80**	29.03±9.95
Sitting after Walk	RSA *(ln(ms^2))*	5.66±0.35	6.39±0.64	5.67±0.26	5.32±0.36	5.38±0.43
	SI *(s^{-2})*	43.73±6.56	75.95±23.55	60.86±8.43	±78.80±15.39	58.82±8.55
	RMSSD *(ms)*	45.18±8.21	41.91±9.97	31.59±3.74	33.83±8.18	37.78±11.19
	HF Power *(ms^2)*	882.55±448.76	1068.21±614.91	418.47±87.76	465.46±205.39	626.11±390.8
	SI/RSA	9.18±1.78	13.29±5.06	12.04±2.50	18.22±4.84	10.40±1.57

Table 6-4:Comparison of ANS activity and reactivity of the patient groups with various health conditions and healthy controls

		Control (n=20; Age_{av}= 28.65±11.70)	**Scoliosis, Spinal bifida, Thoracic Outlet Syndrome, Meningtis, Tarlov Syst** (n=6; Age_{av}= 29.50±12.15)	**Anxiety/Depression, Suicide thoughts** (n=8; Age_{av}= 42.13±11.69)	**Back Pain** (n=16; Age_{av}= 37.94±14.18)	**Constipation** (n=14; Age_{av}= 38.71±18.84)	**Upper GI Symptoms** (n=12; Age_{av}=34.83±13.9)	**Bladder Symptoms** (n=3; Age_{av}= 42.67±16.4)
Supine	RSA *(ln(ms^2))*	6.57±0.30	6.13±0.78	5.99±0.26	***5.38±0.35**	5.90±0.36	***5.31±0.45**	5.57±0.36
	SI *(s^{-2})*	28.71±4.72	48.49±14.76	***52.41±9.14**	****69.46±10.45**	****62.22±11.99**	***73.97±13.20**	***66.80±17.32**
	RMSSD *(ms)*	59.36±7.38	60.54±21.43	41.03±5.04	***30.52±4.15**	***43.94±10.15**	***39.97±12.11**	29.57±4.94
	HF Power*(ms^2)*	1392.28±346.5	1788.07±1080.51	532.37±158.23	***467.96±125.9**	984.84±495.82	***842.04±580.03**	319.31±115.28
	SI/RSA	5.24±1.17	11.39±6.02	***9.33±1.85**	*****16.37±3.57**	****12.34±3.07**	***17.77±4.55**	12.73±3.85
Sitting	RSA *(ln(ms^2))*	6.20±0.35	5.60±0.40	5.42±0.34	***5.02±0.27**	***5.25±0.29**	***4.98±0.32**	5.07±0.52
	SI *(s^{-2})*	33.62±4.77	***42.59±10.56**	***64.56±17.44**	*****82.21±12.97**	****86.05±18.59**	*****89.11±15.21**	***84.05±19.86**
	RMSSD *(ms)*	49.97±8.31	38.53±9.55	28.99±5.11	***26.61±4.52**	***29.95±5.36**	***27.57±6.00**	22.73±4.67
	HF Power*(ms^2)*	1295.90±438.4	467.80±232.36	362.11±128.4	***272.38±76.79**	***356.13±124.2**	***295.58±130.50**	243.49±129.73
	SI/RSA	6.65±1.36	11.96±2.85	13.75±4.50	****19.13±3.94**	****19.00±4.98**	*****20.99±4.93**	***18.17±5.15**
Standing	RSA *(ln(ms^2))*	5.54±0.27	5.09±0.40	***4.42±0.29**	*****4.08±0.19**	4.69±0.22	****4.37±0.28**	****4.08±0.05**
	SI *(s^{-2})*	61.19±6.10	86.01±32.59	129.32±42.43	*****164.52±24.66**	107.01±27.74	****89.11±15.21**	***116.95±28.39**
	RMSSD *(ms)*	28.06±3.42	23.44±4.38	23.51±5.40	****15.83±2.06**	***21.56±2.41**	***17.26±3.04**	***12.74±1.23**
	HF Power*(ms^2)*	524.10±179.79	260.21±110.21	***113.95±32.93**	*****81.30±17.88**	149.37±32.70	****144.16±63.16**	****59.59±3.18**
	SI/RSA	12.17±1.54	20.62±9.83	35.57±15.10	******45.12±8.46**	27.58±9.50	***41.79±11.64**	***28.89±7.24**
Sitting after Walk	RSA *(ln(ms^2))*	5.66±0.35	6.15±0.54	5.83±5.83	5.29±1.25	5.56±1.11	5.32±1.42	5.60±0.64
	SI *(s^{-2})*	43.73±6.56	59.61±11.81	57.89±19.92	76.85±12.05	71.64±10.32	94.25±14.91	73.66±22.47
	RMSSD *(ms)*	45.18±8.21	48.03±19.28	44.32±8.49	32.69±6.35	34.37±8.12	33.59±10.35	24.05±6.12
	HF Power*(ms^2)*	882.55±448.76	1048.55±643.79	662.92±280.18	428.18±157.82	568.44±274.83	605.47±353.52	327.02±131.41
	SI/RSA	9.18±1.78	10.35±2.79	13.66±6.86	17.54±3.83	13.39±2.55	21.08±5.59	9.54±3.82

Chapter 7

Propagation of Light in Biological Tissue and Energy Dosage Calculations

7.1 Introduction:

Non-invasive sacral neuromodulation, such as transcutaneous electrical nerve stimulation (TENS) and lumbosacral low-level laser therapy (LLLT), are potential treatments for chronic left colon dysmotility[47], [48]. Sacral nerve stimulation by implanted electrodes caused immediate changes in rectal blood flow, indicating stimulation of autonomic innervation and improving bowel function and relieving symptoms[49], [50]. Electro-acupuncture has proven successful and increased parasympathetic tone based on HRV analysis[51]. In response to sacral nerve stimulation with implanted electrodes, increased parasympathetic and decreased sympathetic activity were observed in rats [16]. After establishing the association between the autonomic nervous system activity with normal colonic motility and identifying the abnormal autonomic nervous system activity of the motility disorder patients, it is required to identify the potential treatment to restore the normal autonomic function. Neuromodulation of lumbar and sacral autonomic nerves by using Low-Level-Laser Therapy (LLLT) has been tested as a potential treatment to restore the normal autonomic activity in this thesis. We have simultaneously used two LLLT professional therapy systems developed by Bioflex Inc. for neuromodulation [53]. The light sources in the system include infrared laser probe (825 nm) and LED array containing 240 LEDs emitting both RED (660 nm) and infrared light (860 nm). Before discussing the effects of neuromodulation of the Lumbar and sacral autonomic nerves by LLLT on ANS, it is essential to

discuss how light penetrates inside the biological tissue and how much energy is delivered at the target site. In this chapter, the properties of light and its propagation from one medium to another medium like biological tissue are discussed, and the of energy delivered at required penetration depth is calculated for Bioflex IR laser probe, Red and IR LED arrays. The functional test of the LLLT is conducted by stimulating the lumbar and sacral autonomic nerves, and the response of LLLT on the ANS is recorded via heart rate variability, which is discussed in the next chapter.

7.2 Interaction and Propagation of Light in Biological Tissue

The interaction of light with biological matter is of utmost importance due to its significant role in diagnosing and treating various health conditions. Several factors impact the outcome of light-tissue interaction and, if not selected carefully, may damage the tissue. The biological tissues are multilayered with nonuniform optical properties. Therefore, the interaction of light with them is a complex process. The optical properties of each layer of the tissue may change abruptly at the material boundaries, for example, at the interfaces between the soft tissues, nerves, organ tissues and bones.

When the light interacts with a layer of biological tissue, a part of it is reflected from the tissue surface while the remaining portion is refracted (transmitted into the tissue) due to different refractive indexes of the layers. The transmitted light on its way into the biological tissue is either scattered or absorbed or both, depending upon the various factors like wavelength, intensity, refractive index, absorption coefficient, scattering coefficient and angle of incidence (Figure below adapted from [54]). The absorption and scattering attenuate the light, and its intensity decreases as it penetrates deeper until it reaches the end of the layer,

where it meets another layer with different optical parameters. The process restarts when some portion of already attenuated light is reflected. The rest is transmitted into the next layer and so on. These properties of light tissue interaction are widely used for various medical applications; for example, the energy absorbed by the tissue can be used to stimulate the cells and destroy the cancerous cells in case a very high-intensity laser light is used. In addition, the transmission, reflection, scattering, or remission can be used for diagnostic purposes of various diseases.

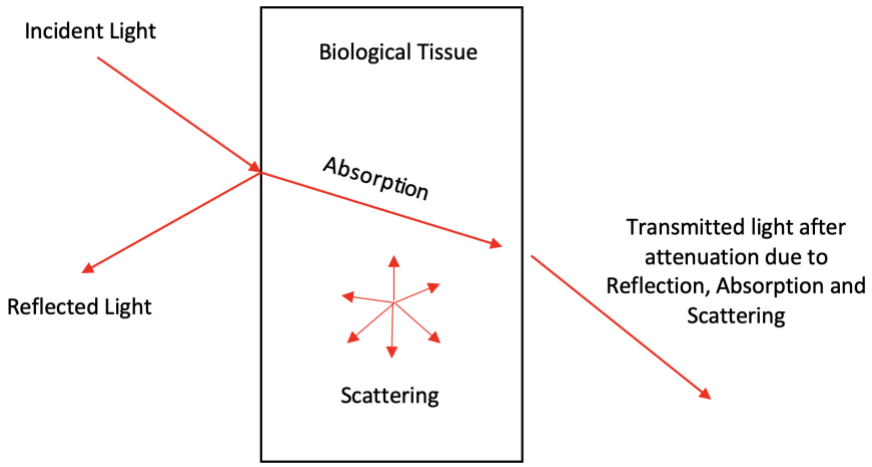

Figure 7-1: Light-Tissue Interaction

7.2.1 Dual Nature of Light:

The transmission of light is explained by the wave theory of light, while the quantum theory of light explains the interaction of light with tissue involving absorption and emission. The absorption or emission of light always occurs in discrete units of energy called photons. The photon's energy depends upon the frequency (v), which is again explained by the wave theory. Hence light exhibits dual nature, which is explained by Planks' law:

$$E = hv = hc/\lambda$$

Where E is the energy of the photon, $h = 6.625^{-34}$ J.s. is the Planks' constant, λ is the wavelength, and c is the velocity of light.

7.2.2 Reflection and Refraction:

When a light ray meets a smooth interference separating two different dielectric media, i.e. a layer of biological tissue, a part of it is reflected from the surface of the layer into the first medium (reflection), and the remainder is refracted after entering the layer of the tissue, the second medium.

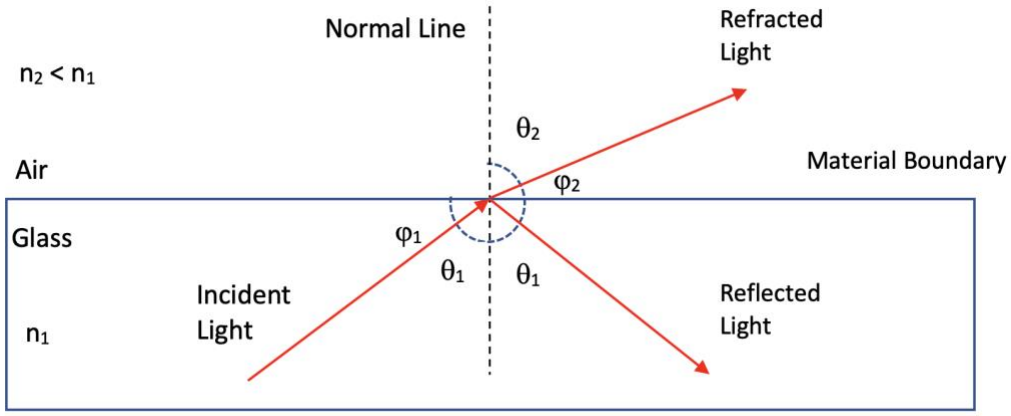

Figure 7-2: The reflection and refraction of light

According to Snell's law, the reflection and refraction depend upon the refractive indexes of the two mediums and the angle of incidence of light measured from the normal to the boundary separating the two mediums. The figure above shows an incident light ray making an angle θ_1 with the line perpendicular to the material boundary, a part of which is refracted (red) at an angle θ_2 to the normal after entering from glass (first medium with a refractive index of n_1) to the air (second medium with a refractive index of n_2) and the remaining portion of the incident

ray is reflected to the glass (the first medium) making the same angle as the angle of incident (θ_1) [55].

Mathematically,

$$n_1 sin\theta_1 = n_2 sin\theta_2$$

The value of the incident angle θ_1 for which the refracted angle θ_2 becomes 90° is called critical angle (θ_c). At this angle the light is refracted parallel to the boundary if the angle of incidence is further increased beyond the critical angle, $\theta_1 > \theta_c$, there will be no refracted ray, and all the light will be reflected to the first medium; this phenomenon is called total internal reflection Figure below [55].

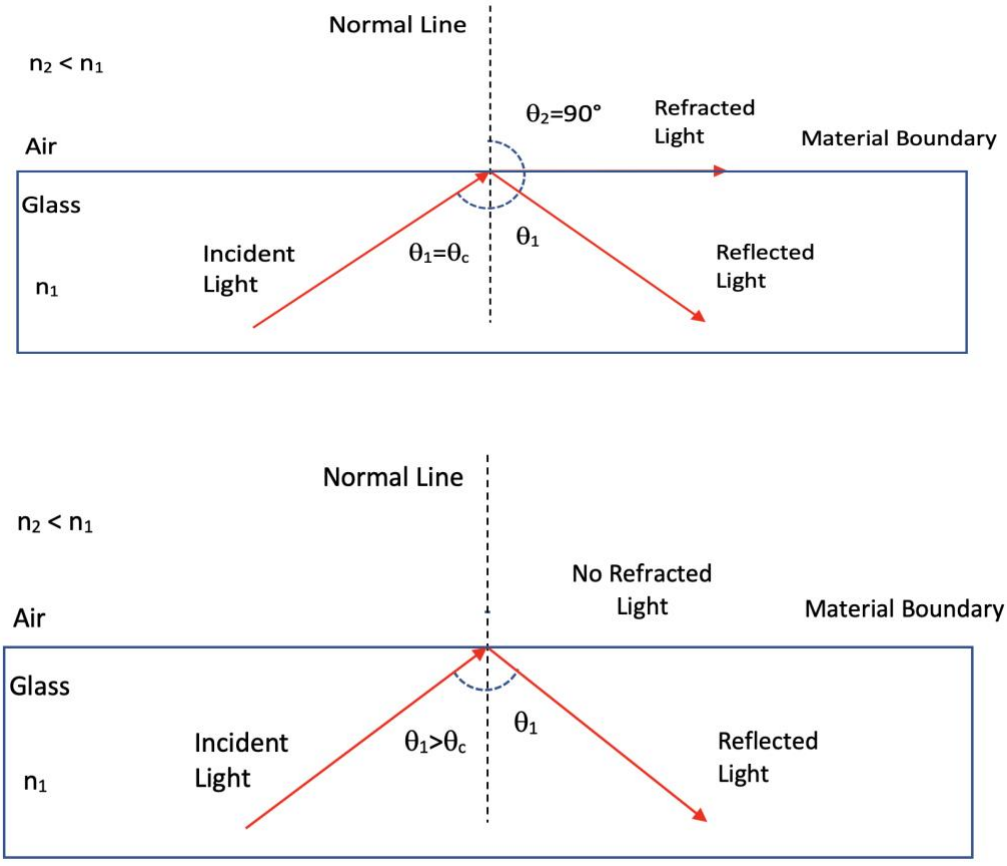

Figure 7-3: Critical angle and total internal reflection

The Fresnel equations are used to calculate the amount of light reflected and refracted at the material interface. The equations are given in terms of perpendicular and parallel coefficients of reflection r_x and r_y as well as those of refraction (or transmission) t_x and t_y respectively.

$$r_{\perp} = r_x = (\frac{E_{0r}}{E_{0i}})_x = \frac{n_1 cos\theta_1 - n_2 cos\theta_2}{n_1 cos\theta_1 + n_2 cos\theta_2}$$

$$r_{||} = r_y = (\frac{E_{0r}}{E_{0i}})_y = \frac{n_2 cos\theta_1 - n_1 cos\theta_2}{n_2 cos\theta_1 + n_1 cos\theta_2}$$

$$t_{\perp} = t_x = (\frac{E_{0t}}{E_{0i}})_x = \frac{2n_1 cos\theta_1}{n_1 cos\theta_1 + n_2 cos\theta_2}$$

$$t_{||} = t_y = (\frac{E_{0t}}{E_{0i}})_y = \frac{2n_1 cos\theta_1}{n_1 cos\theta_2 + n_2 cos\theta_1}$$

Where E_{0i}, E_{0r} and E_{0t} are the amplitudes of the incident, reflected and transmitted waves. To make the maximum amount of light enter from one medium to the next, the refraction should be enhanced, and reflection should be minimized. This can be achieved by making the angle of incident (θ_1) equal to 0° with the normal, in which case, according to Snell's law equation, the angle of refraction (θ_2) will also become 0°, and most of the light will enter the second medium with minimal reflection. In this case, the reflection and transmission coefficients will be:

$$r_x = \frac{n_1 - n_2}{n_1 + n_2}$$

$$r_y = \frac{n_2 - n_1}{n_2 + n_1}$$

$$t_x = \frac{2n_1}{n_1 + n_2}$$

$$t_y = \frac{2n_1}{n_2 + n_1}$$

Because ($cos\theta_1 = cos\theta_2 = 1$)

These ratios can be used to calculate the reflectance (R) and transmittance (T) as follows:

$$R_{\perp} = R_x = (\frac{E_{0r}}{E_{0i}})_x^{\ 2} = {r_x}^2$$

$$R_{||} = R_y = (\frac{E_{0r}}{E_{0i}})_y^{\ 2} = {r_y}^2$$

$$T_{\perp} = T_x = \frac{n_2 cos\theta_2}{n_1 cos\theta_1}(\frac{E_{0t}}{E_{0i}})_x^{\ 2} = \frac{n_2 cos\theta_2}{n_1 cos\theta_1}(t_x)^2$$

$$T_{||} = T_y = \frac{n_2 cos\theta_2}{n_1 cos\theta_1}(\frac{E_{0t}}{E_{0i}})_y^{\ 2} = \frac{n_2 cos\theta_2}{n_1 cos\theta_1}(t_y)^2$$

Substituting $\theta_1 = \theta_2 = 0$

$$R = R_x = Ry = (\frac{n_1 - n_2}{n_1 + n_2})^2$$

And

$$T = T_x = T_y = \frac{4n_1 n_2}{(n_1 + n_2)^2}$$

According to these equations, if the incident light is perpendicular to the surface ($\theta_1 = \theta_2 = 0$) of the smooth tissue (n_2=1.35) travelling from the air (n_1=1), 97.8% of the light will be transmitted (or refracted) into the tissue, and only 2.2% will be reflected to the air. Therefore, to apply the light using low-level laser therapy where the maximum transmission is desired, the incident light is applied perpendicular to the skin's surface, making an incident angle (θ_1) of 0° with the normal line.

7.2.3 Absorption:

When the photon's energy is equal to the energy difference between the two quantum energy levels in an atom, the photon is usually absorbed by the atom. Upon entering the tissue, some of the light will be absorbed due to the interaction between the electromagnetic fields of the incoming photons and the molecular medium. The incoming photon will give its energy to the atom's electron, which will move to a higher energy level. The absorption phenomenon is highly dependent upon the electronic structure of the atoms, wavelength of light, temperature, and thickness of the layer.

The coefficient of absorption (μ_a) is defined as the probability of absorption of a photon per unit length of a material and is calculated as:

$$\mu_a = \rho\sigma_a$$

Where ρ is the density and σ_a are the light absorption cross-section and is calculated from the power of the incident light (P_0) falling upon the cross-section area (A) and power absorbed by the area (P_{abs}) as:

$$\sigma_a = \frac{P_{abs}}{P_0/A}$$

According to Beer-Lambert Law, as the light travels through a tissue layer, a portion of it is absorbed along the way, and its intensity decreases as it penetrates deeper.

$$I(x) = (I - R)I_0 exp(-\mu_a x)$$

I(x) is the intensity of light at a distance x after entering the tissue, I_0 is the intensity of the incident light, μ_a is the coefficient of absorption, R is the coefficient of reflection calculated from the Fresnel equations for light beam incident perpendicular to the surface, and x is the distance at which the intensity is calculated.

The coefficient of absorption is also dependent upon the wavelength (λ) of the light as per the following equation:

$$\mu_a = \sum_{n=1}^{N} c_n \varepsilon_n(\lambda)$$

Where, c_n is the concentration of the nth molecule type, and $\varepsilon_n(\lambda)$ is the molar absorption coefficient nth molecule type. The penetration depth of the light, also known as absorption length (L_a), is the inverse of the coefficient of absorption of the layer.

$$L_a = \frac{1}{\mu_a}$$

Biological tissues primarily consist of water molecules, proteins and chromophores. Water is the largest constituent; therefore, its absorption characteristics are essential in light tissue interaction. The figure below shows the absorption coefficients of some components of biological tissue at different wavelengths of light [55]. It is clear from the figure that hemoglobin, water, melanin, and epidermis all have the lowest absorption coefficient in the wavelength of 0.60µm-1.00µm, which is equivalent to 600 nm to 1000 nm. This range of wavelength is known as the diagnostic or therapeutic window. Due to the lowest absorption coefficient of the constituents of the biological tissue, the attenuation in light intensity due to absorption is minimal, and it penetrates deeper inside the tissue.

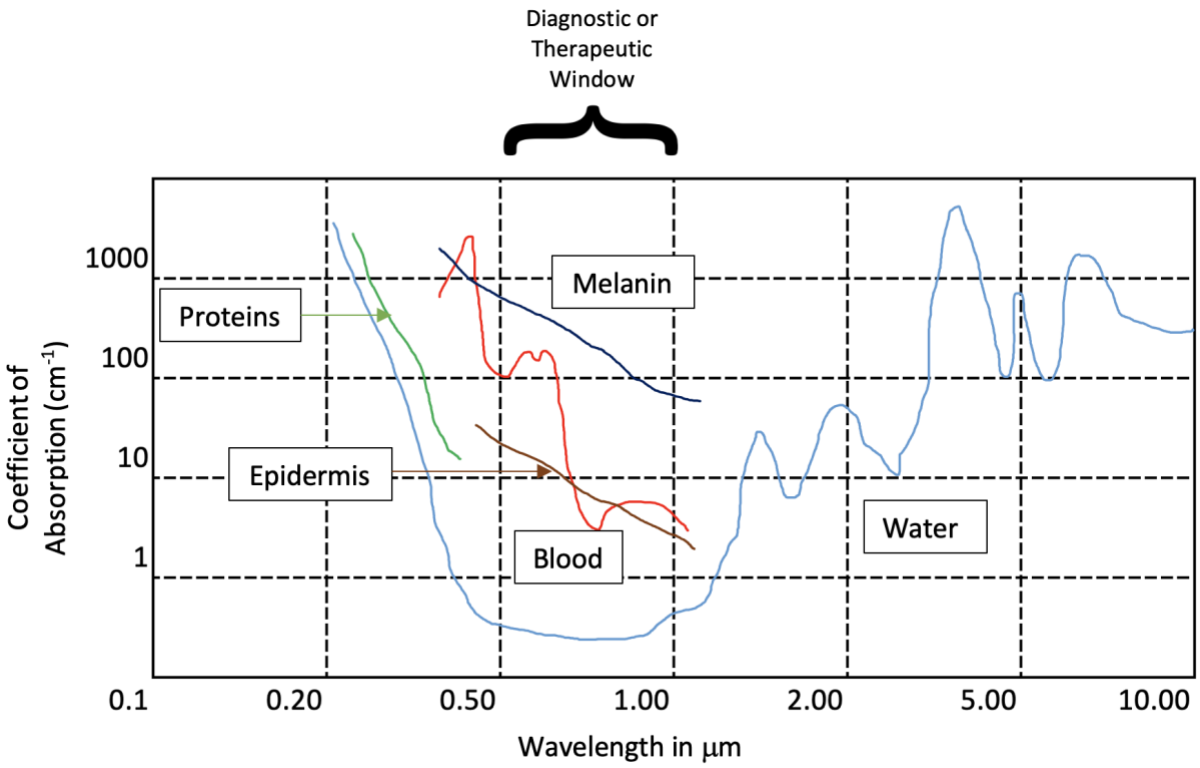

Figure 7-4: Coefficient of absorption of some constituents of biological tissues at different wavelengths of light

7.2.4 Scattering:

While travelling through a medium, if a photon encounters a compact object with a different refractive index compared to the medium, it will be diverted to a new direction; this process is called the scattering of light. The biological tissues have a complex, multilayered structure with heterogeneous optical properties; therefore, they strongly scatter light. If the losses due to absorption are lower than that of scattering, the light is scattered multiple times in each layer, as shown in the figure below [55]. The wavelength of light, the structure, refractive indices, and the size of the tissue components are the factors that contribute to the scattering of light within biological tissue. The two strong scattering elements in biological tissues are the cell nuclei and mitochondria because of their larger size. The scattering event when both the incident and

scattered photons have the same amount of energy is called elastic scattering. When the energy exchange takes place between a photon and the molecule responsible for the scattering, it is called inelastic scattering. In the event of inelastic scattering, the energy can be transferred from the photon to the molecule or vice versa. If the molecule involved in the scattering process is in its ground state, then upon interaction with the photon, it will absorb the energy from the photon and move to a short-lived excited state. However, if the molecule is already in high energy or excited state before the scattering event, then upon interaction with the incoming photon, it will release its energy to the photon and return to its ground state.

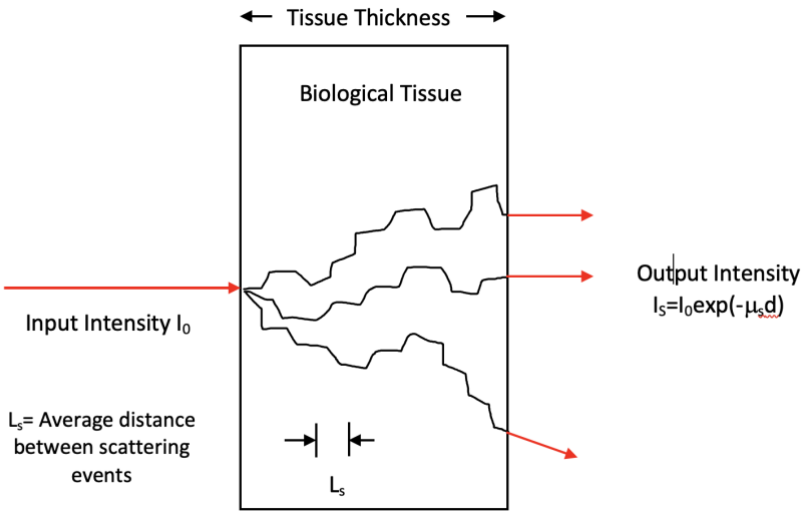

Figure 7-5: Scattering of Photon in biological tissue

The non-scattered intensity of light after travelling a distance "x" in biological tissue can be discovered by Beer-Lambert law:

$$I(x) = I_0 \exp(-\mu_s x)$$

The coefficient of scattering (μ_s), which is defined as the probability of scattering of a photon per unit length of a material and is calculated as:

$$\mu_s = \rho \sigma_s$$

Where ρ is the density and σ_s are the light scattering cross-section and is calculated from the power of the incident light (P_0) falling upon the cross-section area (A) and power scattered by the area (P_s) as:

$$\sigma_s = \frac{P_s}{P_0/A}$$

The *scattering mean free path* (L_s), which is defined as the distance travelled by photon without being scattered, and it is the inverse of the scattering coefficient.

$$L_s = \frac{1}{\mu_s}$$

Ansari et al. have mentioned that the scattering in most biological tissues is defined by the phase function g, and its value ranges from -1 to 1, with g=-1 indicating total backward scattering and g=1 indicating total forward directional scattering. Most biological tissues have g>0.7, which indicates that the scattering in biological tissues is very much near the full forward scattering (g=1) [54].

7.2.5 Simultaneous absorption and scattering

Scattering and absorption co-occur in biological tissues; therefore, they can be measured together in the form of a total interaction coefficient (μ_t), the sum of absorption and scattering coefficients.

$$\mu_t = \mu_a + \mu_s$$

Hence, the total mean free path will be:

$$L_t = \frac{1}{\mu_t}$$

The intensity of light at a distance "x" after travelling in biological tissue is calculated as:

$$I(x) = I_0 b_s \exp(-\mu_{eff} x)$$

Where, b_s is the additional irradiation due to the reflection from the upper layers due to multiple backscattering, and its value ranges from 1 to 5.[56] The values of μ_{eff} is calculated as:

$$\mu_{eff} = [3\mu_a(\mu_a + \mu_s)]^{\frac{1}{2}}$$

7.3 Calculations for energy delivered to the Autonomic Nerves by LLLT:

The above formulae will be used to calculate the intensity of light and energy delivered to the autonomic nerves using Bioflex IR laser Probe, Red and IR LED array during the LLLT session. It is assumed that the sacral or lumbar autonomic nerves are located inside the fat layer, which is located under the dermis and epidermis layers. The thickness of the epidermis and dermis are assumed to be 0.5 mm and 2.5 mm, respectively, and the target location (autonomic nerve fibres) is assumed to be 2.5 mm below the junction of dermis and fat layers. The irradiance coefficient for epidermis, dermis and fat layers are assumed as 1.8,3 and 4, respectively, as shown in figure 8.7 below.

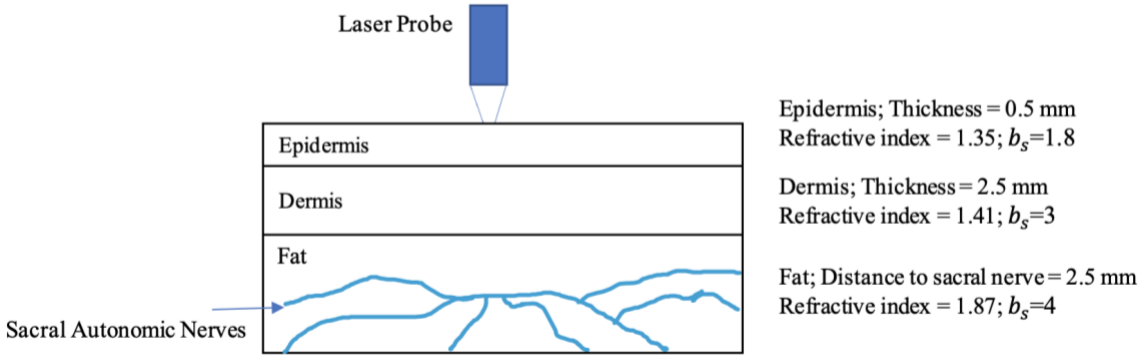

Figure 7-6: Sample of light propagation to Lumbar or sacral autonomic nerves

7.3.1 IR laser probe:

Incident Energy:

According to manufacturer's specifications, the IR laser probe consists of one laser diode with following parameters:

Average power = 180.0 mW

Wavelength (λ) = 825 nm

Spot size = 0.10 cm^2 = 10 mm^2

Power density (I_0) = 1800 mW/cm^2 = 18 mW/mm^2

Time of application. = 10 min

Total Energy = 10800 J = 10.8 kJ

Energy Density = 1080 J/cm^2 = 10.8 J/mm^2

Reflection and Refraction:

For IR laser probe application, the incident angle is 0° with the normal because the probe is kept perpendicular to the skin. Therefore, the amount of light reflected and Refracted (or transmitted) can be calculated from the refractive indexes of the glass and the epidermis. From literature, the epidermis has a refractive index is 1.35, and the refractive index of glass is 1.52.

$$R = \left(\frac{n_1-n_2}{n_1+n_2}\right)^2 = \left(\frac{1.52-1.35}{1.52+1.35}\right)^2 = 0.00351 = 0.35\%$$

$$T = \frac{4n_1n_2}{(n_1+n_2)^2} = \frac{4(1.52)(1.35)}{(1.52+1.35)^2} = 0.9965 = 99.65\%$$

Therefore, 0.35% of the total energy will be reflected, and 99.65% will enter the epidermis at an incident angle of 0°.

The amount of energy refracted into the epidermis = 0.9965 x 10.8 kJ = 10.76 kJ

And the intensity of the light entering the epidermis layer will be 1793.7 mW/cm^2 (17.94 mW/mm^2).

Coefficients of Absorption and Scattering:

Inside the epidermis, the energy can be lost due to the absorption and scattering phenomenon on its way, depending upon the wavelength of light and the coefficients of absorption and

scattering. Each constituent of biological tissue has its own optical properties and hence, its own coefficient of absorption and scattering. According to Colabro et. al., the combined absorption coefficient of a given biological tissue sample can be calculated from the coefficients of absorption of their constituents as follows [57]:

$$\mu_a(\lambda) = B\left(S\mu_{a,Hbo}(\lambda) + (1-S)\mu_{a,Hb}(\lambda)\right) + W\mu_{a,Water}(\lambda) + F\mu_{a,fat}(\lambda) + M\mu_{a,melanine}(\lambda) + L\mu_{a,bile}(\lambda) + C\mu_{a,collagen}(\lambda) + 2.3c_{\beta c}\epsilon_{\beta c}(\lambda)$$

Where, $\mu_{a,Hbo}$, $\mu_{a,Hb}$, $\mu_{a,Water}$, $\mu_{a,fat}$, $\mu_{a,melanine}$, $\mu_{a,bile}$ and $\mu_{a,collagen}$ are the coefficients of absorption respectively for oxygenated hemoglobin, deoxygenated hemoglobin, water, fat melanin, bile and collagen at wavelength of λ. B, W, F, M, L and C are the volume fractions of blood, water, fat, melanin, bile, and collagen respectively and S is the oxygen saturation of blood, $c_{\beta c}$and $\epsilon_{\beta c}$are the average and molar concentrations of hemoglobin in the given tissue sample.

The coefficient of scattering of a biological tissue can be calculated as:

$$\mu_s' = a(f_{Ray}\left(\frac{\lambda}{\lambda_0}\right)^{-4} + \left(1 - f_{Ray}\right)\left(\frac{\lambda}{\lambda_0}\right)^{-b})$$

Where, $f_{Ray}$is the fraction of Rarleigh scattering, a represents the reduced scattering coefficient at λ_0 and b depends upon the particle size. The experimental values of each of the parameters required in the above formulae for both the absorption and reduced scattering coefficients are given in the literature for various types of biological tissues [57]. *Salomatina et al.* has presented the coefficients of absorption and reduced scattering for epidermis, dermis, and fat layer for different wavelengths of light from which we have selected 825 nm, 660 nm and 840nm for our calculations [58].

Table 7-1: Coefficients of absorption and scattering for Epidermis, Dermis, and fat layers

	Epidermis		**Dermis**		**Fat**	
Wavelength(λ)	μ_a (mm^{-1})	μ_s'(mm^{-1})	μ_a(mm^{-1})	μ_s'(mm^{-1})	μ_a(mm^{-1})	μ_s'(mm^{-1})
825 nm	0.14	3.48	0.14	2.2	0.1	2
660 nm	0.18	3.6	0.15	3.2	0.12	2.5
840 nm	0.11	3.42	0.13	2.1	0.09	1.9

Mean free path:

$$L_s = \frac{1}{\mu_a + \mu_s'}$$

The mean free path is calculated using the values given in the table above for the IR laser probe, LED array RED and LED array IR for each epidermis, dermis, and fat.

For Laser Probe (825 nm)

Epidermis:

$$L_s = \frac{1}{(0.15 + 3.4)mm^{-1}} = 0.28\, mm$$

Dermis:

$$L_s = \frac{1}{(0.14 + 2.2)mm^{-1}} = 0.43\, mm$$

Fat:

$$L_s = \frac{1}{(0.1 + 2)mm^{-1}} = 0.48\, mm$$

For LED array RED (660nm):

Epidermis:

$$L_s = \frac{1}{(0.18 + 3.6)mm^{-1}} = 0.26\ mm$$

Dermis:

$$L_s = \frac{1}{(0.15 + 3.2)mm^{-1}} = 0.30\ mm$$

Fat:

$$L_s = \frac{1}{(0.12 + 2.5)mm^{-1}} = 0.38\ mm$$

For LED array IR (840nm):

Epidermis:

$$L_s = \frac{1}{(0.11 + 3.40)mm^{-1}} = 0.28\ mm$$

Dermis:

$$L_s = \frac{1}{(0.13 + 3.21)mm^{-1}} = 0.45\ mm$$

Fat:

$$L_s = \frac{1}{(0.09 + 1.9)mm^{-1}} = 0.50\ mm$$

The summary of these calculations is given in table 8.2 below:

Table 7-2: Calculated Mean Free paths for IR Laser probe, LED array Red and IR for Epidermis, Dermis and Fat layers

	Mean Free Path (mm)		
	Epidermis	Dermis	Fat
IR Laser Probe	0.28	0.43	0.48
LED Array Red	0.26	0.30	0.38
LED Array IR	0.28	0.45	0.50

The energy delivered to autonomic nerves by IR Laser Probe:

The epidermis layer's thickness at the target area for LLLT (lower back) is assumed to be 0.5 mm, which is larger than the mean free path (0.28 mm); hence there will be losses in light energy due to absorption and scattering in the epidermis. Assuming the additional irradiation factor for IR laser probe to be 2 for epidermis due to total internal reflection of scattered photons from the upper layer of the epidermis. The intensity of light at the end of the epidermis layer (after travelling 0.5 mm) is calculated from the Lambert-bear law as discussed previously:

$$I(x) = I_0 b_s \exp(-\mu_{eff} x)$$

$$\mu_{eff} = [3\mu_a(\mu_a + \mu_s)]^{\frac{1}{2}} = 1.23$$

$$I(0.5mm) = (17.94 \frac{mW}{mm^2})(2)\exp(-1.23(0.5mm)) = 17.43 \text{ mW/mm}^2$$

Accordingly, the energy delivered in 10 min at the distance of 0.5 mm will be 10.45 kJ, which is also calculated from the above equations using E instead of I.

At the junction of epidermis and dermis, there will be again some losses due to reflection depending upon the refractive indices of epidermis (n_1 = 1.35) and dermis layers (n_2=1.41). The amount of light reflected (R) and refracted (T) will be:

$$R = (\frac{n_1 - n_2}{n_1 + n_2})^2 = (\frac{1.35 - 1.41}{1.35 + 1.41})^2 = 0.00047 = 0.047\%$$

$$T = \frac{4n_1 n_2}{(n_1 + n_2)^2} = \frac{4(1.35)(1.41)}{(1.35 + 1.41)^2} = 0.9965 = 99.95\%$$

99.95% of the total energy incident at the dermis layer will be transmitted, while 0.047% will be reflected into the epidermis.

Intensity of transmitted light in dermis = (99.95) x17.43 mW/mm^2 = 17.42 mW/mm^2

The energy transmitted into dermis in 10 minutes = 0.9995 x 10.45 kJ = 10.45 kJ

Assuming the thickness of the dermis layer is equal to 2.5 mm, which is more than the calculated mean free path of 0.43 mm for the IR probe. Due to absorption and scattering, there will be losses, and from lambert-beer law with assumption $b_s = 3$.

The light intensity at the end dermis layer = 4.38 mW/mm^2

And

The energy delivered at the end of the dermis layer in 10 minutes = 2.63 kJ

where the light will meet the boundary of the dermis and fat layer, and again, some amount of light will be reflected into the dermis, and the remaining will be transmitted into the fat layer. Using the same calculations for R and T with n_1=1.41(refractive index of dermis) and n_2=1.87 (refractive index of fat) [59], the values of R and T are 1.97% and 98.03% respectively.

Therefore:

The intensity of light entering the fatty layer =(0.983)x 4.38 mW/mm^2 =4.30 mW/mm^2

And

The amount of energy transmitted in the fat layer in 10 minutes = 0.9803 x 2.63 kJ = 2.58 kJ

Suppose that the light meets the sacral nerves in the fatty layer after travelling another 2.5 mm from the junction and the energy redeposition coefficient value is 4 for the fatty layer.

According to Lambert-Beer law, the light intensity at the lumbar or sacral nerve will be

$$I(Autonomic\ Nerve) = (4.30\ mW/mm^2)(4)\exp\big(-0.79(2.5mm)\big) = 2.36\ mW/mm^2$$

And the energy delivered at the sacral nerve in 10 minutes will be calculated as:

$$E(Autonomic\ Nerve) = (2.58\ kJ)(4)\exp\big(-0.79(2.5mm)\big) = 1.42\ kJ = 1420\ J$$

The total energy delivered to the lumbar or sacral autonomic nerve will be 1.42 kJ in 10 minutes.

However, this energy is delivered if the laser probe is kept continuously at one point for ten minutes. As discussed in chapter 8, in our LLLT protocol for lumber and sacral stimulations, two laser probes will be used simultaneously and will be used to stimulate 60 points around the lumbar and sacral spine in 10 minutes which means the energy calculated above for one probe will be divided equally at 30 stimulation points.

Energy delivered at each point = 1420 J /30 = 47.33 J

7.3.2 LED Array:

The LED array consists of 240 LEDs arranged in a rectangular shape with an area of 100 cm^2 (10000 mm^2), and they can generate both red and infrared light. A continuous wave is used for the red light, and a pulsed wave for infrared light is used in the LLLT protocol.

LED Array RED Light:

Average power = 1000 mW

Wavelength (λ) = 660 nm

Spot size = 100 cm^2 = 10000 mm^2

Power density (I_0) = 10 mW/cm^2 = 0.1 mW/mm^2

Time of application. = 5 min

Total Energy = 30000 J = 30 kJ

Energy Delivered per LED = 30000 J/240 = 125 J =0.125 kJ

Energy Density = 3 J/cm^2 = 0.03 J/mm^2

Using the above data for LED array RED light and following the calculations used for the IR Laser probe and using the coefficients of absorption and reduced scattering for 660nm (table 1), the energy delivered per LED at the lumbar or sacral autonomic nerve is 3.89 J (0.00389 kJ).

LED Array IR Light:

Average power = 1000 mW

Peak Power = 2000 mW

Wavelength (λ) = 840 nm

Spot size = 100 cm^2 = 10000 mm^2

Power density (I_0) = 10 mW/cm^2 = 0.1 mW/mm^2

Time of application. = 5 min

Total Energy = 30000 J = 30 kJ

Energy Delivered per LED = 30000 J/240 = 125 J =0.125 kJ

Energy Density = 3 J/cm^2 = 0.03 J/mm^2

Using the above data for IR LED array light, following the method of IR Laser probe, and using the coefficients of absorption and reduced scattering for 840 nm (table 1), the energy delivered per LED at the lumbar or sacral autonomic nerve is 23.9 J (0.0239 kJ).

7.4 Discussions

With current input parameters, the laser light delivers more energy than the LED array stimulations at the target site inside the biological tissue, and the energy delivered by an infrared pulsed LED light is higher than the continuous RED light. Its intensity decreases as the light travels deep down the biological tissue layers. Therefore, the LED light may only stimulate the superficial nerve fibres, while laser light can penetrate the nerves located deeper.

For continuous light, the critical parameters for power calculations are irradiance time and spot size of the beam, while pulsed light depends upon the energy delivered per pulse, number of pulses delivered, irradiation time, pulse frequency and spot size. The energy delivered to the autonomic nerves can be varied using different combinations of these parameters. However, the different combinations of the input parameters may have different effects, as LLLT produces both excitatory and inhibitory effects based on these parameters [13] [55]. Similarly, the LED and Laser light stimulation may have a different effect on the autonomic nervous system due to their different energy dosage and penetration power. Therefore, to alter the amount of energy delivered, it is safer to only change the stimulation time and keep the other parameters unchanged as a first step. However, other parameters may also be modulated to improve the effect of LLLT. Since we are unaware of the lumbar and sacral autonomic nerves' exact location and depth, several assumptions were made during calculations. Therefore, a functional test is necessary to study the effect of LLLT on the autonomic nervous system with the current input parameters and protocols (chapter 8).

Chapter 8

Modulation Of The Autonomic Nervous System By One Session Of Spinal Low-Level Laser Therapy In Patients With Chronic Constipation

Submitted for Publication to *Frontiers in Neuroscience | Autonomic Neuroscience* on March 03, 2022

M. Khawar Ali[1,2], Shrayasee Saha[2], Natalija Milkova[2], Lijun Liu[2], Kartik Sharma[2,] Jan D. Huizinga[1,2], Ji-Hong Chen[2]

McMaster University, Hamilton ON, Canada

1. Faculty of Engineering, School of Biomedical Engineering, McMaster University, Hamilton, ON, Canada
2. Division of Gastroenterology, Department of Medicine, Faculty of Health Sciences, Farncombe Family Digestive Health Research Institute, McMaster University, Hamilton, ON, Canada

8.1 Abstract:

Patients with a defecation disorder may not evoke a normal defecation reflex executed by the spinal autonomic nervous system. Various forms of lumbar and sacral neuromodulation have shown positive results. Here we evaluate the effects of a single session of sacral low-level laser therapy (LLLT) on the lumbar and sacral spine in 41 patients with chronic gastrointestinal motor dysfunction. The LLLT protocol used red LED light at a wavelength of 660 nm for 10 minutes and infrared LED light at a wavelength of 840 nm for 10 minutes, followed by infrared laser light at a wavelength of 825 nm for 20 minutes. Effects on the autonomic nervous system were assessed by measuring heart rate variability (HRV) changes. Respiratory Sinus Arrhythmia (RSA) and Root Mean Square for Successive Differences (RMSSD) were used to quantify

parasympathetic reactivity; the Baevsky's Stress Index (SI) reflected sympathetic reactivity while the ratios SI/RSA and SI/RMSSD were used to represent shifts in autonomic dominance. The results indicate that lumbar and sacral neuromodulation using LLLT using light arrays reduced, whereas the laser probe significantly increased parasympathetic reactivity. The light arrays increased whereas the laser probe significantly decreased sympathetic reactivity (SI), the entire protocol shifted the autonomic balance towards parasympathetic activity. The comparison of actual versus sham neuromodulation proved that the change in HRV parameters was due to actual light stimulation and not due to touching of the arrays and probe to the skin. In conclusion, a single session of LLLT markedly affects autonomic nervous activity reflected in changes in HRV. These results warrant a study into the effects of LLLT on restoring autonomic dysfunction in chronic refractory colonic motility disorders.

8.2 Introduction

Sacral neuromodulation is explored as a treatment for chronic refractory gastrointestinal motility disorders (Payne *et al.*, 2019). Chronic stimulation of the spinal cord with implanted electrodes in patients with fecal incontinence has been shown to be effective (Wexner *et al.*, 2010). The inference from many studies on chronic stimulation with implanted electrodes is that the sustained effects are caused by neuromodulation in response to repeated stimulation of both sensory and efferent fibres, causing changes in organ function and improved organ blood flow (Vaizey *et al.*, 1999) (Veiga *et al.*, 2016) (Kenefick *et al.*, 2003). When implanted electrodes were stimulated while exploring brain areas with MRI, it was shown that sensorimotor learning centers were stimulated (Blok *et al.*, 2006). Neuromodulation for chronic constipation is explored to a lesser extent than for fecal incontinence. In a prospective study at

5 European Sites, 39 out of 45 achieved improvement with stimulation of implanted electrode, from 2.3 to 6.6 evacuations per week (Kamm *et al.*, 2010). Less invasive stimulation is also pursued (Chen *et al.*, 2017). Transcutaneous electrical nerve stimulation (TENS) has been shown to improve constipation symptoms in children) (Veiga *et al.*, 2013; Leong *et al.*, 2011) (Kim & Yi, 2014). A systematic review showed that TENS had a significantly larger effect on stool frequency compared to placebo (Zheng *et al.*, 2019). In rats, it was shown that TENS improved constipation via modulation of the autonomic nervous system, increased vagal activity and decreased sympathetic activity, assessed by spectral analysis of heart rate variability (HRV) (Huang *et al.*, 2019).

Neuromodulation can also be achieved by low-level laser therapy (LLLT) or photobiomodulation. This involves applying specific frequencies of light to tissues to promote regeneration and healing. LLLT has a photochemical effect, where the application of light and its absorption causes a chemical change in the tissue. There is ongoing research about the cellular and molecular mechanisms through which LLLT promotes healing. It is well established that LLLT improves wound healing and reduces pain and inflammation (Mester *et al.*, 1976). Activation of photoreceptor molecules inside mitochondria results in increased adenosine triphosphate and reactive oxygen species, followed by activation of transcription factors producing anti-apoptotic, anti-oxidant, and pro-proliferation gene products (Hashmi *et al.*, 2010; Chung *et al.*, 2012). Increased ATP production from LLLT also upregulates the production of nitric oxide, which is a potent vasodilator and allows for increased blood flow and, therefore, nutrient delivery to the areas being stimulated (Hashmi *et al.*, 2010; Chung *et al.*, 2012). LLLT was able to enhance neural regeneration in rats following chronic depression of dorsal root

ganglia and improve their ambulatory behaviour (Chen *et al.*, 2014); the neuro-reparative effect through photobiomodulation has thus far been proven in painful diabetic neuropathy and various other neurological conditions (Yamany & Sayed, 2012; Hashmi *et al.*, 2010) (Rola *et al.*, 2014) (Chen *et al.*, 2014) (Andreo *et al.*, 2017).

Our objective is to develop new treatments for patients with severe chronic refractory colonic motility disorders (Camilleri *et al.*, 2017) (Rao *et al.*, 2016). Our specific objective is to evaluate if sacral neuromodulation can relieve symptoms and restore autonomic dysfunction (Huizinga *et al.*, 2021). Patients with chronic constipation may not be able to generate spontaneous bowel movements. Constipation is the inability to generate one or more defecation reflexes that are orchestrated by the extrinsic autonomic nervous system involving propulsive motor activity and anal sphincter relaxation (Bharucha *et al.*, 1993; Callaghan *et al.*, 2018) (Milkova *et al.*, 2020; Ali *et al.*, 2021). A propulsive colonic motor pattern may start with triggering of afferent neurons whose cell bodies lie within the dorsal root ganglia (DRG) of the lumbar and sacral portions of the spinal cord (Brookes *et al.*, 2009). Then, sacral parasympathetic nerves may initiate motor patterns in the descending colon, stimulate the rectum, and relax the internal anal sphincter in preparation for defecation (Brookes *et al.*, 2009). At the same time, sacral information projects to the Barrington's nucleus and the nucleus tractus solitarius through spinal pathways (Valentino *et al.*, 1999). Barrington's nucleus can then project the information to the vagus nerve through the dorsal motor nucleus of the vagus. The vagus nerve can invoke propulsive motor patterns in the ascending and transverse parts of the colon, thus transporting more colonic content in the anal direction (Valentino *et al.*, 1999; Brookes *et al.*, 2009). Through the neural activity in the brain stem, particularly the NTS, the neural traffic

originating in the sacrum can influence autonomic innervation to the heart and hence affect HRV. We used HRV successfully to show that propulsive motor patterns generated by the human colon are associated with an increase in parasympathetic activity and a decrease in sympathetic activity (Ali *et al.*, 2021; Yuan *et al.*, 2020)

The goal of neuromodulation of the spinal cord then is to affect the neural circuitries that are underlying the defecation reflexes; to drive them into their normal state. It was, therefore, important to investigate whether or not LLLT can trigger autonomic nerves. The aim of the present study was to examine whether one treatment session of low-level laser therapy would show autonomic reactivity assessed via HRV (Thayer *et al.*, 2012; Baevsky & Chernikova, 2017; Ali *et al.*, 2021), which would prove its ability to activate autonomic neural pathways.

8.3 Methods

8.3.1 Participants

Forty-one patients with chronic constipation refractory to pharmacological therapies took part in this study, carried out at McMaster University with ethics approval from the Hamilton Integrated Research Ethics Board and written consent from all participants. All participants underwent concurrent one session of low-level laser therapy, ECG and impedance recording. Six healthy volunteers without any motility and cardiac disorders took part in a sham study.

8.3.2 Heart rate and impedance measurements

ECG signals were recorded using MindWare BioLab Recording Software. MindWare HRV 3.1 software was used for artifact correction and to calculate the values of the beat-to-beat intervals (RR intervals), RSA and RMSSD (Thayer *et al.*, 2012) (Ali *et al.*, 2021). The sampling frequency was 500 Hz. Baevsky's stress index (Baevsky & Chernikova, 2017) (SI) was calculated

using programs developed in MATLAB using the RR interval time series. RSA and RMSSD were used as measures of parasympathetic reactivity; SI was used as a measure of sympathetic reactivity. The ratios SI/RSA and SI/RMSSD were used to measure shifts in combined parasympathetic and sympathetic activity. The HRV parameters were calculated for 6 minutes (baseline) before the low-level laser therapy session, during the three stages of the low-level laser therapy protocol, as well as 6 minutes recovery after the low-level laser therapy.

8.3.3 Low-Level Laser Therapy Protocol

Two BioFlex Duo+ Professional Systems were used simultaneously to provide light therapy to the lower back; each BioFlex Duo+ system included a control unit connected to a computer, an LED array containing 240 LEDs (each LED provided red light with a wavelength of 660 nm and infrared LED light at a wavelength of 840 nm) and a laser probe which provided infrared light with a wavelength of 825 nm (Kahn, 2022). We applied a single session of our low-level laser therapy protocol to target the lumbar and sacral area using parameters developed by Dr. Fred Kahn and colleagues (Kahn, 2022). Two arrays were used simultaneously at positions A and C for 10 minutes and then at positions B and D for 10 minutes. The array positions are shown in Figure 1a, and the LLLT protocol is given in Table 1. The LED arrays generated continuous red light for the first 5 minutes and infrared light pulses at 20 Hz for the next 5 minutes at each position. The arrays were followed by IR Laser Probe stimulations generating infrared laser light at 825 nm for ten minutes. The laser probe contains one laser diode with a touch sensor to turn ON only upon touching the skin. Two laser probes were used simultaneously, one on each side of the spinal cord starting from the lumbar spine points L1-A as shown in Figure 1b for 10 seconds and then moving laterally on both sides by 1 cm marked as point L1-B and again

stimulated for 10 seconds and in the third step, moving further away from the previous point by 1 cm marked as L1-C and stimulated for 10 seconds (Figure 1b).

Similarly, for L2-L5 and S1-S5 to target the sacral parasympathetic nerves. Stimulating L1-S5 (three points lateral to the spinal cord for each) took 5 minutes using two probes simultaneously, the procedure then repeated for the second time and the total stimulation time for the IR laser probe was 10 minutes. The placements of the Laser probes are shown in Figure 1b.

Technical specifications: the IR laser probe consists of one laser diode with following parameters:

Average power = 180.0 mW

Wavelength (λ) = 825 nm

Spot size = 0.10 cm^2 = 10 mm^2

Power density ($I0$) = 1800 mW/cm^2 = 18 mW/mm^2

Time of application. = 10 min

Total Energy = 10800 J = 10.8 kJ

Energy Density = 1080 J/cm^2 = 10.8 J/mm^2

The specifications of the LED array are as follows:

Average power = 1000 mW

Wavelength (λ) = 660 nm

Spot size = 100 cm2 = 10000 mm^2

Power density ($I0$) = 10 mW/cm^2 = 0.1 mW/mm^2

Time of application. = 5 min

Total Energy = 30000 J = 30 kJ

Number of LEDs in array = 240

Energy Delivered per LED = 30000 J/240 = 125 J =0.125 kJ

Energy Density = 3 J/cm^2 = 0.03 J/mm^2

8.3.4 Sham Study

To rule out a placebo effect, the LLLT protocol was repeated twice in six healthy volunteers such that the arrays and probe were not turned ON during the first round while they were turned ON during the second round. The sham protocol included baseline (6 min) followed by simultaneously placing LED arrays at positions A and C (10 min) followed by simultaneous array placement at positions B and D (10 min) and in the next step, two IR laser probes were used to work simultaneously on both sides of the spinal column for 10 min with a 6 min recovery period (Figure 8.1).

8.3.5 Visual representation of ANS activity

The HRV spectrogram of the RR intervals signal was generated as an image for each step of the LLLT protocol. The ECG and impedance signals were imported into ImageJ using Cardio Images plugins [http://www.scepticalphysiologist.com]. In the Cardio Images plugins, the peak detection and correction of the ECG signal was carried out by the Pan-Tomkins algorithm and a neural networks model generated and trained in TensorFlow with manual checking and editing of wrongly detected/edited R peaks. The tachogram of RR intervals was plotted as a raster image using a sampling frequency of 10 Hz, an image width of 5 seconds with cubic interpolation in the Intervals plugin. The Frequency Win plugin was used to calculate FFT spectra of the tachogram raster image using a window length of the 60s and intervals of 10s.

The power spectra were collated into an image with time on the y-axis and frequency on the x-axis with pixel intensity as amplitude. The Win frequency plugin generated the HRV spectrogram from 0 to 5 Hz to study the RSA/HF (0.15-0.5 Hz.) band only, which represents the parasympathetic activity (Berntson *et al.*, 1997), the lower frequency band (0-0.14 Hz.), as well as the frequency band above 1Hz, was removed in MATLAB. The spectrogram with the frequency band of 0.14 to 1 Hz was plotted as an image. The raster image of RR intervals was also read into MATLAB and was used to calculate RMSSD and SI, which were also plotted as aligned images. RMSSD and SI measured parasympathetic and sympathetic activity, respectively. These images were generated for the whole recording of the patients before low-level laser therapy - during array at AC - during array at BD - during IR laser probe - during recovery. The same procedure was used for the sham study.

8.3.6 Statistical Analysis

The HRV parameters (RSA, RMSSD, SI, SI/RSA, SI/RMSSD) and HR were calculated from the recorded ECG signal for each stage of the low-level laser therapy protocol, including baseline and recovery for each patient. The changes in each parameter during each stage were assessed statistically for 41 patients using GraphPad Prism software. The data were first checked for normality (gaussian distribution) using the Shapiro-Wilk Normality test. A dataset was normally distributed if all the columns (before-Array AC-Array BD-Probe-Recovery) passed the Shapiro-Wilk Normality test. In the case of the normally distributed data set One-Way-ANOVA followed by Holm-Sidak, multiple comparison tests were used to see the changes in the HRV parameter during each stage of the low-level laser therapy protocol. If data was not normally distributed, the Friedman test followed by Dunn's multiple comparison test was applied to check the

changes in that parameter. For the Sham protocol, Two-way Anova followed by Bonferroni's multiple comparison test was used to compare the changes in HRV parameters during the actual and sham protocol. The significance level was set at $p<0.05$.

The data are presented as the effect of the light arrays, focusing on the outcome measured during activation of the BD array combination and the laser probe effect. The figures will show the data from each part of the stimulation protocol.

8.4 Results

Parasympathetic reactivity in response to light arrays and laser probe activation

Activation of light arrays decreased, whereas laser probe stimulation increased parasympathetic activity.

Activation of the light arrays significantly decreases RSA from 5.98 to 5.80 ln(ms^2) (Figure 2a), consistent with a significant decrease in RMSSD (Figure 2b).

Laser probe stimulation increased the RSA significantly to 6.22 ln(ms^2) (Figure 2a). After the IR laser probe stimulation, the RSA decreased back to 5.99 during recovery. The RMSSD significantly increased compared to the light arrays' effect upon activating the laser probe.

The RSA and RMSSD values at baseline and recovery were not significantly different (Figures 2a, b). The percentage change in RSA due to laser probe stimulation and its subsequent recovery for each patient are shown in Figure 3.

Figure 4 shows a continuous assessment of the HRV parameters during the entire low-level laser therapy protocol in one patient. Figure 4b represents the HF power band from which the

RSA is derived. A dramatic increase in parasympathetic activity occurs, measured by HF power and RMSSD during probe stimulation.

Sympathetic reactivity in response to light arrays and laser probe activation

Laser probe stimulation decreased sympathetic activity without immediate recovery.

The sympathetic index (SI) measured the sympathetic nervous system response to the LLLT stimulations. The SI value numerically but not significantly increased during light array stimulation but significantly decreased from 41.31 to 34.84 s^{-1} (Figure 8.2c). The SI values did not recover within five minutes following laser probe stimulation. The percentage change in SI due to laser probe stimulation and the subsequent recovery values for each patient are shown in Figure 8.3.

Assessing shifts in parasympathetic or sympathetic dominance

The ratios SI/RSA and SI/RMSSD showed a shift towards the parasympathetic activity in response to the one-time low-level laser therapy session, dominated by a reduction in sympathetic activity during the laser probe stimulation.

The laser probe stimulation significantly decreased the SI/RSA from 7.60 to 6.12 (Figure 2d). This is a 19.5% decrease compared to baseline and a 29.7% decrease compared to the light arrays' effect. The value of SI/RSA remained at 6.34 during the recovery period suggesting a sustained effect of the probe. SI/RMSSD showed numerically the same direction of change with a significant effect of the laser probe compared to the effect of the light arrays (Figure 2e).

Figure 8.3 shows the percentage change in SI/RSA during probe stimulation of all patients, indicating a shift towards parasympathetic activity in 30 out of the 41 patients.

Assessing heart rate changes during a one-time low-level laser therapy session

Comparing before and after the low-level laser therapy session, there was no significant change in heart rate. However, the average heart rate decreased by 2.7 beats per minute during laser probe stimulation compared to baseline. It recovered back to its baseline value after laser stimulation (Figure 8.2f).

Sham neuromodulation on healthy subjects

Sham activation of light arrays and laser probe did not significantly change HRV parameters.

In six healthy volunteers, laser probe stimulation increased RSA significantly from 6.16 during baseline to 7.00 ln(ms^2); this decreased back to 6.20 ln(ms^2) during recovery (Figure 8.5a). The sham procedure did not show any marked change in RSA during any step (Figure 8.5a). Similarly, the RMSSD increased significantly to 70.70 *ms* during laser probe stimulations compared to the baseline value of 59.19 ms (Figure 8.5b). RMSSD did not show any significant change during the sham protocol (Figure 8.5b).

The average value SI decreased significantly from 53.27 s^{-1} during baseline to 30.07 s^{-1} during laser probe stimulation (Figure 8.5c). The sham procedure did not show a significant change in SI during any step (Figure 8.5c).

During laser probe stimulation, the SI/RSA markedly decreased from its average baseline value of 10.41 to 5.41. This is almost a 50% decrease, which indicated the shift of the autonomic balance towards the parasympathetic nervous system during laser probe stimulation. The sham procedure did not affect SI/RSA values during any step (Figure 8.5d). SI/RMSSD changed numerically from 2.59 to 0.91, but this did not reach significance (Figure 8.5e). No change was observed during the sham procedure (Figure 5e). During actual and sham

procedures, the average heart rate changed slightly during the laser probe stimulation (Figure 8.5f).

Figure 8.6 shows a continuous assessment of HRV parameters during the sham and laser probe stimulation of a single subject. The high-frequency band power of the RR interval signal indicates that during sham probe stimulation, there was no significant change in HF parasympathetic activity. In contrast, the amplitude of the HF power band increased markedly during actual laser probe stimulation compared to baseline, sham and recovery (Figure 8.5b). This was also reflected in an increased RMSSD amplitude during actual laser probe stimulations (Figure 8.5c). A decrease in SI amplitude during the actual laser probe stimulation was observed, compared to sham probe, baseline, and recovery.

8.5 Discussion

The overall effect of a single low-level laser therapy session was increased parasympathetic activity, decreased sympathetic activity, resulting in shifting the autonomic balance into the parasympathetic domain. The protocol involved stimulation using light arrays followed by a laser probe, with the arrays decreasing and the laser probe increasing parasympathetic activity. The sham study showed that the change in autonomic activity was due to activation by light and not due to touching or pressing the probes onto the skin.

Our only objective was to investigate if a single session of low-level laser therapy would demonstrably affect the autonomic nervous system. The fact that HRV parameters significantly changed shows that the autonomic innervation to the heart was affected; hence a signal from the sacral-lumbar area evoked by the low-level laser therapy session reached the brain stem.

This will happen when nerve action potentials are evoked in the ascending autonomic nerves. A study on hippocampal neurons used light at 970 nm, and a dorsal root ganglion study used light at 1875 nm to trigger action potential generation (Liang *et al.*, 2009) (Paris *et al.*, 2017). We used light at 660 nm and 840 nm for 5 minutes at each placement. The study on hippocampal neurons of rats showed that low-power infrared light triggers action potentials through changes in local temperature of the neuron's cell membrane that increased the activity of voltage-dependent Na channels, leading to depolarization (Liang *et al.*, 2009). The dorsal root ganglion expresses temperature-sensitive transient receptor potential channels, which are also sensitive to stimulation by infrared light (Liang *et al.*, 2009). An infrared pulse of 20 ms emitting 1875 nm light was able to trigger depolarization through action potentials in sensory neurons of the dorsal root ganglion (Paris *et al.*, 2017). Both studies show that the temperature changes in the cell membranes were reversible and non-damaging, unlike what is observed with heat-emitting devices and high-power lasers (Liang *et al.*, 2009) (Paris *et al.*, 2017).

The arrays and the probe gave different responses, likely because the probe light has a much higher intensity and will penetrate deeper in the tissue, potentially activating different neuronal circuitries.

The goal of low-level laser therapy concerning colonic motility disorders is to neuromodulate the circuitry of the autonomic nervous system so that normal reflexes are restored. Stimulation with low-level laser therapy may stimulate neurons to fire action potentials with, as a consequence, the strengthening of the functionality of the synapses while also stimulating increased energy production and nutrient delivery through cellular activation and vasodilation (Chung *et al.*, 2012; Rola *et al.*, 2014). This would allow for recovery of the functionality of the

neurons in the sacral defecation center and neural regeneration (Chen *et al.*, 2014) and ultimately help in the restoration of the defecation reflex (Furness *et al.*, 2014; Milkova *et al.*, 2020). The data of the present study do not inform about the likelihood of success of this therapy but give credence to exploring sacral neuromodulation using low-level laser therapy as a treatment for chronic constipation.

Acknowledgements

This study was supported by the Natural Sciences and Engineering Research Council (NSERC) Grant 386877 to JDH. MKA was supported by a fellowship from the Farncombe Family Digestive Health Research Institute and NSERC. We gratefully acknowledge that Dr. Sean Parsons provided all ImageJ plug-ins. We are grateful for the training provided by the Bioflex laser therapy clinic, in particular Dr. Fred Kahn and Slava Kim.

Conflict Of Interest

The authors declare that they have no conflict of interest of any kind.

Author Contributions

MKA analyzed all the data, contributed to interpretation, and wrote a manuscript draft. SS made a significant contribution to data analysis and data interpretation at the beginning of the project. NM and LL contributed to patient assessment and data analysis. KS made a substantial contribution to data analysis. JDH and J-HC designed the study and contributed to data collection, data analysis, interpretation, and revisions to the manuscript.

Table 8-1: LLLT protocol

Session	Head Used	Position	Light	Pulse Frequency	Duty Cycle	Duration (min)
1	Baseline					6
2	LED Arrays	A and C	Red, 660 nm	Continuous		5
			IR, 840 nm	20 Hz.	50%	5
3	LED Arrays	B and D	Red, 660 nm	Continuous		5
			IR, 840 nm	20 Hz.	50%	5
4	Laser Probes		IR, 825 nm	Continuous		10
5	Recovery					6

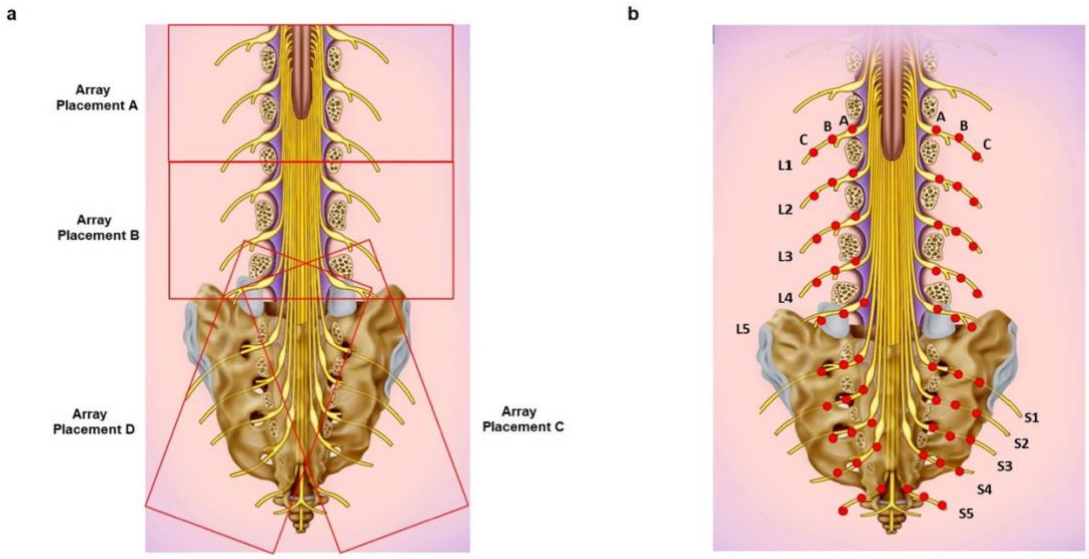

Figure 8-1: a LED array placements A, B, C and D. b Target areas for laser probe stimulation marked as red dots. Each point is stimulated for 20 seconds. Basic image obtained from dreamstime.com with permission

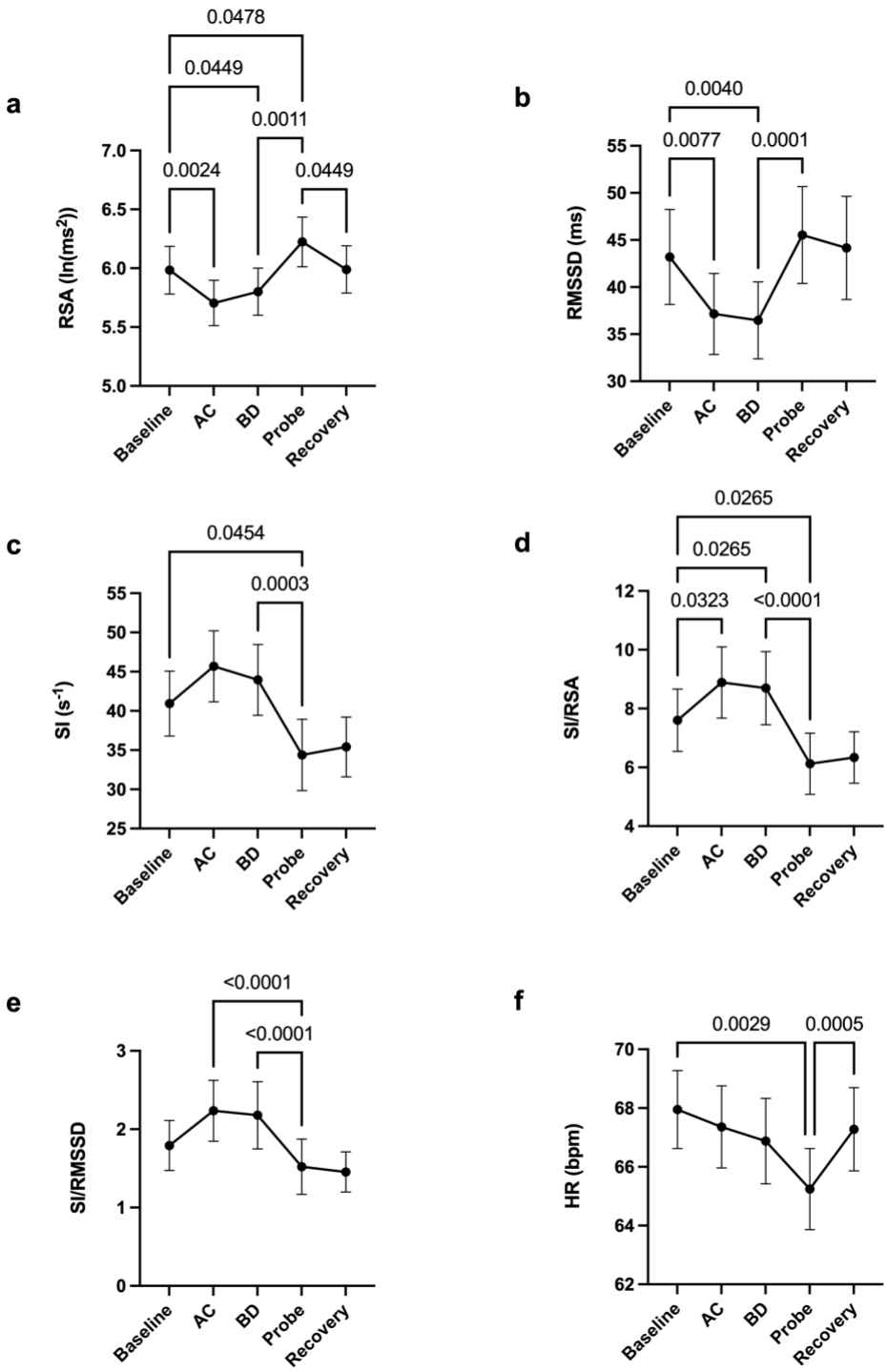

Figure 8-2: Autonomic nervous system modulation as deduced from HRV changes during one session of low-level laser therapy, stimulating the lumbar and sacral spine. Average values ± SD from 41 patients with chronic refractory constipation

	△SI		△RSA		△(SI/RSA)	
Patient#	△SI (IR Probe-Baseline)	△SI (Recovery-IR Probe)	△RSA (IR Probe-Baseline)	△RSA (Recovery-IR Probe)	△(SI/RSA) (IR Probe-Baseline)	△(SI/RSA) (Recovery-IR Probe)
pt1	-7.65%	-28.62%	40.65%	-14.98%	-34.34%	-16.04%
pt2	-53.14%	106.62%	3.17%	9.81%	-54.58%	88.17%
pt3	4.25%	-11.30%	9.26%	8.03%	-4.58%	-17.89%
pt4	50.52%	-37.72%	-9.18%	-1.34%	65.74%	-36.87%
pt5	-39.96%	21.91%	13.10%	-13.79%	-46.91%	41.40%
pt6	-13.89%	-2.11%				
pt7	-75.02%	63.52%	49.36%	-6.65%	-83.28%	74.40%
pt8	-25.05%	104.30%	5.51%	3.11%	-28.97%	97.94%
pt9	-47.12%	136.17%	15.42%	-2.86%	-54.18%	142.92%
pt10	-14.33%	1.70%	-5.64%	9.96%	-9.21%	-8.43%
pt11	13.06%	-12.34%	-33.82%	20.05%	70.82%	-29.91%
pt12	73.11%	-58.13%	-3.64%	0.00%	79.64%	-58.13%
pt13	-28.50%	-17.20%	-5.21%	-1.03%	-24.56%	-16.34%
pt14	-69.74%	22.62%	30.71%	-11.82%	-76.85%	37.12%
pt15	-62.58%	9.86%	-6.02%	5.97%	-60.18%	3.30%
pt16	-40.81%	63.90%	21.13%	-18.42%	-51.14%	94.09%
pt17	-48.36%	15.95%	11.81%	6.05%	-53.81%	8.94%
pt18	106.22%	-35.83%	-0.36%	5.70%	106.98%	-39.49%
pt19	-47.88%	25.46%	3.49%	-3.72%	-49.64%	30.13%
pt20	-56.54%	34.29%	0.17%	1.19%	-56.61%	32.69%
pt21	-22.99%	8.73%	12.58%	-0.29%	-31.60%	9.05%
pt22	54.10%	3.91%	2.07%	-6.50%	50.98%	10.67%
pt23	-65.31%	52.83%	24.09%	-18.04%	-72.05%	80.40%
pt24	-5.09%		-1.07%		-4.06%	-100.00%
pt25	-25.58%	-17.72%	8.02%	-0.43%	-31.11%	-14.69%
pt26	-19.46%	0.96%	1.84%	3.90%	-20.91%	-2.97%
pt27	-44.27%	60.52%	5.05%	-11.07%	-46.95%	181.37%
pt28	60.38%	-20.60%	-1.06%	-4.15%	62.10%	-13.64%
pt29	-44.45%		-0.45%		-44.20%	
pt30	111.85%	-74.04%	-14.64%	-0.52%	148.20%	-42.24%
pt31	-42.34%	29.95%	4.95%	-18.88%	-45.06%	69.69%
pt32	-15.06%	30.66%	3.53%	-0.26%	-17.96%	44.60%
pt33	-1.53%	-145.13%	-3.49%	15.10%	2.04%	-65.36%
pt34	56.11%	-12.17%	-11.46%	7.07%	76.31%	-17.15%
pt35	16.96%	16.46%	-10.13%	1.46%	30.14%	17.95%
pt36	-34.30%		11.43%		-41.04%	
pt37	8.96%	-5.89%	-9.08%	3.18%	19.84%	-8.56%
pt38	-36.22%	40.93%	7.73%	0.35%	-40.80%	68.71%
pt39	-58.43%	48.58%	6.17%	-18.07%	-60.84%	129.60%
pt40	-44.28%	60.77%	0.48%	-4.91%	-44.55%	167.45%
pt41	1.61%	41.89%	-2.77%	-3.32%	4.50%	77.80%

Figure 8-3: Change in RSA, SI and SI/RSA due to laser probe stimulation and recovery in all 41 patients

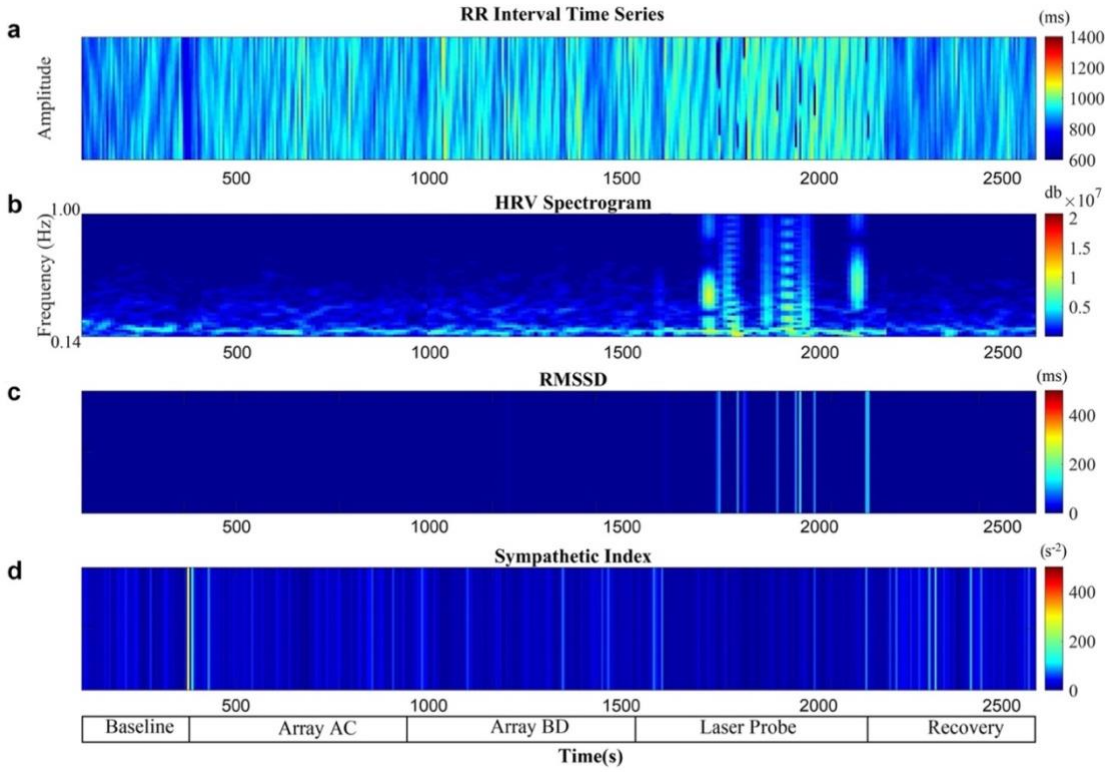

Figure 8-4: Autonomic nervous system modulation as deduced from HRV changes during the entire protocol of one session of low-level laser therapy in one patient.

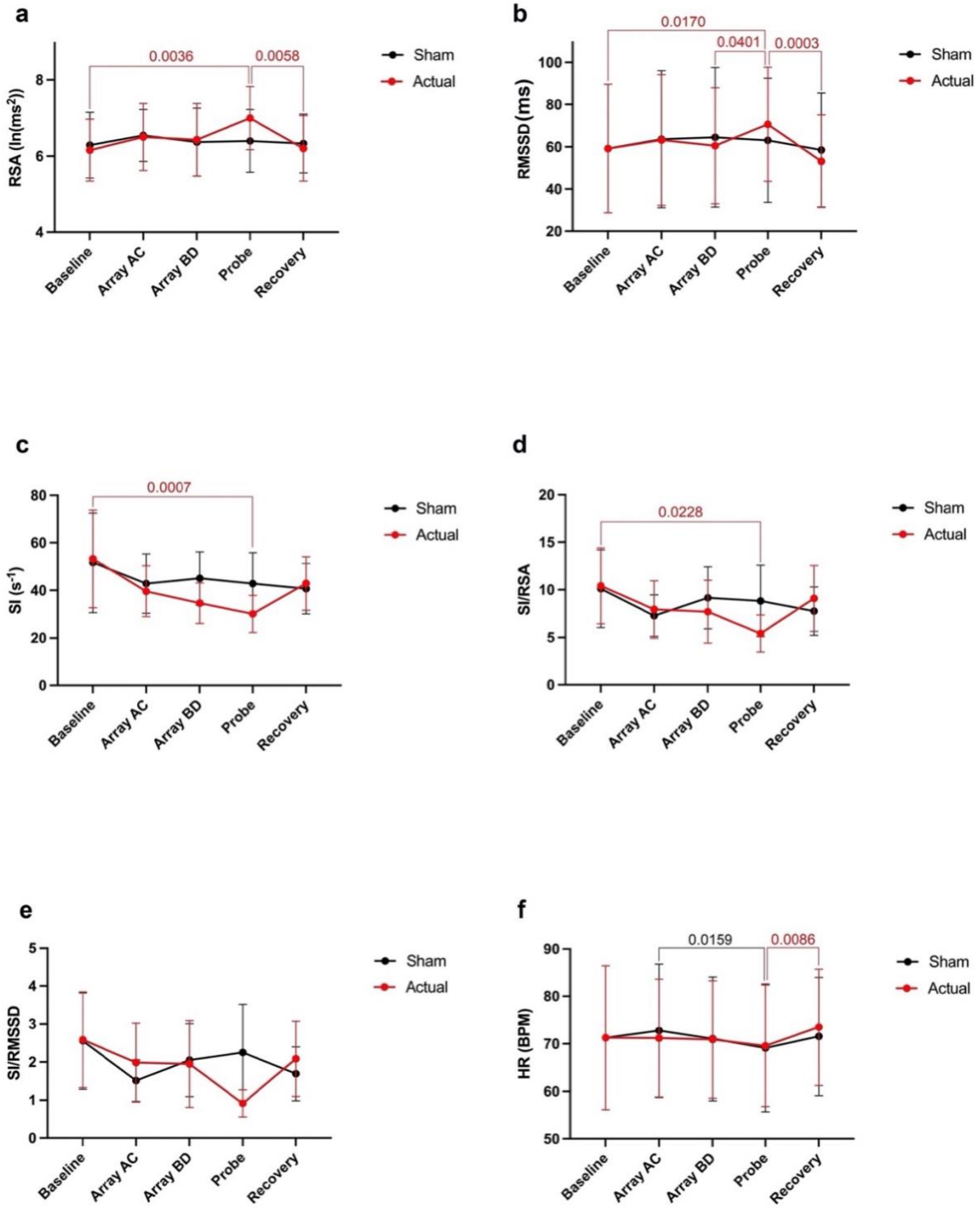

Figure 8-5: Autonomic nervous system modulation as deduced from HRV changes during the entire protocol of one session of low-level laser therapy in one patient.

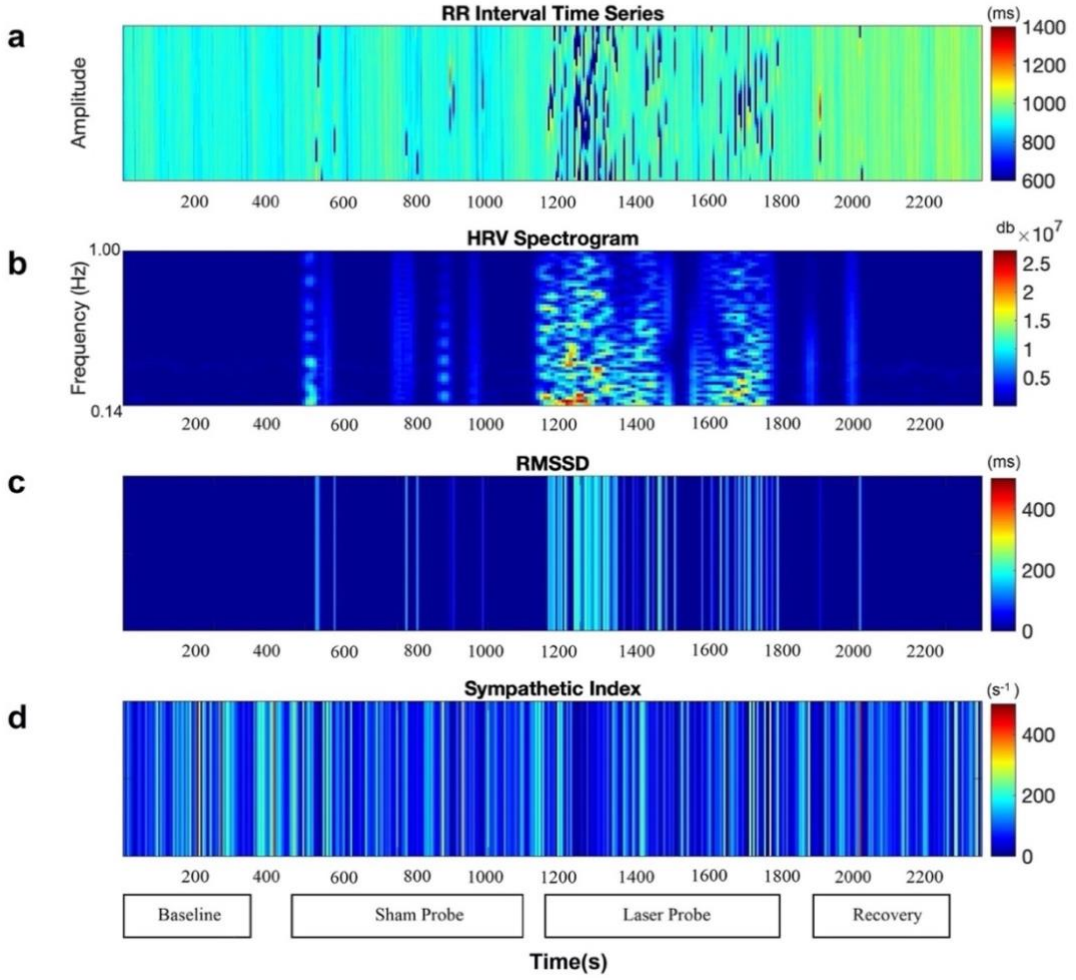

Figure 8-6: Comparison of autonomic nervous system activity during the application of the probe procedure with and without (sham) activating the probe.

8.6 References:

Ali MK, Liu L, Chen JH & Huizinga JD (2021). Optimizing Autonomic Function Analysis via Heart Rate Variability Associated With Motor Activity of the Human Colon. *Front Physiol* **12**, 1–14; doi: 10.3389/fphys.2021.619722.

Andreo L, Soldera CB, Ribeiro BG, de Matos PRV, Bussadori SK, Fernandes KPS & Mesquita-Ferrari RA (2017). Effects of photobiomodulation on experimental models of peripheral nerve injury. *Lasers Med Sci* **32**, 2155–2165.

Baevsky RM & Chernikova AG (2017). Heart rate variability analysis: physiological foundations and main methods. *Cardiometry* **DOI: 10.12710/cardiometry.2017.6676**, 10: 66–76.

Berntson GG, Bigger JT, Eckberg DL, Grossman P, Kaufmann PG, Malik M, Nagaraja HN, Porges SW, Saul JP, Stone PH & van der Molen MW (1997). Heart rate variability: origins, methods, and interpretive caveats. *Psychophysiology* **34**, 623–648.

Bharucha AE, Camilleri M, Low PA & Zinsmeister AR (1993). Autonomic dysfunction in gastrointestinal motility disorders. *Gut* **34**, 397–401.

Blok BF, Groen J, Bosch JL, Veltman DJ & Lammertsma AA (2006). Different brain effects during chronic and acute sacral neuromodulation in urge incontinent patients with implanted neurostimulators. *BJU Int* **98**, 1238–1243.

Brookes SJ, Dinning PG & Gladman MA (2009). Neuroanatomy and physiology of colorectal function and defaecation: from basic science to human clinical studies. *Neurogastroenterol Motil* **21 Suppl 2**, 9–19.

Callaghan B, Furness JB & Pustovit RV (2018). Neural pathways for colorectal control, relevance to spinal cord injury and treatment: a narrative review. *Spinal Cord* **56**, 199–205.

Camilleri M, Ford AC, Mawe GM, Dinning PG, Rao SS, Chey WD, Simrén M, Lembo A, Young-Fadok TM & Chang L (2017). Chronic constipation. *Nat Rev Dis Primers* **3**, 17095.

Chen JD, Yin J & Wei W (2017). Electrical therapies for gastrointestinal motility disorders. *Expert Rev Gastroenterol Hepatol* **11**, 407–418.

Chen YJ, Wang YH, Wang CZ, Ho ML, Kuo PL, Huang MH & Chen CH (2014). Effect of low level laser therapy on chronic compression of the dorsal root ganglion. *PLoS One* **9**, e89894.

Chung H, Dai T, Sharma SK, Huang YY, Carroll JD & Hamblin MR (2012). The nuts and bolts of low-level laser (light) therapy. *Ann Biomed Eng* **40**, 516–533.

Furness JB, Callaghan BP & Rivera LR (2014). The enteric nervous system and gastrointestinal innervation: integrated local and central control. *Adv Exp Med Biol* **817**, 39–71.

Hashmi JT, Huang YY, Osmani BZ, Sharma SK, Naeser MA & Hamblin MR (2010). Role of low-level laser therapy in neurorehabilitation. *Physical Medicine and Rehabilitation (PM&R)* **2**, S292–305.

Huang Z, Li S, Foreman RD, Yin J, Dai N & Chen JDZ (2019). Sacral nerve stimulation with appropriate parameters improves constipation in rats by enhancing colon motility mediated via the autonomic-cholinergic mechanisms. *Am J Physiol Gastrointest Liver Physiol* **317**, G609–G617.

Huizinga JD, Liu L, Barbier A & Chen JH (2021). Distal Colon Motor Coordination: The Role of the Coloanal Reflex and the Rectoanal Inhibitory Reflex in Sampling, Flatulence, and Defecation. *Front Med (Lausanne)* **8**, 720558.

Kahn F (2022).
Kamm MA, Dudding TC, Melenhorst J, Jarrett M, Wang Z, Buntzen S, Johansson C, Laurberg S, Rosen H, Vaizey CJ, Matzel K & Baeten C (2010). Sacral nerve stimulation for intractable constipation. *Gut* **59**, 333–340.
Kenefick NJ, Emmanuel A, Nicholls RJ & Kamm MA (2003). Effect of sacral nerve stimulation on autonomic nerve function. *Br J Surg* **90**, 1256–1260.
Kim JS & Yi SJ (2014). Effects of Low-frequency Current Sacral Dermatome Stimulation on Idiopathic Slow Transit Constipation. *J Phys Ther Sci* **26**, 831–832.
Leong LC, Yik YI, Catto-Smith AG, Robertson VJ, Hutson JM & Southwell BR (2011). Long-term effects of transabdominal electrical stimulation in treating children with slow-transit constipation. *J Pediatr Surg* **46**, 2309–2312.
Liang S, Yang F, Zhou C, Wang Y, Li S, Sun CK, Puglisi JL, Bers D, Sun C & Zheng J (2009). Temperature-dependent activation of neurons by continuous near-infrared laser. *Cell Biochem Biophys* **53**, 33–42.
Mester E, Nagylucskay S, Döklen A & Tisza S (1976). Laser stimulation of wound healing. *Acta Chir Acad Sci Hung* **17**, 49–55.
Milkova N, Parsons SP, Ratcliffe E, Huizinga JD & Chen JH (2020). On the nature of high-amplitude propagating pressure waves in the human colon. *Am J Physiol Gastrointest Liver Physiol* **318**, G646–G660.
Paris L, Marc I, Charlot B, Dumas M, Valmier J & Bardin F (2017). Millisecond infrared laser pulses depolarize and elicit action potentials on in-vitro dorsal root ganglion neurons. *Biomed Opt Express* **8**, 4568–4578.
Payne SC, Furness JB & Stebbing MJ (2019). Bioelectric neuromodulation for gastrointestinal disorders: effectiveness and mechanisms. *Nat Rev Gastroenterol Hepatol* **16**, 89–105.
Rao SS, Rattanakovit K & Patcharatrakul T (2016). Diagnosis and management of chronic constipation in adults. *Nat Rev Gastroenterol Hepatol* **13**, 295–305.
Rola P, Doroszko A & Derkacz A (2014). The Use of Low-Level Energy Laser Radiation in Basic and Clinical Research. *Adv Clin Exp Med* **23**, 835–842.
Thayer JF, Ahs F, Fredrikson M, Sollers JJ & Wager TD (2012). A meta-analysis of heart rate variability and neuroimaging studies: implications for heart rate variability as a marker of stress and health. *Neurosci Biobehav Rev* **36**, 747–756.
Vaizey CJ, Kamm MA, Turner IC, Nicholls RJ & Woloszko J (1999). kEffects of short term sacral nerve stimulation on anal and rectal function in patients with anal incontinence. *Gut* **44**, 407–412.
Valentino RJ, Miselis RR & Pavcovich LA (1999). Pontine regulation of pelvic viscera: pharmacological target for pelvic visceral dysfunctions. *Trends Pharmacol Sci* **20**, 253–260.
Veiga ML, Costa EV, Portella I, Nacif A, Martinelli Braga AA & Barroso U (2016). Parasacral transcutaneous electrical nerve stimulation for overactive bladder in constipated children: The role of constipation. *J Pediatr Urol* **12**, 396.e1–396.e6.
Veiga ML, Lordêlo P, Farias T & Barroso U (2013). Evaluation of constipation after parasacral transcutaneous electrical nerve stimulation in children with lower urinary tract dysfunction--a pilot study. *J Pediatr Urol* **9**, 622–626.
Wexner SD, Coller JA, Devroede G, Hull T, McCallum R, Chan M, Ayscue JM, Shobeiri AS, Margolin D, England M, Kaufman H, Snape WJ, Mutlu E, Chua H, Pettit P, Nagle D, Madoff

RD, Lerew DR & Mellgren A (2010). Sacral nerve stimulation for fecal incontinence: results of a 120-patient prospective multicenter study. *Ann Surg* **251**, 441–449.

Yamany AA & Sayed HM (2012). Effect of low level laser therapy on neurovascular function of diabetic peripheral neuropathy. *Journal of Advanced Research* **3**, 21–28.

Yuan Y, Ali MK, Mathewson KJ, Sharma K, Faiyaz M, Tan W, Parsons SP, Zhang KK, Milkova N, Liu L, Chen J-H & Huizinga JD (2020). Associations between colonic motor patterns and autonomic nervous system activity assessed by high-resolution manometry and concurrent heart rate variability. *Front Neurosci* **13**, 1447.

Zheng H, Chen Q, Chen M, Wu X, She T, Li J, Huang D, Yue L & Fang J (2019). Nonpharmacological conservative treatments for chronic functional constipation: A systematic review and network meta-analysis. *Neurogastroenterology & Motility* **31**, e13441.

Chapter 9

General Discussions

The objective of this study was to establish methodologies to study the autonomic nervous system activity using heart rate variability parameters and to identify the role of the autonomic nervous system in colonic motility disorders and the effect of sacral nerve stimulation to restore autonomic functioning. Heart rate variability parameters for sympathetic and parasympathetic nervous system activity were explored. Since the parasympathetic reactivity decreases and the sympathetic reactivity increases from supine to standing, HRV parameters were tested using the postural change test. Almost all the parasympathetic HRV parameters indicated decreased PNS activity during standing. RSA, RMSSD and SD1 were identified as the best measures of PNS activity. For the sympathetic nervous system activity, the LF power has been used in the literature; however, it is affected by both the sympathetic and parasympathetic activity. To find a pure measure of SNS activity, pre-ejection period was explored, but it was not sensitive enough to identify small changes in SNS activity. Baevsky's Stress Index or Sympathetic Index (SI) was found to be the best HRV parameter for SNS activity. SI was found to be highly sensitive to sympathetic nervous system changes in response to active standing. Detrended fluctuation analysis and complex correlation methods were also explored, but the results were not consistent with the changes in the autonomic nervous system as shown by SI or RSA. For sympathovagal balance, we tested LF/HF power ratio and SD2/SD1 ratio and introduced SI/RSA and SI/RMSSD ratios, the latter two were found to be very sensitive and accurately predicted the shift in sympathovagal balance during the active standing test.

These parameters were then tested against the tilt table test; patients with both motility disorders and cardiac dysfunctions were selected. During the tilt table test, the patients who had a postural orthostatic tachycardia syndrome attack had a very high sympathetic index value in the baseline supine and standing. Similarly, in patients who had a syncopal attack during the tilt table test, their autonomic reactivity to standing during the active standing test was the opposite of healthy controls. Usually, the sympathetic activity increases, and parasympathetic activity decreases during standing, but for those patients, it was the opposite in the active standing test; therefore, it was concluded that the active standing test could also predict the POTS and syncope, and the selected HRV parameters correctly predicted the sympathetic and parasympathetic nervous system activity. However, the number of patients available for this study were enough to generate hypotheses but not to make definitive conclusions. To reconfirm, it is recommended to include more patients in a future project. Age is also an important factor for autonomic nervous system activity and reactivity to the postural change; old age is associated with a low RSA during baseline. For future studies, it is intended to recruit more volunteers to generate HRV control values for different age groups. Our immediate goal is to establish control values based on our analysis of HR data from data banks such as Physionet database, Biosec Lab database at University of Toronto and MIT ECG database. However, our initial observations are that it will be difficult to find studies that use the same conditions and the same data analysis methods. In particular, many studies do not report the specifics needed to assess differences with our methods and conditions. We have now established a final protocol for autonomic assessment, and we will embark on a major study to obtain control values.

To establish the association between the autonomic nervous system and colonic motility, ECG and impedance cardiography were recorded along with high-resolution colonic manometry. The colon's motor patterns were evoked using different stimuli: meal, proximal and distal balloon distention, prucalopride and bisacodyl. Heart rate variability parameters were calculated for HR measurements before, during and after each recorded colonic motor pattern. It was identified that the parasympathetic activity increases, and sympathetic activity decreases during the motor patterns, and both PNS and SNS recover back afterwards. Upon visual representations of parasympathetic activity and the colonic motility recordings, we found, a sudden increase in the baseline parasympathetic activity and a decrease in sympathetic activity during the motor patterns. During motor complexes, rhythmic parasympathetic activity was observed, which diminished slowly after the end of the motor complexes.

Based on these results, it was hypothesized that the autonomic nervous system is highly involved in generating the normal colonic motor patterns. A stimulus is needed to modulate the autonomic nervous system such that the parasympathetic neural input to the colon from vagal and sacral nerves increases in order to generate colonic motor patterns. Conversely, there is also a requirement to decrease the sympathetic input to the colon. Based on these results, it was hypothesized that the patients with colonic motility disorders have very high sympathetic tone and very low parasympathetic tone, or they may not be able to modulate their autonomic nervous system to generate the colonic motor patterns.

To test this hypothesis, we have compared the autonomic activity of patients with motility disorders with that of the healthy controls. The results indicated that many patients with motility disorders have a very high sympathetic tone and a very low parasympathetic tone

during each posture of the active standing test. Patients were also hypersensitive to the postural change, and they had a very high sympathetic reactivity to standing. Their abnormal autonomic nervous system activity might be contributing to their abnormal motility. They may not be able to modulate their autonomic nervous system as required to generate the normal colonic motor patterns. Therefore, correcting their normal autonomic function may help to restore the normal colonic motility. Several factors contribute to the high sympathetic and low parasympathetic tone, including age, physical and mental stress, lifestyle, diet, and more. To test the effect of some of these factors, the next part of this study was to compare different groups of patients based on age and health conditions with healthy controls. The only issue was, we had a limited number of healthy controls (n=20) and if we further divided them based on the conditions mentioned above, the number of the controls (n) in each group further decreased. The study therefore generated hypotheses and it is recommended for future studies to increase the number of controls, generate control values for different age groups and compare each of the patients' groups to its respective control group based on age.

After establishing that a normal autonomic nervous system is critical to perform normal colonic functions and that autonomic dysfunction contributes to colonic motility disorders, we hypothesized that restoring the normal autonomic functions might help restore normal motility. Low-Level Laser Therapy is assumed to restore autonomic function by stimulating the lumbar and sacral autonomic nerves. Treating autonomic dysfunction by low-level laser therapy involves multiple treatments (three times a week for eight weeks). However, to test the hypothesis, we have used one session of LLLT in patients with motility disorders. The results indicated that the parasympathetic activity increased, and sympathetic activity decreased

significantly using a protocol that involved stimulation by arrays followed by an infrared laser probe. We also tested the placebo effect of LLLT, and It was identified that the parasympathetic reactivity increased, and sympathetic activity decreased only when the real stimulations were applied, which ruled out the sham effect. The autonomic nervous system recovered back after the one-time low-level laser therapy session, which indicates that the effect of low-level laser therapy may not be permanent, but these are the results for only one session. It is assumed that low-level laser therapy stimulates the neuronal circuitry of the autonomic nervous system, and multiple treatments may restore this permanently by providing energy to the system. Since the light cannot penetrate inside the spinal cord, magnetic nerve stimulations may be used to stimulate the nerves located inside the spinal cord. It is hypothesized that the low-level laser therapy restores the neuronal circuitry by providing energy to the cells, while the magnetic nerve stimulation is known to generate the action potentials by depolarizing the nerves which may initiate an immediate autonomic activity which can affect the colonic activity. The effect of low-level laser therapy might be slow compared to that of magnetic nerve stimulation but long-lasting. Combination of LLLT, TENS and Magnetic nerves stimulation may be tested to enhance the treatment.

Future Recommendations

9.1.1 Multiple sessions of LLLT

Since one session of LLLT can modulate the ANS activity, it is required to study the effect of multiple sessions of LLLT to verify its ability to permanently restore normal autonomic function and hence colonic motility. Our lab has recently started clinical trials on LLLT, which consists of a 3-week treatment with a total of 8 sessions. Treatment effects will be assessed using symptoms

and quality of life questionnaires, as well as physiological anorectal motility tests and autonomic nervous system functioning assessments before, during and after the LLLT treatment.

9.1.2 Mathematical Modelling

In a preliminary study, we found that lumbar and sacral neuromodulation by magnetic nerve stimulations can also modulate the ANS; however, the parameters of magnetic stimulations (intensity, frequency, duty cycle, duration) were not optimised. Similarly, for LLLT, we used light parameters recommended for pain modulation. The treatment for autonomic dysfunction can be optimised by selecting the type (or combination) of neuromodulation (LLLT, TENS, Electromagnetic) and the parameters of the modulation individualized for each patient. A mathematical model for ANS control of the colon and the effects of neuromodulation can be developed to:

1. predict the functionality of the human colon based on the ANS tone measured by HRV during the supine and ANS reactivity to standing, considering the gender and age of the person.
2. recommend the type and amount of neuromodulation and parameters for neuromodulation required to bring the ANS tone to normal ranges to restore the normal colonic function.

The ANS activity of the healthy volunteers can be recorded in association with their colonic motility and the effect of neuromodulation on ANS as well as colonic motility via LLLT, transcutaneous electrical nerve stimulation (TENS) and magnetic stimulation techniques. This data can be used to train the model using machine learning and to make the above predictions.

9.1.3 Neuromodulation via a feedback control system

The above model can be interfaced with ECG recorder and the neuromodulation equipment, to generate live HRV values to indicate the ANS activity and use it as feedback to continually adjust

the parameters of the applied neuromodulation. This model integrated with ANS activity recording and neuromodulation may prove to be very beneficial in clinical settings. It can be further extended to other organs of the human body that are controlled by the autonomic nervous system.

9.1.4 Understand the brainstem autonomic centers involved in the defecation reflex, in TENS-Magnetic stimulation and Laser induced autonomic activities

Evaluate the autonomic neural pathways involved in the defecation reflex and neuromodulation using functional MRI. The defecation reflex can be evoked by injecting 10 mg bisacodyl in the rectum of healthy volunteers. The goal of this will be to fully understand the brain stem regions affected by TENS, Magnetic Stimulation and LLLT to enhance our understanding of their mechanism of action.

9.1.5 Development of a non-invasive method to differentiate the parasympathetic activity of the sacral and vagal pathways

The proximal and transverse colon is innervated by vagal parasympathetic pathways while the distal colon is innervated by the sacral parasympathetic pathways. However, the HRV parameters used to measure the parasympathetic activity cannot differentiate between the vagal or sacral pathways. Therefore, there is a requirement to generate a new method to non-invasively record the parasympathetic activity that can differentiate the two pathways. It will enable us to study the two innervations separately and identify and treat the problem accordingly. This can be done by using a large variety of stimuli to stimulate the proximal and distal colon and study their effect on various parameters of HRV.

9.1.6 Remote assessment of the Autonomic nervous system tone and reactivity

The COVID 19 pandemic has made it clear that remote diagnostics and treatment will be the future. We can develop a mobile phone application to record the Autonomic Nervous System tone and reactivity remotely. The phone camera or chest band can be used to record the heart rate variability or pulse rate variability which will generate the HRV parameters for ANS activity. There are several applications already available for HRV, but we need HRV parameters, used as an input in our model discussed above, which will be able to accurately predict the organ function and recommend the required neuromodulation treatment. We have tried to record the HRV parameters using Kubios and Elite HRV apps using a chest band as a sensor, but these applications have their limitations. They do not provide the values of all the HRV parameters we require especially SI, secondly, the raw RR interval data cannot be downloaded. In addition to that, the frequency bands used to record the HF power could not be adjusted to consider the deep breathing. Therefore, to incorporate the recorded HRV into the model, we need to either be able to download the raw data and further process it to generate the input values for the mathematical model or to develop our own application for this purpose.

BIBLIOGRAPHY

[1] A. E. Bharucha and S. J. H. Brookes, “Neurophysiologic Mechanisms of Human Large Intestinal Motility ☆,” in *Physiology of the Gastrointestinal Tract*, Elsevier, 2018, pp. 517–564. doi: 10.1016/B978-0-12-809954-4.00023-2.

[2] K. N. Browning and R. A. Travagli, “Central Nervous System Control of Gastrointestinal Motility and Secretion and Modulation of Gastrointestinal Functions,” in *Comprehensive Physiology*, 1st ed., R. Terjung, Ed. Wiley, 2014, pp. 1339–1368. doi: 10.1002/cphy.c130055.

[3] T. J. Hibberd, W. P. Yew, B. N. Chen, M. Costa, S. J. Brookes, and N. J. Spencer, “A Novel Mode of Sympathetic Reflex Activation Mediated by the Enteric Nervous System,” *eNeuro*, vol. 7, no. 4, p. ENEURO.0187-20.2020, Aug. 2020, doi: 10.1523/ENEURO.0187-20.2020.

[4] H. Duan *et al.*, “Regulation of the Autonomic Nervous System on Intestine,” *Front. Physiol.*, vol. 12, 2021, Accessed: May 27, 2022. [Online]. Available: https://www.frontiersin.org/article/10.3389/fphys.2021.700129

[5] “INNERVATION OF THE GASTROINTESTINAL TRACT - Gastrointestinal Physiology - Physiology 5th Ed.” https://doctorlib.info/physiology/physiology-2/70.html (accessed May 13, 2022).

[6] Y. Taché, “The parasympathetic nervous system in the pathophysiology of the gastrointestinal tract,” in *Handbook of the Autonomic Nervous System in Health and Disease*, 2002, pp. 463–503.

[7] “Gastrointestinal Physiology - Physiology 5th Ed.” https://doctorlib.info/physiology/physiology-2/68.html (accessed May 13, 2022).

[8] M. T. La Rovere, A. Porta, and P. J. Schwartz, “Autonomic Control of the Heart and Its Clinical Impact. A Personal Perspective,” *Front. Physiol.*, vol. 11, 2020, Accessed: May 13, 2022. [Online]. Available: https://www.frontiersin.org/article/10.3389/fphys.2020.00582

[9] “CV Physiology | Autonomic Innervation of the Heart and Vasculature.” https://www.cvphysiology.com/Blood%20Pressure/BP008 (accessed May 13, 2022).

[10] F. Shaffer and J. P. Ginsberg, “An Overview of Heart Rate Variability Metrics and Norms,” *Front. Public Health*, vol. 5, p. 258, Sep. 2017, doi: 10.3389/fpubh.2017.00258.

[11] G. Ernst, “Heart-Rate Variability—More than Heart Beats?,” *Front. Public Health*, vol. 5, p. 240, Sep. 2017, doi: 10.3389/fpubh.2017.00240.

[12] P. Gupta, M. Swami, and H. Patel, “Light–Tissue Interactions,” in *Handbook of Photomedicine*, Taylor & Francis, 2013, pp. 25–34. doi: 10.1201/b15582-5.

[13] M. R. Hamblin, M. V. P. de Sousa, and T. Agrawal, *Handbook of low-level laser therapy*. Singapore: Pan Stanford publishing, 2017.

[14] G. N. Georgieva-Tsaneva, “Time and Frequency Analysis of Heart Rate Variability Data in Heart Failure Patients,” *Int. J. Adv. Comput. Sci. Appl.*, vol. 10, no. 11, 2019, doi: 10.14569/IJACSA.2019.0101163.

[15] D. L. Eckberg and M. J. Eckberg, “Human sinus node responses to repetitive, ramped carotid baroreceptor stimuli,” *Am. J. Physiol.*, vol. 242, no. 4, pp. H638-644, Apr. 1982, doi: 10.1152/ajpheart.1982.242.4.H638.

[16] L. Nguyen *et al.*, “Autonomic function in gastroparesis and chronic unexplained nausea and vomiting: Relationship with etiology, gastric emptying, and symptom severity,” *Neurogastroenterol. Motil. Off. J. Eur. Gastrointest. Motil. Soc.*, vol. 32, no. 8, p. e13810, Aug. 2020, doi: 10.1111/nmo.13810.

[17] J. Colombo, R. Arora, N. L. DePace, and A. I. Vinik, “Drawbacks of Heart Rate Variability Analysis and Application of Parasympathetic and Sympathetic Monitoring,” in *Clinical Autonomic Dysfunction: Measurement, Indications, Therapies, and Outcomes*, J. Colombo, R. Arora, N. L. DePace, and A. I. Vinik, Eds. Cham: Springer International Publishing, 2015, pp. 27–52. doi: 10.1007/978-3-319-07371-2_3.

[18] Z. Issa, J. M. Miller, and D. P. Zipes, *Clinical Arrhythmology and Electrophysiology: A Companion to Braunwald’s Heart Disease E-Book: Expert Consult: Online and Print*. Elsevier Health Sciences, 2012.

[19] “All About HRV Part 4: Respiratory Sinus Arrhythmia – MindWare Technologies Support.” https://support.mindwaretech.com/2017/09/all-about-hrv-part-4-respiratory-sinus-arrhythmia/ (accessed May 27, 2022).

[20] T. Minato *et al.*, "Relationship Between Short Term Variability (STV) and Onset of Cerebral Hemorrhage at Ischemia-Reperfusion Load in Fetal Growth Restricted (FGR) Mice," *Front. Physiol.*, vol. 9, p. 478, 2018, doi: 10.3389/fphys.2018.00478.

[21] A. H. Khandoker, C. Karmakar, M. Brennan, M. Palaniswami, and A. Voss, *Poincaré Plot Methods for Heart Rate Variability Analysis*. Boston, MA: Springer US, 2013. doi: 10.1007/978-1-4614-7375-6.

[22] P. Contreras, R. Canetti, and E. R. Migliaro, "Correlations between frequency-domain HRV indices and lagged Poincaré plot width in healthy and diabetic subjects," *Physiol. Meas.*, vol. 28, no. 1, pp. 85–94, Jan. 2007, doi: 10.1088/0967-3334/28/1/008.

[23] "About HRV," *Kubios*. https://www.kubios.com/about-hrv/ (accessed Apr. 08, 2022).

[24] C. K. Karmakar, A. H. Khandoker, J. Gubbi, and M. Palaniswami, "Complex Correlation Measure: a novel descriptor for Poincaré plot," *Biomed. Eng. OnLine*, vol. 8, no. 1, p. 17, Aug. 2009, doi: 10.1186/1475-925X-8-17.

[25] N. S. Salem and B. Eng, "Nonlinear Dynamics of the Heart Rate Variability Signal," p. 111.

[26] C. Kamath, "A NEW APPROACH TO DETECT CONGESTIVE HEART FAILURE USING DETRENDED FLUCTUATION ANALYSIS OF ELECTROCARDIOGRAM SIGNALS," vol. 10, p. 15, 2015.

[27] "All About Cardiac Impedance Part 1: Introduction to Cardiac Impedance – MindWare Technologies Support." https://support.mindwaretech.com/2017/05/all-about-cardiac-impedance-part-1-introduction-to-cardiac-impedance/ (accessed May 27, 2022).

[28] R. van Lien, N. M. Schutte, J. H. Meijer, and E. J. C. de Geus, "Estimated preejection period (PEP) based on the detection of the R-wave and dZ/dt-min peaks in ECG and ICG," *J. Phys. Conf. Ser.*, vol. 434, p. 012046, Apr. 2013, doi: 10.1088/1742-6596/434/1/012046.

[29] Institute of Biomedical Problems of the Russian Academy of Sciences, R. M. Baevsky, and A. G. Chernikova, "Heart rate variability analysis: physiological foundations and main methods," *Cardiometry*, no. 10, pp. 66–76, May 2017, doi: 10.12710/cardiometry.2017.10.6676.

[30] M. K. Ali, L. Liu, J.-H. Chen, and J. D. Huizinga, "Optimizing Autonomic Function Analysis via Heart Rate Variability Associated With Motor Activity of the Human Colon," *Front. Physiol.*, vol. 12, p. 619722, Jun. 2021, doi: 10.3389/fphys.2021.619722.

[31] P. Grossman and E. W. Taylor, "Toward understanding respiratory sinus arrhythmia: Relations to cardiac vagal tone, evolution and biobehavioral functions," *Biol. Psychol.*, vol. 74, no. 2, pp. 263–285, Feb. 2007, doi: 10.1016/j.biopsycho.2005.11.014.

[32] I. S. Curthoys, "Concepts and Physiological Aspects of the Otolith Organ in Relation to Electrical Stimulation," *Audiol. Neurootol.*, vol. 25, no. 1–2, pp. 25–34, 2020, doi: 10.1159/000502712.

[33] J. R. Carter and C. A. Ray, "Sympathetic responses to vestibular activation in humans," *Am. J. Physiol. Regul. Integr. Comp. Physiol.*, vol. 294, no. 3, pp. R681-688, Mar. 2008, doi: 10.1152/ajpregu.00896.2007.

[34] H. Nishimura and M. Yamasaki, "Changes in blood pressure, blood flow towards the head and heart rate during 90 deg head-up tilting for 30 min in anaesthetized male rats," *Exp. Physiol.*, vol. 103, no. 1, pp. 31–39, Jan. 2018, doi: 10.1113/EP086543.

[35] D. S. Goldstein and Y. Sharabi, "Neurogenic orthostatic hypotension: a pathophysiological approach," *Circulation*, vol. 119, no. 1, pp. 139–146, Jan. 2009, doi: 10.1161/CIRCULATIONAHA.108.805887.

[36] K. M. Smith-Edwards, S. A. Najjar, B. S. Edwards, M. J. Howard, K. M. Albers, and B. M. Davis, "Extrinsic Primary Afferent Neurons Link Visceral Pain to Colon Motility Through a Spinal Reflex in Mice," *Gastroenterology*, vol. 157, no. 2, pp. 522-536.e2, Aug. 2019, doi: 10.1053/j.gastro.2019.04.034.

[37] K. N. Browning and R. A. Travagli, "Central control of gastrointestinal motility," *Curr. Opin. Endocrinol. Diabetes Obes.*, vol. 26, no. 1, pp. 11–16, Feb. 2019, doi: 10.1097/MED.0000000000000449.

[38] S. M. Altschuler, J. Escardo, R. B. Lynn, and R. R. Miselis, "The central organization of the vagus nerve innervating the colon of the rat," *Gastroenterology*, vol. 104, no. 2, pp. 502–509, Feb. 1993, doi: 10.1016/0016-5085(93)90419-D.

[39] K. N. Browning and R. A. Travagli, “Central control of gastrointestinal motility:,” *Curr. Opin. Endocrinol. Diabetes Obes.*, vol. 26, no. 1, pp. 11–16, Feb. 2019, doi: 10.1097/MED.0000000000000449.

[40] W. C. De Groat and J. Krier, “The sacral parasympathetic reflex pathway regulating colonic motility and defaecation in the cat.,” *J. Physiol.*, vol. 276, no. 1, pp. 481–500, 1978, doi: 10.1113/jphysiol.1978.sp012248.

[41] G. Devroede and J. Lamarche, “Functional Importance of Extrinsic Parasympathetic Innervation to the Distal Colon and Rectum in Man,” *Gastroenterology*, vol. 66, no. 2, pp. 273–280, Feb. 1974, doi: 10.1016/S0016-5085(74)80114-9.

[42] B. Callaghan, J. B. Furness, and R. V. Pustovit, “Neural pathways for colorectal control, relevance to spinal cord injury and treatment: a narrative review,” *Spinal Cord*, vol. 56, no. 3, Art. no. 3, Mar. 2018, doi: 10.1038/s41393-017-0026-2.

[43] K. Krogh, N. Olsen, P. Christensen, J. L. Madsen, and S. Laurberg, “Colorectal transport during defecation in patients with lesions of the sacral spinal cord,” *Neurogastroenterol. Motil.*, vol. 15, no. 1, pp. 25–31, Feb. 2003, doi: 10.1046/j.1365-2982.2003.00381.x.

[44] A. E. Lomax, K. A. Sharkey, and J. B. Furness, “The participation of the sympathetic innervation of the gastrointestinal tract in disease states,” *Neurogastroenterol. Motil.*, vol. 22, no. 1, pp. 7–18, 2010, doi: 10.1111/j.1365-2982.2009.01381.x.

[45] K. N. Browning and R. A. Travagli, “Central Nervous System Control of Gastrointestinal Motility and Secretion and Modulation of Gastrointestinal Functions,” *Compr. Physiol.*, vol. 4, no. 4, pp. 1339–1368, Oct. 2014, doi: 10.1002/cphy.c130055.

[46] J.-H. Chen, H. S. Sallam, L. Lin, and J. D. Z. Chen, “Colorectal and rectocolonic reflexes in canines: involvement of tone, compliance, and anal sphincter relaxation,” *Am. J. Physiol.-Regul. Integr. Comp. Physiol.*, vol. 299, no. 3, pp. R953–R959, Sep. 2010, doi: 10.1152/ajpregu.00439.2009.

[47] M. L. Veiga, P. Lordêlo, T. Farias, and U. Barroso, “Evaluation of constipation after parasacral transcutaneous electrical nerve stimulation in children with lower urinary tract dysfunction – A pilot study,” *J. Pediatr. Urol.*, vol. 9, no. 5, pp. 622–626, Oct. 2013, doi: 10.1016/j.jpurol.2012.06.006.

[48] L. C. Y. Leong, Y. I. Yik, A. G. Catto-Smith, V. J. Robertson, J. M. Hutson, and B. R. Southwell, "Long-term effects of transabdominal electrical stimulation in treating children with slow-transit constipation," *J. Pediatr. Surg.*, vol. 46, no. 12, pp. 2309–2312, Dec. 2011, doi: 10.1016/j.jpedsurg.2011.09.022.

[49] N. J. Kenefick, "Sacral Nerve Neuromodulation for the Treatment of Lower Bowel Motility Disorders," *Ann. R. Coll. Surg. Engl.*, vol. 88, no. 7, pp. 617–623, Nov. 2006, doi: 10.1308/003588406X149174.

[50] M. A. Kamm *et al.*, "Sacral nerve stimulation for intractable constipation," *Gut*, vol. 59, no. 3, pp. 333–340, Mar. 2010, doi: 10.1136/gut.2009.187989.

[51] C.-Y. Chen, M.-D. Ke, C.-D. Kuo, C.-H. Huang, Y.-H. Hsueh, and J.-R. Chen, "The influence of electro-acupuncture stimulation to female constipation patients," *Am. J. Chin. Med.*, vol. 41, no. 2, pp. 301–313, 2013, doi: 10.1142/S0192415X13500225.

[52] M. E. Jarrett *et al.*, "Balance of Autonomic Nervous System Predicts Who Benefits from a Self-management Intervention Program for Irritable Bowel Syndrome," *J. Neurogastroenterol. Motil.*, vol. 22, no. 1, pp. 102–111, Jan. 2016, doi: 10.5056/jnm15067.

[53] "BIOFLEX Laser Therapy | Restore your quality of life with BIOFLEX® Laser Therapy." https://bioflexlaser.com/ (accessed May 29, 2022).

[54] mohamamd ali Ansari and E. Mohajerani, "Mechanisms of Laser-Tissue Interaction: I. Optical Properties of Tissue," *J. Lasers Med. Sci.*, vol. 2, Jun. 2011.

[55] G. Keiser, *Biophotonics: Concepts to Applications*. Singapore: Springer Singapore, 2016. doi: 10.1007/978-981-10-0945-7.

[56] A. Douplik, G. Saiko, I. Schelkanova, and V. Tuchin, "The response of tissue to laser light," 2013. doi: 10.1533/9780857097545.1.47.

[57] K. Calabro, "Modeling Biological Tissues in LightTools," p. 14.

[58] E. Salomatina, B. Jiang, J. Novak, and A. N. Yaroslavsky, "Optical properties of normal and cancerous human skin in the visible and near-infrared spectral range," *J. Biomed. Opt.*, vol. 11, no. 6, p. 064026, 2006, doi: 10.1117/1.2398928.

[59] E. Berry *et al.*, "Optical properties of tissue measured using terahertz-pulsed imaging," San Diego, CA, Jun. 2003, p. 459. doi: 10.1117/12.479993.

[60] J.-J. Chen et al., “A Pilot Study Exploring the Relationship between Short-Term HRV and Self-Rated Health Status among Elderly People,” Arch. Community Med. Public Health, vol. 3, no. 1, pp. 001–007, Feb. 2017.

[61] “Postural Changes on Heart Rate Variability among Older Population: A Preliminary Study.” https://www.hindawi.com/journals/cggr/2021/6611479/ (accessed Jun. 09, 2022).

[62] G. R. Geovanini et al., “Age and Sex Differences in Heart Rate Variability and Vagal Specific Patterns – Baependi Heart Study,” Glob. Heart, vol. 15, no. 1, p. 71, doi: 10.5334/gh.873.

[63] G. Ravé et al., “Heart Rate Variability is Correlated with Perceived Physical Fitness in Elite Soccer Players,” J. Hum. Kinet., vol. 72, pp. 141–150, Mar. 2020, doi: 10.2478/hukin-2019-0103.

[64] O. F. Barak, D. G. Jakovljevic, J. Z. Popadic Gacesa, Z. B. Ovcin, D. A. Brodie, and N. G. Grujic, “Heart Rate Variability Before and After Cycle Exercise in Relation to Different Body Positions,” J. Sports Sci. Med., vol. 9, no. 2, pp. 176–182, Jun. 2010.

[65] B. Julia and B. Reiner, “The postural orthostatic stress syndrome in childhood: HRV analysis and the active standing test,” Prev. Med. Community Health, vol. 3, no. 2, 2020, doi: 10.15761/PMCH.1000148.

[66] A. Voss, R. Schroeder, A. Heitmann, A. Peters, and S. Perz, “Short-Term Heart Rate Variability—Influence of Gender and Age in Healthy Subjects,” PLOS ONE, vol. 10, no. 3, p. e0118308, Mar. 2015, doi: 10.1371/journal.pone.0118308.